THE PATHOGENESIS OF BOVINE OSTERTAGIASIS

DISSERTATION FOR THE DEGREE

OF

DOCTOR OF PHILOSOPHY

IN

THE FACULTY OF MEDICINE

OF

THE UNIVERSITY OF GLASGOW

BY

MAXWELL MURRAY

DEPARTMENT OF EXPERIMENTAL VETERINARY MEDICINE

UNIVERSITY OF GLASGOW

1968

AUTHOR'S NOTE

This thesis is presented in two volumes because it contains a large number of micrographs; the first contains the text and the second, the illustrations.

VOLUME I

CONTENTS

CONTENTS - MATERIALS AND METHODS

CONTENTS - SECTION I

PREPARATION OF BOVINE GASTRIC MUCOSA FOR ELECTRON MICROSCOPICAL EXAMINATION

CONTENTS - SECTION II

THE FINE STRUCTURE OF THE ABOMASAL MUCOSA OF THE PARASITE-FREE BOVINE

CONTENTS - SECTION III

THE DISEASE PROCESS

CONTENTS - SECTION IV

STRUCTURAL AND FUNCTIONAL CHANGES ASSOCIATED WITH THE USE OF THIABENDAZOLE IN BOVINE OSTERTAGIASIS

CONTENTS - SECTION V

THE GLOBULE LEUKOCYTE AND ITS DERIVATION FROM THE SUBEPITHELIAL MAST CELL

CONTENTS - SECTION VI

THE STRUCTURAL CHANGES IN THE BOWEL WALL ASSOCIATED WITH INCREASED PERMEABILITY TO MACROMOLECULES

GENERAL INTRODUCTION

Parasitic disease is responsible for considerable economic loss to agriculture throughout the world. Efficient anthelmintics, enlightened husbandry and immunisation procedures have done much to reduce this. Yet it is still not possible to treat and control certain types of parasitism. This is mainly due to lack of knowledge of the basic pathogenic and immunological mechanisms involved. In the last few years the increasing use of modern techniques in parasitological research has helped to clarify many of these phenomena.

In Britain Ostertagia ostertagi infection in cattle is the most common cause of the widespread morbidity and mortality associated with bovine gastrointestinal parasitism (Ritchie, Anderson, Armour, Jarrett, Jennings and Urquhart, 1966) (Figure 1). The main clinical signs of this disease are diarrhoea, inappetance and weight loss. The pathogenesis and epidemiology of bovine ostertagiasis has several unexplained features which are reflected in inability to treat and control certain severe forms of the disease (Anderson, Armour, Jarrett, Jennings, Ritchie and Urquhart, 1965).

Since 1890 when Ostertag first attributed abomasal lesions in cattle to Ostertagia ostertagi, there have been a number of reports of outbreaks of parasitic gastritis in animals at grass (Stiles, 1900; Moras, 1907; Gardener, 1911; Ackert and Muldoon, 1920; Bruford and Fincham, 1945; Bailey, 1956; Gracey, 1960). In these, there was little detailed information on the epidemiology of the outbreaks or on the pathology of the disease process.

The situation became more complicated when Martin, Thomas and Urquhart (1957) found severe abomasal lesions due to O. ostertagi in young housed cattle with

chronic dairrhoea. These animals had completed one grazing season and when initially housed in autumn they were clinically healthy. After a period which ranged from 3 to 20 weeks, diarrhoea developed. This history was one which up till that time would not have been associated with parasitic gastritis but would have suggested a non-parasitic aetiology.

Anderson et al. (1965), in a detailed investigation of field outbreaks of bovine ostertagiasis, did much to resolve the understanding of this condition. They classified the disease into 3 phases, 2 of which (Type I and Type II) were clinically obvious and one which was not (Pre-Type II); these were described as follows:-

Type I This corresponded to the classical description of clinical parasitic gastritis in which calves, at grass for the first time, showed a loss of weight and diarrhoea; outbreaks occurred any time from late July until the end of the grazing season. The majority of the ingested larvae developed to maturity in the expected period of 3 weeks.

Pre-Type II (or the Stage of Inhibition). In this stage, which preceded Type II, large populations of O. ostertagi (over 100,000 in many cases) were present, and of these over 80% were inhibited in the early 4th stage. These animals had grazed infected pasture in autumn, but had no history of diarrhoea and usually appeared healthy to the farmer.

Type II The history in this type was that calves in which diarrhoea or weight loss had not been prominent during the grazing season, had been housed about the beginning of November. After a lapse of time which ranged from 3 weeks to 6

months, the animals started to lose weight and showed profuse watery diarrhoea. The appearance of these clinical signs coincided with the development to maturity of large numbers of inhibited larvae. This syndrome also occurred in outwintered animals.

In Type I and Type II, the principal lesions found in the abomasum were umbilicated nodules in the mucosa which resulted in diffuse irregular epithelial hyperplasia (Fig. 1), sloughing of epithelium, congestion and oedema. Histologically, the most significant changes occurred in the specialised cells lining the gastric glands. These cells were replaced by rapidly dividing and apparently undifferentiated epithelial cells in the parasitised glands and in the surrounding glands. It was noted that globule leukocytes were numerous and that lymphoreticular and plasma cell activity could be marked. In Pre-Type II cases the macroscopic changes and microscopic changes were minimal and were confined to the parasitised glands housing the inhibited 4th stage larvae. These authors found elevation of the pH of abomasal contents of animals with Type I and Type II ostertagiasis and attributed this to loss of the specialised secretory cells responsible for HCl production, namely the parietal cells. In both phases, the plasma pepsinogen levels were raised; hypoalbuminaemia occurred but only in Type II ostertagiasis. It was theorised that the cell junctions responsible for the integrity of the epithelial sheet were seriously interfered with, thereby allowing pepsinogen, not activated in the alkaline conditions in the abomasum, to leak into the circulation and likewise plasma macromolecules to leak out. Using isotopically labelled albumin and the non-digestible macromolecule polyvinylpyrrolidone (P.V.P.), it has been shown that, in calves infected with O. ostertagi, the half life of albumin was significantly

shortened and that P.V.P. was lost into the gut (Mulligan, Dalton and Anderson, 1963).

Ross, Todd and Dow (1963) and Ross and Todd (1965) also observed elevation of the pH of the abomasal contents of cattle severely affected with O. ostertagi; in addition, they found a marked reduction in the pepsin concentration of the abomasal contents.

Experimental inoculations of O. ostertagi larvae were given to susceptible calves by Threkeld and Johnson (1948), Osborne, Batte and Bell (1960) and Mahrt, Hammond and Miner (1964). In these experiments a standard dose of inoculum was not employed and necropsies were carried out at long intervals after inoculation; little data were given on the development or consequences of the lesions.

More recently, Ross and Dow (1965) and Ritchie et al. (1966) studied the sequential development of the abomasal lesions following experimental inoculations of 100,000 third stage O. ostertagi larvae. Ritchie et al. (1966) used 8 to 10-week old worm-free calves and these were necropsied in pairs at selected intervals from 2 to 90 days after infection. It was found that a single dose of 100,000 O. ostertagi larvae produced all of the abomasal lesions seen in typical field cases of Type I ostertagiasis. This infecting dose was too low to produce widespread confluence of lesions and hence the main clinical features of the severely affected case were not produced. Ritchie et al. (1966) described the pathogenesis in terms of 3 phases.

1) The larva is located in a gastric gland by day 2; it grows and matures in the gland, the epithelium of which becomes stretched and replaced by mucous cells.

2) Emergence of the adult parasite commences about 16 days after infection and a loss of a large part of the adult worm population takes place over the next 10 to 12 days. At about the time of emergence the functional cells lining the glands surrounding the parasitised gland are replaced by an undifferentiated and hyperplastic epithelium. The unit lesion produced is a raised nodule at the centre of which is the gastric gland originally dilated by the presence of a larva. The emerged parasites lie apposed to the surface epithelium and at this point cytolysis and sloughing of the superficial cells may occur. There is an increase of plasma cells in the lamina propria and globule leukocytes appear within the mucosa.

3) As the infection subsides the epithelium resumes its normal appearance and content of differentiated cells. Some of the glands, which have contained larvae, remain lined by tall mucus-secreting epithelium.

In further experiments, which were done to give quantitative dose-response data, Anderson, Armour, Eadie, Jarrett, Jennings, Ritchie and Urquhart (1966) infected groups of 15-week old parasite-free calves with doses of O. ostertagi larvae ranging from 50,000 to 800,000. All calves were killed 21 days after infection. Doses of 400,000 larvae and upwards produced marked diarrhoea, anorexia and loss of weight, severe abomasal lesions, considerable elevation of the pH of the abomasal contents and raised plasma pepsinogen levels. It was found that doses of 200,000 and over resulted in coalescence and overlapping of unit lesions and led to a morocco leather appearance of a thickened, hyperplastic,

non-differentiated and non-functional mucosa. The degree of cytolysis and epithelial sloughing of the superficial mucosa was directly related to the dose level. In all calves there were marked reactive changes in the regional lymph nodes. In calves given doses of 400,000 and 800,000 larvae, a purulent lymphadenitis was superimposed on the reactive changes.

Jennings, Armour, Lawson and Roberts (1966) inserted abomasal cannulae into calves and subsequently infected them with 300,000 O. ostertagi larvae. Studies of the daily biochemical changes in the abomasal fluid and in the blood were made. This allowed the biochemical findings on the abomasal fluid and on the blood to be correlated with the development of the abomasal lesions. The period of maximal change occurred immediately after the emergence of the parasites from the gastric glands at day 19 and lasted till about 27 days after infection. In the abomasum there was an increase in sodium ion concentration and a decreased concentration of hydrogen, potassium and chloride ions. During this period, pepsin activity was reduced and there was an increase in plasma pepsinogen levels. With the loss of the adult worm population there was a gradual return to normal function.

From the results of the investigations described a hypothesis of the pathogenesis of bovine ostertagiasis can be formulated. The period immediately after infection, when larvae are developing to the adult stage in the gastric glands, is associated with cellular changes which are confined to the parasitised glands; during this period, significant changes do not occur in the biochemical values of either the abomasal fluid or the blood, and clinical signs are not detectable. By day 16 after infection, adult worms begin to emerge from the

parasitised glands, and this leads to an apparent loss of parietal cells; when these areas become confluent, giving a morocco leather appearance to the mucosa, then complete loss of parietal cells appears to have occurred and the pH of the abomasal fluid rises markedly. This undifferentiated and hyperplastic mucosa has increased permeability to macromolecules (Mulligan et al., 1963), which is possibly reflected in the increased plasma pepsinogen levels and also in the excess loss of albumin into the gut. The principal clinical sign, i.e. severe diarrhoea, also occurs after emergence of the adult O. ostertagi from the glands and coincides with the increase in the pH of the abomasal fluid to more than 7.

The primary purpose of this work was to study by light and electron microscopy the development of the structural changes in the gastrointestinal tract of cattle infected experimentally and naturally with O. ostertagi and to relate these to alterations in functional activity. In addition, a cytochemical and ultrastructural study was made of certain cell types which appear to be particularly involved in parasitic infections.

MATERIALS AND METHODS

1. Experimental Animals

(i) Parasite-free calves

Ayrshire bull calves, purchased when 3 to 5 days old, were housed individually indoors. They were reared on whole milk at the rate of one pint of milk per 10 lbs. live weight per day. During the 3rd and 4th weeks, hay and calf weaner pellets (British Oil and Cake Mills Ltd.) were introduced and milk feeding was stopped by the end of the 4th week. From then until slaughter, the calves were fed on 3 lbs. of pelleted ration daily with hay and water available *ad lib*. Reared in this way, the calves had a mean growth weight of 1 lb. per day. Regular faecal examination for nematode eggs gave negative results.

(ii) Tissues were taken from 10 young cattle, aged 12 to 15 months, with Type II ostertagiasis (Anderson *et al.*, 1965). The animals had severe diarrhoea.

Their plasma pepsinogen levels were elevated being greater than 4,000 milliunits of tyrosine (*vide* p. 12 ; normal is 326 ± 8 milliunits of tyrosine). They had marked hypoalbuniaemia, serum albumin levels being less than 1.5 gms.% (normal is 2.9 ± 0.4 gms.%). At necropsy the pH of abomasal fluid of every case was greater than 6 (normal is 2.4 ± 0.1). The normal levels quoted are from Anderson *et al.* (1965). In all cases at least 50,000 *O. ostertagi* were recovered; in one the number was greater than 500,000.

(iii) Sheep

Material was taken from the abomasum of 2 sheep experimentally infected with Haemonchus contortus. They were subjected to repeated infections, receiving in the course of one year, approximately 15 million larvae.

Tissue was examined from the biliary tract of 2 sheep which had been vaccinated against Fasciola hepatica with Freund's adjuvant-whole worm antigen preparation and then experimentally infected with 500 F. hepatica metacercariae. These sheep were killed 19 weeks after infection.

(iv) Rats

Tissue was taken from the intestine of normal adult rats and from rats at various intervals after infection with 3,000 or 10,000 N. brasiliensis. Material was also examined from hyperimmune rats infected with successive doses of 3,000, 5,000 and 7,000 N. brasiliensis.

2. Histological Techniques

(i) Fixation

A range of fixatives was used. These were isotonic-formaldehyde acetic acid (IFAA) (Enerbäck, 1966a), Carnoy's fluid (Clayden, 1955) and corrosive formal (CF) (Carleton and Drury, 1957). Tissues were fixed for 24 - 48 hours, dehydrated and cleared in an alcohol-amyl acetate-chloroform series and embedded in paraffin wax.

With respect to the cytochemical investigations carried out in Section V, it was found that IFAA gave poor overall fixation of tissues

although the subepithelial mast cells and globule leukocytes (GL) were well preserved. Carnoy's fluid was the fixative of choice in the rat; in the bovine and sheep, most of the GL granules were not adequately fixed by this method. Tissues from the bovine and sheep were best preserved by corrosive formal, although the mast cells did not stain as metachromatically with toluidine blue nor as brightly with astra blue as those cells fixed in Carnoy's fluid.

(ii) Staining Procedures

Paraffin sections were stained with haemalum and eosin, picro-Mallory, phosphotungstic acid haematoxylin, periodic acid-Schiff and Southgate's mucicarmine (Pearse, 1961).

The following special staining procedures were employed in the study of mast cells and globule leukocytes.

(a) Thiazine dyes. Toluidine blue was used in a 0.5% aqueous solution at pH 4 or 4.5 (McIlvaine's citric acid-disodium phosphate buffer; staining time 45 seconds) (Enerbäck, 1966b). Sections were stained with a 0.1% aqueous solution of toluidine blue at pH 0.3 (dye diluted in 0.7 N HCl) for 10 minutes followed by rinsing in 0.7 N HCl for 10 minutes (Enerbäck, 1966b).

(b) Copper phthalocyanine dyes. Astra blue (G. T. Gurr Ltd.) was used in a 0.5% solution at pH 0.3 (Bloom and Kelly, 1960); staining time was 30 minutes. Sections treated with astra blue as described were counterstained with 0.5% safranin O (Hopkin and William Ltd.

in 0.125 N HCl (about pH 1) for 30 seconds (Enerbäck, 1966b)

(c) Acridine orange was used as a 0.001% solution (Jagatic and Weiskopf, 1966) and also as a 0.1% solution in distilled water (pH 7.2) and as a 0.1% solution in 0.01M acetic acid (pH 3.2). (Saunders, 1964).

(d) Biebrich scarlet (Spicer and Lillie, 1961) was used as a 0.04% solution in glycine buffers at pH 8.15, 8.9 and 9.9; staining time was 30 minutes.

3. Freeze-drying Technique for Fluorescent Demonstration of Monoamines (Falck, Hillarp, Thieme and Torp, 1962).

Tissues 3 - 4 mm in size were quenched in isopentane and cooled in liquid nitrogen; these were placed in an Edwards-Pearse Tissue Drier and left overnight under a vacuum of 0.001 torr at -40°C. They were then exposed to paraformaldehyde vapour at 80°C for 1 hour and impregnated with de-gassed molten paraffin wax in the tissue drier at 60°C under vacuum of 0.001 torr for 15 minutes. The tissues were embedded in molten paraffin wax. Material was stored in the dark until sectioned. Prior to cutting, the wax blocks containing the tissues were left for 30 minutes at +4°C. Sections were cut on a Cambridge Rocking Microtome at 6 μ and mounted on warm slides to melt the wax; surplus wax was removed with warm liquid paraffin, the mounting medium. The block was then re-covered with soft wax to seal it from moisture.

Acridine orange-stained sections and sections treated for monoamines were examined with a Leitz Ortholux microscope; A BG 12, 3 mm exciting filter and a

K 530 barrier filter were used. The light source was a mercury vapour lamp (Wotan HBO 200 w).

4. Electron Microscopical Techniques

For fixation, concentrations of glutaraldehyde ranging from 1% to 4% were prepared in a 0.067 M Sorensen's phosphate buffer at pH 7.4. Tissues from the abomasum and small intestine of sheep and cattle, from the biliary tract of sheep and the small intestine of rats were removed under barbiturate or trichloroethylene anaesthesia or after stunning and exsanguination. In Section I the methods and requirements for adequate fixation are described in detail.

Thick sections, 1 - 1.5μ were cut on an LKB Mark III Ultratome. They were mounted on glass slides and stained with Mallory's borax-methylene blue or aqueous toluidine blue after the methods of Richardson, Jarret and Finke (1960) and Trump, Smuckler and Benditt (1961). These sections were used to locate lesions for electron microscopical examination.

5. Biochemical Analysis

(i) Plasma pepsinogen

15 ml. of blood were collected into a tube containing 2 - 3 drops of 1:1000 solution of heparin. The heparinised sample was centrifuged at room temperature at 1500 x g for 20 minutes. The plasma was then pipetted into plastic tubes and immediately forzen and stored at -5°C. The method of estimation was essentially similar to that described by Edwards, Jepson

and Wood (1960) in that plasma was incubated at pH 2 with a bovine serum albumin substrate (Armour's Fraction V. Armour Pharmaceutical Co. Ltd.) for 24 hours at 37°C. The liberated tyrosine, non-precipitable with trichloroacetic acid, was estimated with Folin-Ciocalteau reagent (British Drug Houses) and read in a spectrophotometer (Unicam, Cambridge). The activity was expressed as millunits (mU) tyrosine (μ mols tyrosine per litre of plasma per minute x 100).

(ii) Total Serum Protein Concentration

Total serum protein concentration was estimated by the biuret method of Weichselbaum (1946).

(iii) Serum Protein Fractionation

Separation of serum protein fractions were carried out by electrophoresis. Cellulose acetate strips (Oxoid Ltd.) were saturated with barbitone buffer (pH 8.6) and placed in a horizontal electrophoresis tank (Shandon Scientific Co.). Serum (0.03 ml.) was pipetted on to strips and a voltage of 150 volts was applied for one hour from a Vokam power pack (Shandon Scientific Co.). The strips were then removed and dried in an oven at 80 - 100°C for ten minutes and developed by staining with 0.2% Ponceau S (G. T. Gurr Ltd. : for electrophoresis) in 3% aqueous trichloroacetic acid for 5 minutes. After staining, the strips were washed in 5% acetic acid until the background was white. The strips were evaluated automatically as described by Neil (1963) using a Chromoscan recording

densitometer (Joyce Loebl and Co. Ltd.). The results were expressed as grams per 100 ml. of serum albumin, total globulin and gamma globulin.

(iv) pH of Abomasal Contents

This was determined using a glass electrode (Beckman Instruments Ltd.) immediately after collection.

6. Parasitological Techniques

The details of parasitological techniques used in the experimental studies in Sections III and IV are those described by Armour (1967).

SECTION I

PREPARATION OF BOVINE GASTRIC MUCOSA FOR ELECTRON MICROSCOPICAL EXAMINATION

INTRODUCTION

Up to the present time all studies of the ultrastructure of the gastric mucosa have employed osmium tetroxide or potassium permanganate ($KMnO_4$) as fixatives. While the results are useful, the information obtained is limited by the fact that these fixatives do not preserve protein structures in the cell. With the introduction of glutaraldehyde (Sabatini, Bensch and Barnett, 1963), a major advance was made in the stabilisation of protein structures for electron microscopical examination.

Early in this study glutaraldehyde fixation gave rise to many technical undesirable effects including cell shrinkage, myelin configurations, breakdown of cristae mitochondriales and uneven fixation. It was realised that several properties of the fixative solution influenced the ultrastructure of gastric mucosa. Such properties included the concentration of the fixative, the buffer system, the osmolality of the fixative solution and the pH of the fixative itself and of the buffered fixative solution.

As some components of aldehyde-fixed tissues, such as membranes, are extracted during dehydration, primary aldehyde fixation was followed by treatment with osmium tetroxide.

To date the embedding medium used in most electron microscopical studies of the gastric mucosa has been methacrylate. This substance produces considerable shrinkage and distortion of tissues; these deleterious effects can largely be eliminated by the use of epoxy resins such as Araldite and Epon as embedding media.

In this work, a study was made on the influence of glutaraldehyde concentration, osmolality of the fixative solution and type of buffer system on cell ultrastructure in the bovine gastric mucosa. The experimental design is shown in Table 1. Firstly, glutaraldehyde concentrations were varied from 1 to 4%, maintaining a constant buffer solution (0.067 M Sorensen's phosphate buffer). Secondly, the osmolality of the Tyrode buffer was gradually increased by adding sodium chloride, maintaining constant glutaraldehyde concentrations.

MATERIALS

1. Tissues Tissue was taken from the gastric mucosa of 2 parasite-free bovines under barbiturate anaesthesia. The fixatives used penetrate tissues very slowly (Glauert, 1965) and so it was found essential to limit the size of the specimen to 1-2 mm for optimal results.

2. Glutaraldehyde Stock Solutions In preliminary investigations, solutions were prepared from 25% glutaraldehyde supplied by Union Carbide Ltd. The pH of this solution was frequently less than 3 due to free glutaric acid produced by spontaneous auto-oxidation of glutaraldehyde. When the stock glutaraldehyde solution has a pH of less than 3.5, the quality of fixation is poor (Glauert, 1965). In our initial studies the solution was purified by adding a small quantity of barium carbonate. A precipitate was formed, and after centrifugation the clean supernatant was removed and used as fixative. The resultant pH was greater than 3.5. In the present experiment, a 25% solution of glutaraldehyde, specially

purified and stabilised at pH 5-6 by Taab Laboratories, was used.

3. Buffers The composition of the 0.067 M Sorensen's phosphate buffer was as follows:

$Na_2 HpO_4$	-	9.118 gm/litre	- 3 parts
$K H_2PO_4$	-	9.512 gm/litre	- 1 part

The final pH of the buffered fixative solution was between 7.2 and 7.4.

The composition of Tyrode solution was as follows: KCl, 0.2 gms., $CaCl_2$, 0.2 gms., $MgCl_2$ 6 H_2O, 0.1 gms., distilled water ad 1,000 ml. In addition, variable amounts of sodium chloride (2, 4, 6, 8 and 10 gms.) were added to vary the final osmolality of the solution. The pH of the fixative solution was adjusted to 7.2 to 7.4 by bubbling a mixture of 95% oxygen-5% carbon dioxide through the solution.

Millonig's phosphate buffer was prepared as follows:

NaH_2PO_4 $2H_2O$	(2.26%)	83 ml.
NaOH	(2.52%)	17 ml.
H_2O		10 ml.
Sucrose		0.54 gms.

The final osmolalities of the fixative solutions shown in Table 1 were measured by depression of the freezing point on a Knauer Semimicroosmometer (Shandon Ltd.).

4. Embedding Material The embedding medium used was the epoxy resin Araldite or a mixture of Araldite and Epon. The composition of the Araldite was as follows:

Mixture 1	Resin CY 212	1 lb. (Ciba (A.R.L.) Ltd.)
	Hardener HY 964	1 lb.
Mixture 2	Accelerator DY 064	5 mls.
	Dibutyl Phthalate	25 mls.
Mixture 3	Mixture 1	19 mls.
	Mixture 2	1 ml.

All Araldite preparations were mixed together very thoroughly, usually being stirred overnight.

The Araldite-Epon mixture was prepared in the following proportions:

25 ml. Epon 812 (Epikote 812) (Shell Chemicals Ltd.)

55 mls. DDSA (Dodecenyl Succinic Anhydride) (Cambrian Chemicals Ltd.)

15 mls. Araldite CY 212

4 mls. Dibutyl Phthalate

This mixture was kept at +4°C before use. Just prior to using, 1.5 ml. DMP 30 were added as accelerator.

METHODS

Tissues were sliced into small blocks in drops of chilled buffered glutaraldehyde. The blocks were left for 1½ hours at +4°C, rinsed in Millonig's phosphate buffer and post-fixed for 1 hour in 1% osmium tetroxide. In addition, tissues were fixed for 1½ hours in 1% osmium tetroxide prepared in Millonig's phosphate buffer at pH 7.4. Dehydration was through an ascending series of 70%, 90% and absolute alcohol. The blocks were then treated with propylene oxide and embedded in the epoxy resin preparation in gelatine capsules. Araldite-embedded tissues were left at 57°C for 48 hours and Araldite-Epon embedded tissues were kept at 80°C for 36 hours, to allow the resins to polymerise. Sections were cut on an LKB Mark III Ultratome, mounted on copper mesh grids and double-stained with saturated uranyl acetate in methanol and then with lead citrate (Reynolds, 1963); they were examined with an AEI electron microscope 6B.

RESULTS

Due to the poor penetrative qualities of the fixatives used, fixation was found to be variable in the deeper parts of the blocks; therefore sections were cut only from the superficial parts.

The criteria used for judging the quality of fixation were, breakage of cristae mitochondriales, tissue tears, myelin configurations, density of the cytoplasm and cell apposition.

It was found that glutaraldehyde concentrations could be varied over a wide range without inducing cell swelling or shrinkage. At osmolalities less than

360 milliosmoles/litre and even more so at less than 310 milliosmoles/litre, cell swelling was obvious. This was indicated by loss of density of the cytoplasm, swelling of mitochondria with breakage of their cristae and separation and dilatation of the cisternae of the rough surfaced endoplasmic reticulum (RSER) and of the membranes surrounding the nucleus (Fig. 2). At osmolalities greater than 430 milliosmoles/litre, the tissues became shrunken as shown by dilatation of intercellular spaces, increased cytoplasmic density and shrinkage of mitochondria (Fig. 3). In all preparations used, fixation was found to be rather variable and in each case some areas of fixation were excellent.

Using Tyrode solution as fixative vehicle and buffering with carbon dioxide, the quality of fixation was poorer in comparison with phosphate buffer preparations. However, changes in osmolality of the fixative solutions of 50 - 60 milliosmoles/litre were clearly reflected in tissue preparations. Solutions 8 and 12 (Table 1) showed swelling of cells (Fig. 4), while 11, 16 (Fig. 5) and to a lesser extent 15 (Fig. 6) showed shrinkage of cells. Solutions 9, 10, 13 and 14 showed little evidence of cell swelling or shrinkage.

Epithelial cells in the gastric mucosa were much more sensitive to changes in osmolality than cells in the lamina propria which were adequately fixed by most fixative solutions.

With solution 17, fixation was good and cell apposition was exact (Fig. 7).

It was found that the quality of the sections and their ability to withstand electron bombardment was directly dependent on the time the epoxy resin medium was left to mature.

DISCUSSION

In this study no one preparation gave completely satisfactory results.

Adequate fixation was obtained using glutaraldehyde concentrations from 1.5% - 4% in Sorensen's phosphate buffer. Optimal apposition was obtained using fixative solutions between 350 and 430 milliosmoles/litre. Small changes in the number of osmotically active ions (Na^+, Cl^-) of 50 - 60 milliosmoles/litre could be detected by changes in cell ultrastructure; glutaraldehyde concentrations could be altered over a wide range without changes in cell structure. Similar conclusions were reached by Maunsbach (1966) in a study of fixation of the rat kidney. Maser, Powel and Philpott (1967) emphasised the importance of the osmolality of the fixative solution. They considered that osmolality could affect cell structure to the extent that it should be recorded when describing results.

The quality of fixation given by phosphate-buffered solutions was superior to that given by Tyrode/CO_2 buffered solutions.

It was considered that, in order to aid interpretation of results, the concentration of fixative used and the final osmolality of the fixative solution should always be stated.

Using osmium tetroxide alone, good fixation and cell apposition were obtained using a fixative solution approximately isotonic with the blood serum of the bovine, i.e. 290 - 300 milliosmoles/litre (McEwan, 1967). The value of this fixative was limited in this study by its inability to preserve certain structures.

Although fixation techniques used in the preparation of one tissue or in one species may not be valid in another tissue or species, it was found that in

the case of ovine abomasal and biliary mucosa and rat small intestine, adequate fixation was given by 1.5 - 4% glutaraldehyde solutions in 0.067 M Sorensen's phosphate buffer.

TABLE 1

Concentration of Fixative, Buffer System and Osmolality of Fixative Solution

Solution No.	Concentration of Fixative	Buffer	Osmolality milliosmoles/litre
1	1 % Glutaraldehyde	0.067 M Phosphate	250
2	1.25% "	"	280
3	1.5 % "	"	310
4	1.75% "	"	330
5	2 % "	"	360
6	2.5 % "	"	425
7	4 % "	"	450
		Tyrode/NaCl in gms.	
8	1.5 % "	4	330
9	1.5 % "	6	380
10	1.5 % "	8	445
11	1.5 % "	10	510
12	2.0 % "	2	310
13	2.0 % "	4	370
14	2.0 % "	6	430
15	2.0 % "	8	480
16	2.0 % "	10	550
17	1.0 % Osmium Tetroxide	Millonig's Phosphate	290

SECTION II

THE FINE STRUCTURE OF THE ABOMASAL MUCOSA OF THE PARASITE-FREE BOVINE.

INTRODUCTION

The abomasum forms the fourth division of the ruminant stomach and corresponds to the secretory stomach of other animals. It constitutes 7 to 8% of the capacity of the bovine stomach (Sisson, 1958). It is divided by a transverse constriction into two main areas, the fundus and pylorus. The fundus is lined by a glandular mucosa which forms a dozen or more spiral folds with an interfold area between (Fig. 1). These folds commence at the omaso-abomasal junction, rapidly attain their maximum depth which may be 3 to 4 cms., and then gradually become smaller as they approach the pyloric region. The pylorus is narrower than the fundus and is covered with a smooth mucous membrane thrown into a few small rugae which resemble those of the simple stomach. There is a transition area between the fundus and pylorus known as the transverse fold area in which the abomasal folds become smaller and smaller in depth.

To date the fine structure of the bovine abomasum has not been described. Since the introduction of glutaraldehyde as a fixative and epoxy resins as embedding media, there have been no reports in which these materials were used to study the ultrastructure of the gastric mucosa in any species. Existing publications have employed osmium tetroxide or potassium permangenate as fixatives and usually methacrylate as an embedding medium (Kurosumi, Shibasaki, Uchida and Tanaka, 1958; Shibasaki, 1961; Helander, 1962; Ito and Winchester, 1963; Sedar, 1964; Lillibridge, 1964; Corpron, 1966).

In these publications general agreement exists concerning the ultrastructural characteristics of the cells present. Surface mucous cells are recognised by their apical content of electron-dense granules arranged in rouleaux formation and by an extensive golgi complex capping the nucleus; their lateral plasmalemmata are usually elaborately interdigitated. Parietal cells are packed with large mitochondria with numerous transversely oriented cristae mitochondriales; intracellular channels lined by microvilli and termed canaliculi pursue a tortuous course around the nucleus and communicate directly with the gland lumen. The main ultrastructural features of zymogen cells are numerous stacks of rough-surfaced endoplasmic reticulum (RSER) in the basal cytoplasm, an extensive paranuclear golgi complex and an apical content of granules of variable electron density. Enterochromaffin cells are characterised by small membrane-bound granules in their basal cytoplasm; the base of the cell rests on the basement membrane but its apical part rarely reaches the gland lumen. At one time there was some controversy as to whether mucous neck cells, readily recognised in light microscopy, could be distinguished ultrastructurally from surface mucous cells; Helander (1962), working with the mouse, was unable to differentiate them and criticised earlier identification and description of mucous neck cells in the rat by Kuromsumi et al. (1958) and Shibasaki (1961) on the grounds of poor fixation. Since then the ultrastructural features of the mucous neck cell have been delineated in several species, the bat, dog, man and rat by Ito and Winchester (1963), Sedar (1964), Lillibridge (1964) and Corpron (1966) respectively. It is recognised by its apical content of granules which

are larger than those in surface mucous cells and by relatively straight lateral plasmalemmata.

Apart from Ito and Winchester's (1963) description of the pyloric gland cell in the bat, there are no reports on the ultrastructural characteristics of the cell types found in the pylorus. These workers noted a similarity between the pyloric gland cell and the mucous neck cell.

For many years it was generally assumed, on the basis of light microscopy, that cells were joined together by bands of condensed intercellular substance called terminal bars. In an electron microscopical study, Farquhar and Palade (1963) showed that the terminal bar is a tripartite complex between juxtaluminal segments of adjacent cells and that it consists of modifications of the lateral plasmalemmata and the associated cytoplasm. They demonstrated this complex between a wide variety of epithelial cells in glands and cavitary organs of the rat and guinea pig.

In this section, a description is given of tissues which were examined from the abomasum of 4 parasite-free bovines; these animals were aged 12, 16, 20 and 24 weeks. The objects were to define the cell types present and to examine the appearance of normally functioning cells.

In order to stabilise protein structures for ultrastructural examination, glutaraldehyde was used as fixative followed by osmium tetroxide. To reduce tissue shrinkage and distortion Araldite and Araldite-Epon were employed as embedding media.

RESULTS

The microarchitecture of the fundic and pyloric parts of the bovine gastric mucosa resembles that described by Ham (1965) in other mammals. Figure 8 shows the gastric pit descending through the mucosa to reach the gastric gland which opens into the pit. In the bovine, the gastric gland is a relatively simple tubular structure. It is in the gastric gland that the highly acidic proteolytic gastric juice is produced. Figure 9 shows the pyloric mucosa with a much longer gastric pit traversing the mucosa to the pyloric glands.

On electron microscopical examination it was found that the epithelial cells of the bovine gastric mucosa are joined by a tripartite junctional complex. The nomenclature used in the following description follows that adopted by Farquhar and Palade (1963).

The first part of the complex, the zonula occludens (or tight junction), is located immediately behind the line of reflection of the plasma membrane from the apical to the lateral surface of the cell body (Fig. 10). It is characterised by fusion of the adjacent cell membranes resulting in obliteration of the intercellular space over variable distances (0.2 to 0.5 u). Within the obliterated zone, the dense outer lamina of adjoining cell membranes converge to form a single intermediate line. A thin accompanying zone of electron-dense material is obvious in the adjacent cytoplasm. In view of the fact that the zonula occludens is constantly found, irrespective of the plane of section, it is concluded that this structure encircles the cell completely. This is in agreement with Farquhar and Palade (1963). In a few cases, one or more focal

splittings of the fusion line may be found (Fig. 11).

Basally, the zonula occludens separates into 2 lines, the emerging outer leaflets of the lateral cell membrane forming what is termed the zonula adhaerens (Figs. 10 and 11). This is characterised by a true intercellular space of approximately 200 Å and by conspicuous condensation of the adjacent cytoplasmic matrices. The triple-layered plasma membranes of the adjoining cells are distinct. Throughout the junction the apposed membranes run parallel to each other over a straight or wavy course for 0.2 to 0.5 u. The intercellular space is occupied by material of moderate electron density occasionally bisected by a faint band of higher density. The zones of cytoplasmic condensation along this junctional element have a tightly matted fine fibrillar texture with most of the fibrils appearing to run parallel to the cell surface. It is thought that the fibrillar material is a local condensation of the terminal web. The zonula adhaerens is found in all planes of section and is therefore assumed to form a complete belt round the cell.

The third element of the junctional complex, the macula adhaerens or desmosome is located at the basal end of the zonula adhaerens (Fig. 12). It consists of 2 straight plaques of dense material each disposed parallel to the inner leaflet of the corresponding trilaminar plasma membrane. The two apposed plaques are aligned in perfect phase, measuring from 0.1 u to 0.5 u. The intercellular space of 200 to 250 Å is occupied by a disc of moderately dense material bisected by a denser central layer sometimes called the intercellular contact layer. Bundles of cytoplasmic fibrils, coarser and more distinct

than those of the terminal web, converge on the inner aspect of each desmosomal plaque approaching at an angle or occasionally running parallel to it (Fig. 11). In most fields several desmosomes are present along the lateral cell membranes (Fig. 10). The occurrence of these structures is irregular and it is considered that they are probably discrete.

Elsewhere along the lateral wall of the cell, the apposed plasmalemmata run parallel to one another with a gap of about 200 Å between them. Occasionally they are thrown into tortuous interdigitations especially between surface mucous cells (Fig. 10).

Electron microscopical examination of the small intestine of the same animals demonstrated that the cells are joined by a similar type of tripartite complex (Fig. 13).

In the fundus at least 6 cell types are present: (1) the surface mucous cell, (2) the mucous neck cell, (3) the parietal cell, (4) the zymogen cell, (5) a "fibril-containing" cell and (6) the enterochromaffin cell.

In the pylorus at least 4 cell types are present: (1) the surface mucous cell, (2) the pyloric gland cell, (3) the enterochromaffin cell and (4) the parietal cell.

In all 4 calves the lamina propria contained very few cells; only in parasitised animals did cells become numerous enough for electron microscopical examination.

Fundus

(1) The Surface Mucous Cell

A single layer of surface mucous cells lines the gastric lumen and extends

into the gastric pit and upper gland where they mingle with parietal cells (Fig. 8). They contain a considerable quantity of apical mucus which decreases in the deepest part of the pit and in the gland isthmus.

Ultrastructurally surface mucous cells range from cuboidal to columnar. On their free surface a few stubby microvilli are present while the lateral plasmalemmata, although usually straight near the apical border, are elaborately interdigitated and closely apposed along most of the lateral border (Figs. 14 and 15). The apical cytoplasm is packed with membrane-bound granules. The number present depends on the location of the cells; in the lower pit and upper gland area the number of granules present is markedly reduced. The granules assume a spherical, ovoid, or discoid profile and range in size up to 1 u. The density of granules varies considerably, and is not affected by the concentration of glutaraldehyde used; the granules are either of low (Fig. 16) or marked electron density (Fig. 15). Occasionally both types are present in the same cell and some granules contain patches of electron-dense material (Fig. 17). In osmium tetroxide-fixed material the granules are of high electron density (Fig. 14).

The nucleus is located towards the base of the cell and is most often oval or pear shaped. Prominent central nucleoli are frequently present. A sizeable golgi complex usually caps the nucleus (Figs. 14 and 15). It consists of several parallel arrays of flat cisternae with dilated vacuoles and small vesicles. Mitochondria are confined to the lower two-thirds of the cell and assume an oval or elongated shape and contain a moderate number of transversely

oriented cristae mitochondriales. Numerous ribosomes are present in the cytoplasmic matrix. Cisternae of RSER are present mainly in the basal part of the cell; they are wide, tortuous and contain moderately dense material. RSER never occurs in such high concentrations as in zymogen cells. An occasional feature of the cytoplasmic matrix is bundles of fibrils.

(2) The Mucous Neck Cell

These cells are located in the middle segment of the gastric gland. They occur singly or in clusters among the parietal cells. When stained with periodic acid-Schiff, the apical cytoplasm is full of foamy pink mucus. The nuclei are frequently flattened against the cell bases.

The shape of these cells is generally columnar (Figs. 18 and 19) but marked variations are encountered. Some are flask-shaped with a narrow apex and a broad base resting on the basement membrane. Others have a wide luminal border and a narrow base (Fig. 20). The free surface of the mucous neck cells has a sparse covering of short microvilli. Although interdigitations of the lateral plasmalemmata occur, they are not as frequent as in surface mucous cells; in many cells the lateral plasmalemmata are, for the most part, straight.

Membrane-bound spherical granules measuring up to 1.5 u are present in the apical cytoplasm. In some cells the granules occupy the entire supranuclear part of the cytoplasm and often appear to indent the nucleus (Figs. 19 and 20). In other cells where granules are not so numerous the extent of the golgi complex can be delineated and granules are frequently in close proximity to it (Fig. 18). In most cells granules are located lateral and basal to the

nucleus (Fig. 20). The electron-density of the granules varies with the type and concentrations of fixative used. After glutaraldehyde fixation, the granules assume a patchy appearance with irregular areas of electron-dense material scattered in the granule. After osmium tetroxide fixation, the granules are consistently less dense than those of the surface mucous cell. The cytoplasm contains a moderate number of mitochondria some of which are markedly elongated. Scattered irregular and dilated profiles of RSER are present, particularly towards the cell base (Fig. 18); there is an abundance of free ribosomal particles in the cytoplasmic matrix. The golgi complex is well developed and is located in a supranuclear position and also lateral to the nucleus (Fig. 18). It consists of arrays of several smooth-surfaced profiles with dilated vacuoles and small vesicles. The nucleus is irregular in outline with deep infoldings and is often indented with granules.

(3) The Parietal Cell

Parietal cells are located principally in the neck and isthmus region scattered between surface mucous cells and mucous neck cells and occasionally among zymogen cells (Fig. 8). These cells have abundant eosinophilic cytoplasm, are round or triangular in shape and have round centrally-placed nuclei.

Electron micrographs reveal a well developed canaliculus within the cell (Figs. 21, 22, 23 and 24). This structure is continuous with the gland lumen and appears to run a tortuous course within the cell, often appearing to completely encircle the nucleus (Figs. 21 and 23). The canaliculus is lined by numerous irregularly oriented microvilli and is limited by a membrane which is continuous

with the plasmalemmata at the apex of the cell. The degree of patency of the lumen of the canaliculus varies markedly from cell to cell. In some cells the microvilli are closely intermeshed and almost completely fill the lumen of the canaliculus (Fig. 22). Most frequently the microvilli are less closely packed and the canaliculus is relatively open with a free lumen (Fig. 21). The cytoplasmic matrix contains a limited number of vesicles in the vicinity of the intracellular canaliculi (Fig. 23). The cytoplasm of the parietal cell, particularly in the vicinity of canaliculi and occasionally within the microvilli, is crowded with mitochondria. The mitochondria are more numerous and larger than those in other gastric epithelial cells. The cristae mitochondriales are abundant and closely spaced transversely (Fig. 24). The golgi complex is poorly developed and can be identified only in a few cells where it consists of a few cisternae and vesicles. While lateral plasmalemmata are usually straight, the basal plasmalemmata frequently form complicated infoldings or interdigitations (Fig. 21).

(4) The Zymogen Cell

These cells occupy the base of the gastric glands and intermingle with parietal and mucous neck cells in the neck region (Fig. 8). Their apical cytoplasm is packed with granules while the cytoplasm in the paranuclear area is highly basophilic.

Ultrastructurally, the apical border of the cell has a few small microvilli (Figs. 25, 26 and 27). The lateral plasmalemmata are relatively straight with occasional interdigitations (Figs. 26 and 27). The nucleus is located

basally and the outer layer of the nuclear envelope is studded with numerous ribosomes.

The apical and paranuclear cytoplasm contain numerous round or oval membrane-bound granules which measure up to 2 u in diameter (Figs. 25, 26 and 27). Their contents vary in density depending on the method of fixation. With glutaraldehyde fixation the granules are highly electron-dense while after osmium tetroxide fixation the granules are electron-lucid and often have patches of electron-dense material. This latter appearance can be related to different degrees of extraction during tissue preparation.

Stacks of RSER are very much more abundant in the zymogen cell than in any other cell type in the gastric mucosa. The cisternae are arranged in parallel stacks and dominate the basal cytoplasm. They tend to orientate more or less parallel to the basal and lateral cell surfaces (Figs. 25 and 27). Large numbers of free ribosomes are scattered throughout the cytoplasmic matrix.

The golgi complex is well developed and is located in a paranuclear position. It consists of several arrays of membranes with dilated vacuoles and vesicles associated with which are small secretory granules (Figs. 25 and 26).

The mitochondria are neither as numerous nor as large as those in the parietal cell and are generally similar in structure to those in mucous cells. They are lodged between cisternae of RSER at the cell base and only rarely are found in the granule-laden apical cytoplasm.

(5) The "fibril-containing" Cell

These cells are located singly in the isthmus and neck of the gastric gland between surface mucous cells (Figs. 28 and 29), mucous neck cells (Fig. 30) and zymogen cells (Fig. 31), to which they are joined by a tripartite junctional complex. Apically a few microvilli are present while the lateral plasmalemmata are straight in the apical part of the cell but are often interdigitated in the basal half. Desmosomes are occasionally located along the lateral border of the cell.

The characteristic feature of this cell is bundles of fibrils scattered throughout the cytoplasmic matrix and encircling the nucleus. These fibrils become concentrated near the apex of the cell where they project into the microvilli. Longitudinal and transverse sections of fibrils are observed.

The golgi complex is prominent and is situated mainly in a supranuclear position (Figs. 28 and 29). It is composed of stacks of cisternae with dilated vacuoles and numerous small vesicles. In some of these cells a few membrane-bound granules are located in the vicinity of the golgi complex and in the apical cytoplasm. When granules are present they closely resemble in size and appearance the granules within adjacent cells (Figs. 28 and 30).

The cytoplasmic matrix is apparently lost and assumes a pseudo-vacuolated appearance. A few irregular cisternae of RSER and clusters of ribosomes are scattered throughout the cytoplasmic matrix. One or two small mitochondria are also present. The nuclei in these cells are located in the basal part of the cell and are often deeply indented.

(6) The Enterochromaffin Cell

Of the cell types in the gastric mucosa the enterochromaffin cells are smallest and least numerous. They are situated mainly in the basal part of the gastric gland where they are isolated among other epithelial cells. They can be distinguished from other cells by demonstrating the presence of 5-hydroxytryptamine using the technique of Falk, Hillarp, Thieme and Torp (1962) (Section V of this study).

In electron micrographs, these cells are oval or pyramidal with their apices pointing towards, but rarely reaching, the lumen. Most of them are wedged between the basal halves of adjacent gland cells. A few cells have thin prolongations extending to the gland lumen into which elongated microvilli project (Fig. 35). Their lateral borders are relatively straight and occasional desmosomes are present.

The enterochromaffin cells contain granules which are located mainly in the basal part of the cell (Fig. 35). These granules are electron-dense, round, oval or elliptical and measure 0.2 - 0.3 u in diameter (Fig. 32). Each is enveloped by a trilaminar membrane which occasionally has a loose fitting appearance. The number of granules present tends to vary from cell to cell; in some the cytoplasm is packed with granules while in others separate and small groups of granules are scattered in the cytoplasmic matrix.

A few elements of RSER and some free ribosomes are present in the cytoplasmic matrix. Mitochondria are small and usually spherical. The golgi complex is of moderate proportions and consists of parallel cisternae with some dilated vacuoles and a few vesicles (Fig. 32).

Pylorus

(1) The Surface Mucous Cell

These cells are identical in structure to those found in the fundus. They cover the luminal surface of the pylorus and line the deep gastric pits which open into glands lined by mucus-secreting cells (Fig. 9).

(2) The Pyloric Gland Cell

Ultrastructurally these cells are mainly columnar and often assume a conical shape (Figs. 33 and 34). A few apical microvilli are present and the lateral plasmalemmata are usually straight with only an occasional interdigitation. The apical cytoplasm is packed with membrane-bound granules of variable size and electron density. The granules measure up to 1.5 u although many smaller granules measuring about 0.2 u are also present (Figs. 33 and 34). The electron-density of the granules varies from moderate to the marked degree of zymogen granules. Granules are also located in a paranuclear position lateral and basal to the nucleus. A well-developed golgi complex of several stacks of cisternae with dilated vacuoles and small vesicles is usually present in a paranuclear position (Fig. 34).

A few irregular, often branching and dilated, cisternae of RSER are in the basal part of the cell and clusters of ribosomes are scattered throughout the cytoplasmic matrix. Mitochondria are usually oval although sometimes they are markedly elongated.

The nuclei of these cells are usually round or oval and when oval the long axis is frequently parallel to the basement membrane.

Enterochromaffin Cell and Parietal Cell

These cells are identical to those in the fundus (Fig. 35).

DISCUSSION

Previous workers studying the fine structure of gastric epithelial cells have employed osmium tetroxide or potassium permanganate, fixatives of restricted use in preserving protein structures in cells, e.g. the granules in zymogen cells, known to contain the protein pepsinogen, showed complete or partial loss of contents. In this study the use of glutaraldehyde gave superior protein fixation and allowed more meaningful interpretation of results.

All epithelial cells in the bovine abomasum and in the small intestine are joined by a tripartite junctional complex similar in structure to that described in the rat and guinea pig by Farquhar and Palade (1963). The purpose of this complex is not fully understood but it is thought to be important in preserving cell apposition and structure; there is evidence to suggest that the zonula occludens is a site of maximum constraint against macromolecules moving into and out of the epithelial sheet (Section VI).

In the fundus there are 2 mucus-secreting cells, the surface mucous cell and the mucous neck cell. Histologically, these cells are recognised by their position and appearance. However, there has been some controversy as to whether they can be distinguished ultrastructurally. In this study they appear as two distinct types. The main distinguishing feature is the morphology of the granules. In the mucous neck cells the granules are larger, more uniformly

spherical and exhibit a patchy electron density. Unlike surface mucous cell their granules are frequently located in the perinuclear or the basal cytoplasm. Some mitochondria in mucous neck cells are markedly elongated, a feature not observed in surface mucous cells. In addition, the lateral plasmalemmata of the mucous neck cells usually contain fewer interdigitations. The function of these cells is not precisely understood. It is generally considered that the mucus secreted by these cells has a protective role against the proteolytic gastric juice, preventing autodigestion and also protects the surface mucosa from abrasion by ingesta.

The bovine parietal cell is characterised by the presence of intracellular canaliculi which are lined by numerous microvilli with only a few vesicles in the adjacent cytoplasm. The cytoplasm is packed with large mitochondria with numerous transverse cristae mitochondriales. The parietal cell is responsible for HCl production and the maintenance of an acid medium in the bovine abomasum (pH 2.4 $\pm$ 0.1, Anderson et al. (1965)). Continuous basal secretion of gastric juice occurs in the bovine (Hill, 1961; Hirschowitz, 1967). Studies have been made on the structural changes found in parietal cells of species in which gastric secretion is intermittent (Vial and Orrego, 1960, working with the cat; Sedar and Friedman, 1961, in the dog; Helander, 1962, in the mouse; Sedar, 1964, in the dog; Rohrer, Scott, Joel and Wolf, 1965, in the human; Orrego, Navia and Vial, 1966, in the toad). Tissues were examined after a period of inanition, i.e. cell inactivity and after stimulation of gastric secretion by a variety of techniques. It was found that after stimulation the intracellular canaliculi become more extensive and the microvilli more numerous; the number of vesicles

in the adjacent cytoplasm is reduced. Most bovine parietal cells show similar ultrastructural characteristics; this probably indicates that they are active cells. The above workers concluded that acid secretion is directly related to the surface area of the canaliculi and that the numerous vesicles in the cytoplasm of inactive cells act as a reserve of cell membrane and are incorporated into the surface during the process of secretion.

Zymogen cells are mainly located at the base of gastric glands. Apically-situated membrane-bound electron-dense granules and extensive areas of RSER are the main structural features of these cells. The pepsinogen in their granules is secreted into the lumen of the gastric gland where it is activated in the acid medium to the proteolytic enzyme pepsin.

It is considered that the cell type recognised by its fibrils and pseudo-vacuolated cytoplasm is a discharged or degenerated secretory cell; these cells are found scattered among surface mucous cells, mucous neck cells and zymogen cells.

Enterochromaffin cells are characterised by small membrane-bound granules located in the basal part of the cell; these granules contain 5-hydroxytryptamine (Falck, Nystedt, Rosengren and Stenflo, 1964). The functional significance of the 5-hydroxytryptamine and of these cells is not known.

The gland cell in the pylorus is structurally similar to the mucous neck cell. In addition to the large granules of variable electron density similar to those in mucous neck cells, large and small electron-dense granules are present. It is possible that the electron-dense granules contain pepsinogen as

they are similar in size and morphology to those in zymogen cells; in the dog and in man, at least, pepsinogen is secreted by the pyloric glands (Grossman and Mark , 1960; Turner, Miller and Segal, 1967). On the other hand, gastrin which is found in high concentrations in the pyloric mucosa of many species (Blair, 1966) may be present in these granules.

SECTION III

THE DISEASE PROCESS

INTRODUCTION

In the General Introduction, published information on bovine ostertagiasis was reviewed and a hypothesis of the pathogenesis was formulated. The main study of the sequential development of abomasal lesions in calves infected with O. ostertagi was made by Ritchie et al. (1966) using a single inoculum of 100,000 larvae. It was found that this was too low to produce a syndrome analogous to the field disease. Anderson et al. (1966) showed that in order to produce this, infecting doses of over 200,000 larvae were required.

In the present experiment a single inoculum of 300,000 O. ostertagi larvae was used, i.e. a dose large enough to produce clinical signs and severe abomasal lesions. The object was to study with the light and electron microscopes, the sequential development of abomasal lesions at different stages of the life cycle of O. ostertagi and attempt to relate these to clinical and biochemical findings.

In addition, it was considered that bovine ostertagiasis might afford an opportunity to study the mode of differentiation of gastric epithelial cells as little is known about this field. It has been shown in colchicine studies that surface mucous cells and mucous neck cells arise in the lower pit - upper gland region and that there is a rapid turnover of these cells (Stevens and Leblond, 1953). Mitoses are rare in zymogen and parietal cells and their mode of differentiation is controversial. Using 48/80 to stimulate mitotic activity and Thymidine-H^3 as a marker, Hunt and Hunt (1962) showed that parietal and zymogen cells were capable of dividing. In light microscope studies Townsend

(1961) and Hunt and Hunt (1962) concluded that parietal and zymogen cells arose from mucous neck cells. With the electron microscope Lawn (1960) and Corpron (1966) described a cell, the neck parietal cell, in the neck region of rat gastric gland, and considered it to be a developing parietal cell. Corpron (1966) found mucous granules in some of these cells and concluded that the neck parietal cells arose from immature surface mucous cells. In suckling and foetal rabbits, it has been shown that parietal cells develop from undifferentiated cells (Hayward, 1967a and 1967b).

EXPERIMENTAL DESIGN

Twenty-two Ayrshire male calves, reared parasite-free from birth, were given a single oral inoculum of 300,000 O. ostertagi larvae. At the time of inoculation (Day 0), the calves were ten weeks old. They were necropsied singly on days 4, 10, 17 and then daily until day 30, and thereafter at weekly intervals from day 35 to day 70.

OBSERVATIONS

A daily clinical examination was made of all calves. The five calves due to be necropsied from day 42 onwards were weighed thrice weekly and the quantity of concentrates consumed at each feed measured. Blood samples were also collected thrice weekly from these five calves and plasma pepsinogen and serum protein estimations were made.

Faecal examinations were collected daily and examined for consistency. Faecal egg counts were done on days 0 and 17 and thereafter daily until the end of the experiment.

At necropsy, the calves were stunned with a captive bolt and exsanguinated. The abomasum was removed intact as quickly as possible and opened along its greater curvature. Tissue was removed from the fundus, pylorus, small intestine and regional lymph nodes for electron microscopic and histological examination.

The pH of the abomasal contents was measured and a parasitological examination of the abomasal contents and mucosa was made.

RESULTS

The clinical and parasitological results have been described in detail by Armour (1967). A brief description is given of these because of their relevance to the present investigation.

CLINICAL OBSERVATIONS

The mean body weight of the group of five calves is shown in Graph 1; in addition, the onset and severity of diarrhoea and reduction of appetite for concentrates are recorded.

PARASITOLOGICAL OBSERVATIONS

Details of the numbers, sex ratios and stage of development of O. ostertagi present at necropsy are given in Table 2. A plot of the log number of O. ostertagi against time is shown in Graph 2. Regression analysis of this data showed that through days 17 - 35, there was an inverse linear, functional relationship between log worm numbers and time, i.e. - the loss of worms was exponential.

The mean faecal egg counts from day 18, i.e. when eggs first appeared in the faeces, are shown in Graph 3. The mean egg count increased to a maximum of 1,000 eggs per gram on day 24 and thereafter decreased to 0 by day 63.

BLOOD ANALYSIS

There were no significant alterations in serum protein values (Appendix 1, Tables 1 and 2).

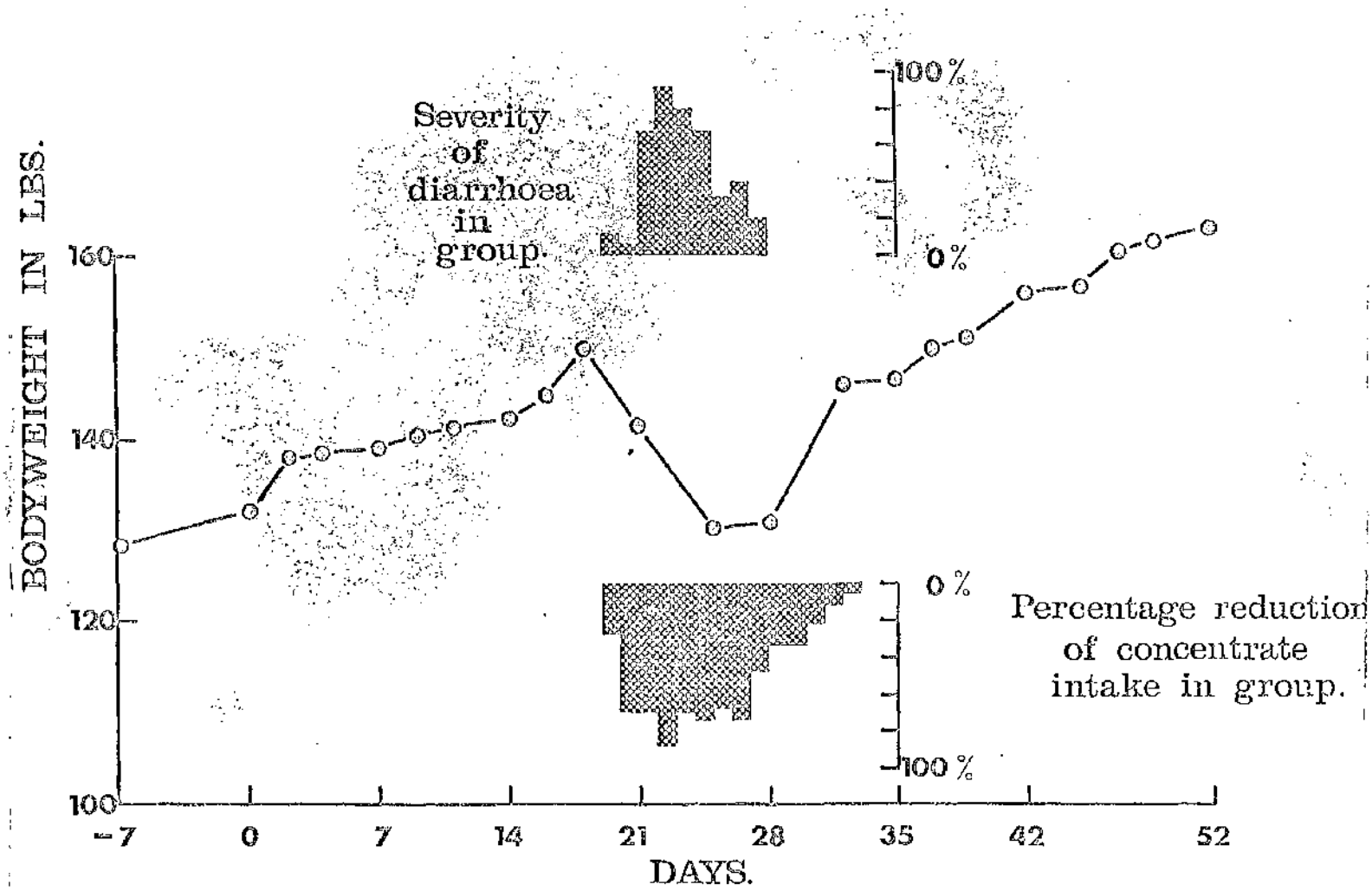

Graph 1. The mean bodyweights, classification of diarrhoea and reduction of concentrate in a group of 5 calves inoculated with 300,000 O. ostertagi larvae.

Table 2

Worm Counts at Necropsy of Calves

Given a Single Dose of 300,000 O. ostertagi Larvae

Day Killed	No. of Adult Worms	No. of Developing Stages i.e. late 4th, 4th moult & 5th larval stages	No. of Early 4th Larval Stages	Percentage of Inoculum Established	Sex Ratio M:F
4	-	-	50,000	17	...
10	-	34,000	-	11	...
17	12,200	56,800	-	23	1:1
18	5,600	38,700	-	15	1:1
19	36,600	40,000	-	26	1:1
20	33,600	8,000	-	14	1:1
21	28,000	24,200	-	18	1:1
22	50,000	10,500	-	20	1:1
23	24,000	1,800	-	9	2:1
24	33,800	2,200	-	12	3:2
25	12,600	-	100	4	9:4
26	10,000	500	-	4	5:4
27	9,600	-	-	3	3:2
28	21,000	900	-	7	2:1
29	15,000	200	-	5	2:1
30	28,000	200	-	9	3:1
35	10,600	-	200	4	4:1
42	10,000	-	-	3	7:3
49	2,000	-	200	1	5:4
56	6,700	-	-	3	5:1
63	200	-	-	<1	0:1*
70	600	-	-	<1	1:7

* No Male Worms Found

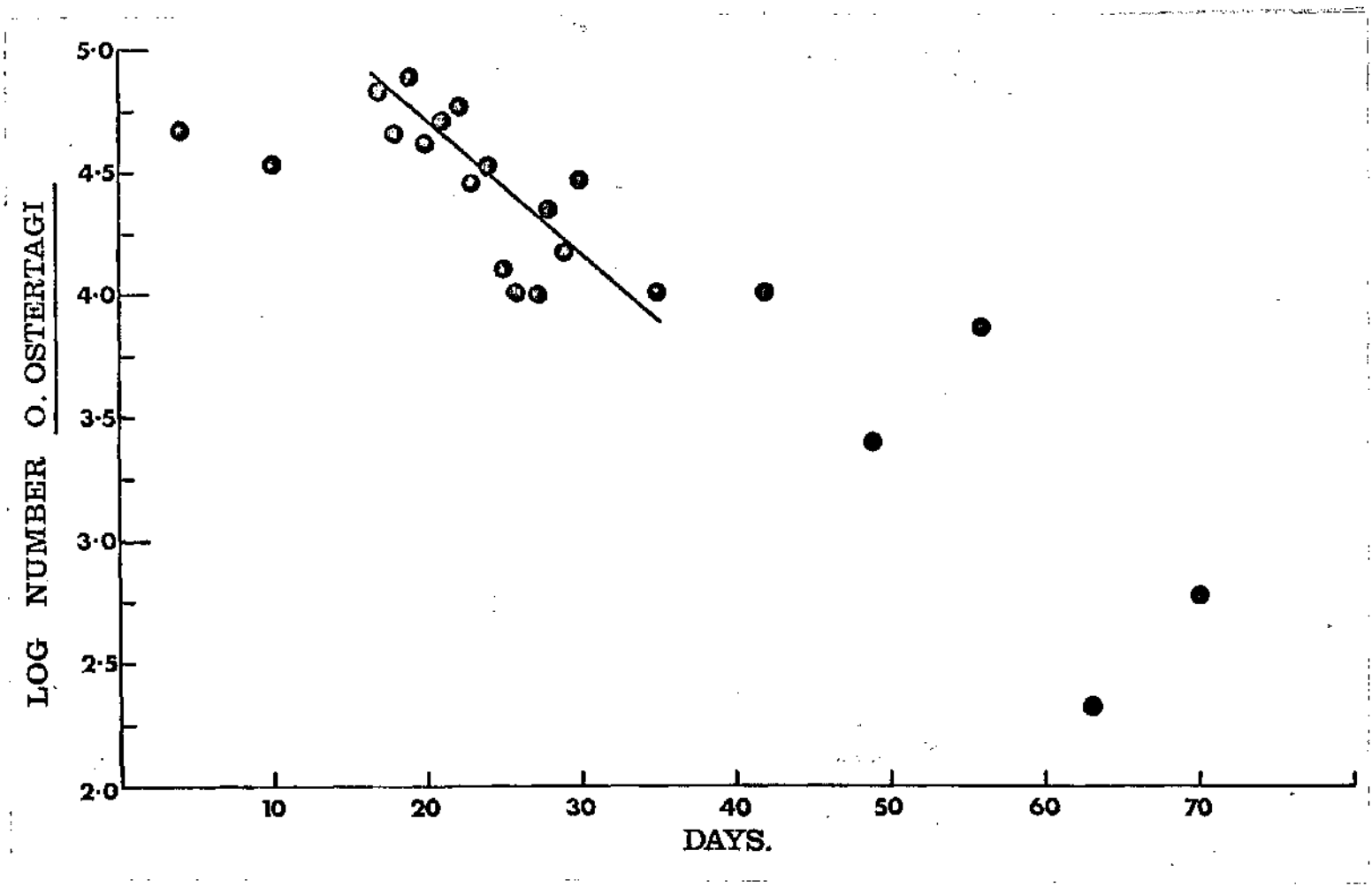

Graph 2. Logarithm of worm burden found at different times after infection. The slope of the line between days 17 and 35 (b) is 1 in 20. Each calf was inoculated on day 0 with 300,000 O. ostertagi larvae.

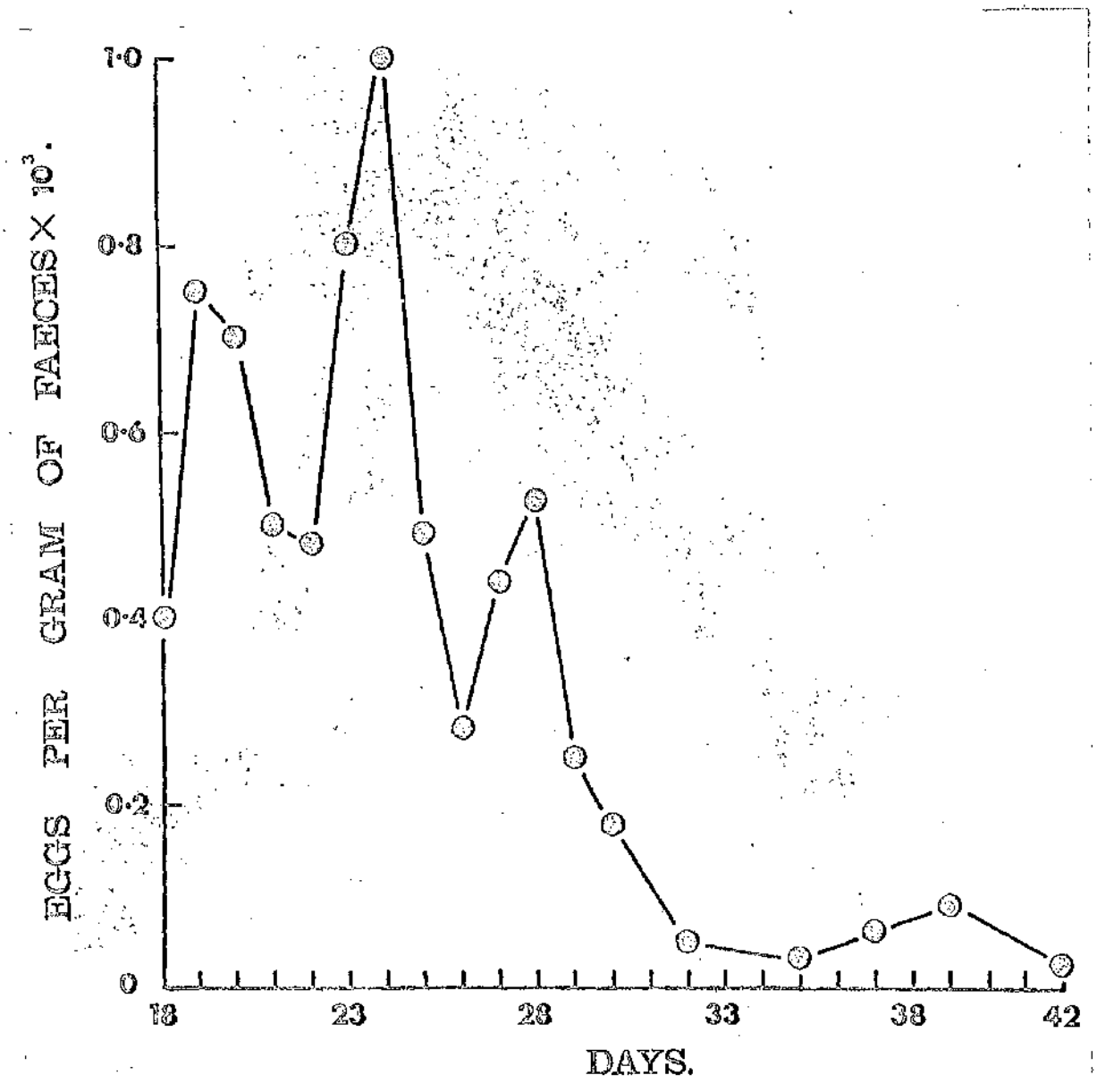

Graph 3. Mean faecal egg count for group of 5 calves inoculated with 300,000 O. ostertagi larvae on day 0.

There were marked changes in plasma pepsinogen levels (Graph 4). A slight increase occurred by day 4 (1,100 millunits of tyrosine) and this became elevated to 2,200 milliunits of tyrosine by day 14. During the next few days the level increased sharply to a maximum mean value of 7,400 milliunits of tyrosine on day 23. Details of individual plasma pepsinogen results are given in Appendix 1, Table 3.

ABOMASAL pH

The pH of the abomasal contents in calves necropsied up to day 21 was not significantly altered. Thereafter, a marked increase in pH occurred and this was maintained in calves necropsied till day 30. From day 35, the pH gradually returned to normal (Table 3).

PATHOLOGICAL FINDINGS

The disease process was divided into three phases.

Phase 1 - the lesion produced by the parasite within the mucosa, termed 'the primary nodule' by Jarrett (1966).

Phase 2 - the lesion which results from emergence of the adult parasite from within the gastric mucosa, termed 'the secondary nodule' by Jarrett (1966) (> day 17).

Phase 3 - the structure of the gastric mucosa after the loss of the adult worm population (> day 35).

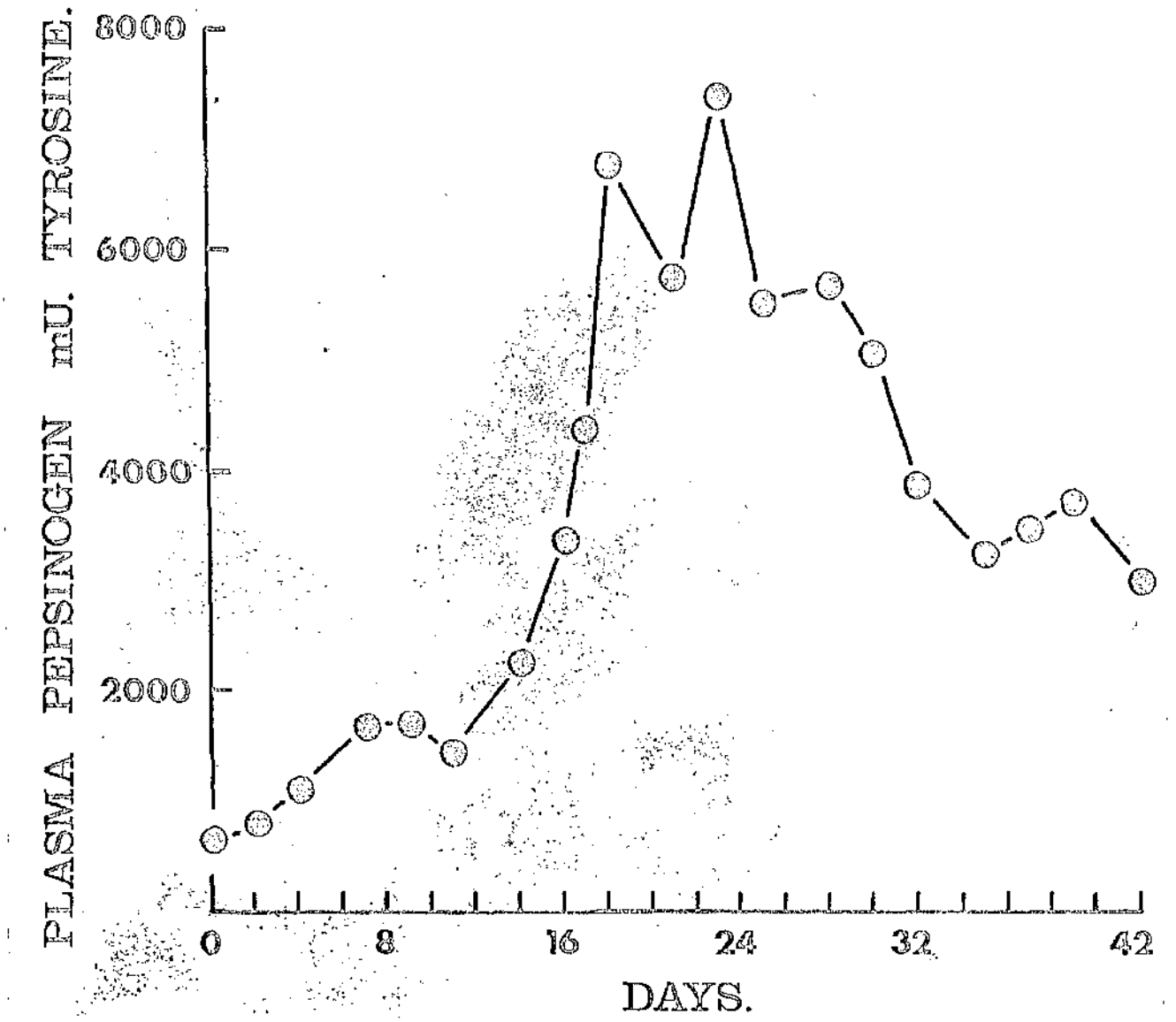

Graph 4. Mean plasma pepsinogen from group of 5 calves inoculated with 300,000 O. ostertagi larvae on day 0.

Table 3

Mean pH of Abomasal Contents from Calves Necropsied during Three Different Periods of Infection Following Inoculation with 300,000 *O. ostertagi* Larvae.

	Day of Necropsy		
	4 - 20	21 - 30	35 - 70
No. of calves	6	10	6
Mean pH	3.27 ± s.e. 0.39	6.42 ± s.e. 0.32	3.56 ± s.e. 0.21

s.e. = standard error

Phase 1 - The Development of the Primary Nodule

Gross and histopathological findings

Four days after infection, lesions could be seen in all parts of the abomasum, the largest number being located in the fold areas of the fundus. Small white nodules about 1 - 2 mms. in diameter were raised above the surface of the mucosa; in some areas, the nodules had become conjoined, giving the mucosa a granular appearance. At the centre of the nodule was the gland moderately dilated by the presence of a larva, giving an umbilicated appearance which was to become marked in longer-standing infections (Fig. 36a). Histologically, the epithelium of the parasitised gland had lost the clarity of delineation of mucous, parietal and zymogen layers; the lining epithelium was mainly of a low cuboidal nature and was undifferentiated and rapidly dividing (Fig. 36b). The eosinophilic staining of some cells indicated their formal parietal cell identity. Where the larva did not touch the epithelium, it was often hyperplastic and was differentiating into mucous cells.

In the lamina propria in the vicinity of parasitised glands, a few eosinophils and neutrophils were present as were accumulations of lymphoid cells.

By day 10 of the infection, the glands had basically similar appearances, the pattern being one of larval growth, lengthening of the gland, complete conversion of the lining cells of the gland to mucous cell types, varying from cuboidal to columnar (Fig. 37). The surrounding glands were structurally normal although some glands had become slightly dilated and were lined by stretched, flattened epithelium; this occurred particularly in the neck-isthmus region.

Granulocyte infiltration was evident, but not marked in the lamina propria. In addition, focal accumulations of plasma cells and lymphoid cells were occasionally found. The number of mast cells had increased. Moderate stromal oedema and congestion occurred around the upper part of the gastric glands and the pits.

Grossly, the nodules had increased in size, ranging from 2 - 3 mm. They were distinctly raised and had dark, translucent centres produced by the contained larvae. They were particularly numerous in the fundus of the abomasum, being confluent in some areas. Some fold oedema and patches of congestion were obvious. The abomasal lymph nodes were enlarged and contained numerous follicles with active germ centres.

By day 17, just prior to emergence, the nodules had become distinctly raised and umbilicated over the parasitised glands (Fig. 38). They were approximately 3 mms. in diameter and many areas had started to coalesce.

The parasitised gland was now considerably dilated by the mature adult parasite which often measured up to 10 mm. The gland was lined by mucus-secreting cells whose height varied from cuboidal to columnar (Fig. 39 a and b). The surrounding gland epithelium could still be differentiated into several layers. Some glands in the immediate vicinity were dilated and lined by stretched epithelial cells the structural features of which could still be recognised; it was in this area, during the ensuing days, that the major structural changes were found.

By this stage, the granulocyte and mononuclear cell response was much more intense and the number of mast cells had increased markedly.

Ultrastructural Features of the Primary Nodule

As described histologically, the consequence of the presence of a parasite within the gastric gland was the loss of the functional gastric epithelial cells, namely mucous neck, parietal and zymogen cells. Initially, these were replaced by low cuboidal, rapidly dividing cells, which, by day 10, had developed into mucus-secreting cells. The height of these cells depended on their relationship to the parasite. Where the parasite was in close apposition to the gland, the cells tended to be low and flattened with the long axis of their nuclei parallel or tangential to the basement membrane. Elsewhere, the cells were taller and often arranged in a pseudostratified fashion.

The apical cytoplasm of the low cuboidal cells (Figs. 40, 41 and 42) had only a few stumpy, flattened microvilli, while their lateral plasmalemmata were tangential to the basement membrane. Interdigitations of the lateral plasmalemmata occurred at all the levels, but were more elaborate near the base of the cell. Even at day 4, a few membrane-bound granules of moderate electron density were found in the apical cytoplasm. These were round or oval and measured up to 1 u in diameter. A fairly well-developed golgi complex was usually in a paranuclear position. It consisted of parallel stacks of cisternae with dilated vacuoles and some associated vesicles. The cytoplasmic matrix was rich in ribosomes. A few irregular cisternae of RSER were present mainly in the basal cytoplasm. Scattered throughout the cytoplasm were mitochondria which were round, oval or occasionally elongated and contained a moderately well-developed internal membrane system.

By day 17, nearly all cells were columnar and mucus-secreting (Fig. 43). The apical cytoplasm of these cells showed short, stumpy microvilli. Their lateral plasmalemmata exhibited marked cytoplasmic interdigitations, particularly in the basal part of the cell. The apical cytoplasm contained a variable number of membrane-bound granules with a range of electron-density. These granules were oval or discoid, measuring up to 1.2 u in diameter although most granules were less than 1 u; they were positive for mucin when stained with periodic acid-Schiff and Southgate's mucicarmine. In most cells, a prominent golgi complex was found in a paranuclear position and showed similar features to that described in low cuboidal cells. The nuclei were elongated or oval with their long axis perpendicular to the basement membrane; they were frequently indented and nucleoli were occasionally present. These cells were structurally similar to surface mucous cells (Section II).

The tripartite junctional complexes between cells lining the parasitised glands were invariably intact, although the zonula occludens was sometimes shortened.

The cells in the glands surrounding the parasitised gland showed the ultrastructural features of normal functional cells, although in some dilated glands the cells were rather stretched and flattened.

The Functional Consequences of the Primary Nodule

Up to day 17, the plasma pepsinogen levels rose gradually (Graph 4). However, the pH of the abomasal contents did not alter significantly (Table 3). No diarrhoea was observed up to this stage, and the animals continued to eat and gain weight normally (Graph 1).

Phase 2 - The Development of the Secondary Nodule

Gross and Histopathological Findings

About the time the parasites reached maturity and started to emerge a striking change took place in the surrounding glands and this was reflected in equally striking clinical and biochemical changes. Between days 17 and 30 of infection, there was a considerable overlap of daily structural changes. Therefore, the description of the development of the secondary nodule is not dealt with on a daily basis. Between day 17 and 25, adult worms were found emerging or had emerged from the gastric glands (Figs. 44a and b, 45, 46). Tall, fully differentiated mucous cells now lined the parasitised glands (Fig. 47a); the immediate surrounding glands were stretched and sometimes dilated and their epithelium was flattened, low cuboidal and non-functional (Figs. 46, 47 a and b). The next few glands were still lined by differentiated gastric epithelial cells (Figs. 47 a and b). In the ensuing days, these changes became more widespread and most of the glands surrounding the parasitised gland, (after emergence of the parasite) were lined by low cuboidal, rapidly dividing cells which showed no functional differentiation (Fig. 48). It was the rapid division of these cells, particularly in the lower pit, upper gland areas, which resulted in the marked hyperplasia and thickening of the gastric mucosa which occurred during Phase 2.

Where the nodules were situated close together, these lesions overlapped, so that the functional gastric mucosa was lost over a considerable area (Fig. 49).

However, in these areas, parietal cells could still be identified (Fig. 50).

The dose of 300,000 O. ostertagi was sufficiently high to produce considerable coalescence of the secondary nodules (Fig. 51). The individual nodules were raised with a visible central orifice surrounded by an elevated area of hyperplastic cells (Fig. 52). These individual lesions coalesced to form an intensely hyperplastic mucosa; to the naked eye, this had a characteristic morocco-leather or crazy-paving appearance (Fig. 1).

A lesion which followed emergence was necrosis and sloughing of the surface mucous cells. Here the worm lay apposed to the hyperplastic mucosa, embedded in an exudate of protein, polymorphs and clumps of bacteria (Fig. 53). A striking feature in the top layer of the mucosa was the accumulation of large aggregates of plasma cells (Fig. 54). Grossly, this lesion appeared as irregular grey-white plaques of diphtheresis (Fig. 55).

Oedema, particularly of the folds of the abomasum, was a common, but not constant finding. Occasionally, the surface mucous cells were stretched and flattened by the presence of oedema (Fig. 56); in the adjacent lamina propria, lymphatics became markedly dilated. The gastric mucosa was frequently congested and on occasions haemorrhagic (Fig. 57).

Following emergence, the cellular reaction in the lamina propria became marked and had many striking features. The high mast cell content in the mucosa found at day 17, was maintained during phase 2, and from day 25 the number of globule leukocytes within the epithelium gradually increased. There was an increase in the number of eosinophils; these were found in blood

vessels in the lamina propria and migrating through epithelia to the gland lumen. The number of polymorphonuclear leukocytes also increased. Occasionally, post-parasitised glands were distended with pus (Fig. 58); grossly, these lesions were recognised by cream-white cores at the centre of the nodule. As described earlier, the plasma cell reaction, especially in the surface layer of the mucosa, was intense. In the lower mucosa and in the submucosa, lymphoid nodules, many with germ centres, were frequently found encircling small blood vessels, particularly in the vicinity of parasitised glands (Fig. 59). Occasionally, parasites had penetrated the lining epithelium of the gland, resulting in giant cell or eosinophil granulomata around the aberrant parasite (Fig. 60).

Following emergence, the abomasal lymph nodes became reactive; in some cases there was a marked, superimposed purulent lymphadenitis.

Ultrastructural Features of the Secondary Nodule

The cells lining glands which formerly contained parasites had developed into columnar mucous cells (Fig. 61). They exhibited structural features similar to surface mucous cells although they usually contained fewer granules. These cells were often piled on top of one another in a pseudostratified fashion (Fig. 62). Scattered among mucous cells were a number of undifferentiated cells (Fig. 62); these were devoid of any of the structural features of mature end cells. Their golgi complexes were extensive, often encircling the nucleus. Mitochondria were fairly numerous and some had well-developed internal structures. The cytoplasm and nucleoplasm was of low electron density. RSER was sparse while clusters of ribosomes were fairly numerous.

Electron-dense material was occasionally found between cells lining parasitised glands (Figs. 61 and 62). Examination of the junctional complexes between these cells showed that in many instances the zonula occludens was shortened and the intercellular spaces were dilated by electron-dense material (Fig. 63).

The dilated and stretched glands in the vicinity of the parasitised glands were lined by flattened mucous neck cells (Fig. 64) and zymogen cells (Fig. 65). An occasional parietal cell was also stretched, but in most cases they maintained their oval or triangular outline. Many zymogen cells contained few or no granules; those that were present were smaller than normal (Fig. 66). In the stretched parietal cells, the intercellular canaliculi were greatly dilated and were exposed to the lumen of the gland (Fig. 67). In these glands, the cells were sometimes pulled completely apart or junctional complexes were shortened and obviously under considerable pressure. Some cells were held together only by a shortened zonula occludens, others only by a desmosome (these lesions are fully illustrated in Section VI).

The cells lining these glands were soon replaced by rapidly dividing undifferentiated cells. These cells lacked the structural features of any gastric epithelial cells, e.g. granules, extensive RSER, intracellular canaliculi (Figs. 68 and 69). They had a few apical microvilli, moderate interdigitations of the lateral plasmalemmata, while the basal plasmalemmata were straight. Their nuclei were mainly round, and in some, nucleoli were present. The nucleoplasm and the cytoplasmic matrixwere of low electron density. The golgi complex was located in a paranuclear position and was well-developed. It consisted of stacks of

parallel cisternae, many of which were dilated to form vacuoles and of numerous associated vesicles. Cisternae of RSER were present throughout the cytoplasm; they were irregular in outline and were dilated by the presence of electron-dense material. Clusters of ribosomes were scattered throughout the cytoplasm. Mitochondria were prominent; they were large, round, oval or occasionally elongated and usually had a well-developed internal structure. In some cells, a few apical electron-dense granules were present. Invariably, electron-dense material lay between these cells (Figs. 68 and 69). Examination of the junctional complexes betwee them revealed that in a number of instances, there was separation of the plasma-lemmata forming the zonula occludens and electron-dense material lay between (Fig. 70).

Although large areas of the mucosa consisted mainly of undifferentiated cells, differentiated cells were still present in many glands; these cells showed distinct changes in their structural features. In parietal cells, intracellular canaliculi were either absent (Fig. 71) or greatly reduced in extent. In most cells, the cytoplasm had assumed a degenerate pseudo-vacuolated appearance (Fig. 71). When canaliculi were present, they were greatly dilated and were lined by only a few microvilli (Figs. 72 and 73.cf. Fig 22, Section II). The adjacent cytoplasm contained numerous mitochondria, but was devoid of other organelles, such as vesicles.

Zymogen cells showed a marked reduction in the number and size of pepsinogen granules present (Fig. 74). The fibril-containing cells described in Section II were observed with increased frequency. No structural changes were found in enterochromaffin cells.

In some areas, the outline of differentiated gastric gland cells and surface mucous cells was delineated by electron-dense material dilating the intercellular space and lying between the lateral plasmalemmata of adjacent cells (Fig. 75).

After emergence, severe submucosal oedema became a common, but not a constant finding. Ultrastructural examination of these areas showed marked dilatation of the intercellular spaces between the superficial surface mucous cells and often breakdown of their junctional complexes. Material of moderate electron density was present in the dilated intercellular spaces (Figs. 76 and 77).

In the lamina propria, striking changes took place in the micro-circulation. The vessels became packed with red blood cells (Figs. 78 and 79) eosinophil leukocytes (Fig. 80), polymorphonuclear leukocytes (Fig. 81) and lymphocytes (Fig. 80); these cells were found migrating across the walls of post-capillary venules. In the post-capillary venules, many zonulae occludentes were separated (Fig. 82) and lymphatics became greatly distended and their cell junctions widely separated (Fig. 83). Junctional complexes between endothelial cells lining capillaries remained intact (Figs. 84 and 85).

Functional Consequences of the Development of the Secondary Nodule

Biochemically, there was a marked elevation of the pH of the abomasal fluid (Table 3) and an increase in plasma pepsinogen levels (Graph 4). By day 22, the calves had developed severe diarrhoea and were partially anorexic. There was a resultant decline in weight gain (Graph 1).

3. Phase 3

Gross and Histopathological Findings

With the gradual loss of the adult worm population, lesions regressed. There was a gradual return of the parietal and zymogen cell mass. By day 63 and 70, the gastric mucosa had almost completely returned to normal, although the glands which had formerly contained larvae, were still obvious by their mucous cell lining (Fig. 85).

Grossly, the nodules gradually disappeared and the former areas of necrosis were recognised by thumb-print lesions in which the sloughed mucosa was being replaced by rapidly-dividing epithelial cells (Fig. 87).

The number of cells found in the lamina propria gradually decreased although globule leukocytes within epithelium increased.

Ultrastructural Features of the Recovery Phase

With the expulsion of the adult worm burden, there was a gradual return to normal structure.

From day 28 of the infection, a number of incompletely differentiated cells was found in the gastric mucosa. These showed some of the structural features of the undifferentiated cells described in phase 2 and also some features of mature gastric epithelial cells.

A series of cells, considered to be immature surface mucous cells, was found (Figs. 88 and 75). Although similar to undifferentiated cells, these cells showed some increase in the density of the cytoplasmic matrix; more strands of RSER and ribosomes were present. In these cells the mitochondria were largely

confined to the basal cytoplasm. In the apical cytoplasm some granules were present; they were round, oval or discoid, always less than 1 u in diameter, and of variable electron density, i.e. similar to those found in mature surface mucous cells (Section II). Their lateral plasmalemmata were often elaborately interdigitated, particularly towards the base of the cell.

Cells showing many of the structural features of mucous neck cells were present in areas of undifferentiated epithelium (Figs. 89 and 90). These were recognised by the presence of a few apical granules; granules were also located lateral to the nucleus. The granules were round and measured up to 1.5 u; they contained patches of electron-dense material, i.e. similar to mature mucous neck cells (Section II). The golgi complex was well-developed. Elongated mitochondria, a feature of mucous neck cells, were often present. Irregular stacks of RSER were situated mainly in the basal cytoplasm. Their lateral plasmalemmata were commonly but not constantly straight. It was considered that these cells were differentiating mucous neck cells.

A series of cells, thought to be developing parietal cells was located in the isthmus - neck region of gastric glands. In these cells, intracellular canaliculi were present, but were less extensive and contained fewer microvilli than mature parietal cells; also mitochondria were not as numerous, nor was their internal structure as elaborate (Figs. 91 and 92). Membrane-bound granules of moderate electron-density, measuring up to 0.6 u in diameter were sometimes found (Fig. 91). In all cases interdigitation of the basal plasmalemmata occurred (Figs. 91, 93, 94 and 95); this is a constant feature of the mature parietal cell. Some cells, in which the intracellular canaliculi were poorly

developed (Figs. 94 and 95), contained mitochondria similar in size, morphology and numbers, to those in mature parietal cells. In these cells there was a fairly extensive golgi complex, not a feature of the mature parietal cell (Fig. 93).

Scattered among undifferentiated cells, were cells with few or no granules; when granules were present, they were electron-dense. They contained fairly extensive stacks of RSER located in the basal cytoplasm and clusters of ribosomes scattered throughout the cytoplasmic matrix (Fig. 96). These cells were mainly cuboidal, with a few stumpy, apical microvilli; the lateral plasmalemmata were straight, but occasionally were elaborately interdigitated. An extensive golgi complex was situated paranuclearly. The nucleus was basal and usually had a prominent nucleolus. It was considered that these cells were differentiating zymogen cells.

Cells were located in the basal part of the gastric gland. These were oval or pyramidal, and were mostly wedged between the basal half of adjacent gland cells. Their lateral plasmalemmata were occasionally interdigitated and desmosomes were found. In the cytoplasm, a few electron-dense, membrane-bound granules, up to 0.3 u in diameter were present (Fig. 97). A golgi complex of moderate proportions was located in a paranuclear position; it consisted of a few cisternae with some dilated vacuoles and a few vesicles. Centrioles were occasionally found in association with the golgi complex. The mitochondria were mainly small and oval, but were occasionally elongated. These cells showed many of the structural characteristics of enterochromaffin cells; it is likely that they were differentiating cells and their ability to divide was indicated by the presence of centrioles.

Functional Changes in Phase 3

Biochemically, the pH of the abomasal fluid (Table 3) and the plasma pepsinogen levels (Graph 4) gradually returned to normal. Diarrhoea stopped and the calves started to eat and gain weight.

Ultrastructural Studies on Cells in the Lamina Propria of the Bovine Abomasum in Ostertagiasis.

With the development of the secondary nodule, Phase 2, the cell reaction in the lamina propria of the gastric mucosa became marked. This presented an opportunity to study the fine structure of bovine immuno-inflammatory cell types.

Mononuclear Cells

Lymphoid Cells. These cells were scattered throughout the lamina propria but were most often found in follicles surrounding small vessels in the lower part of the mucosa (Fig. 59). They had a round nucleus with large clumps of chromatin surrounded by a rim of cytoplasm containing one or two mitochondria and clusters of ribosomes. In some cells centrioles were present (Fig. 98) and occasionally a few Auer bodies were found (Fig. 99). In lymphoid cell follicles a series of cells was identified which appeared to link small lymphocytes and immunoglobulin-producing cells (plasma cells); this was based on the amount of RSER present (Fig. 100).

Immunoglobulin-Producing Cells (Plasma Cells).

These cells became numerous and active after emergence, particularly in the superficial part of the mucosa (Figs. 54 and 101). The nucleus was eccentric and contained large patches of chromatin. The golgi complex was located in a paranuclear position and was well-developed; it consisted of numerous stacks of cisternae and many vesicles. An associated centriole was occasionally found. The main features of this cell type were numerous parallel

stacks of cisternae of RSER interspersed between which were oval or elongated mitochondria and an occasional lysosome (Fig. 102). As the cells produced more antibody, the cisternae of the RSER became distended (Fig. 103). Some cells showed uncoiling of their cisternae of RSER (Fig. 104), a possible mode of immunoglobulin discharge. Others showed enormously distended cisternae of undischarged immunoglobulins termed Russell body-containing cells (White, 1954), (Fig. 105).

Macrophages These cells were scattered throughout the lamina propria. They were large with abundant cytoplasm which was irregular in outline (Fig. 106). A moderately well-developed golgi complex was often found. Irregular stacks of RSER were scattered throughout the cytoplasm. Membrane-bound granules and vacuoles of various sizes were frequently present. Occasionally these cells were found in the vicinity of mast cells and it was considered that they were phagocytosing mast cell granules (Fig. 107). On the other hand, many of these membrane-bound vacuoles contained degenerating organelles such as mitochondria. Their nuclei were round or oval and often showed distinct margination or clumping of chromatin.

Fibroblasts These were mainly elongated cells which were often found in the vicinity of the basement membrane of epithelial cells (Fig. 108). Their main feature was an abundance of irregularly-dilated and orientated cisternae of RSER with numerous interspersed small oval or elongated mitochondria (Fig. 109). Their nuclei were round or oval with margination of the chromatin and an occasional nucleolus.

Granule Containing Cells

Eosinophil-leukocytes These cells were found in large numbers at all levels of the gastric mucosa especially during Phase 2. They were oval or elongated in outline and were characterised by numerous electron-dense membrane-bound granules. These granules were round or oval, pear-shaped, or occasionally angular, measuring up to 1 u in diameter (Figs. 110 and 111). Central bars, a feature of eosinophil granules in many species (Hudson, 1967 and Bessis, 1964) including sheep (Figs. 112, 113, 114 and 115), were not found after either glutaraldehyde or osmium tetroxide fixation. Golgi complexes of moderate extent were usually located in a paranuclear position, often with an associated centriole. Other organelles were fairly scant. Their nuclei assumed a reniform, bilobed, or occasionally trilobed, shape and contained large amounts of chromatin.

Polymorphonuclear leukocytes These cells were scattered throughout the lamina propria, but were particularly numerous in areas of superficial diphtheresis (Fig. 53) or gastric gland abscesses (Fig. 58). The cells were oval or elongated in outline and their cytoplasm was packed with electron-dense, membrane-bound granules, measuring up to 0.5 u in diameter. These granules assumed a variety of shapes, being round, oval or elongated (Figs. 116 and 117). Their golgi complex was moderately well-developed and was located in a paranuclear position with an occasional associated centriole. Other features of the cytoplasm were a few irregular cisternae of RSER and electron-dense particles of the nature of glycogen.

Mast Cells and Globule Leukocytes In the course of this experiment there was a marked increase in the numbers of these cells. GLs were located mainly within epithelium and it is shown in Section V that they are derived from subepithelial mast cells. The structural features, the cytochemical characteristics and the significance of mast cells and globule leukocytes are discussed in Section V.

All cell types described above, apart from fibroblasts, were found at some time within the epithelium of the gastric mucosa.

DISCUSSION

Functional Consequences of Bovine Ostertagiasis

A single inoculum of 300,000 O. ostertagi larvae proved to be sufficient to give severe clinical signs and extensive pathological changes in the abomasum. These occurred about the time the parasite reached maturity and emerged from the gastric glands. The main pathogenic effect of the parasite was to produce a reduction in the functional gastric gland mass responsible for the production of the highly acidic proteolytic gastric juice. The biochemical consequences were elevation of pH of abomasal fluid due to reduction in the functional parietal cell mass and diminution in pepsin activity (Jennings et al., 1966). As the peptic activity is negligible above pH 5 (Piper and Fenton, 1965), a serious impairment of digestion must occur, hence the animals become anorexic and start to lose weight. The cause of diarrhoea was not clear, but its course appeared to follow

closely the elevated pH of the abomasal fluid; it has also been observed that during Phase 2 there is an increase in the number of viable bacteria present in the abomasal fluid (Jennings et al., 1966).

Structural Changes Associated with the Loss of Gastric Function

Although the gastric gland mass was largely replaced by rapidly-dividing undifferentiated cells, many parietal cells were still present. Their fine structural appearance was suggestive of a state of reduced functional activity. The cytoplasm of many had a pseudovacuolated and degenerate appearance and the intracellular canaliculi when present were reduced in extent; although dilated, the canaliculi were lined by only a few microvilli, i.e., their surface area was diminished. It is known that the amount of acid produced by parietal cells is directly related to the surface area of the intracellular canaliculi (Section II). The structural appearance of the bovine parietal cell in a state of reduced activity bore a striking resemblance to that described by Vial and Orrego (1963) who examined the ultrastructure of the parietal cell of the rat after depressing acid secretion with 2, 4-dinitrophenol and with iodoacetate. It is possible that the adult O. ostertagi parasite secrete chemicals of a similar nature, perhaps acting as enzyme inhibitors. On the other hand, during this phase, a large number of immunoglobulin-producing cells appear (Fig. 101) suggesting the possibility of an immunological reaction.

Zymogen cells showed ultrastructural features suggestive of reduced pepsinogen production; the number of pepsinogen granules present in most cells was greatly reduced in size and in number. It is likely that most of the pepsinogen which was secreted was not activated in the alkaline conditions found

in the abomasum in Phase 2.

Structural Changes Possibly Associated with Increased Permeability of Bowel Wall to Macromolecules (vide Section VI)

Following emergence, it was found that in certain areas, the outline of epithelial cells was delineated by electron-dense material. Examination of the zonula occludens between such cells showed that they were shortened or their plasmalemmata had become separated. It was estimated that this occurred most commonly between rapidly-dividing, undifferentiated cells. This observation may be biased by the fact that these were the main cell types in the hyperplastic mucosa after emergence. The integrity of the mucosa was also breached in dilated glands found in the vicinity of parasitised glands; the lining epithelium, which was stretched and flattened, was often completely pulled apart. In areas of severe oedema, there was marked dilatation of the intercellular spaces between surface mucous cells; the junctional complexes between some of these cells were separated. There is considerable structural and physiological evidence to suggest that the breakdown of zonulae occludentes allows the leakage of macromolecules into and out of the mucosa. It was considered mainly on the basis of its electron density, that the material found between cells was protein, possibly plasma proteins leaking out of the mucosa or non-activated pepsinogen leaking through the mucosa into the circulation and giving rise to the elevated plasma pepsinogen levels recorded during Phase 2 (Graph 4).

A number of changes occurred in the microcirculation during Phase 2. The zonulae or maculae occludentes joining endothelial cells in post-capillary venules

became separated. Mast cells, known to contain the vasoactive amine 5-hydroxytryptamine (Section V) were often located in the vicinity of these vessels. Lymphatic channels became greatly distended. These changes probably indicate an increased permeability of the post-capillary venules and a leakage of plasma protein into the lamina propria (Majno, Palade and Schoeofl, 1961; Movat and Fernando, 1964; Cotran, 1967 and Karnovsky, 1967).

Biochemical results similar to those described above have been reported in a number of parasitic infections in a variety of species. Elevation of the pH of gastric fluid has been recorded in sheep with Ostertagia circumcincta (Armour, Jarrett and Jennings, 1966) and with H. contortus (Christie, Brambell and Mapes, 1967) and in pigs with Hyostrongylus rubidus (Davidson, Murray and Sutherland, 1967). Raised plasma pepsinogen levels have been found in sheep infected with O. circumcincta (Armour et al., 1966). Although hypoalbuminaemia was not found in experimental Type I ostertagiasis, it occurs in Type II ostertagiasis and a number of other parasitic conditions (Section VI, Table 5).

Differentiation of Gastric Epithelial Cells

Following emergence of adult O. ostertagi parasites, the gastric mucosa became lined largely by undifferentiated cells. It was thought probable that these represented stem cells. They showed none of the structural features of mature gastric epithelial cells, namely granules, extensive RSER or intracellular canaliculi. Their cytoplasmic matrix was largely devoid of organelles apart from an extensive golgi complex and some mitochondria. Similar cell types were located in areas of cell hyperplasia in parasitised glands.

From the latter half of Phase 2 onwards a series of cells which showed structural evidence of differentiation was found in the gastric mucosa.

It would appear that surface mucous cells differentiated directly from stem cells; a number of intermediate cell types was recognised. As these cells matured there was a gradual increase in the number of apically-situated granules; these were of the size and shape of those in mature cells. The density of the cytoplasm increased and most organelles became confined to the lower two-thirds of the cell.

In parasitised glands a complete range of cells from stem to mature surface mucous cells was recognised (Figs. 62, 40, 41, 42, 43 and 61).

Cells thought to be immature mucous neck cells were present. These were identified by the size and shape of granules, the number of which gradually increased in the apical cytoplasm. The mitochondria were occasionally elongated and the lateral plasmalemmata straight; these are features of mature mucous neck cells.

Some cells showed progressive differentiation towards parietal cells. These cells had elaborate interdigitations of the basal plasmalemmata and poorly developed intracellular canaliculi. Initially, the internal structure of the few mitochondria which were present was relatively poorly developed. A prominent golgi complex was present in the early parietal cells but it decreased in extent as the cells matured. In a few of these cells, mucus-like granules were found, an observation also made by Corpron (1966). This author suggested that parietal cells arose from early surface mucous cells. In this study, it was considered that a cell differentiating into a surface mucous cell is unlikely to have the

ability to change and differentiate into the structurally highly complex parietal cell. It was concluded that parietal cells arose de novo and possibly by cell division. Hayward (1967b and 1967a), found that parietal cells developed directly from undifferentiated cells in suckling and foetal rabbits. Lawn (1960) and Corpron (1966) described a cell type in the rat similar to Figs. 91 and 92 and called it the neck parietal cell; they suggested that it was an immature parietal cell.

Cells were found which showed some of the structural features of zymogen cells namely, stacks of cisternae of RSER in the basal cytoplasm, a well-developed golgi complex and occasional electron-dense granules. It has been suggested that zymogen cells differentiate from mucous neck cells (Townsend, 1961; Hunt and Hunt, 1962). The present findings indicate that this is unlikely. Also, mucous neck cells are packed with mucous granules and appear fully differentiated; it is unlikely that such cells can act as a source of zymogen cells.

The function of the enterochromaffin cell and its relationship to other cell types in the gastric mucosa remains unknown. In this study, poorly-differentiated cells with centrioles, showing some of the features of enterochromaffin cells, were located within the mucosa. This would suggest that this cell arises directly from an undifferentiated cell and at least at this stage is capable of division. By virtue of the fact that this cell occurs at all levels of the gastrointestinal tract, it is unlikely to be related to any other cell type in the gastric mucosa.

Possible Stimuli of Cell Hyperplasia

The nature of the stimulus leading to cell hyperplasia and replacement of functional gastric gland epithelial cells is unknown. Townsend (1961) found that,

after localised surgical trauma to the rat gastric mucosa, the denuded area was quickly relined by flattened non-differentiated cells and that the differentiated gastric gland cells lining the surrounding glands were replaced by non-functional cuboidal cells. In the same way, it is possible that necrosis and sloughing of the surface mucosa, a lesion which follows emergence, stimulates proliferation of stem cells in the upper gland-lower pit region in an attempt to replace the damaged mucosa. It is also possible that the physical stretching effect exerted on the gastric mucosa by O. ostertagi parasites as they matured had an effect similar to the surgical damage induced by Townsend (1961). Weight is possibly added to this theory by the findings of Armour et al. (1966) in sheep experimentally infected with O. circumcincta. Structural and functional changes similar to those found in bovine ostertagiasis were described; however, these occurred at a much earlier stage in the life cycle of the parasite, while the parasite was still within the mucosa. O. circumcincta is a much larger parasite than O. ostertagi and it is possible that because of this the physical stretching produced by the parasite had an effect at an earlier stage.

Possible Mechanism of Parasite Expulsion (vide Section V)

It was shown that there was an exponential expulsion of the adult worm burden between day 17 to 35 of the infection. With the onset of the expulsive phase, there was an increase in cell activity in the lamina propria; in particular, there was a marked increase in mast cell numbers and towards the end of Phase 2 and during Phase 3, many GLs appeared within the epithelium. Jarrett, Jarrett, Miller and Urquhart (1967) established a definite quantitative

relationship between the kinetics of mast cell and globule leukocyte populations in rats infected with N. brasiliensis. They showed that a sudden episode of mast cell activity occurred at the commencement of the expulsion of the worm burden. Due to the extensive hyperplasia of the gastric mucosa in O. ostertagi infections, it was not possible to apply quantitative methods to mast cell and GL counting; the observations made were visual estimations. In the ultrastructural and cytochemical studies made in Section V, it was concluded that GLs were the end product of a series of changes in subepithelial mast cells, namely discharge of amines and an accompanying alteration in the relationship between the acid mucopolysaccharide and the basic protein of the granules. Following emergence and the onset of the expulsive phase, there was a marked increase in immunoglobulin-producing cells in the lamina propria of the abomasum. From their structural features, i.e. distended cisternae of RSER, it would appear that they were producing large quantities of antibody. It has been shown that the antibody present in such cells in the human gastrointestinal tract is mainly IgA (Crabbé and Heremans, 1966). Mast cells were frequently located in close apposition to active plasma cells (Fig. 134).

It is possible that the mast cell-GL transformation might be associated with an effector mechanism involved in the transport of locally-produced immunoglobulins into the lumen of the gastrointestinal tract and expulsion of the adult worm burden.

The cellular activity at the time of expulsion of both N. brasiliensis and O. ostertagi is remarkably similar. This would suggest that the mechanism of the expulsive processes are alike. Preliminary observations, which I have made on the cytological and ultrastructural features of cellular reactions in the biliary

tract of sheep infected with F. hepatica and the abomasum of sheep infected with H. contortus and of sheep infected with O. circumcincta, indicate that the nature of the cellular response is almost identical to that described in bovine ostertagiasis.

Plasma cells were especially numerous in the upper mucosa on which lay adult O. ostertagi in a diphtheritic membrane. It has been suggested that superficial necrosis of the epithelium may be the result of an antigen-antibody reaction (Jarrett, 1966).

Phase 1 and Phase 3

Up to day 17 (Phase 1) the structural changes were more or less confined to the parasitised gland. No significant biochemical or clinical findings were noted apart from slight elevation of the plasma pepsinogen level. This could be accounted for by limited breakdown of tripartite junctional complexes initially in dilated parasitised glands and later in associated dilated glands. After day 35 (Phase 3)with the expulsion of the adult worm burden, there was a gradual return of normal structure and function and at day 63 and 70 the gastric mucosa was virtually normal except for the presence of post-parasitised glands and occasional globule leukocytes.

SECTION IV

STRUCTURAL AND FUNCTIONAL CHANGES ASSOCIATED WITH THE USE OF THIABENDAZOLE IN BOVINE OSTERTAGIASIS

INTRODUCTION

It has been shown earlier in this work that clinical ostertagiasis is associated with reduction in the functional parietal cell mass. This results in a rise in pH of the abomasal fluid and impairment of peptic digestion. With the loss of the adult worm burden there is a gradual return of parietal cell function and normal digestion.

Thiabendazole (Thibenzole; Merck, Sharp and Dohme, Rahway, New York, U.S.A. and Hoddesdon, Hertfordshire, England) is an anthelmintic widely used in the treatment and prophylaxis of bovine ostertagiasis. It was thought desirable to study in precise detail its effect in this disease. In this study particular reference is made to the biochemical and pathological changes in the abomasum after treatment with Thiabendazole to ascertain if the removal of the adult O. ostertagi worm population accelerates the resolution of the pathological changes and a more rapid return to normal gastric function.

EXPERIMENTAL DESIGN

The objects of this experiment were : 1) to test the anthelmintic efficiency of Thiabendazole against adult O. ostertagi at 220 mg. per kg. body weight; these results have been reported in detail by Armour, Jennings, Kirkpatrick, Malczewski, Murray and Urquhart (1967) and Armour (1967).
2) To study the biochemical and pathological changes in the abomasum after treatment of clinical ostertagiasis.

Ten parasite-free calves, aged 8 - 10 weeks, were allotted to two groups of five each (Groups 1 and 2) and inoculated on day 0 with 400,000 O. ostertagi third-stage larvae. Group 1 remained untreated while each calf of Group 2 was treated orally with Thiabendazole at 220 mg. per kg. body weight on the day of onset of clinical signs, i.e. anorexia, weight loss and diarrhoea. One calf in each group had an abomasal cannula inserted after the method of Jennings et al. (1966) to allow samples of abomasal fluid to be withdrawn; this enabled daily changes in the pH of abomasal contents to be followed. All calves in Groups 1 and 2 were necropsied 28 days after infection. A further 2 parasite-free calves were infected with 400,000 O. ostertagi larvae and necropsied fourteen days later to establish the infectivity of the inoculum; in experimental infections of this magnitude, a large proportion of the worm population is expelled between the 17th and 35th day (Section III).

OBSERVATIONS

The calves were examined clinically each day and faecal samples were inspected for assessment of consistency. The calves in groups 1 and 2 were weighed prior to inoculation and on days 7, 14, 20, 25 and 28. Faecal samples for egg counts were collected on day 0 and daily from day 17 to 28. Samples of abomasal fluid for pH estimation were examined daily from the two calves with the abomasal canulae.

At necropsy, parasitological examinations were carried out as in Section III and the pH of the abomasal contents was determined. Tissues were taken from the abomasum and regional lymph nodes for light and electron microscopical examination.

RESULTS

CLINICAL DATA

All calves in both groups developed clinical signs of ostertagiasis, i.e. anorexia, weight loss and diarrhoea, within 17 days to 28 days of infection; these signs persisted in the untreated calves until necropsy on day 28, by which time 3 calves were *in extremis*. Following treatment of calves in Group 2, there was a complete cessation of diarrhoea and return of appetite within 48 hours. These changes were reflected in resumption of weight gains 3 to 4 days after treatment (Graph 5).

PARASITOLOGICAL FINDINGS

Faecal egg counts were positive in calves of both groups on day 17 and increased until day 23 in the untreated calves and thereafter decreased; in the treated calves, faecal egg counts decreased to zero within 24 hours of treatment. The course of the mean faecal egg counts in treated and untreated calves is shown in Graph 6.

In the treated calves the mean numbers of *O. ostertagi* were reduced by 94% compared to the untreated calves (Table 4). The numbers of *O. ostertagi*

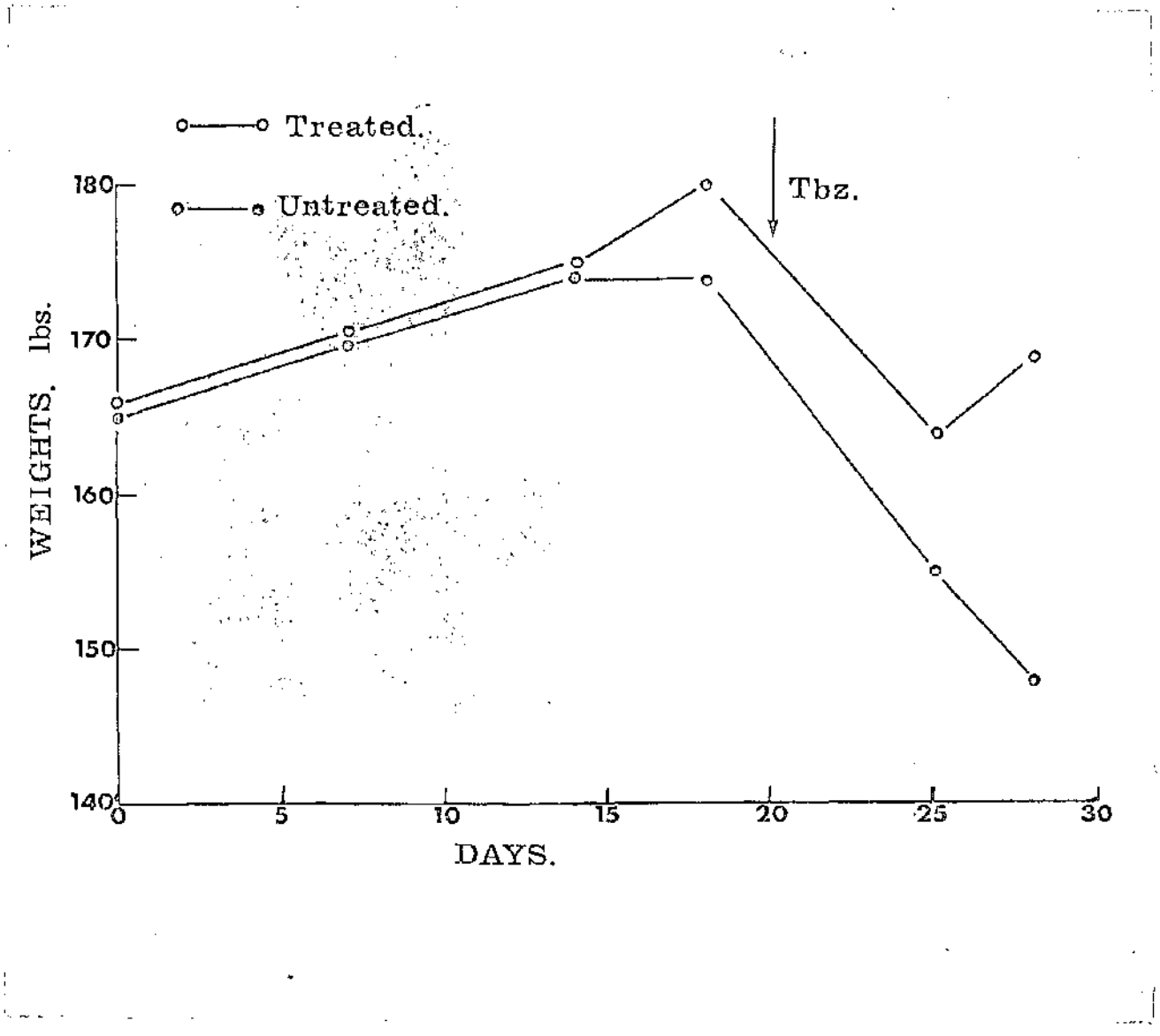

Graph 5. Mean bodyweights from two groups of 5 calves each, following inoculation of 400,000 O. ostertagi larvae on Day 0, one group being treated with thiabendazole (Tbz).

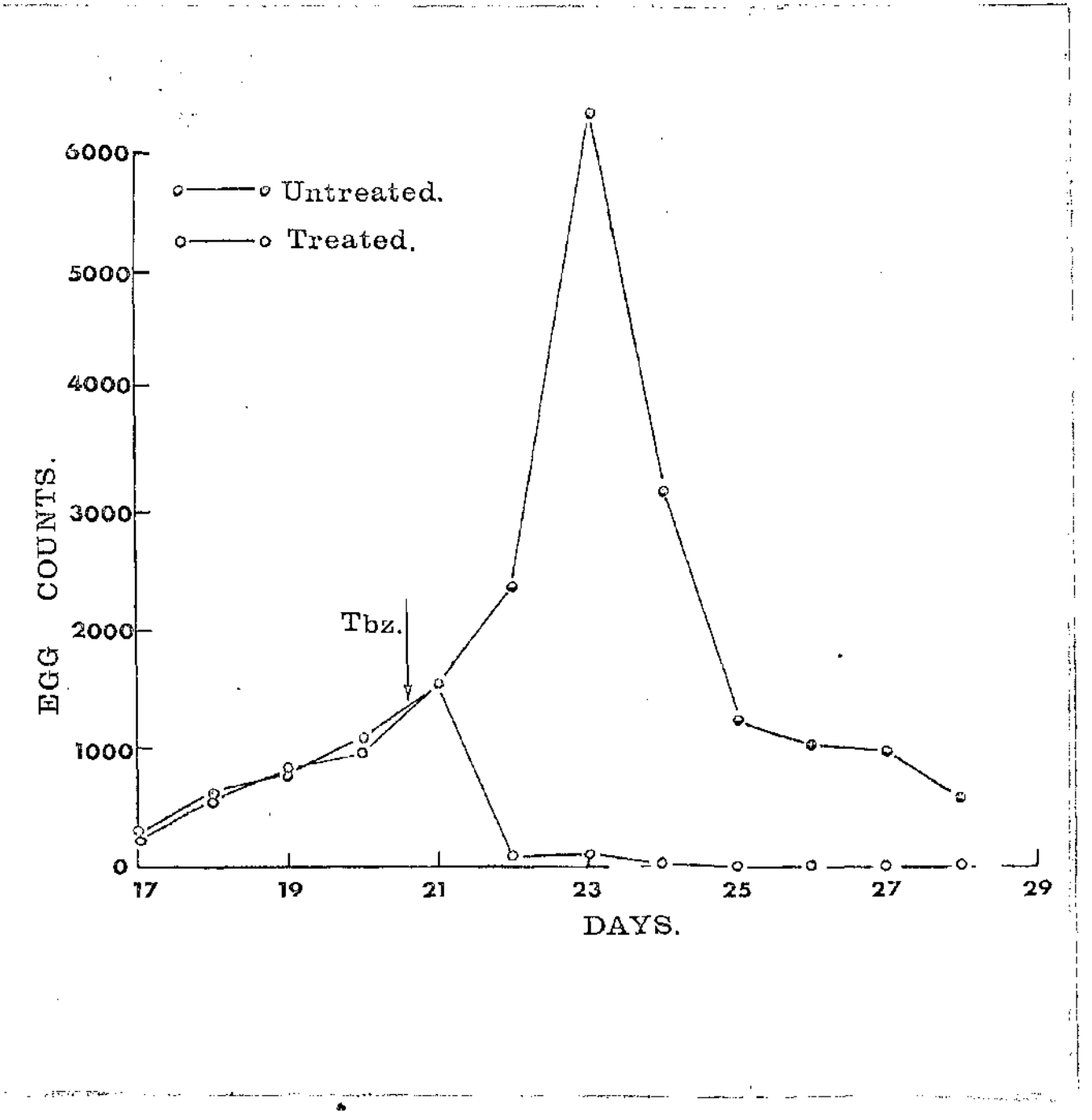

Graph 6. Mean faecal egg counts from two groups of 5 calves each, following inoculation of 400,000 O. ostertagi larvae on day 0, one group being treated with thiabendazole (Tbz).

Table 4

Worm Counts and pH of Abomasal Fluid at Necropsy on Day 28 of Two Groups of Five Calves Inoculated with 400,000 O. ostertagi Larvae on Day 0, One Group being Treated Orally with Thiabendazole on the Day of Onset of Clinical Signs

Group	Nos. of O. ostertagi	pH of Abomasal Fluid
1 Untreated	12,500	6.7
	13,900*	7.0
	19,800	6.9
	14,600*	7.2
	11,500*	7.1
Mean	14,460	7.0
2 Thiabendazole 220 mg/Kg	300	2.3
	100	4.9
	1,700	2.0
	700	2.8
	1,700	4.1
Mean	900	3.2

Percentage reduction compared with controls — Mean 94; Range 88 - 99

* Killed in extremis

found in the two calves necropsied on day 14 were 138,000 and 110,000 respectively; this indicated that the larvae used in the experiment were of normal infectivity.

BIOCHEMICAL RESULTS

In the treated calves, the pH of the abomasal contents (Table 4) had returned to normal levels (mean 3.2) whereas in untreated calves they remained elevated (mean 7.0). Daily changes in the pH of abomasal contents in the two calves with abomasal canulae are outlined in Graph 7 and show that the pH of the abomasal contents became markedly elevated in both calves after day 19 and remained so in the untreated calf until necropsy on day 28; in the treated calf, the pH of the abomasal contents decreased steadily until necropsy on day 28.

PATHOLOGY

Macroscopic Findings

The gross lesions found at necropsy of calves in Groups 1 and 2 were similar to those described in Section III in that the unit lesions, the nodules, had coalesced to give rise to a morocco leather like appearance. There were areas of superficial necrosis and diphtheresis which were more extensive in the untreated calves (Group 1). The abomasal lymph nodes were highly reactive in both groups. The mucosa in the untreated calves was more thickened and oedematous than in the treated ones.

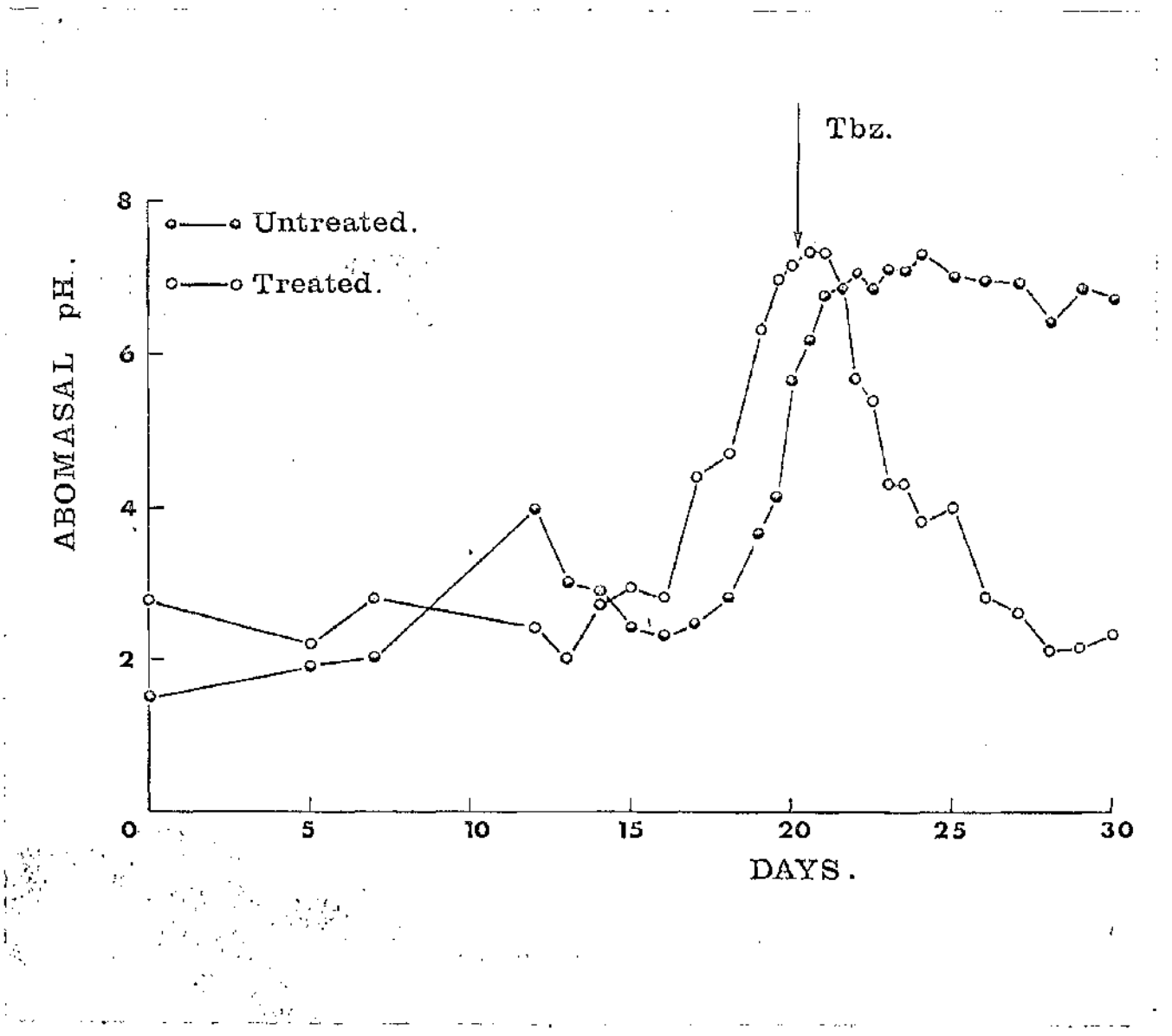

Graph 7. The pH of abomasal contents from two calves (with abomasal cannulae) following inoculation of 400,000 O. ostertagi larvae on day 0, one calf being treated with thiabendazole (Tbz).

Histopathological Findings

In both treated and untreated calves, emergence of parasites from glands was almost complete and there were numerous dilated post-infected gastric glands lined by columnar mucus-secreting cells. The glands surrounding these cells in the untreated calves of Group 1 showed a marked apparent loss of functional differentiation (Fig. 118 and Fig. 49, Section III), although many parietal cells could still be found amongst the rapidly dividing non-differentiated cells. By contrast, in the treated calves, many of the surrounding glands showed a return of normal functional cells, particularly parietal cells (Figs. 119 a and b, 120 a and b) although the mucosa was still thickened as the result of hyperplasia of undifferentiated and mucous cells. The cell response in the lamina propria was marked in both treated and untreated calves; however, the number of plasma cells present in the superficial part of the gastric mucosa was reduced in untreated calves. Cytolysis and necrosis of the superficial gastric mucosa was more extensive and severe in untreated calves.

Ultrastructural Findings

The changes found in the untreated calves (Group 1) were similar to those in Phase 2 of the experimental infection described in Section III. Those parietal cells which were still present had a degenerate appearance with a pseudovacuolated cytoplasm and in some cases complete loss of intracellular canaliculi. The intracellular canaliculi which remained showed a marked reduction of the surface area available for acid secretion, i.e. they were less extensive and although often markedly dilated, were lined by only a few

microvilli (Fig. 121 cf. Section III Figs. 71, 72 and 73).

On the other hand, in calves treated with Thiabendazole, the parietal cells showed structural features indicative of a return to normal functional activity. These cells were more akin to those described in the normal functional gastric mucosa in Section II, Figs. 21, 22 and 24, i.e. they contained extensive and elaborately developed intracellular canaliculi lined by numerous microvilli (Fig. 122). In some of these cells the structural changes were graded and evidence of previous inactivity, i.e. dilated intracellular canaliculi with only a few microvilli, was present (Figs. 123 and 124).

DISCUSSION

The results of this experiment demonstrated the high efficiency of Thiabendazole at 220 mg. per kgm. body weight as shown by a dramatic cessation of diarrhoea, resumption of normal appetite within 48 hours and almost complete elimination of the adult worm burden. It is probable that this dramatic expulsion of the adult worm burden facilitated the rapid return of the functional parietal cell mass. In treated calves, the pH of the abomasal contents returned to a functional level within 48 hours. That a new parietal cell mass could have differentiated in this time is possible, but the data available indicate that this is unlikely. In treated calves, no mitotic figures were found and no developing parietal cells were identified. Most of the parietal cells present contained extensive canaliculi lined by numerous microvilli, although some showed areas with dilated canaliculi lined only by a few microvilli, i.e. areas

of inactivity (Section III, Discussion); this would suggest that the inactive cells, seen in controls, were capable of returning to normal function. The mechanism of the depression of HCl production in the parietal cells is possibly a chemical one (Section III, Discussion) or it may be immunological; the treated calves showed a marked reduction in the superficial mucosa of the number of plasma cells, cells likely to be producing antibody.

With the return of the functioning parietal cell mass and normal pH, peptic activity was resumed and allowed digestion to start and normal weight gains to be made.

SECTION V

THE GLOBULE LEUKOCYTE AND ITS DERIVATION FROM THE SUBEPITHELIAL MAST CELL

INTRODUCTION

Despite its striking morphology, the globule leukocyte (GL) is one of the few cells in the body whose origin has remained unknown and whose function is uncertain. It is found within epithelia (Figs.125a &132a), and characteristically contains large acidophilic granules or globules. It occurs in many species and is particularly prominent in parasitic infections.

A number of investigations have been carried out in an attempt to find the origin and function of this cell. Kirkman (1950) considered that the GL was of connective tissue origin and that there was probably a close relationship between it and the Russell body-containing cell. Kent (1952) suggested that the GL originated from the small lymphocyte. In histochemical studies, Dobson (1966) and Whur and Gracie (1967) decided that the mast cell and the GL were unrelated and that the GL originated from immunoglobulin-producing cells; they postulated that its function was to carry antibody into the intestinal lumen.

Preliminary histochemical and ultrastructural evidence has been presented to show that in parasitic infections the GL originates from the mast cell of the lamina propria of mucous surfaces (subepithelial mast cell). (Jarrett, Miller and Murray, 1967; Miller, Murray and Jarrett, 1967).

Globule leukocytes occur in large numbers in the intestines of rats experimentally infected with Nippostrongylus brasiliensis (Paliaferro and Sarles, 1939). Kirkman (1950) related the appearance of these cells in the

urinary tract of the rat to infection with the bladder worm Trichosomoides crassicanda and found them to be absent in uninfected rats. Sommerville (1956) noted their presence in parasitised lambs but was unable to find them in lambs raised free of parasites. Whur (1966a) found that there was a relationship between the appearance of GLs in the intestinal mucosa and the onset of expulsion of the worm burden in rats infected with N. brasiliensis. It has also been shown that in such rats there is an increase in the numbers of intestinal mast cells (Wells, 1962). Jarrett, Jarrett, Miller and Urquhart (1967) established a definite quantitative relationship between the kinetics of mast cell and GL populations in rats infected with N. brasiliensis.

Little published data are available on the histochemical properties of mast cells in the bovine or the sheep. Many histochemical studies have been done on the connective tissue and peritoneal mast cell of the rat. The classical connective tissue mast cell granule is known to contain a sulphated acid mucopolysaccharide (Schiller and Dorfman, 1959; Benditt and Lagunoff, 1964) associated with a highly basic protein (Spicer, 1963; Benditt and Lagunoff, 1964). The granule also contains the vasoactive amines, histamine and 5-hydroxytryptamine (Benditt and Lagunoff, 1964).

On the other hand, mast cells of the rat gastrointestinal lamina propria have been the subject of conflicting reports. Some workers have found very few or no mast cells in this region (Mota, Ferri and Yoneda, 1956; Whur, 1966b) while others have shown that there is a high density of these cells in the lamina propria (Lindholm, 1960; Wells, 1962). Enerbäck (1966a; 1966b) showed that the demonstration of such gastrointestinal mast cells depends on the method

of fixation. He found that the granules of these cells stained differently from those of the connective tissue mast cells. In addition, the rat gastrointestinal mast cells were found to contain a monoamine, possibly dopamine (Enerbäck, 1966c). It has been shown that the mast cells of the gastrointestinal tract and the liver of cattle and sheep may also contain a catecholamine, probably dopamine (Coupland and Heath, 1961; Falck, Nystedt, Rosengren and Stenflo, 1964; Jarrett, Miller and Murray, 1967; Miller et al., 1967).

Little has been published on the ultrastructural features of the subepithelial mast cell in the gastrointestinal tract of the bovine or rat or on the subepithelial mast cell of the ovine biliary tract (Jarrett, Miller and Murray, 1967; Miller et al., 1967). Several observations have been made on the fine structure of the rat connective tissue and the peritoneal mast cell (Smith and Lewis, 1957; Smith, 1963; Benditt and Lagunoff, 1964; Fujita, 1965; Singleton and Clark, 1965; Bloom and Haegermark, 1965; Combs, 1966; Kent, 1966).

On the basis of ultrastructural studies, Toner (1965) in the chicken and Kent (1966) in the rat, were unable to find any functional significance for the presence of GLs and suggested that they were derived from lymphocytes. Kent (1966) stated that, of the cells found in the vicinity of GLs, mast cells were most like them in ultrastructure and gross cytology. Whur and Johnstone (1967), in an electron microscopic investigation, concluded that the GL of the rat was a migratory cell and considered that it structurally resembled immunoglobulin-producing cells. In this section detailed cytochemical and ultrastructural data are presented to show that the GL is derived from the mast cell and is

not a member of the immunoglobulin-producing cells. Tissues were examined from bovines infected with O. ostertagi, sheep infected with F. hepatica or H. contortus and rats infected with N. brasiliensis. The studies in the rat were made by my colleague H. R. P. Miller (Ph.D. Thesis, in preparation) and details are given in a conjoint paper (Murray, Miller and Jarrett, 1968). In summary, it was found that mast cells and globule leukocytes in the rat were similar cytochemically and ultrastructurally to their bovine and ovine counterparts.

RESULTS

CYTOCHEMISTRY

The Bovine

The Mast Cell Mast cells were located both subepithelially and intraepithelially in the abomasum. These showed a deep violet metachromasia at pH 4.5 after toluidine blue staining (Fig. 125 a and b); when stained with toluidine blue at pH 0.3, metachromasia was reduced or absent in many cells but was still obvious in some. The granules bound astra blue strongly (Fig. 126a), even when counterstained with safranin, and fluoresced orange with acridine orange (Fig. 127). Biebrich scarlet stained the granules at pH 8, 9 and 10 (Fig. 126b); this reaction was not found in all mast cells. Biebrich scarlet also stained eosinophil leukocyte granules at pH 10.

In the lamina propria, the granules of most mast cells fluoresced bright

apple-green with the monamine reaction (Fig. 128b); others were packed with small granules which fluoresced bright yellow (Fig. 128a). Some cells contained green and yellow fluorescing granules (Fig. 129).

The Globule Leukocyte This cell was readily recognised intraepithelially by its large intracytoplasmic globules or granules which frequently indented the nucleus.

With toluidine blue at pH 4.5, the granules showed a range of reactions from deep violet metachromasia (Figs. 125 a and b) through blue to almost colourless; the reactivity found at pH 0.3 was much less. With astra blue-safranin the granules of most cells also bound astra blue to a varying extent, staining from bright blue through pale blue to colourless. A feature found in some was a halo effect, the granules being rimmed by astra blue-positive material (Fig. 126a). With acridine orange they sometimes fluoresced yellow, sometimes green (Fig. 127). The granules bound biebrich scarlet up to pH 10 to varying extents (Fig. 126b). Some stained bright red, some pale red, while others had a bright red halo.

Using the technique for monoamines, it was found that the granules fluoresced dull green but not uniformly so (Fig. 128 b); many were only rimmed with green fluorescence while others contained green fluorescing centres. In general, the intensity was much less than in mast cells (Fig. 129).

The Transitional Cell This cell was found predominantly within epithelia. It contained granules of a similar size and cytochemical nature to those of the mast cell and also larger granules showing a range of staining affinity similar to those of the classical GL. With acridine orange, cells were found containing

small granules which fluoresced orange in the same way as mast cells but also having larger granules which fluoresced yellow or green similar to those of the classical GL (Fig. 130).

The Sheep

Tissues were examined from the abomasums and biliary tracts of parasitised animals. The range of cells defined by morphological and cytochemical features was similar to the bovine; subepithelial and intraepithelial mast cells, GLs and transitional cell types, were all recognised. Each of these cells had cytochemical features identical to those of its bovine counterpart (Figs. 131a and b, 132a and b, 133).

ULTRASTRUCTURE

The Bovine

The Mast Cell Very few mast cells were seen in the parasite-free abomasal mucosa of the bovine and these were difficult to locate on electron microscopic examination. The following description is of those found in the gastric mucosa of parasitised animals.

Subepithelial mast cells were often located in close apposition to plasma cells which had markedly distended cisternae of RSER (Fig. 134), to eosinophils and polymorphonuclear leukocytes and to macrophages. Mast cells were also identified close to small blood vessels or bordering epithelial basement membranes (Fig. 135). These cells assumed oval, triangular, or sometimes elongated forms

(Fig. 136). There were cytoplasmic finger-like projections around the borders of many mast cells. Their nuclei were frequently eccentric and most often round or oval in shape and were usually indented by granules. Margination of chromatin was present as were occasional nucleoli. The cytoplasmic matrix contained round or oval granules which ranged in size up to 1.3 u; most were less than 1 u diameter. These were bounded by smooth-surfaced unit membranes (Fig. 137). After glutaraldehyde fixation the electron density of the granules varied considerably from cell to cell, from granule to granule and within granules (Figs. 134 and 136). Some granules had an amorphous, homogeneous appearance (Fig. 138), others had dense homogeneous cores rimmed by less electron-dense material, while the contents of others had a reticulated or moth-eaten appearance (Fig. 136). The matrices of a few granules could be seen spilling through ruptured granule membranes (Fig. 137); in others there were distinct halos between the granule content and surrounding membranes. The number of granules varied from cell to cell. Throughout the cytoplasmic matrix ribosomes and RSER were present in variable amounts although they were sparse when the cell was fully granulated. In some cells, well-developed golgi complexes, often with an associated centriole, were located in paranuclear positions (Figs. 139 and 140). Each complex was composed of parallel arrays of flattened cisternae which were dilated at the ends to form vacuoles; they had numerous associated vesicles. Some vacuoles contained electron-dense material (progranules) (Fig. 140). Occasional small round, or oval or elongated mitochondria were interspersed between granules. Cytoplasmic fibrils were frequently present in the vicinity of the nucleus. Dense particles similar to glycogen granules were scattered in the cytoplasm.

The Globule Leukocyte Within the epithelium itself, classical GLs were found at all levels (Fig. 141). Occasionally, small cytoplasmic prolongations projected from these cells into the intercellular space. No desmosomal or other attachments were found between GLs and epithelial cells.

The cytoplasm of the GL contained a variable number of granules which were surrounded by smooth-surfaced unit membranes (Fig. 142). Granules measured from 1 - 5 u diameter and frequently indented the nucleus. The matrices of the small granules showed a similar range of appearances to those of the subepithelial mast cell. In most GLs the granules were up to 3 u diameter. Some cells contained only large granules, i.e. the classical globule leukocytes (Fig. 143); some cells had only small granules, i.e. the intraepithelial mast cells while in others, a mixture of large and small granules was present, i.e. the transitional cell (Fig. 144). The matrices of the larger granules were electron-dense although some had a reticulated or moth-eaten appearance (Fig. 145) while others had lost their contents. In some cells, a few large electron-lucent granules were present.

Well-developed golgi complexes similar to those of the subepithelial mast cells were present in paranuclear positions. In some cells, particularly those with large granules, the cytoplasmic matrix was devoid of organelles and had a pseudo-vacuolated appearance (Fig. 145). In others, some ribosomes were scattered throughout the matrix and a few cisternae of RSER were found (Fig. 143). A few small round or oval mitochondria were present. Cytoplasmic fibrils, similar to those of subepithelial mast cells, were identified in paranuclear

positions. The nuclei of these cells were most often eccentric and were similar in appearance to those of subepithelial mast cells.

A few transitional cells and GLs were found in the lamina propria (Fig. 146).

The Sheep

The Mast Cell The structural features of the subepithelial ovine mast cell found in the biliary tract resembled those of the bovine. The mast cell was characterised by a variable complement of granules surrounded by smooth unit membranes. These granules showed a range of electron densities (Fig. 147). A point of difference from the bovine mast cell was that the cytoplasm of the ovine mast cell contained a much greater number of small membrane-bound vacuoles (Fig. 147).

The Globule Leukocyte The intraepithelial GL contained large membrane-bound granules (Figs. 148 and 149). Some were extremely electron-dense; some were reticulated or moth-eaten, others appeared to have lost their granule content. Within some of these (transitional) cells, granules of a similar size and nature to those of the subepithelial mast cell were found (Fig. 150). A feature which the GL had in common with the subepithelial mast cell was the presence of numerous small membrane-bound vacuoles in the cytoplasmic matrix (Fig. 148).

The nuclei of both the GL and the subepithelial mast cell were similar in appearance to the bovine nuclei and were frequently indented by granules. In

the biliary tract of the sheep examined, classical GLs and transitional cells were also found in the subepithelial lamina propria.

DISCUSSION

Experimental infections with parasites afford an excellent opportunity to study the formation of GLs. In N. brasiliensis infections in the rat it has been clearly shown that there is a quantitative relationship between episodes of mast cell activity and the appearance of waves of GLs in the epithelium (Jarrett, Jarrett, Miller and Urquhart, 1967). A similar situation exists in parasitic infections of the bovine and sheep. In these circumstances, one might expect to find the series of changes which shows the development of GLs.

We have demonstrated that the granules of the gastrointestinal mast cell of the rat and the great majority of the subepithelial and intraepithelial mast cells in the bovine and the sheep contain a sulphated acid mucopolysaccharide, which stains metachromatically with aqueous toluidine blue at pH 4 and 4.5 but not at pH 0.3 and which binds astra blue strongly. A mucopolysaccharide of similar affinities was found in the transitional cell types and GLs of the bovine and sheep and also in the GL of the rat. With acridine orange the acid mucopolysaccharide of the granules of the mast cells of all three species and the granules of the GLs of the rat fluoresced orange. In the bovine and sheep, a striking series of changes was seen as mast cells transformed to GLs; as the granules became larger, the orange fluorescence changed to yellow and then to green. In individual transitional cells, all phases of acridine orange

fluorescence were demonstrated. This range of staining affinities within individual transitional cells probably indicates a structural change in the mucopolysaccharide leading to loss of the stacking effect (Saunders, 1964).

Spicer (1963), using the acid dye biebrich scarlet at high pH, demonstrated a basic protein in certain mast cells of the rat. Our results show that mast cells, transitional cells and GLs of the three species bind this dye up to at least pH 10, indicating that the granules of the GLs like those of the mast cells, contain a highly basic protein.

The relationship of the subepithelial mast cell to the mature connective tissue mast cell remains unclear. In the developing rat connective tissue mast cell (CTMC), maturation accompanied by increasing degrees of sulphation is reflected by changing histochemical properties of the granule. The granules of the mature cells stain with safranin in preference to astra blue in contradistinction to those of the less mature forms. Whereas mature cells bind toluidine blue and stain metachromatically at pH 0.3, the immature cells do not stain metachromatically below pH 4 (Combs, Lagunoff and Benditt, 1965). The gastrointestinal mast cells of the rat resemble these developing cells in that their granules do not have the full range of staining characteristics of the heparin of the mature CTMC (Murray et al. , 1968).

The mature CTMC of the rat contains 5-HT which is demonstrable by its yellow fluorescence in the Falck reaction (Miller, 1968). This is the typical reaction of the perivascular mast cells in the submucosa of the intestine. In a rat which has just expelled its population of N. brasiliensis (e.g. 19 days

after primary infection), there is a great increase in mast cells in the lamina propria. Most of the cells in the villi do not show marked 5-HT fluorescence but are weakly greenish-yellow; however, many of the cells around the venules between crypts have a similar colour and intensity to the submucosal mast cells and obviously contain 5-HT. Globule leukocytes usually show the indeterminate green fluorescence but occasionally are bright yellow. Intermediate forms are found between the two mast cell types (Miller, 1968; Murray et al. 1968).

Many of the subepithelial mast cells of the bovine and sheep show bright apple-green fluorescence characteristic of catecholamines. Some mast cells are packed with small bright yellow fluorescing granules and obviously contain 5-HT. Other cells contain a mixture of yellow and green fluorescing granules. The granules of cells within the epithelium have a range of intensity of green fluorescence. The granules of some individual cells show this range of green staining intensity.

It should be emphasised that these data do not show that the so-called subepithelial mast cells are exclusive to this site; cytochemically similar cells have been found in other sites but these have not yet been investigated fully.

The fine structural features of the subepithelial mast cell of the rat (Miller, 1968) and mast cells of the bovine and sheep have been delineated. There are minor differences between the mast cells of the three species, yet the similarities between GLs and subepithelial mast cells in each species are strikingly apparent. Granules bounded by unit membranes, golgi complexes,

microvilli and relatively small amounts of RSER are all features found in GLs that are common to subepithelial mast cells. In the rat, GLs are found whose granules are indistinguishable from the subepithelial mast cells (Miller, 1968; Murray et al., 1968). In the bovine and sheep, the complete range of granule size found in studies with the light microscope is readily seen with the electron microscope. A spectrum of cells covering subepithelial mast cells through transitional cell types to GLs with large granules is demonstrable. The ultrastructural relationship between the subepithelial mast cell and the GL emphasises the already strong histochemical evidence that GLs are derived from subepithelial mast cells.

The variation found in granule structure of the GL may have resulted from several different factors. In the bovine and sheep, histochemical data point to a loss of amine and acid mucopolysaccharide from the granule; the ultrastructural changes in the granules possibly reflect this loss.

Whur and Johnstone (1967) and Dobson (1966) suggested that there were many similarities between GLs and immunoglobulin-producing cells. They elaborated the hypothesis that the globules contain immunoglobulin and that the function of the GL is to transport antibody across the epithelium to the target site. During our studies, many plasma cells were seen, all of which were characterised by the presence of extensive and well-developed RSER. In many cases the cisternae of RSER were markedly dilated for form Russell bodies. The latter were recognised by the presence of rough-surfaced membrane surrounding the dilated cisternae (Fig. 151), and were at all times easily distinguished from mast cells and GLs.

From the quantitative, ultrastructural and cytochemical data which are now available, it is possible to trace the steps in a process which demonstrates that the GL is derived from the subepithelial mast cell. In the experimental conditions used, i.e. active parasitic infections, it can be seen that the cells involved are in a dynamic state. It seems probable that the changes observed are the result of the mast cells discharging amines during the course of migration and of an accompanying alteration in the relationship between the acid mucopolysaccharide and the basic protein of the granules. The end product of this process is a cell with the staining affinities of the classical GL.

Although the details of the functional effects of this cellular process have not yet been fully worked out, recent research has thrown some light on the possibilities. It is clear, for example, that at least some parasities secrete two substances which have an effect on mast cells. It has long been known that Ascaris extracts contain a mast cell degranulator and this has been shown to be a peptide with a molecular weight of about 2000-3000 (Uvnäs and Wold, 1967). N. brasiliensis produces a substance which causes degranulation of mast cells, almost immediately after the worms reach the intestine (Jarrett, Jarrett, Miller and Urquhart, 1967). At this time, a local vascular leak is established and the connective tissue of the villi and the subepithelial spaces becomes markedly oedematous. It is possible that this mechanism is associated with the feeding processes of the worm. During this degranulation, there is a peak production of GLs (Jarrett, Jarrett, Miller and Urquhart, 1967). Later in the infection, the mast cell population regenerates. A sudden episode of mast

cell activity associated with a second peak of production of GLs occurs at the commencement of expulsion of the worm burden (Jarrett, Jarrett, Miller and Urquhart, 1967). This worm is known to produce an allergen capable of reacting with reagins and mast cells with the production of anaphylactic shock (Urquhart, Mulligan, Eadie and Jennings, 1965; Ogilvie, 1964; Jones and Ogilvie, 1967; Wilson, 1967). The expulsive phase of a helminth infection can be accelerated by passively administering antiworm antiserum and simultaneously producing a heterologous anaphylactic shock with albumin-adjuvanted Haemophilus pertussis (Barth, Jarrett and Urquhart, 1966). It has therefore been suggested that the mast cell-GL transformation might be associated with the effector mechanism which is involved in the transport of antibodies from immunoglobulin-producing cells through the bowel wall to the target sites on parasites (Jarrett, Miller and Murray, 1967).

SECTION VI

THE STRUCTURAL CHANGES IN THE BOWEL WALL ASSOCIATED WITH INCREASED PERMEABILITY TO MACROMOLECULES

INTRODUCTION

Isotopically labelled proteins have enabled significant advances to be made in understanding the role of the gastrointestinal tract in the homeostasis of plasma proteins in both normal and pathological states. The gastrointestinal tract has been shown to be involved in the synthesis of immunoglobulins (Crabbé and Heremans, 1966) and lipoproteins (Isselbacher and Budz, 1963; Cardell, Badenhausen and Porter, 1967), in the absorption of intact gamma globulin in newborn animals (Brambell, 1957) and in the loss and degradation of plasma proteins (Holman, Nickel and Sleisenger, 1959; Glass and Ishimori, 1961; Hollander and Horowitz, 1962; Wetterfors, 1964 and 1965; Stanley, 1965).

Excessive loss of plasma protein via the gastrointestinal tract results in hypoproteinaemia, particularly hypoalbuminaemia. This occurs in a variety of diseases in man (Schwartz, 1964; Waldmann, 1966). A large number of techniques have been proposed for the detection and quantitation of gastrointestinal plasma protein loss. These have been reviewed by Waldmann (1966).

Hypoalbuminaemia has been reported in a number of parasitic conditions in cattle and sheep (Table 5). Mulligan *et al.* (1963) and Nielsen (1966) using I^{131}-labelled albumin and I^{131}-labelled polyvinylpyrrolidone (P.V.P.) demonstrated that there is a leak of macromolecules into the gastrointestinal tract of bovines with Type II ostertagiasis, a condition in which severe hypoalbuminaemia occurs (Anderson *et al.*, 1965).

In man, hypoalbuminaemia has been found in association with giant hypertrophy of the gastric mucosa, a condition with many structural features similar

Table 5

Parasitic Conditions in Cattle and Sheep Associated with Hypoproteinaemia

Abomasum	*O. ostertagi*	Bovine	Martin *et al.* (1957) Mahrt *et al.* (1964) Ross and Todd (1965) Anderson *et al.* (1965)
	O. circumcincta	Sheep	Horak and Clark (1964) Armour, Jennings and Urquhart (1968)
	Trichostrongylus axei	Bovine	Leland, Drudge and Wyant (1959) Ross, Purcell, Dow and Todd (1967)
		Sheep	Leland, Drudge and Wyant (1960)
Small Intestine	*Cooperia pectinata*	Bovine	Herlich (1967)
Large Intestine	*Oesophagostomum radiatum*	Bovine	Bremner (1961)
Mixed Infections	*O. ostertagi*, *T. axei*, *T. colubiformis* *C. punctata*	Bovine	Herlich (1962)
	H. contortus, *T. colubiformis*, *Nematodirus spathiger*	Sheep	Shumard, Bolin and Evelett (1957)
	H. contortus, *Nematodirus spathiger*	Sheep	Kuttler and Marble (1960)
Liver	*F. hepatica*	Bovine	Ross, Todd and Dow (1967) Armour, Jennings and Urquhart (1967)
		Sheep	Ross, Dow and Todd (1967)
	F. gigantica	Bovine	Sewell (1965)
Small Intestine	*Paramphistomum microbothrium*	Sheep	Horak and Clark (1963)

to ostertagiasis; it has been shown using I^{131}-labelled albumin and I^{131}-labelled P.V.P. that the hypoalbuminaemia is the result of excessive loss of albumin through the gastric mucosa (Citrin, Sterling and Halstead, 1957; Schwartz and Jarnum, 1961; Dawson, Williams and Williams, 1961; Glass and Ishimori, 1961). Using the same technique it was demonstrated that the hypoalbuminaemia found in association with gastric cancer is the result of excessive loss of albumin into the stomach (Jarnum and Schwartz, 1960; Schwartz and Jarnum, 1961; Dich, Paaby and Schwartz, 1961; Glass and Ishimori, 1961; Wetterfors, 1965).

No detailed electron microscopical studies have been made on the structural changes in the bowel wall associated with increased permeability to macromolecules. There are a number of light microscopic studies which deal with this problem. Schiraldi, Pastore, Strada and Marano (1968) used Cr^{51}-labelled albumin in a histoautoradiographic study of protein loss in the intestine of antifolic-treated rats; it is known that in such rats albumin is lost into the bowel. They showed particles of radioactive material associated with capillaries in the lamina propria and concentrated in the apical cytoplasm of epithelial cells; they concluded that protein loss would seem to occur mainly through epithelial cells. Using the immunofluorescent technique, Gelzayd, Kraft and Fitch (1967) demonstrated IgA in the apical cytoplasm of human rectal mucosal epithelial cells and in adjacent lymphoid cells. They concluded that IgA produced in the lymphoid cells entered the epithelial cells and was transported to the apical cytoplasm. In the foregoing studies labelled material was not

demonstrated in the mid or basal parts of epithelial cells nor between them. Therefore it was not clear whether these macromolecules passed through or between epithelial cells.

A number of workers have presented evidence to show that macromolecules are capable of moving across cell membranes under certain conditions. Green, Fleischer, Barrow and Goldberg,(1959) showed that tissue culture cells, injured by cytotoxic antibody, permit the passage of electrolytes and larger molecules across the cell membrane. Using the fluorescent antibody technique, Kent (1967) demonstrated that, following damage to the cell membrane of cardiac muscle fibres, in patients with myocardial infarction, there was increased permeability of the cell membranes to plasma proteins; he found albumin, IgG and fibrinogen in affected cells. It has been shown that colloidal particles (saccharated iron oxide, thorium dioxide, ferritin) introduced at the basal surface of the simple squamous epithelium of the corneal endothelium, passed across the cell membrane and were transported through the cell in membrane-bound vesicles without appearing in the intercellular spaces (Kaye and Pappas, 1962). In a study of the ultrastructural changes involved in placental transfer of large molecules, Lambson (1966) found that in the visceral yolk sac of the rat, ferritin passed intracellularly through the visceral endodermal cells in a system of vacuoles and vesicles.

A number of authors have suggested that macromolecules may pass between cells and that the junctions joining cells are important in preserving the integrity of mucous surfaces with respect to the movement of macromolecules. In

a discussion on the mechanism of serum protein transfer across the bowel wall Hollander and Horowitz (1962) concluded that intercellular passage was the most likely route. Dilatation of intercellular spaces has been shown to occur between epithelial cells in certain protein-losing enteropathies (Schwartz, 1964; Shnitka, 1964; Gonzalez-Licea and Yardley, 1966). On this basis, Schwartz (1964) concluded that plasma protein loss occurred between cells and not through them. There is no evidence that dilatation of the space between epithelial cells of the intestine is necessarily indicative of plasma protein movement. Cassidy and Tidball (1967) demonstrated that dilatation of the intercellular space in intestinal epithelial cells of the rat occurred under conditions of enhanced permeability and agreed with Diamond and Tormey (1966) who provided evidence of enlargement of intercellular channels under conditions of graded water transport activity in the gallbladder. Hence, dilatation of these spaces would appear to be related primarily to fluid transport and is not evidence of plasma protein movement. Dobbins (1966 a and b) in an ultrastructural study of the small intestine, showed that dilated intercellular spaces were found in normal patients. However, in his electron micrographs, the intercellular spaces demonstrated were not of the extent shown in the protein-losing enteropathies.

It was first suggested in 1895 by Bonnet and later in 1911 by Zimmerman that the terminal bar might act as a diffusion barrier between the lumen and intercellular spaces. It has been shown that haemoglobin administered intraperitoneally to mice was concentrated in the tubules of the nephron and that penetration of haemoglobin between adjacent cell walls stopped invariably at the height of the terminal bar, demonstrating that this structure acted as an effective barrier

against penetration of large molecules (Miller, 1960). Similar results were obtained using the particulated tracers saccharated iron oxide, thorium dioxide and ferritin. It was found that these did not penetrate the terminal bars in the simple squamous epithelium of the rabbit cornea (Kaye and Pappas, 1962). Choi (1962, 1965) showed that thorotrast and saccharated iron oxide did not enter the epithelium of the toad urinary bladder beyond the level of the terminal bar.

For many years it was generally assumed on the basis of light microscopy that the terminal bar consisted of bands of condensed intercellular substance cementing cells together. In 1963, Farquhar and Palade showed that the terminal bar is a tripartite complex between the juxtaluminal segments of adjacent cells and that it consists of modifications of lateral plasmalemmata and the associated cytoplasm. The most apical part of the complex is termed the zonula occludens or tight junction; it was shown that this structure can restrict the flow of macromolecules between cells. To demonstrate this, advantage was taken of the progressive concentration undergone by haemoglobin in the renal tubules of the rat during experimental haemoglobinuria. Haemoglobin, given intravenously or intraperitoneally, filtered through the glomeruli and was concentrated by re-absorption of water in tubules. It eventually formed a dense homogeneous mass that filled the tubular lumina. In all segments, the dense mass was traced along the cellular margins down to the level of the occluding zonulae. Beyond these, the intercellular spaces appeared free of tracer. Since the density of the material in the junctional gaps was considerably lower than that of the luminal haemoglobin and since there was no evidence of a concentration gradient

down the junctional complex, it was concluded that penetration of haemoglobin molecules was effectively stopped along the line of fusion of the adjoining cell membranes at the zonula occludens. Further demonstration of this was obtained by the same workers using zymogen discharged from pancreatic acini and ducts. It was shown that no dense material penetrated the zonula occludens to accumulate in the intercellular space.

Additional evidence that the occluding parts of the intercellular junctions acted as a barrier to the passage of macromolecules was provided by Brightman (1962, 1965). Zonulae adhaerentes (the intermediate part of the tripartite complex)were demonstrated adjoining the luminal parts of ependymal cells lining the ventricles of the rat brain. Maculae occludentes were found at varying intervals along the lateral cell membrane. Brightman injected ferritin into the lateral ventricles and found that this tracer readily passed between the zonula adhaerens but was "occluded", if only temporarily, by the maculae occludentes.

On a morphological basis, Farquhar and Palade (1965) considered that the zonula occludens must be the site of maximal constraint to the diffusion of micro and macromolecules between cells of the amphibian skin.

Horseradish peroxidase (HPO) is a substance with a molecular weight of 40,000 (slightly smaller than that of albumin). Its use as a tracer in electron microscopy has helped in the understanding of how macromolecules pass from the lamina propria through the epithelial sheet to the lumen in normal tissues. Becker, Novikoff and Zimmerman (1967) found that the egress of HPO from the circulation into the cerebrospinal fluid via choroidal cells in the rat was

apparently blocked by apical zonulae occludentes. HPO was also present within cells in coated vesicles which appeared to arise from the lateral plasmalemmata.

Apical intercellular junctions, namely zonulae occludentes, between epithelial cells in the small intestine of normal mice appeared to constitute an effective barrier to HPO which had been administered intravenously and lay between the epithelial cells (Hampton and Rosario, 1967). It was also found in vacuoles free within the epithelial cells.

A possible route for the egress of serum macromolecules, which is known to occur to a limited extent in normal healthy subjects, can be postulated: macromolecules pass from the lamina propria through the epithelial basement membrane into the intercellular space as far as the zonula occludens which acts as a barrier. The macromolecules then pass within the cell to the apical cytoplasm in vesicles and vacuoles and are discharged.

Considerable evidence has been presented above to suggest that the zonula occludens presents a barrier to the movement of macromolecules into and out of epithelia. However, there are two reports that suggest that this might not be the case. Sedar (1966), in a short communication, stated that HPO passed intercellularly between zonulae occludentes, zonulae adhaerentes and maculae adhaerentes (desmosomes) of the ductuli efferentes of the Syrian hamster. In addition, it was shown by Yodaiken (1966) that the zonula occludens did not appear to act as a barrier to the movement of lead-gum acacia combinations from the liver sinusoid to the bile canaliculus, although the passage of this tracer through the zonula occludens was not demonstrated.

Jarrett (1966) discussed the movement of macromolecules through the gastric mucosa of calves infected with O. ostertagi and suggested a breach in the integrity of the epithelium due to improper fusion of the zonula occludens between cells with the resultant egress of macromolecules. In addition it has been suggested that the raised plasma pepsinogen levels found in certain phases of ostertagiasis (Anderson et al., 1965; Jennings et al., 1966) might be a marker of a leaky mucosa. It was theorised that the pepsinogen secreted into the lumen was not activated due to the elevated abomasal pH and then passed back between cells into the circulation (Jarrett, 1966; Jennings, Armour, Kirkpatrick and Murray, 1967).

Based on the knowledge that in Type II ostertagiasis, low serum albumin levels are found and a loss of macromolecules into the gastrointestinal tract occurs, a study was made with the light and electron microscope of the changes in the gastrointestinal tract which might be related to increased permeability to macromolecules. Tissues were examined from 10 young cattle with Type II ostertagiasis.

RESULTS

The main pathological features of Type II ostertagiasis are similar to, but are usually more marked than in Type I (Section III). The lesions are produced by waves of development and emergence of large numbers of previously inhibited larvae (Anderson et al., 1965). Therefore, one finds some lesions of the inhibited phase plus the simultaneous presence of all lesions due to larval development and emergence (Fig.152). The inhibited fourth stage larvae

lie in glands which are lined by mucous epithelium; the associated mesenchymal reaction is minimal. When these larvae start to mature, nodules develop as in Type I (Section III); surrounding these after emergence are areas of epithelial hyperplasia, the gastric mucosa being lined by rapidly-dividing, undifferentiated cells (Fig. 153). Confluence of nodules leads to extensive hyperplastic areas of morocco leather appearance (Fig. 154) which are devoid of functionally differentiated cells. Epithelial sloughing and necrosis can be extensive (Figs 155 and 156); congestion may be marked and oedema is often very severe. In these areas, the surface mucous cells, normally columnar in shape, are stretched and flattened (Fig. 157) and the subepithelial lymphatics are greatly distended. Globule leukocytes are numerous (Fig. 158) and lymphoreticular and plasma cell activity can be marked.

Ultrastructural examination of this hyperplastic mucosa shows that the outline of lateral cell boundaries of many cells is delineated by diffusely distributed electron-dense material which lies between adjacent lateral cell membranes (Figs. 159, 160 and 161). This material traverses the entire length of the cell from the basement membrane to the lumen of the gland and causes irregular dilatation of the intercellular space. In other areas, patches of electron-dense material are found between the lateral boundaries of cells (Fig. 162). In some cells membrane-bound vacuoles, filled with electron-dense material, are present in the cytoplasm close to the lateral border (Fig. 163). They are particularly numerous in the apical cytoplasm.

Examination of the juxtaluminal segments of these cells shows that the electron-dense material lies in the intercellular spaces between the lateral

trilaminar membranes often beyond the macula adhaerens (desmosome) and the zonula adhaerens; these structures are not altered in any way. However, between many cells the lateral cell membranes which form the zonula occludens are separated (Fig. 164) and the spaces are often filled with electron-dense material (Fig. 165); in other cases the zonula occludens is much shorter than normal (Fig. 166). Although the membranes forming the zonula occludens are usually in contact at some point, electron-dense material is often beyond the points of lateral membrane contact. It is likely that these points of contact do not completely encircle the cell and hence cannot act as barriers to this electron-dense material. In some areas, although the lateral plasmalemmata forming the zonula occludens are completely (Fig. 167) or partially separated (Fig. 168), electron-dense material is not present between them. Figure 169 and Figs. 10 and 11 (Section II) show tripartite junctional complexes between gastric epithelial cells in parasite-free animals.

These changes are found between all cell types and at all levels of the fundus and pylorus; they appear to occur most commonly between undifferentiated cells. The last observation may be biased by the fact that in severely hyperplastic mucosae the cells present are mainly undifferentiated. It is estimated that in the cases examined between 50 and 90% of the junctional complexes were affected.

In areas of severe subepithelial oedema (Fig. 157), the intercellular spaces are often markedly dilated (Fig. 170) by material of moderate electron density. The junctional complexes between many of these cells are separated as described above.

The parasite O. ostertagi can measure up to 10 mm. (Armour, 1967) and its presence, therefore, has a considerable physical effect on the gastric mucosa, producing stretching and flattening of epithelial cells in and around parasitised glands (Section III, Fig. 46). Electron micrographs of such fields, show that these flattened cells are stretched to the extent that they are partially or completely torn apart (Figs. 172 and 173). The zonula occludens between many of these cells is shortened (Fig. 171) or completely disrupted (Fig. 174).

Thus, the integrity of the epithelium is breached in two ways: firstly, by separation of the lateral plasmalemmata forming the zonula occludens between cells; secondly, by the tearing apart of flattened epithelial cells lining glands, probably dilated by the physical presence of the parasite.

Structural changes also occur in the microcirculation. Junctions between many endothelial cells lining the post-capillary venules are separated (Fig. 175); other parts of the microcirculation, i.e. capillaries and arterioles show no such change. Lymphatic vessels are greatly distended (Fig. 176).

Electron-microscopic study of the small intestine reveals no structural abnormalities, (Fig. 177).

DISCUSSION

Hypoalbuminaemia, the result of gastroenteropathy, has been reported in association with a wide range of conditions in man (Waldmann, 1966). In cattle and sheep, hypoalbuminaemia occurs in a variety of parasitic conditions (Table 5). In Type II ostertagiasis, Mulligan *et al.* (1963) and Nielsen (1966) and in experimental fasciolaisis in rabbits, Dargie, Holmes, Maclean and Mulligan (1967) have demonstrated a loss of plasma macromolecules into the gut and biliary tract respectively. However, the structural changes in the bowel wall associated with increased permeability to macromolecules, have not been described in man or animals.

Electron-microscopic examination of tissues from cattle infected with *O. ostertagi* shows electron-dense material lying between epithelial cells lining the gastric mucosa, extending from the basement membrane along the lateral boundaries of adjacent cells and passing between open *zonulae occludentes* into the lumen. It is probable that this material is protein; the basis for this argument is that its electron density is similar to known protein-containing structures within cells such as zymogen granules.

Previous workers (Hampton and Rosario, 1967; Becker *et al.*, 1967) have shown that in normal tissue the *zonula occludens* acts as a site of maximum restraint to the egress of macromolecules through epithelial cell sheets; it appears that material blocked at this level passed within cells to the apical cytoplasm in vesicles and vacuoles. Therefore, the enhanced permeability of the bowel wall in bovine ostertagiasis to macromolecules is probably due to

widespread breakdown of zonulae occludentes. In some areas electron-dense material is located in vesicles and vacuoles close to the lateral plasmalemmata; it is possible that these occur where the zonulae occludentes are still intact and are restraining the egress of macromolecules.

It is likely that this material lying between cells is either albumin leaking out of the mucosa and/or non-activated pepsinogen passing from the gastric lumen into the circulation. Hampton and Rosario (1967), using corn oil via stomach tube and HPO intravenously as tracers, demonstrated that these substances, given simultaneously, use the same route to pass into or to pass out of the epithelial sheet, i.e. corn oil was absorbed by the epithelial cells, passed into the intercellular space through the basement membrane to the lymphatics while HPO passed from the circulation, through the epithelial basement membrane to the intercellular space up to the zonula occludens and then moved through the cells in vesicles and vacuoles probably to be secreted into the lumen. By analogy, it is possible that albumin is leaking out of the mucosa while pepsinogen is leaking in.

Although the physical presence of the parasite O. ostertagi is responsible for breakdown of cell junctions within certain glands, most frequently separation of the lateral plasmalemmata forming the zonula occludens occurs between cuboidal and columnar cells which do not appear to be stretched. Many of these cell types are rapidly-dividing non-functional stem cells. It has been demonstrated that in the absorptive epithelial cells of the developing small intestine of the embryo rat, tight junctions (zonulae occludentes) and desmosomes do not appear until

day 16 (Dunn, 1967). In addition, Trelstad, Revel and Hay (1966) were able to find the components of the tripartite junctional complex only in late stages of chick embryo development. It is possible that the zonulae occludentes between rapidly-dividing stem cells in the gastric mucosa of cattle with ostertagiasis, have not had time to become fully formed.

A similar situation may exist in human patients with giant hypertrophy of the gastric mucosa or with gastric cancer. In both conditions, hypoproteinaemia has been shown to be the result of protein loss into the stomach. It is possible that the junctional complexes between the rapidly-dividing cells in giant hypertrophy of the gastric mucosa and between cancer cells, are not completely formed, thereby allowing plasma macromolecules to leak into the stomach.

This hypothesis is not supported by the finding of open zonulae occludentes between fully differentiated gastric epithelial cells.

In many parasitic infections in domestic animals, low blood calcium and magnesium levels have been found. Nielsen (1966) recorded hypocalcaemia in bovine ostertagiasis and suggested that the calcium loss was found to albumin leaking into the gut. There is considerable evidence that the structural and physiological integrity of cells depends on the electrostatic binding of cell-to-cell surfaces by divalent cations. Jones (1966) and Jones (1966) demonstrated the importance of calcium and magnesium in cell adhesiveness. Sedar and Forte (1964), using the chelating agent ethylenediamine tetra-acetic acid (EDTA), produced considerable alteration in tripartite junctional complexes between parietal cells in the gastric mucosa of the frog Rana pipiens. There was marked

separation of the apposed leaflets of the lateral cell membranes of the zonula adhaerens and the macula adhaerens (desmosome). The changes in the zonula occludens were not so obvious and it was suggested that a stronger binding component existed between adjacent cells at this level. However, they did find an increased frequency of separations or openings of the membranes in this area in EDTA-treated sections. These investigators concluded that the reduction of the trans-mucosal potential difference which must lead to increased permeability was produced by calcium depletion and was the result of the creation of extra-cellular channels between epithelial cells. Cassidy and Tidball (1967) found that EDTA provoked a fivefold increase in membrane permeability of the small intestine of the rat to phenolsulphthalein (phenol red); at the same time, the mucosa content of magnesium and calcium decreased significantly. Although they demonstrated areas of intercellular distension beyond the zonula occludens and the zonula adhaerens and in the desmosomes in common with Sedar and Forte (1964), they found changes in the zonula occludens in only one of 200 examined and considered this to be a preparation artefact. They concluded that phenol red with a molecule size of 30 Å could not have passed between cells but must have moved into them. It has been shown that the bladder mucosa of the toad is only slightly permeable to inulin (molecular weight = 5,500) (Hays, Singer and Malamed, 1965). The withdrawal of calcium by means of EDTA resulted in complete dissociation of the cell lateral junctions and a 60 times increase in the permeability of the mucosa. It may be that altered mineral metabolism found in some parasitic conditions interferes with the structural integrity of the

tripartite junctional complexes joining epithelial cells resulting in increased permeability.

On the other hand, it is possible that serum proteins, once released from the circulation, force their way between epithelial cells and by their physical presence break down the zonulae occludentes. This is probably true to some extent in severe ostertagiasis where marked accummulation of protein-rich fluid occurs in the subepithelial tissue of the folds; ultrastructural examination of these areas shows marked dilatation of intercellular spaces of surface mucous cells by moderately electron-dense material, probably proteinaceous fluid, and separation of the lateral plasmalemmata forming the zonula occludens. However, opening up of the zonulae occludentes also occurs between cells in areas where little oedema is present, i.e. hyperplastic areas and in the pylorus where the mucosa is arranged in shallow folds and oedema is never marked; it is likely that some mechanism other than physical force is responsible for the breakdown of these cell junctions.

Neilsen (1966) considered that the leakage of serum proteins into the gut in bovine ostertagiasis was not confined to the diseased organ, the hyperplastic parasitised abomasum, but occurred also in the small intestine. In this study, ultrastructural changes probably related to protein leak were confined to the fundus and the pylorus.

The junctions between endothelial cells lining many post-capillary venules are separated; such a change is indicative of enhanced permeability of the microcirculation to macromolecules (Majno, Palade and Schoefl, 1961; Movat and Fernando, 1964; Cotran, 1967; and Karnovsky, 1967). The use of macromolecular

tracers to determine the site and extent of this vascular leak proved to be technically impossible in the bovine. Mast cells known to contain 5-hydroxytryptamine are located in the vicinity of these blood vessels (Murray et al., 1968; Section V) and it is known that junctions between endothelial cells in venules are particularly sensitive to vasoactive amines such as histamine and 5-HT.

That the release of such amines is responsible for the enhanced permeability of the microcirculation of the bovine gastric mucosa is likely, but has not yet been demonstrated. Vasoactive amines, once released, may also have some effect on the permeability of the epithelial sheet.

Since the gastrointestinal tract is an important site of immunoglobulin synthesis (Crabbé and Heremans, 1966; Gelzayd et al., 1967), the movement of macromolecules across the bowel wall may be important not only in the increased loss of albumin, but also in the transport or passage of locally-produced antibody to target sites on parasites within the gut.

ACKNOWLEDGEMENTS.

I would like to record my appreciation for the help which I received during the course of this work.

I am indebted to Professor W.F.H. Jarrett under whose supervision the work was carried out.

Thanks are due to Dr. J. Armour, Dr. G.M. Urquhart and Dr. F.W. Jennings who made the parasitological and biochemical observations described in Sections III and IV.

I wish to express my appreciation to the following: Mr. A. Finnie who prepared the light micrographs in Section III, Mr. J. Murphy for his help in the post-mortem room and Mrs. Celia Burke, Mrs. Sheila Cranston, Mrs. Carol Maclay and Miss Mona Lyle for technical assistance. For their help in mounting the photomicrographs so carefully, I would like to thank Miss Dorothy Fleming and Miss Rosemary Brown.

For her patience and long hours of secretarial work, I am most grateful to Miss Jacqueline Sommerville.

Finally I wish to express my thanks to the Agricultural Research Council, Allen and Hanburys Ltd. and Merck, Sharp and Dohme with whose financial support this work was carried out.

REFERENCES

Ackert, J.E. and Muldoon, W.E. 1920. J. Am. vet. med. Ass. 58 138 - 148.

Anderson, N., Armour, J., Eadie, R.M., Jarrett, W.F.H., Jennings, F.W., Ritchie, J.S.D., Urquhart, G.M. 1966. Am. J. vet. Res. 27 1259 - 1265.

Anderson, N., Armour, J., Jarrett, W.F.H., Jennings, F.W., Ritchie, J.S.D. and Urquhart, G.M. 1965. Vet. Rec. 77 1196 - 1204.

Armour, J. 1967. Ph.D. Thesis University of Glasgow. Ostertagia ostertagi infections in the Bovine: Field and Experimental Studies.

Armour, J., Jarrett, W.F.H. and Jennings, F.W. 1966. Am. J. vet. Res. 27 1267 - 1278.

Armour, J., Jennings, F.W., Kirkpatrick, K.S., Malezewski, A., Murray, Max and Urquhart, G.M. 1967. Vet. Rec. 80 510 - 514.

Armour, J., Jennings, F.W. and Urquhart, G.M. 1967. Personnal Communication.

Bailey, W.S. 1956. 'Diseases of Cattle' 1st Edition. American Veterinary Publications Inc. 206 - 219.

Barth, E.E.E., Jarrett, W.F.H. and Urquhart, G.M. 1966. Immunology. 10 459 - 464.

Becker, N.W., Novikoff, A.B. and Zimmerman, H.M. 1967. J. Histochem. Cytochem. 15 160 - 165.

Benditt, E.P. and Lagunoff, D. 1964. Prog. Allergy. 8 195 - 223.

Bessis, M. 1964. 'Electron Microscopic Anatomy' editor S.M. Kurtz. Academic Press, New York and London.

Blair, E.L. 1966. Postgraduate Gastroenterology editors T.J. Thomson and I.E. Gillespie. Bailliere, Tindall and Cassell, London.

Bloom, G. and Kelly, J.W. 1960. Histochemie. 2 48 - 57.

Bloom, G.D. and Haegermark, O. 1965. Expl. Cell. Res. 40 637 - 654.

Bonnet, R. 1895. Dt. med. Wschr. 21 58.

Brambell, F.W.R. 1958. Biol. Rev. 33 481 - 531.

Bremner, K.C.B. 1961. Aust. J. agric. Res. 12 498 - 512.

Brightman, M.W. 1962. Anat. Rec. 142 219.

Brightman, M.W. 1965. J. Cell. Biol. 26 99 - 123.

Bruford, J.W. and Fincham, I.H. 1945. Vet. Rec. 57 421 - 424.

Cardell, R.R., Badenhausen, S. and Porter, K.R. 1967. J. Cell. Biol. 34 123 - 155.

Carleton, H.M. and Drury, R.A.B. 1957. 'Histological Technique' 3rd Edition Oxford University Press.

Cassidy, M.M. and Tidball, C.S. 1967. J. Cell. Biol. 32 685 - 598.

Choi, J.K. 1962. Anat. Rec. 142 222.

Choi, J.K. 1965. J. Cell. Biol. 25 175 - 192.

Christie, M.G., Brambell, M.R. and Mapes, C.J. 1967. Vet. Rec. 80 207.

Citrin. Y., Sterling, K. and Halsted, J.A. 1957. New Eng. J. Med. 257 906 - 912.

Clayden, E.C. 1955. 'Practical Section Cutting and Staining' 3rd Edition. J. and A. Churchill Ltd., London.

Combs, J.W. 1966. J. Cell. Biol. 31 563 - 575.

Combs, J.W., Lagunoff, D. and Benditt, E.P. 1965. J. Cell. Biol. 25 577 - 592.

Corpron, R.E. 1966. Am. J. Anat. 118 53 - 89.

Cotran, R.S. 1967. Expl. Mol. Pathol. 6 143 - 155.

Coupland, R.E. and Heath, J.D. 1961. J. Endocr. 22 71 - 76.

Crabbé, P.A. and Heremans, J.F. 1966. Gastroenterology. 51 305 - 316.

Dargie, J.D., Holmes, P.H., MacLean, J.M. and Mulligan, W. 1967. Vet. Rec. 390.

Davidson, J.B., Murray, Max and Sutherland, I.H. 1968. 'Reaction of Host to Parasitism' editor E.L. Soulsby. London Academic Press.

Dawson, A.M., Williams, R. and Williams, H.S. 1961. Br. med. J. 2 667 - 670.

Diamond, J.M. and Tormey, J. McD. 1966. Nature, Lond. 210 817 - 820.

Dich, J., Paaby, H. and Schwartz, M. 1961. Br. med. J. 2 686 - 688.

Dobbins, W.O. 1966. Gastroenterology. 50 195 - 210.

Dobbins, W.O. 1966. Gastroenterology. 51 1004 - 1017.

Dobson, C. 1966. Aust. J. agric. Res. 17 955 - 966.

Dunn, J. Shaw. 1967. J. Anat. 57 - 68.

Edwards, K., Jepson, R.P. and Wood, K.F. 1960. Br. med. J. 1 30 - 32.

Enerbäch, L. 1966a. Acta. path. microbiol. scand. 66 289 - 302.

Enerbäch, L. 1966b. Acta. path. microbiol. scand. 66 303 - 312.

Enerbäch, L. 1966c. Acta. path. microbiol. scand. 67 365 - 379.

Falck, B., Hillarp, N.-Å., Thieme, G. and Torp, A. 1962. J. Histochem. 10 348 - 354.

Falck, B., Nystedt, T., Rosengren, E. and Stenflo, J. 1964. Acta. pharmac. tox. 21 51 - 58.

Farquhar, M.G. and Palade, G.E. 1963. J. Cell. Biol. 17 375 - 412.

Farquhar, M.G. and Palade, G.E. 1965. J. Cell. Biol. 26 263 - 291.

Fujita, T. 1965. Z. Zellforsch. mikrosk. Anat. 55 66 - 82.

Gardner, R.C.B. 1911. Jl. S.-east agric. Coll. Wye. 20 482 - 493.

Gelzayd, E.A., Kraft, S.C. and Fitch, F.W. 1967. Science, N.Y. 157 930 - 931.

Glass, G.B.J. and Ishimori, A. 1961. Am. J. dig. Dis. 6 103 - 133.

Glauert, A.M. 1965. 'Techniques for Electron Microscopy' editor D.H. Kay. 2nd Edition. Blackwell Scientific Publications.

Gonzalez-Licea, A. and Yardley, J.H. 1966. Gastroenterology. 51 825 - 838.

Gracey, J.F. 1960. H.M.S.O. 'Survey of Livestock Diseases in Northern Ireland'.

Graham, R.C. and Karnowsky, M.J. 1966. J. exp. Med. 124 1123 - 1134.

Green, H., Fleischer, R.A., Barrow, P. and Goldberg, B. 1959. J. exp. Med. 109 511 - 521.

Grossman, M.I. and Marks, I.N. 1960. Gastroenterology. 38 343 - 352.

Ham, A.W. 1965. 'Histology' 5th Edition. Pitman Medical Publishing Co. Ltd., London.

Hampton, J.C. and Rosario, B. 1967. Anat. Rec. 159 159 - 170.

Hays, R., Singer, B. and Malamed, S. 1965. J. Cell. Biol. 25 195 - 208.

Hayward, A.F. 1967a. J. Anat. 101 69 - 81.

Hayward, A.F. 1967b. Z. Zellforsch. mikrosk. Anat. 78 474 - 483.

Helander, H.F. 1962. J. Ultrastruct. Res. Suppl. 4 7 - 123.

Herlich, H. 1962. Am. J. vet. Res. 23 521 - 528.

Herlich, H. 1967. Am. J. vet. Res. 28 71 - 77.

Hill, K.J. 1961. Vet. Revs. Annot. 7 83 - 106.

Hirschowitz, B.I. 1967. Ann. N.Y. Acad. Sci. 140 709 - 723.

Holman, H., Nickel Jr. W.F. and Sleisenger, M.H. 1959. Am. J. Med. 27 963 - 975.

Horak, I.G. and Clark, R. 1963. Onderstepoort. J. vet. Res. 30 145 - 159.

Horak, I.G. and Clark, R. 1964. Onderstepoort. J. vet. Res. 31 163 - 176.

Hudson, G. 1967. Expl. Cell. Res. 46 121 - 128.

Hunt, T.E. and Hunt, E.A. 1962. Anat. Rec. 142 505 - 517.

Isselbacher, K.L. and Budz, D.M. 1963. Nature. Lond. 200 364 - 365.

Ito, S. and Winchester, R.J. 1963. J. Cell. Biol. 16 541 - 572.

Jagatic, J. and Weiskopf, R.W. 1966. Archs. Path. 82 430 - 433.

Jarnum, S. and Schwartz, M. 1960. Gastroenterology. 38 769 - 776.

Jarrett, W.F.H. 1966. 'The Pathology of Parasitic Diseases' Fourth Symposium of the British Society for Parasitology. 33 - 40.

Jarrett, W.F.H., Jarrett, E.E.E., Miller, H.R.P. and Urquhart, G.M. 1968. 'Reaction of Host to Parasitism' editor E.L. Soulsby, London Academic Press.

Jarrett, W.F.H., Miller, H.R.P. and Murray, Max. 1967. Vet. Rec. 80 505 - 506.

Jennings, F.W., Armour, J., Lawson, D.D. and Roberts, R. 1966. Am. J. vet. Res. 27 1249 - 1257.

Jennings, F.W., Armour, J., Kirkpatrick, K.S. and Murray, Max. 1968. 'Reaction of Host to Parasitism' editor E.L. Soulsby, London Academic Press.

Jones, B.M. 1966. Nature, Lond. 212 362 - 365.

Jones, P.C.T. 1966. Nature, Lond. 212 365 - 369.

Jones, V.E. and Ogilvie, B.M. 1967. Int. Archs. Allergy appl. Immun. 31 490 - 504.

Karnovsky, M.J. 1967. J. Cell. Biol. 35 213 - 236.

Kaye, G.I. and Pappas, G.D. 1962. J. Cell. Biol. 12 457 - 479.

Kent, J.F. 1952. Anat. Rec. 112 91 - 115.

Kent, J.F. 1966. Anat. Rec. 156 439 - 454.

Kent, S.P. 1967. Am. J. Path. 50 623 - 637.

Kirkman, H. 1950. Am. J. Anat. 86 91 - 131.

Kurosumi, K., Shibasaki, S., Uchida, G. and Tanaka, Y. 1958. Arch. Histol. Japon. 15 587 - 624.

Kuttler, K.L. and Marble, D.W. 1960. Am. J. vet. Res. 21 445 - 448.

Lawn, A.M. 1960. J. biophys. biochem. Cytol. 7 161 - 166.

Lambson, R.O. 1966. Am. J. Anat. 118 21 - 52.

Leland Jr. S.E., Drudge, J.H. and Wyant, Z.N. 1959. Expl. Parasit. 8 383 - 412.

Leland Jr. S.E., Drudge, J.H. and Wyant, Z.N. 1960. Am. J. vet. Res. 21 458 - 463.

Lillibridge, C.B. 1964. Gastroenterology. 47 269 - 290.

Lindholm, S. 1960. Acta. path. microbiol. scand. 48 328 - 334.

McEwan, A.D. 1967. Personnal Communication.

Mahrt, J.L., Hammond, D.M. and Miner, M.L. 1964. Cornell Vet. 54 453 - 474.

Majno, G., Palade, G.E. and Schoefl, G.I. 1961. J. biophys. biochem. Cytol. 11 607 - 626.

Martin, W.B., Thomas, B.A.C. and Urquhart, G.M. 1957. Vet. Rec. 69 736 - 739.

Maser, M.D., Powell III, T.E. and Philpott, C.W. 1967. Stain Technol. 42 175 - 182.

Maunsbach, A.B. 1966. J. Ultrastruct. Res. 15 283 - 309.

Miller, F. 1960. J. biophys. biochem. Cytol. 8 689 - 718.

Miller, H.R.P. 1968. Ph.D. Thesis, University of Glasgow. In preparation.

Miller, H.R.P., Murray, Max and Jarrett, W.F.H. 1968. 'Reaction of Host to Parasitism' editor E.L. Soulsby, London Academic Press.

Moras, J.M. 1907. An. Soc. rur. argent. 49 181 - 187.

Mota, I., Ferri, O.G. and Yoneda, S. 1956. Q. Jl. microsc. Sci. 97 251 - 256.

Movat, H.Z. and Fernando, N.V.P. 1964. Expl. Mol. Pathol. 3 98 - 114.

Mulligan, W., Dalton, R.G. and Anderson, N. 1963. Vet. Rec. 75 1014.

Murray, Max, Miller, H.R.P. and Jarrett, W.F.H. 1968. Lab. Invest. (in press).

Neil, D.W. 1963. Joyce - Loebl Review, Spring Number.

Nielsen, K. 1966. 'Gastrointestinal Protein Loss in Cattle. A clinical pathophysiological study' Carl Fr. Mortensen, Copenhagen.

Ogilvie, B.M. 1964. Nature, Lond. 204 91 - 92.

Orrego, H., Navia, E. and Vial, J.D. 1966. Expl. Cell. Res. 43 351 - 357.

Osborne, J.C., Batte, E.G. and Bell, R.R. 1960. Cornell Vet. 50 223 - 235.

Ostertag, R. 1890. Centbl. Bakt., 1 Abt. 8 457 - 480.

Pearse, A.G.E. 1961. 'Histochemistry' 2nd Edition. J. and A. Churchill Ltd., London.

Piper, D.W. and Fenton, B.H. 1965. Gut. 6 506 - 508.

Reynolds, E.S. 1963. J. Cell. Biol. 17 208 - 212.

Richardson, K.C., Jarret, L. and Finke, E.M. 1960. Stain Technol. 35 313 - 323.

Ritchie, J.D.S., Anderson, N., Armour, J., Jarrett, W.F.H., Jennings, F.W. and Urquhart, G.M. 1966. Am. J. vet. Res. 27 659 - 667.

Rohrer, G.V., Scott, J.R., Joel, W. and Wolf, S. Am. J. dig. Dis. 10 13 - 21.

Ross, J.G. and Dow, C. 1965. Br. vet. J. 121. 228 - 233.

Ross, J.G., Dow, C. and Todd, J.R. 1967. Vet. Rec. 80 543 - 546.

Ross, J.G., Purcell, D.A., Dow, C. and Todd, J.R. 1967. Res. vet. Sci. 8 201 - 206.

Ross, J.G. and Todd, J.R. 1965. Br. vet. J. 121 55 - 64.

Ross, J.G., Todd, J.R. and Dow, C. 1963. Vet. Rec. 75 954.

Ross, J.G., Todd, J.R. and Dow, C. 1966. J. comp. Path. Ther. 76 67 - 81.

Sabatini, D.D. Bensch, K. and Barnett, R.J. 1963. J. Cell. Biol. 17 19 - 58.

Saunders, A.M. 1964. J. Histochem. Cytochem. 12 164 - 170.

Schiller, S. and Dorfman, A. 1959. Biochim. biophys. Acta. 31 278 - 280.

Schiraldi, C., Pastore, G., Strada, C. and Marano, R. 1968. Experentia. 24 45 - 46.

Schwartz, M. 1964. 'Protides of the Biological Fluids' editor H. Peeters. Elsevier Publishing Co., Amsterdam - London - New York.

Schwartz, M. and Jarnum, S. 1961. Dan. med. Bull. 8 1 - 10.

Sedar, A.W. 1964. 'Electron Microscopic Anatomy' editor S.M. Kurtz. Academic Press, New York and London.

Sedar, A.W. 1966. J. Cell. Biol. 31 102A.

Sedar, A.W. and Forte, J.G. 1964. J. Cell. Biol. 22 173 - 188.

Sedar, A.W. and Friedman, M.H.F. 1961. J. biophys. biochem. Cytol. 11 349 - 363.

Sewell, M.M.H. 1965. 83rd Annual Congress of B.V.A. 3 - 10.

Shibasaki, S. 1961. Arch. Histol. Japon. 21 251 - 258.

Shnitka, T. 1964. Can. med. Ass. J. 91 7 - 22.

Shumard, R.F., Bolin, D.W. and Eveleth, D.F. 1957. Am. J. vet. Res. 18 330 - 337.

Singleton, E.M. and Clark, S.L. 1965. Lab. Invest. 14 1744 - 1763.

Sisson, S. 1958. 'The Anatomy of the Domestic Animals' 4th Edition. W.B. Saunders Company, Philadelphia and London.

Smith, D.E. 1963. Ann. N.Y. Acad. Sci. 103 40 - 52.

Smith, D.E. and Lewis, Y. 1957. J. biophys. biochem. Cytol. 3 9 - 14.

Sommerville, R.I. 1956. Aust. vet. J. 32 237 - 240.

Spicer, S.S. 1963. Ann. N.Y. Acad. Sci. 103 322 - 333.

Spicer, S.S. and Lillie, R.D. 1961. Stain Technol. 36 365 - 370.

Stanley, M.M. 1965. Am. J. dig. Dis. 10 993 - 1003.

Stevens, C.E. and Leblond, C.P. 1953. Anat. Rec. 115 231 - 243.

Stiles, C.W. 1900 - 1901. U.S.D.A., Bur. Anim. Indus., 17th Ann. Rpt.

Taliaferro, W.H. and Sarles, M.P. 1939. J. infect. Dis. 64 157 - 192.

Threkeld, W.L. and Johnson, E.P. 1948. Vet. Med. 43 446 - 452.

Toner, P.G. 1965. Acta. anat. 61 321 - 330.

Townsend, S.F. 1961. Am. J. Anat. 190 133 - 147.

Trelstad, R.J., Revel, Jean-Paul and Hay, E.D. 1966. J. Cell. Biol. 31 C6 - C10.

Trump, B.J., Smuckler, E.A. and Benditt, E.P. 1961. J. Ultrastruct. Res. 5 343 - 348.

Turner, M.D., Miller, L.L. and Segal, H.L. 1967. Gastroenterology. 53 967 - 983.

Urquhart, G.M., Mulligan, W., Eadie, R.M. and Jennings, F.W. 1965. Expl. Parasit. 17 210 - 217.

Uvnäs, B. and Wold, J.K. 1967. Acta. physiol. scand. 70 269 - 276.

Vial, J.D. and Orrego, H. 1960. J. biophys. biochem. Cytol. 7 367.

Vial, J.D. and Orrego, H. 1963. Expl. Cell. Res. 30 232 - 235.

Waldmann, T.A. 1966. Gastroenterology. 50 422 - 443.

Weichselbaum, T.E. 1946. Am. J. clin. Path. tech. Suppl. 10 40 - 49.

Wells, P.D. 1962. Expl. Parasit. 12 82 - 101.

Wetterfors, J. 1965. Acta. med. scand. 177 1 - 72.

Wetterfors, J. 1964. 'Protides of the Biological Fluids' editor H. Peeters. Elsevier Publishing Co., Amsterdam - London - New York.

White, R.G. 1954. Br. J. exp. Path. 35 365 - 376.

Wilson, R.J.M. 1967. J. Parasit. 53 752 - 762.

Whur, P. 1966a. J. comp. Path. Ther. 76 57 - 65.

Whur, P. 1966b. Int. Archs. Allergy appl. Immun. 30 351 - 354.

Whur, P. and Gracie, M. 1967. Experentia. 23 655 - 657.

Whur, P. and Johnston, H.S. 1967. J. Path. Bact. 93 81 - 85.

Yodaiken, R.E. 1966. Lab. Invest. 15 403 - 411.

Zimmerman, K.W. 1911. Arch. mikrosk. Anat. Entw. Mech. 78 199 - 231.

APPENDICES

APPENDIX 1 - Table 1

Total Serum Proteins (gms/100 ml) of Calves

Following a Single Oral Inoculation of 300,000 O. ostertagi Larvae

Day	CALF NO. 1	2	3	4	5	Group Mean & Standard Error	
0	6.2	6.4	6.0	6.0	6.1	6.1	0.07
4	6.3	6.6	6.2	6.1	5.8	6.2	0.11
7	6.3	6.5	6.5	6.4	5.7	6.3	0.15
9	5.7	6.0	6.7	5.9	5.3	5.9	0.25
11	5.9	6.0	6.1	6.0	5.4	5.9	0.12
14	6.6	6.3	6.1	6.0	5.1	6.0	0.25
16	6.4	6.5	6.2	6.2	5.2	6.1	0.23
18	6.2	6.7	6.4	6.2	5.2	6.1	0.25
21	6.4	6.6	5.9	6.2	5.4	6.1	0.19
23	6.0	6.9	5.8	6.1	5.5	6.1	0.23
25	6.9	7.0	6.2	6.4	5.6	6.4	0.26
28	5.8	5.5	N	6.8	5.8	6.0	0.29
35	6.1	6.4	-	6.5	5.6	6.2	0.20
42	6.3	6.4	-	6.7	5.9	6.3	0.17
49	6.2	6.3	-	6.3	5.8	6.2	0.12
56	6.7	6.4	-	N	6.0	6.4	0.20
Mean	6.3	6.4	6.2	6.3	5.6		
Standard Error	0.32	0.36	0.26	0.27	0.30		

N = Necropsied

APPENDIX 1 - Table 2

Serum Albumin Levels (gms/100 ml) of Calves

Following a Single Oral Inoculation of 300,000 *O. ostertagi* Larvae

Day	CALF NO. 1	2	3	4	5	Group Mean & Standard Error	
0	2.2	2.9	2.3	2.7	2.7	2.6	0.13
4	2.2	2.4	2.5	2.6	2.4	2.4	0.07
7	2.4	2.4	2.7	2.6	2.3	2.5	0.07
9	2.4	2.5	2.8	2.6	2.4	2.5	0.07
11	2.1	2.3	2.7	2.6	2.3	2.4	0.11
14	2.3	2.5	2.9	2.4	2.2	2.5	0.12
16	2.6	2.3	2.2	2.9	2.5	2.5	0.12
18	2.6	2.8	2.8	2.6	2.2	2.6	0.11
21	2.1	2.3	2.4	2.3	2.5	2.3	0.07
23	2.4	2.1	2.4	2.3	2.2	2.3	0.06
25	2.0	2.4	2.4	2.3	2.3	2.3	0.07
28	2.4	1.9	N	2.5	2.1	2.2	0.14
35	2.1	2.3	-	2.7	2.3	2.4	0.13
42	2.2	2.2	-	2.5	2.1	2.3	0.09
49	2.3	2.3	-	2.3	2.5	2.4	0.05
56	2.4	2.2	-	N	2.5	2.4	0.09
Mean	2.3	2.4	2.6	2.5	2.3		
Standard Error	0.05	0.06	0.07	0.05	0.04		

N = Necropsied

APPENDIX 1 - Table 3

Plasma Pepsinogen Levels (m.U. of Tyrosine) In Calves
Following a Single Oral Inoculation of 300,000 O. ostertagi Larvae

Day	0	2	4	7	9	11	14	16	17	18	21	23
Calf No.												
1	600	800	1,200	1,800	2,200	1,700	3,000	3,600	4,500	7,600	5,400	7,900
2	1,200	1,200	1,500	1,900	1,600	1,500	1,900	2,900	4,000	5,800	6,700	9,700
3	800	N.S.	1,000	1,700	1,300	1,900	3,100	4,600	5,200	7,300	4,400	5,000
4	400	800	900	1,300	2,100	1,200	1,800	3,000	4,400	7,600	7,900	9,300
5	400	400	1,000	1,400	1,600	1,100	1,500	2,800	2,800	5,700	4,500	5,100
Mean	700	800	1,100	1,600	1,800	1,500	2,300	3,400	4,200	6,800	5,800	7,400
Standard Error	100	170	140	160	80	80	330	340	400	430	660	1,010

Day	25	28	30	32	35	37	39	42	49	56	63	70
Calf No.												
1	4,500	6,700	4,100	2,600	1,700	1,800	1,600	1,500	800	800	1,100	400
2	8,200	7,500	7,500	5,700	5,300	6,300	7,700	5,600	2,700	2,300	1,800	N
3	3,200	2,400	N	...	...	...	...	...	...	...	...	...
4	7,700	6,100	4,300	3,400	2,000	2,600	2,400	2,000	1,100	N	...	...
5	4,100	5,600	4,300	3,700	2,900	3,100	3,100	2,900	2,100	2,000	N	...
Mean	5.500	5,700	5,100	3,900	3,000	3,500	3,700	3,000	1,700	1,700	1,400	400
Standard Error	1,010	870	820	660	820	980	1,370	910	440	460	...	...

N = Necropsied

N.B. All Plasma Pepsinogen Values to Nearest 100. Standard Errors to Nearest 10

THE PATHOGENESIS OF BOVINE OSTERTAGIASIS

DISSERTATION FOR THE DEGREE

OF

DOCTOR OF PHILOSOPHY

IN

THE FACULTY OF MEDICINE

OF

THE UNIVERSITY OF GLASGOW

BY

MAXWELL MURRAY

DEPARTMENT OF EXPERIMENTAL VETERINARY MEDICINE

UNIVERSITY OF GLASGOW

1968

AUTHOR'S NOTE

This thesis is presented in two volumes because it contains a large number of micrographs; the first contains the text and the second, the illustrations.

V O L U M E II

KEY TO ABBREVIATIONS

A	=	Auer body	IC	=	intracellular canaliculi
BM	=	basement membrane	IS	=	intercellular space
C	=	centriole	L	=	lymphocyte
Ca	=	capillary	LY	=	lymphatic vessel
CF	=	cytoplasmic fibrils	M	=	mitochondria
E	=	epithelial cell	MA	=	macula adhaerens
ED	=	electron-dense material	MC	=	mast cell
En	=	enterochromaffin cell	MN	=	mucous neck cell
Eo	=	eosinophil leukocyte	MO	=	macula occludens
f	=	fibrils	P	=	parasite
G	=	granule	p	=	progranule
g	=	glycogen	Pa	=	parietal cell
GC	=	golgi complex	Pl	=	plasma cell
GG	=	gastric gland	pl	=	platelet
GL	=	globule leukocyte	Po	=	polymorphonuclear leukocyte
GP	=	gastric pit	PP	=	post-parasitised gland
I	=	interdigitations	R	=	red blood cell

RSER = rough-surfaced endoplasmic reticulum

S = surface mucous cell

TC = transitional cell

U = undifferentiated cell

V = vacuole

v = vesicle

Z = zymogen cell

ZA = zonula adhaerens

ZO = zonula occludens

CONTENTS

GENERAL INTRODUCTION

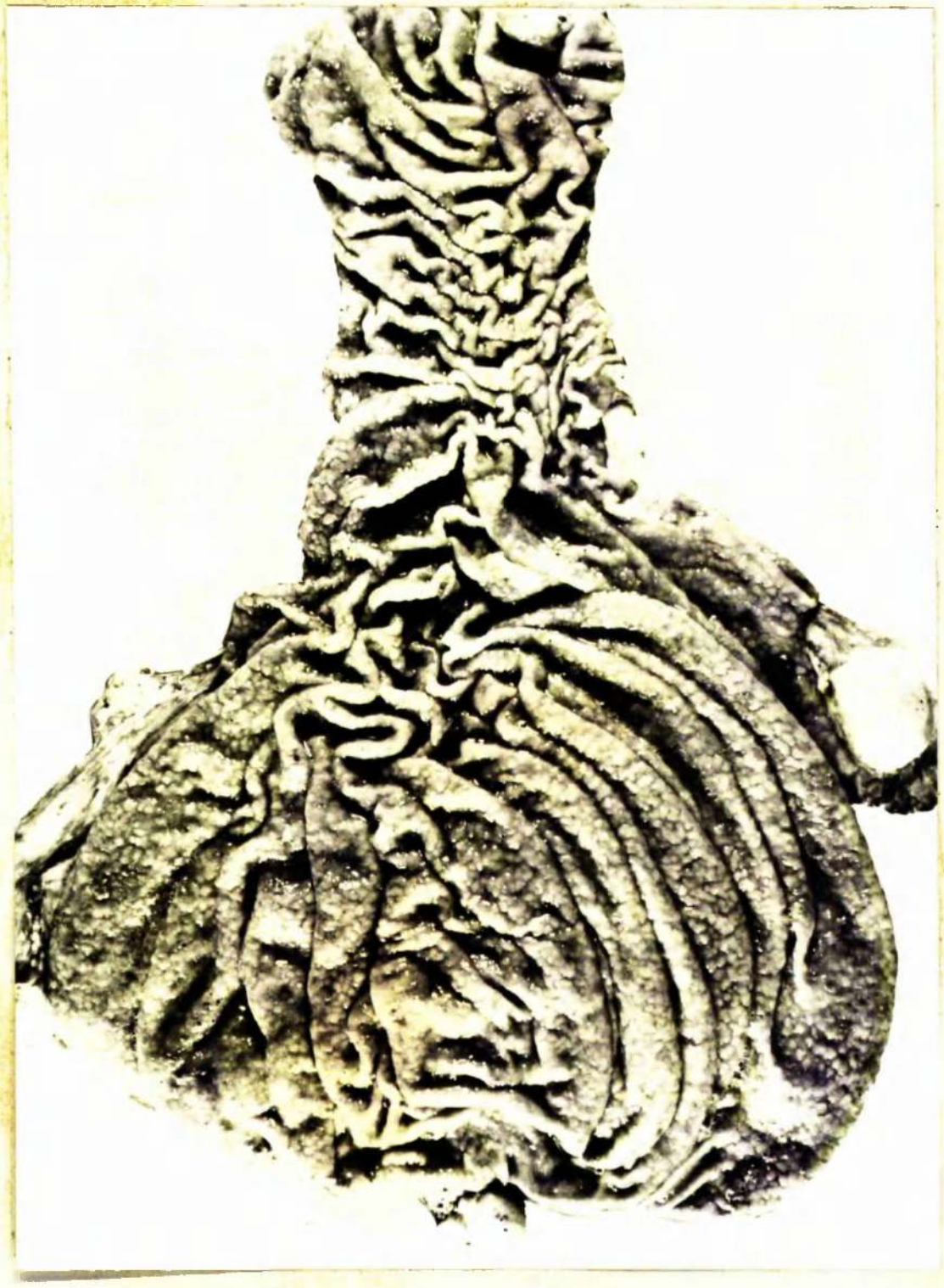

Figure 1. Bovine abomasum with severe ostertagiasis. Note morocco leather appearance of mucosa (confluence of lesions) and reactive lymph nodes.

SECTION I

PREPARATION OF BOVINE GASTRIC MUCOSA FOR ELECTRON MICROSCOPICAL EXAMINATION.

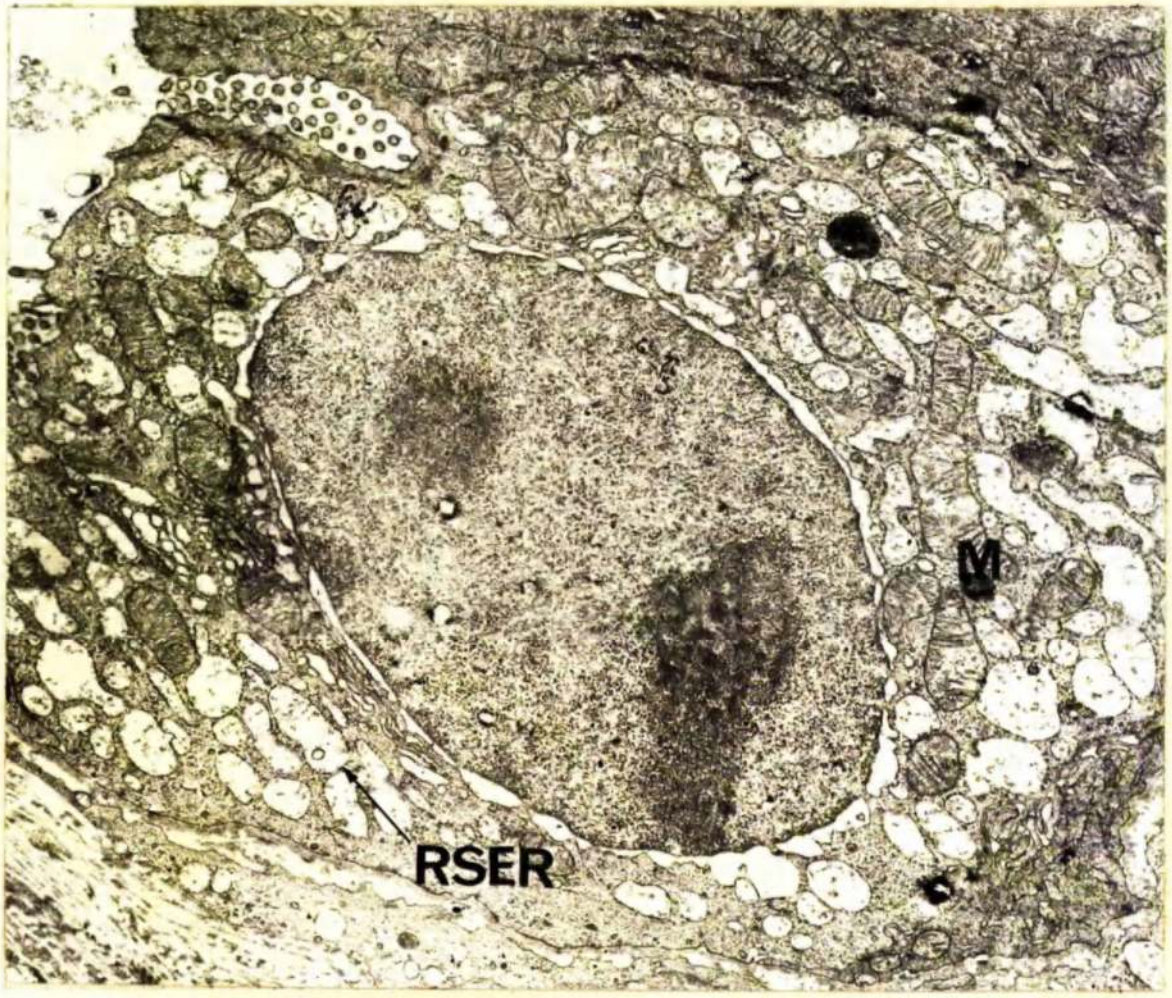

Figure 2. Tissue fixed in solution 1 (osmolality = 250 milliosmoles/ litre) showing swelling of mitochondria with breakage of cristae mitochondriales, dilatation of cisternae of RSER and separation of membranes encircling the nucleus. x 10,000.

Figure 3. Tissue fixed in solution 7 (osmolality = 450 milli-osmoles/litre) showing marked shrinkage and dilatation of intercellular spaces. x 12,500.

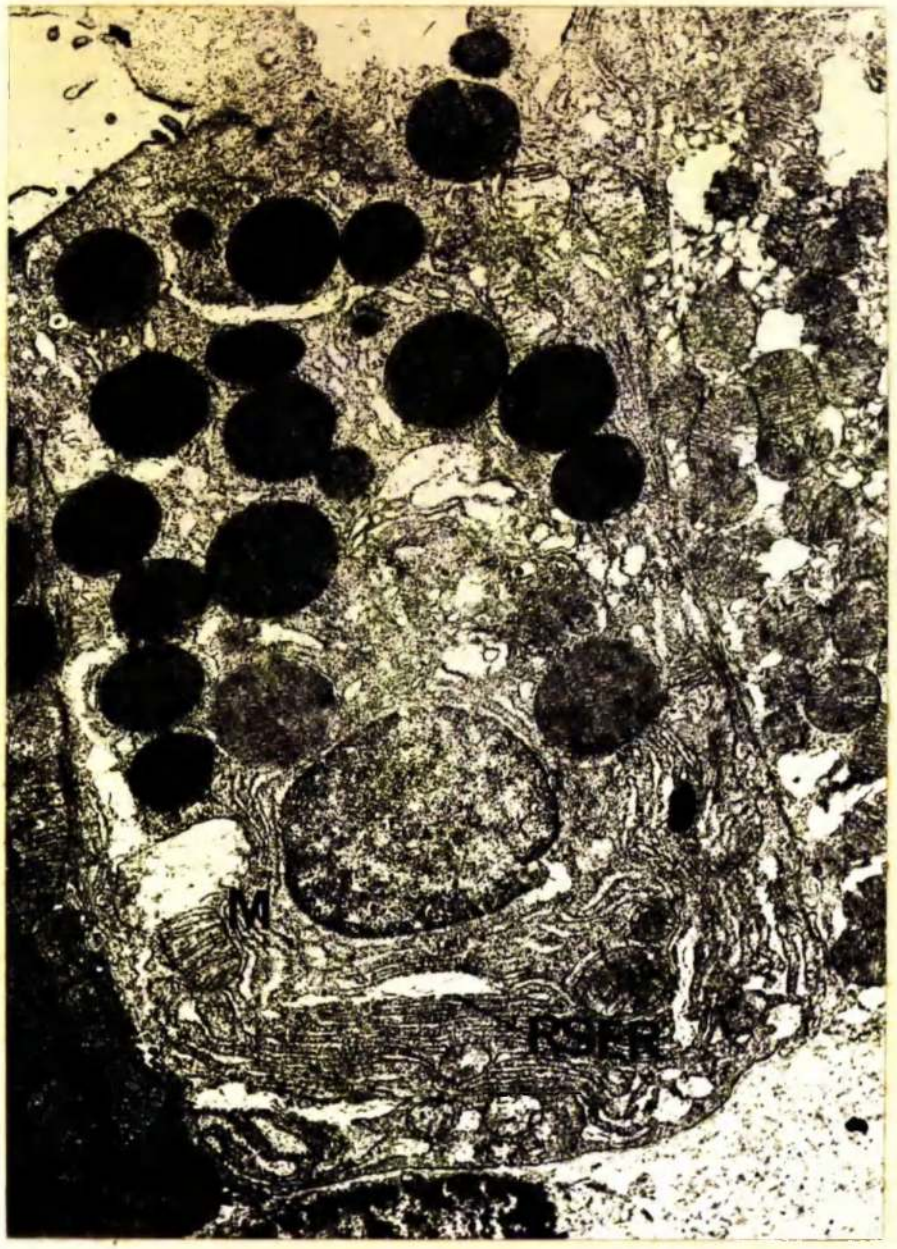

Figure 4. Tissue fixed in solution 12 (osmolality = 310 milliosmoles/litre) showing swelling of mitochondria with breakdown of cristae mitochondriales and some separation of the cisternae of RSER. x 12,500.

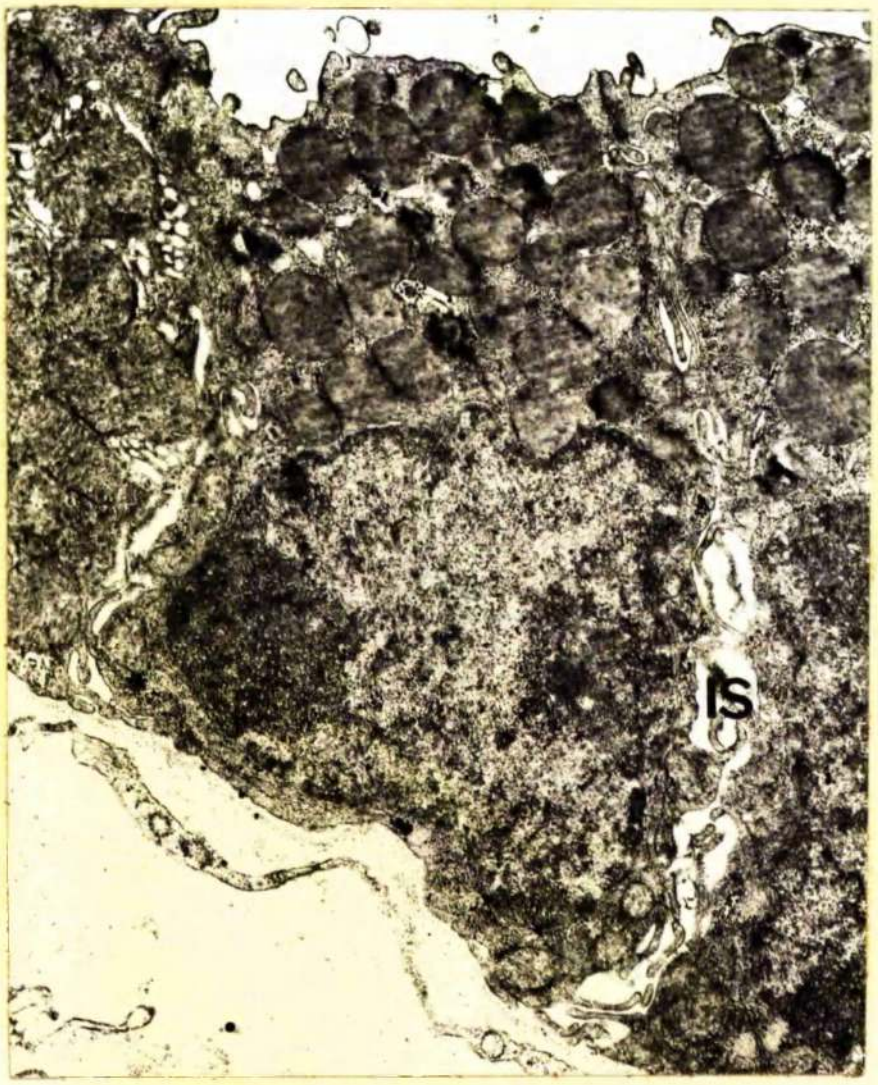

Figure 5. Tissue fixed in solution 16 (osmolality = 550 milliosmoles/litre) showing marked shrinkage and dilatation of intercellular spaces. x 18,750.

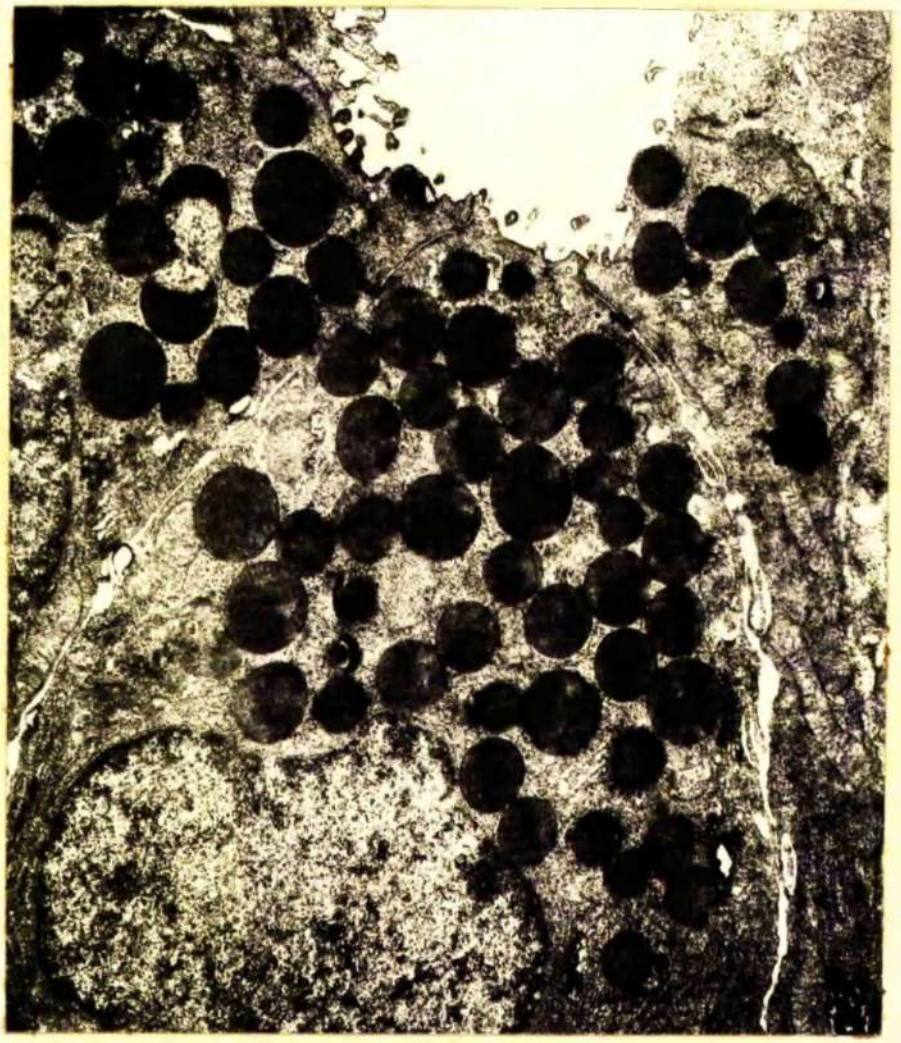

Figure 6. Tissue fixed in solution 15 (osmolality = 480 milliosmoles/litre) showing cell shrinkage and dilatation of intercellular spaces. x 12,500.

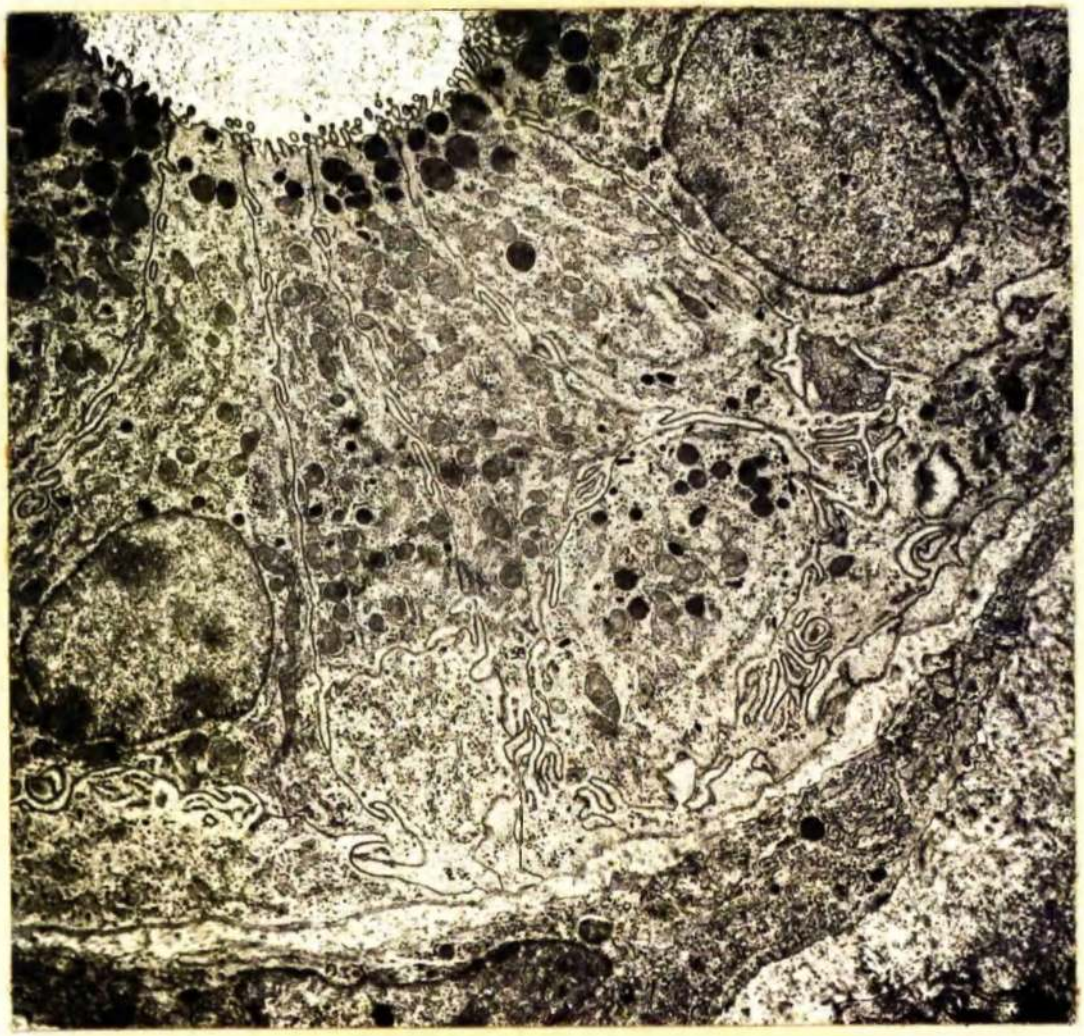

Figure 7. Tissue fixed in solution 17 (osmolality = 290 milli-osmoles/litre) showing good preservation of organelles and exact cell apposition. x 6,000

SECTION II

THE FINE STRUCTURE OF THE ABOMASAL MUCOSA OF THE PARASITE-FREE BOVINE

Figure 8 Gastric mucosa in fundal gland area showing gastric pit (GP) descending into gastric gland (GG). Note that the gastric glands are straight tubules lined by surface mucous and mucous neck cells (S and MN), parietal cells (Pa) and zymogen cells (Z). The gastric pit is about one quarter of the total thickness of the mucosa and is lined by surface mucous cells. picro-Mallory. x 390.

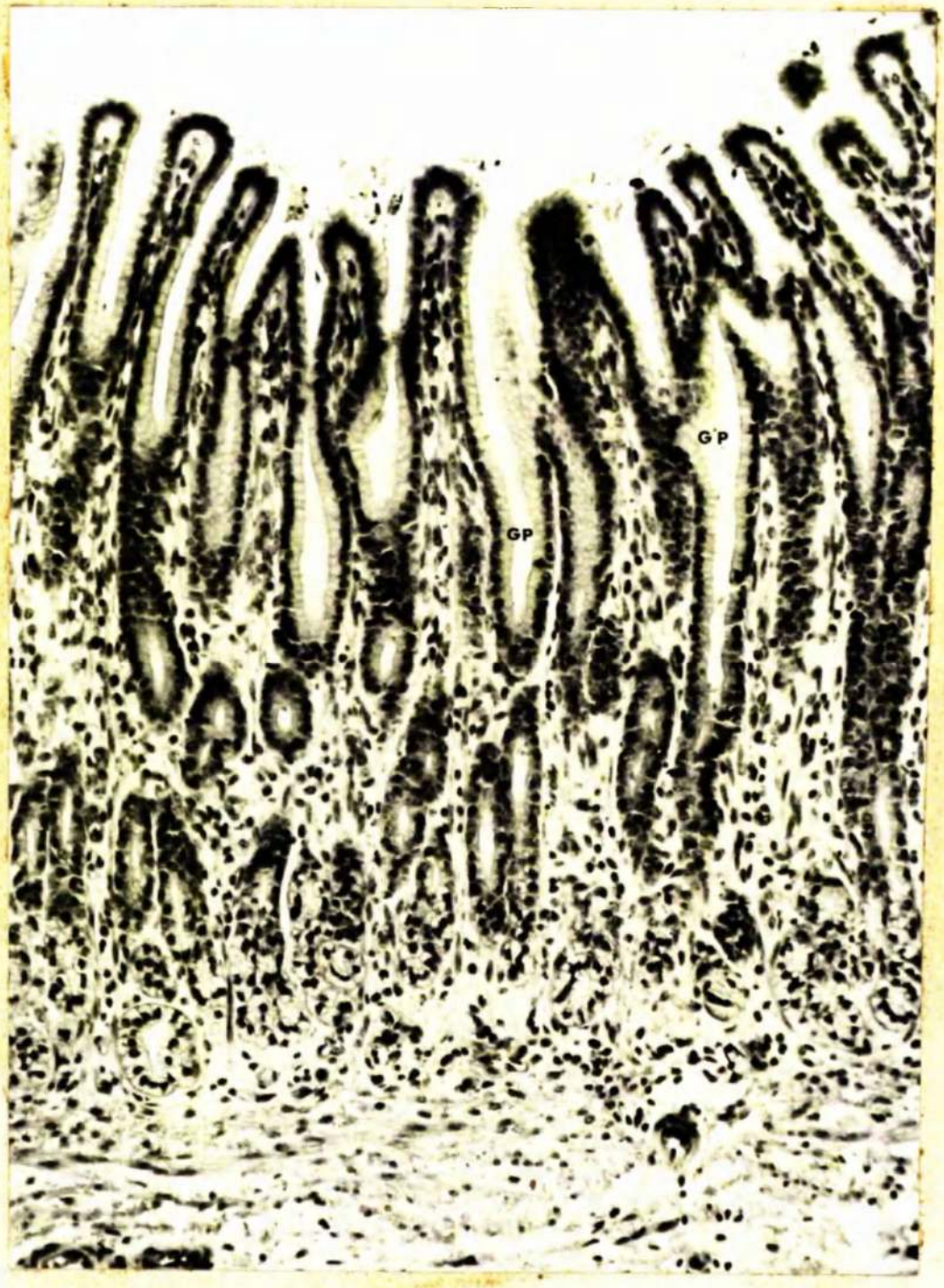

Figure 9. Gastric mucosa in pyloric gland area showing gastric pit (GP) descending into pyloric glands. Note that the gastric pits are deeper than in the fundal area and the pyloric glands are coiled. x 200.

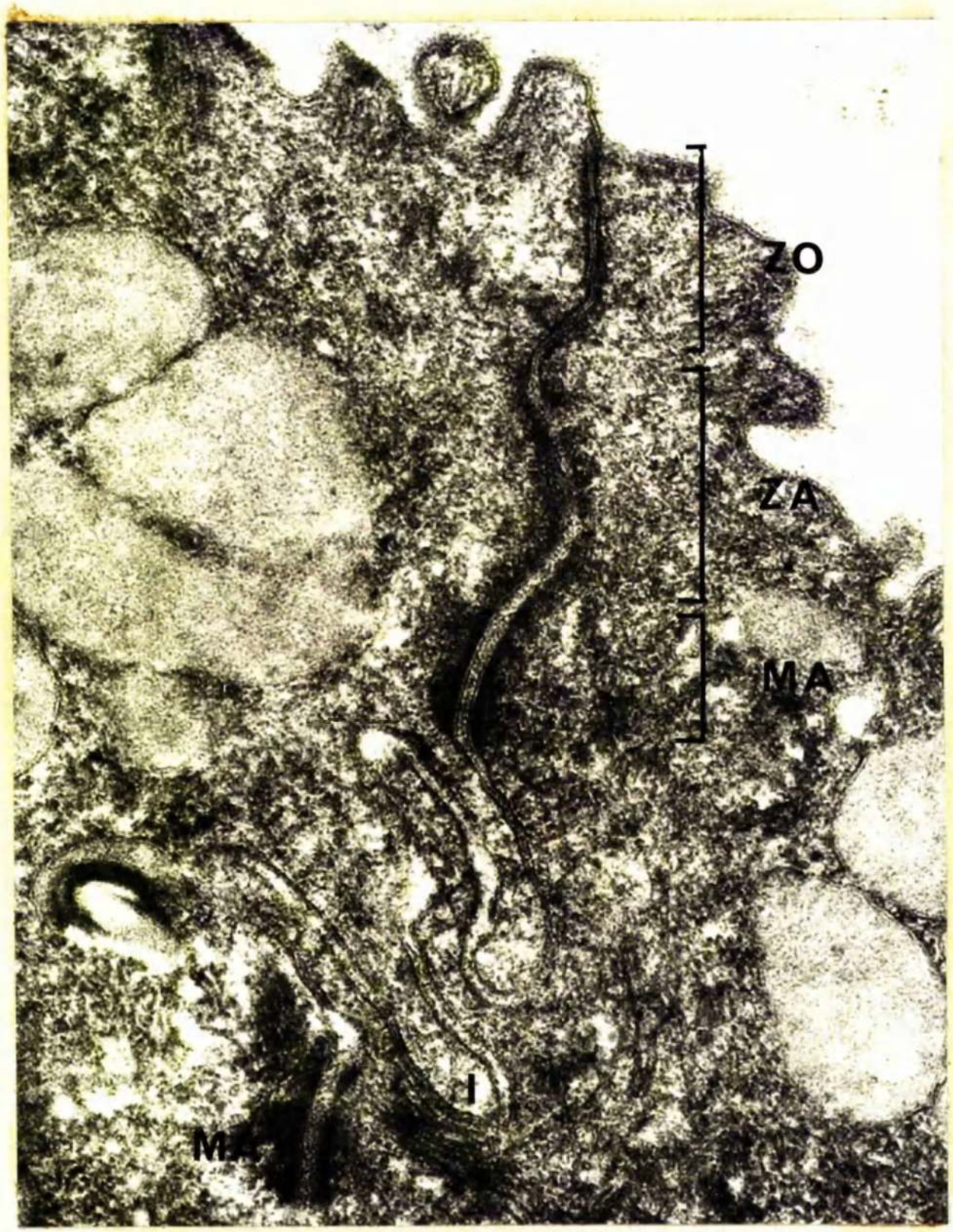

Figure 10. Tripartite junctional complex between surface mucous cells. Note the 3 components of the complex, the zonula occludens (ZO), the zonula adhaerens (ZA) and the macula adhaerens (MA) or desmosome. Fixation 4% glutaraldehyde. x 90,000.

Figure 11. Tripartite junctional complex between pyloric gland cells. Note the focal splitting (↑) in the zonula occludens and the cytoplasmic fibrils converging on the desmosome. Fixation 1.5% glutaraldehyde. x 135,000.

Figure 12. Macula adhaerens (desmosome) between zymogen cells.
Fixation 4% glutaraldehyde. x 135,000.

Figure 13. Tripartite junctional complex between surface epithelial cells in the small intestine. Note that the components present are similar to Figs. 10 and 11.
Fixation 1% osmium tetroxide. x 75,000.

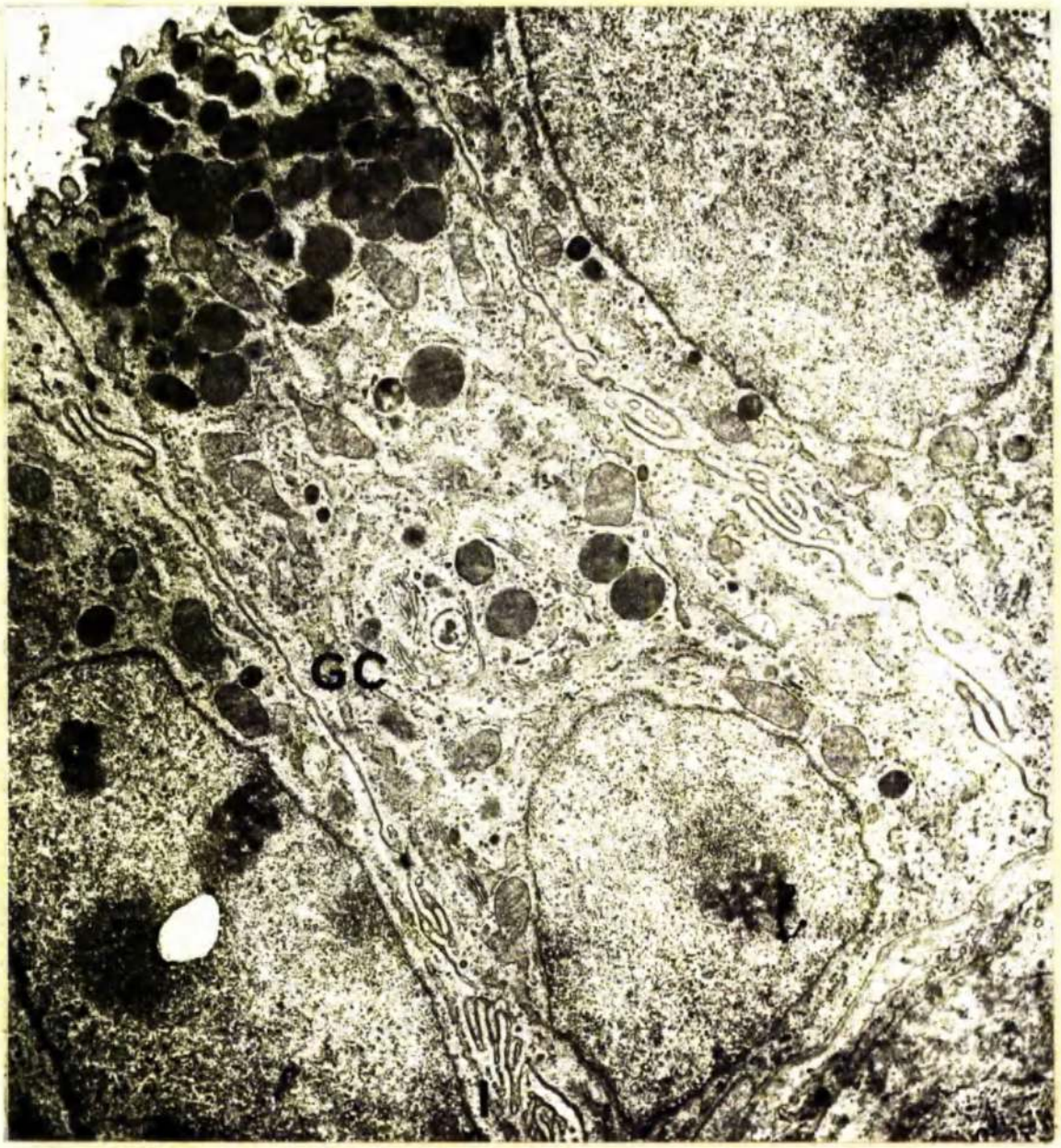

Figure 14. Surface mucous cell with extensive golgi complex (GC) and numerous electron-dense granules. Note elaborate interdigitation of lateral plasmalemmata (I). Fixation 1% osmium tetroxide. x 7,500.

Figure 15. Surface mucous cell with numerous electron-dense granules in apical cytoplasm. Fixation 1.75% glutaraldehyde. x 12,500.

Figure 16. Surface mucous cells with numerous granules of low electron density in the apical cytoplasm. Fixation 4% glutaraldehyde. x 8,000.

Figure 17. Granules of varying electron density in apical cytoplasm of a surface mucous cell. Fixation 4% glutaraldehyde. x 30,000.

Figure 18. Mucous neck cell with prominent golgi complex (GC) and apical granules containing patches of electron-dense material. Fixation 4% glutaraldehyde. x 9,000.

Figure 19. Mucous neck cell with granules packing the apical cytoplasm and indenting the nucleus. Note the elongated mitochondria (M). Fixation 4% glutaraldehyde. x 12,000.

Figure 20. Mucous neck cell with granules in apical and basal cytoplasm. Fixation 4% glutaraldehyde. x 12,500.

Figure 21. Parietal cell between mucous neck cells showing intracellular canaliculi (IC) encircling the nucleus and a large number of mitochondria. Note the interdigitations of the basal plasmalemmata (↑). Fixation 4% glutaraldehyde. x 10,000.

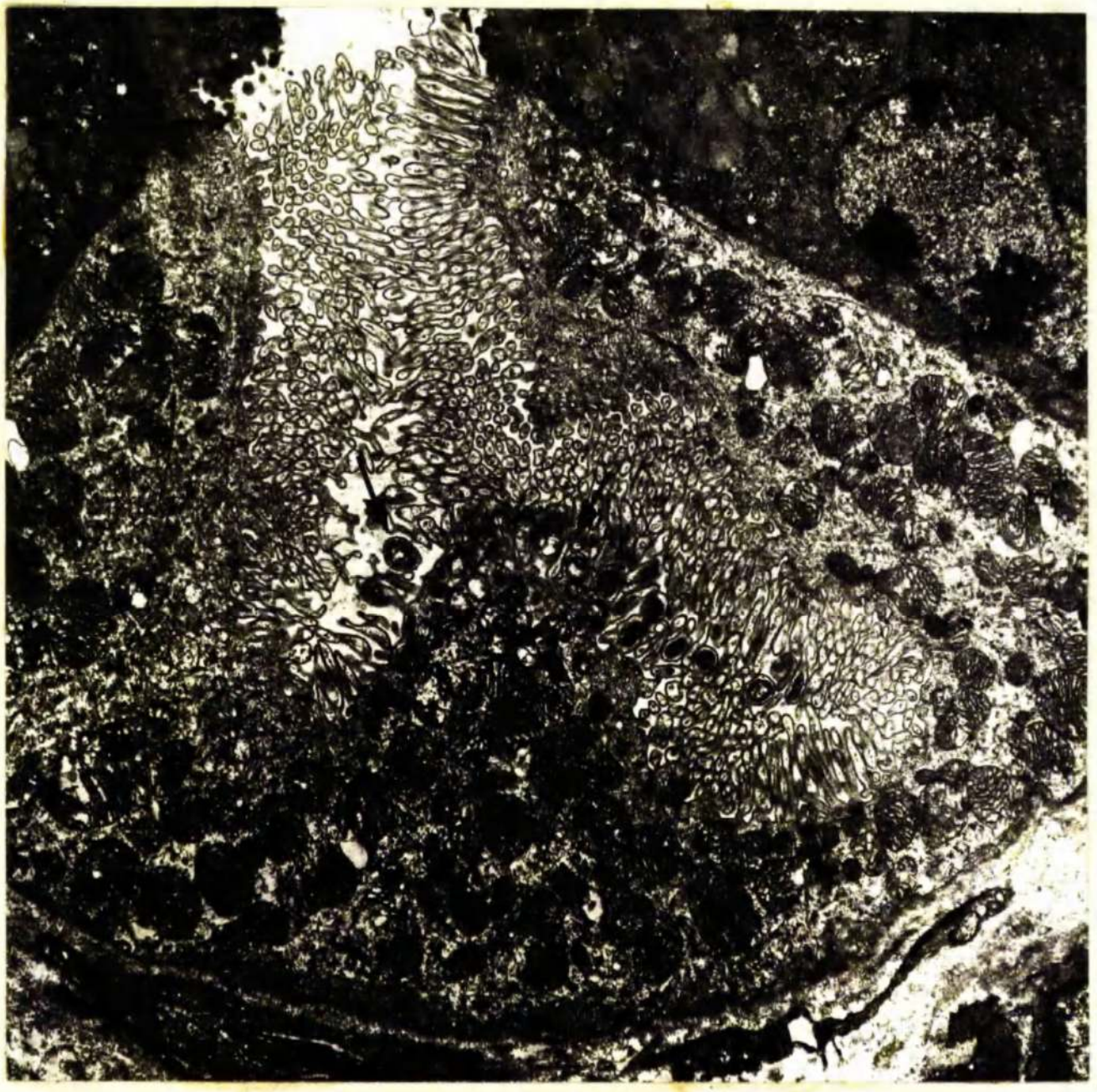

Figure 22. Parietal cell with extensive intracellular canaliculi lined by numerous microvilli some of which contain mitochondria (↑). Fixation 4% glutaraldehyde. x 7,500.

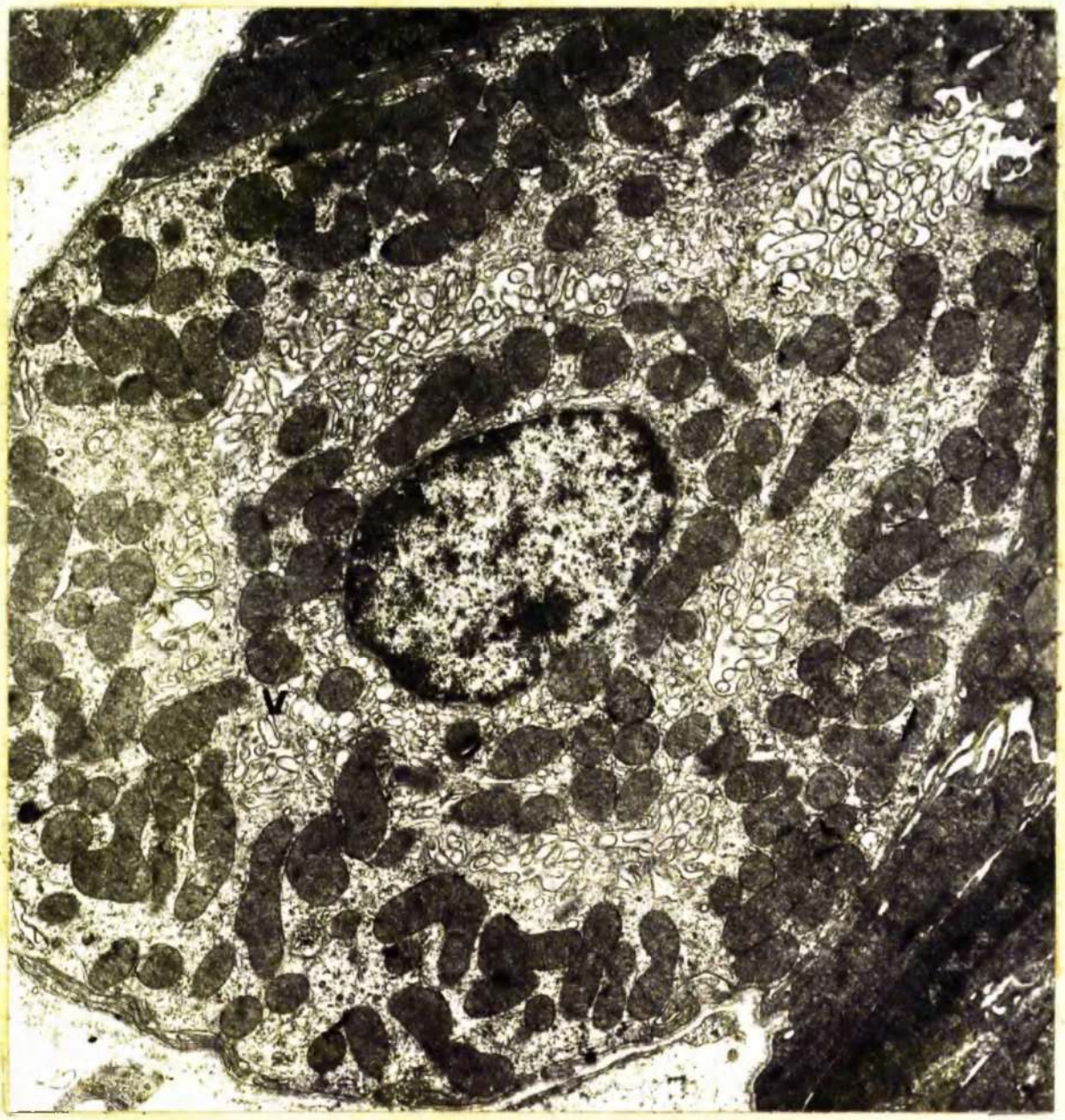

Figure 23. Parietal cell with intracellular canaliculi encircling the nucleus. Note the associated vesicles (v). Fixation 2% glutaraldehyde. x 12,500.

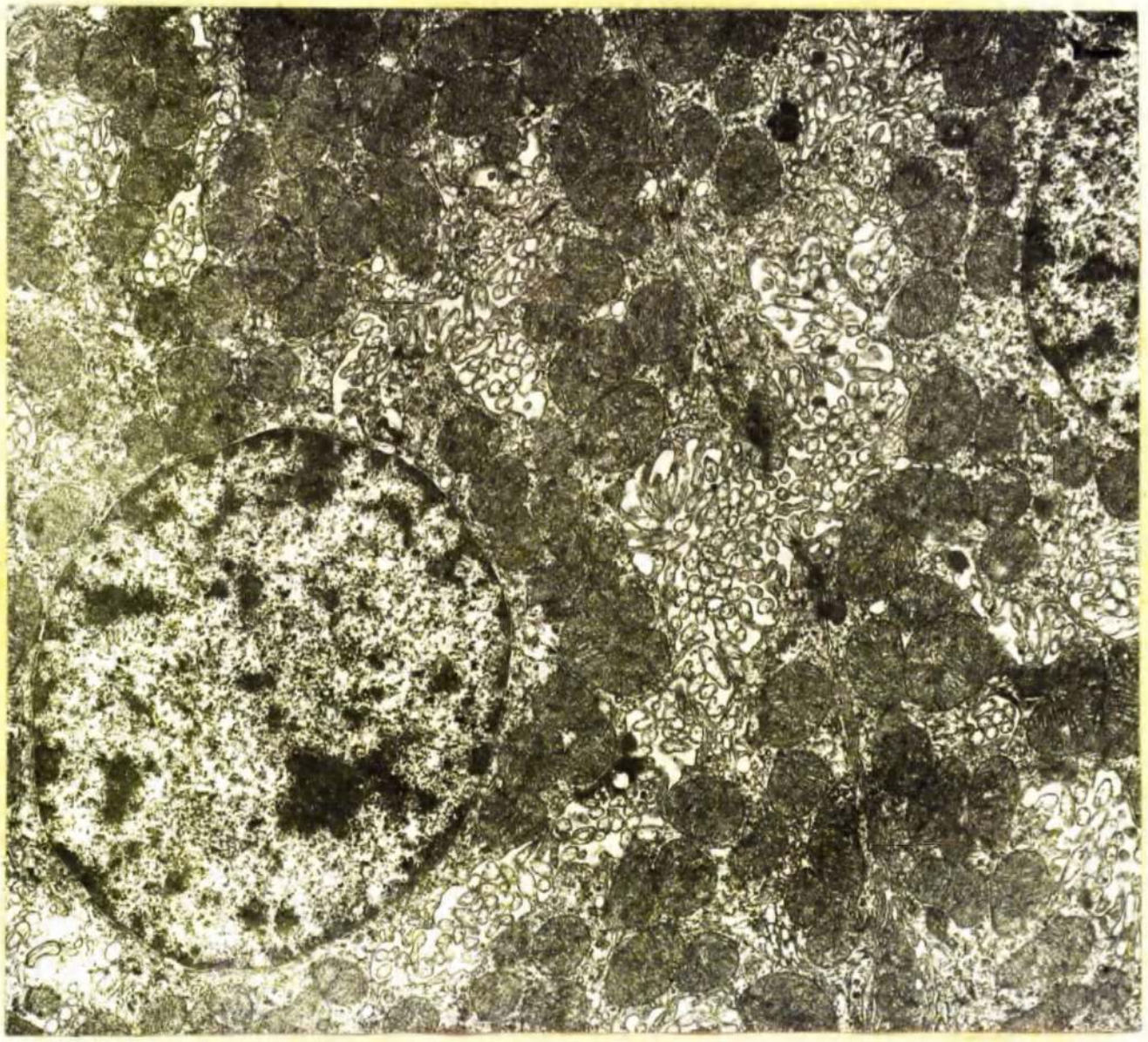

Figure 24. Parietal cells with elaborate intracellular canaliculi and numerous mitochondria lined by closely packed transverse cristae mitochondriales. Fixation 4% glutaraldehyde. x 18,750.

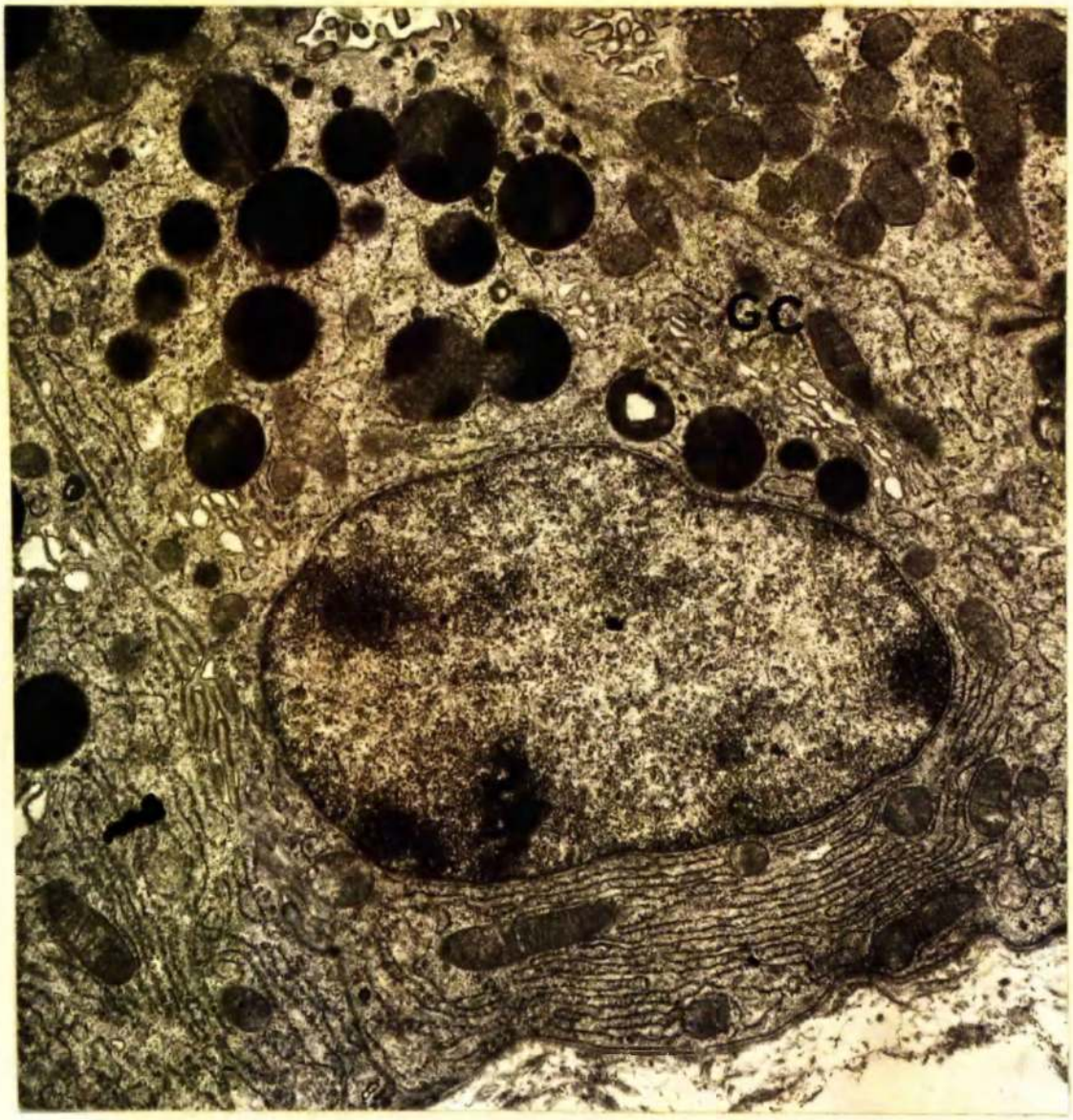

Figure 25. Zymogen cell with electron-dense granules in the apical cytoplasm and an extensive paranuclear golgi complex (GC). Fixation 1.75% glutaraldehyde. x 15,000.

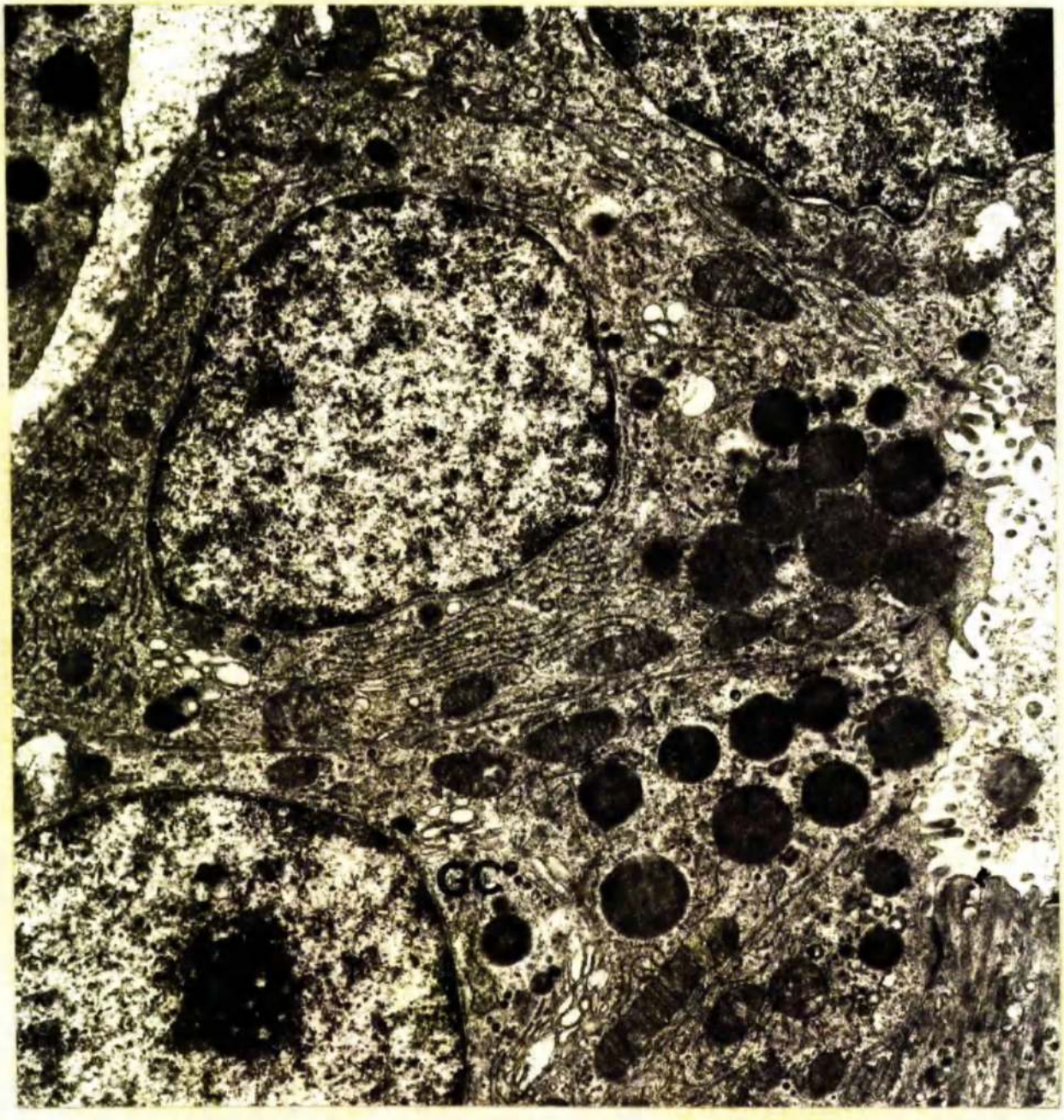

Figure 26. Zymogen cells with electron-dense granules and extensive golgi complex (GC) capping nucleus. Fixation 2% glutaraldehyde in Tyrodes (osmolality = 430 milliosmoles/litre). x 12,500.

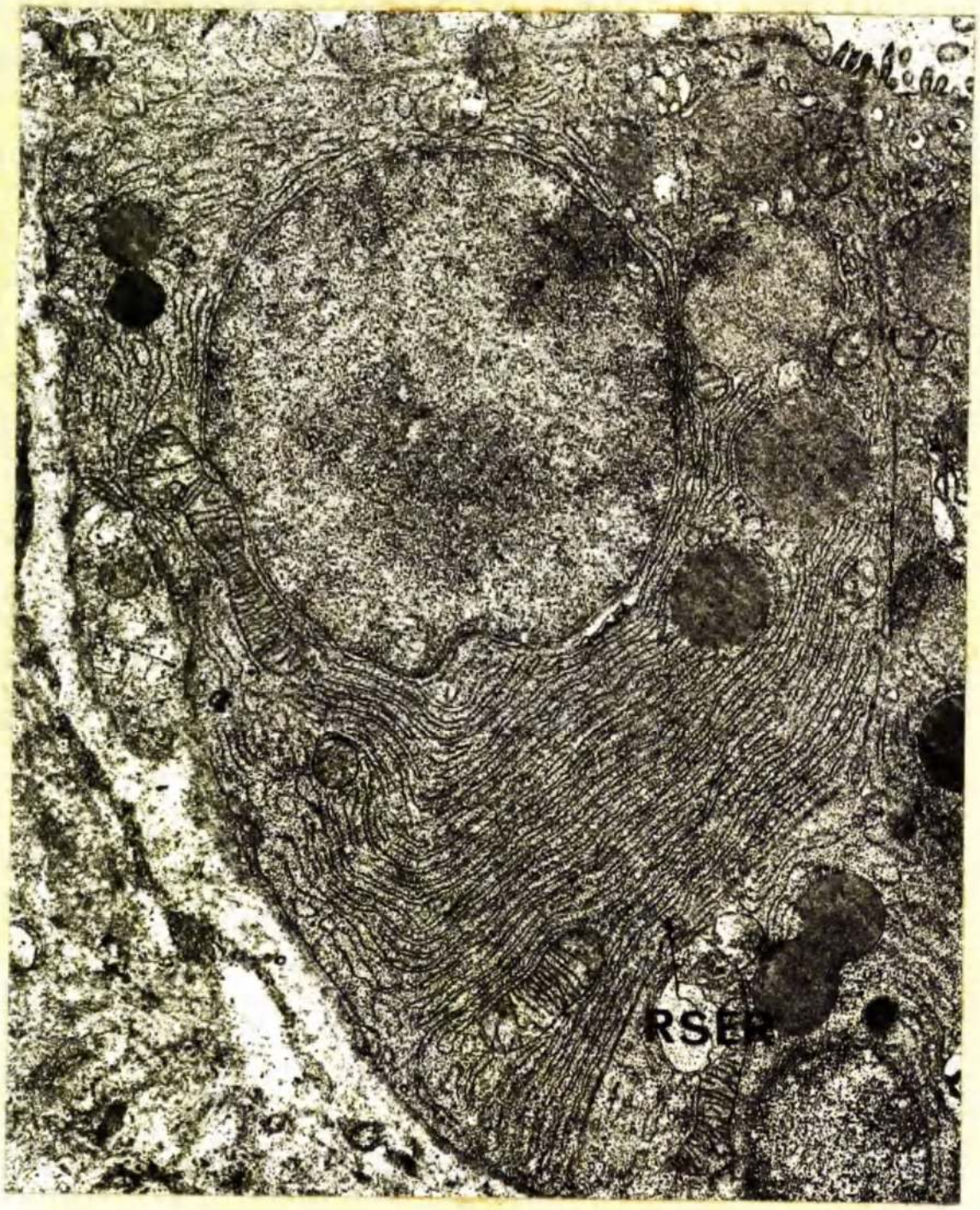

Figure 27. Zymogen cell showing parallel stacks of RSER.
Fixation 1.5% glutaraldehyde. x 15,000.

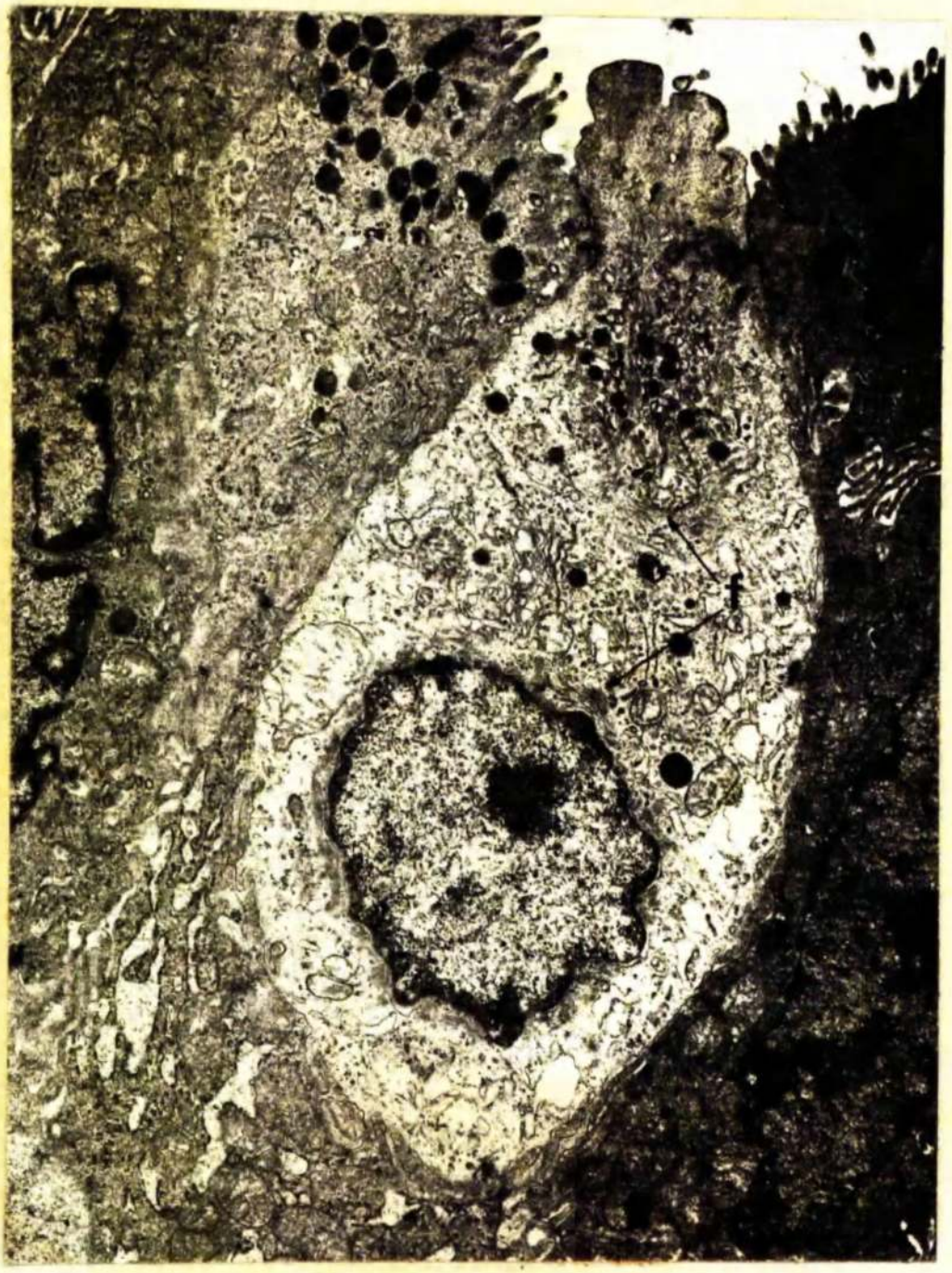

Figure 28. Fibril-containing cell showing bundles of fibrils (f) and pseudovacuolation of cytoplasm. Electron-dense granules of the size and shape of those in the associated surface mucous cells are in the apical cytoplasm. Fixation 1.5% glutaraldehyde. x 18,750.

Figure 29. Fibril-containing cell between surface mucous cells showing longitudinal and transverse bundles of fibrils (f) and an extensive golgi complex (GC). Fixation 1.5% glutaraldehyde. x 22,500.

Figure 30. Fibril-containing cell with bundles of fibrils passing into microvilli and granules similar to those in associated mucous neck cells. Fixation 4% glutaraldehyde. x 17,500.

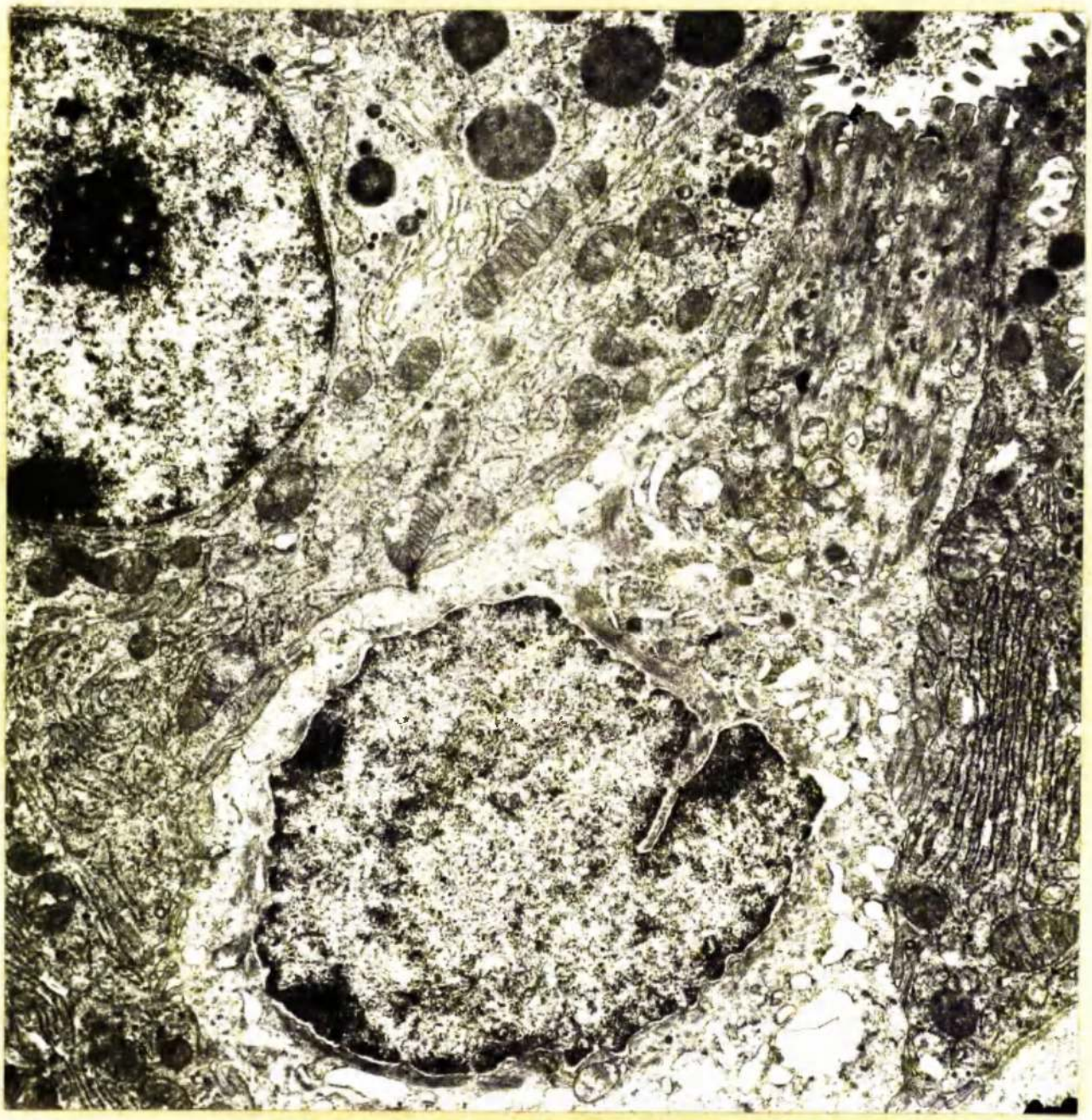

Figure 31. Fibril-containing cell associated with zymogen cells. Note the bundles of fibrils and the degenerate pseudovacuolated cytoplasm. Fixation 2% glutaraldehyde in Tyrodes (osmolality = 430 milliosmoles/litre). x 12,500.

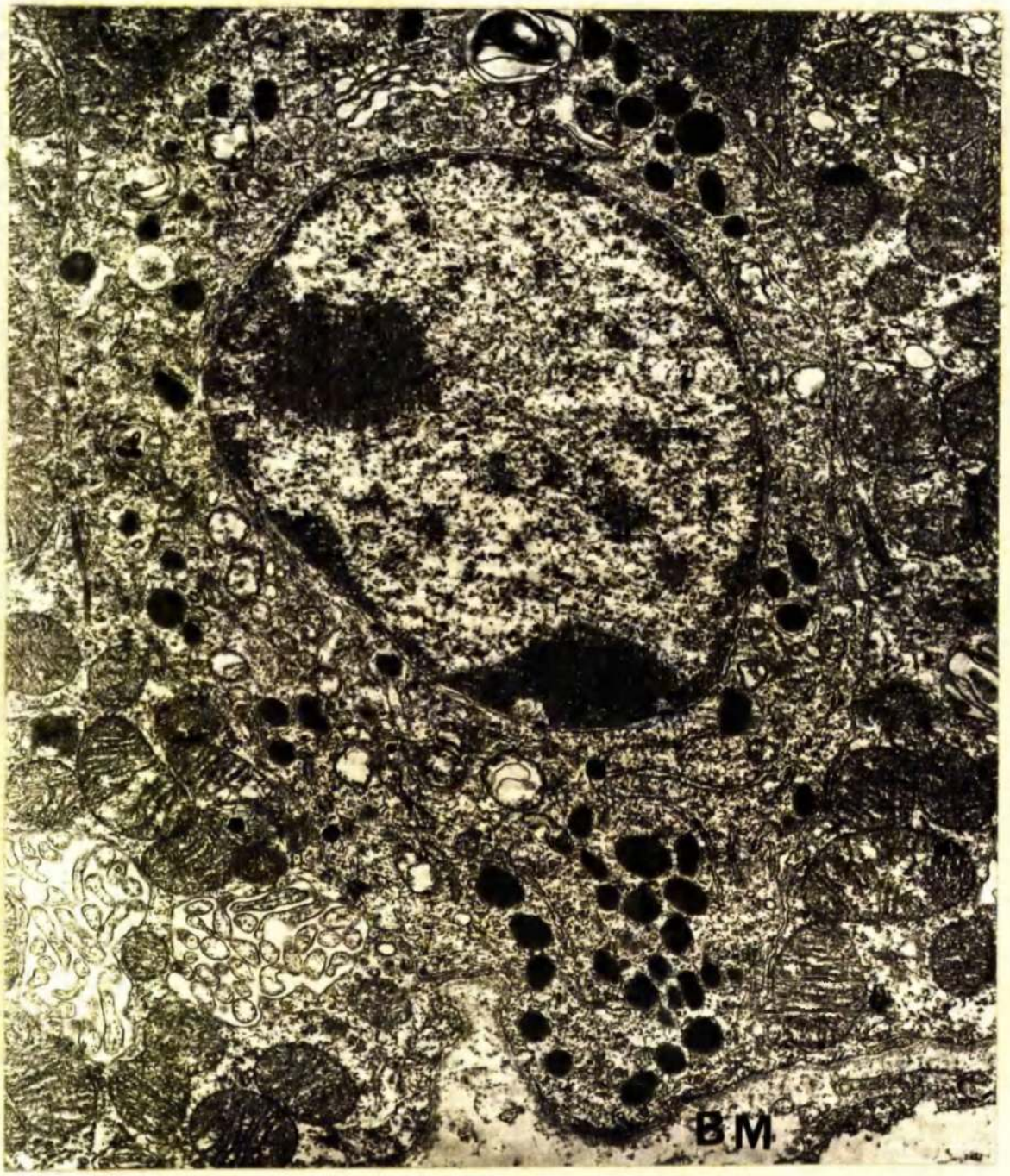

Figure 32. Enterochromaffin cell with small electron-dense granules. Fixation 4% glutaraldehyde. x 18,750.

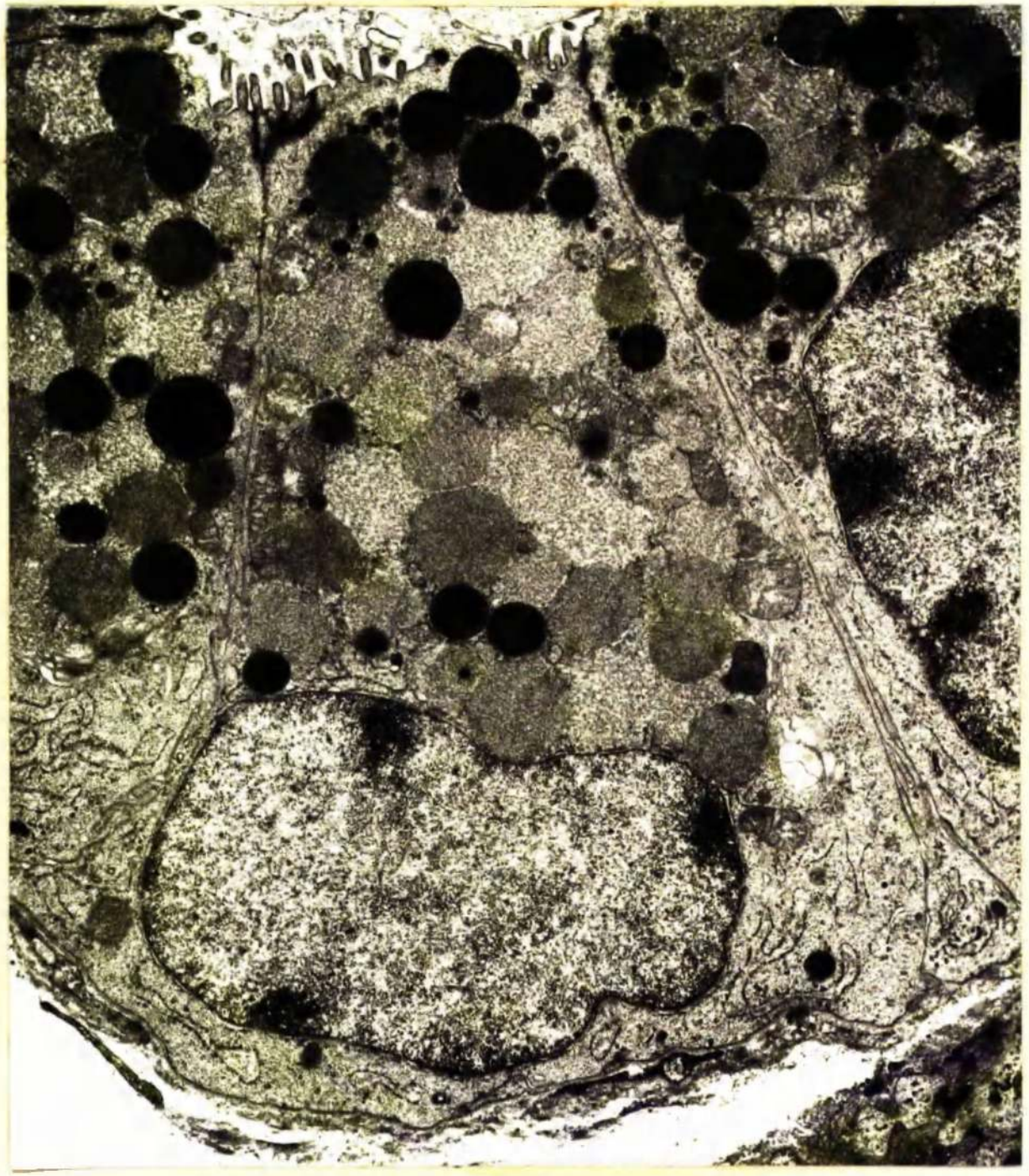

Figure 33. Pyloric gland cell packed with granules of varying size and electron density. Fixation 1.5% glutaraldehyde. x 12,500.

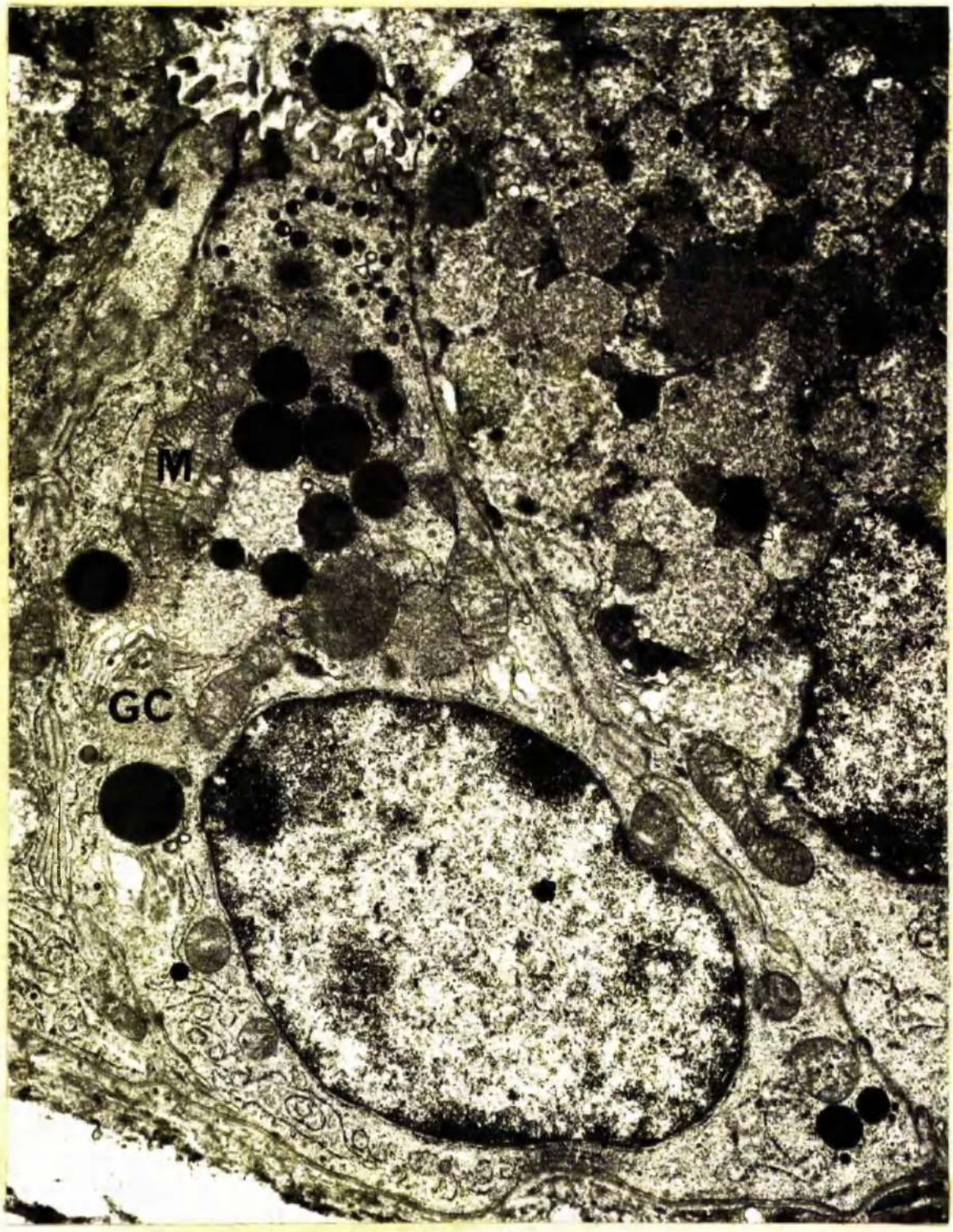

Figure 34. Pyloric gland cell with granules of varying size and electron density and a prominent paranuclear golgi complex (GC). Fixation 1.5% glutaraldehyde. x 12,500.

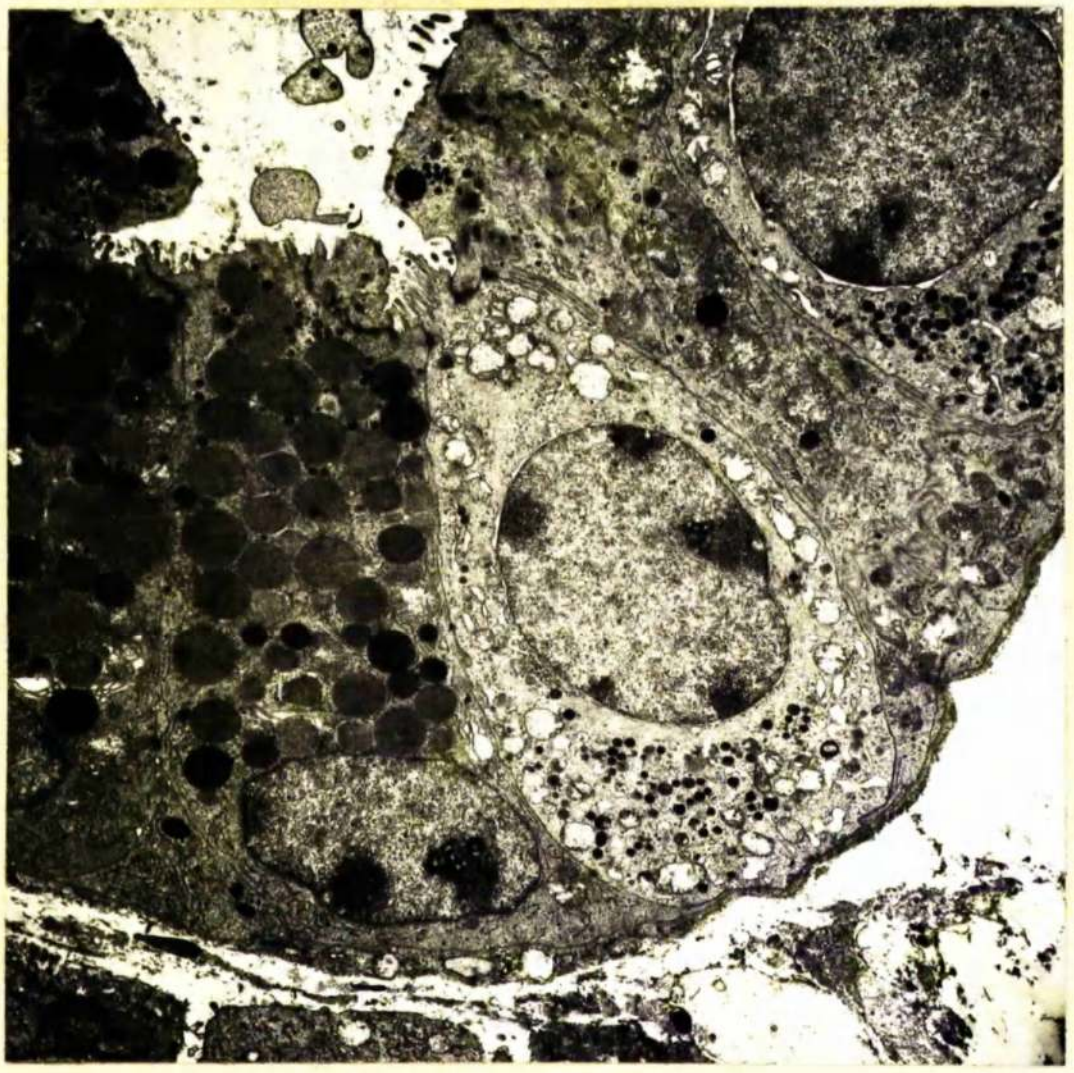

Figure 35. Enterochromaffin cell in pylorus. Note the basally located granules and thin apical prolongation extending to gland lumen. Fixation 1.5% glutaraldehyde. x 6,000.

SECTION III

THE DISEASE PROCESS

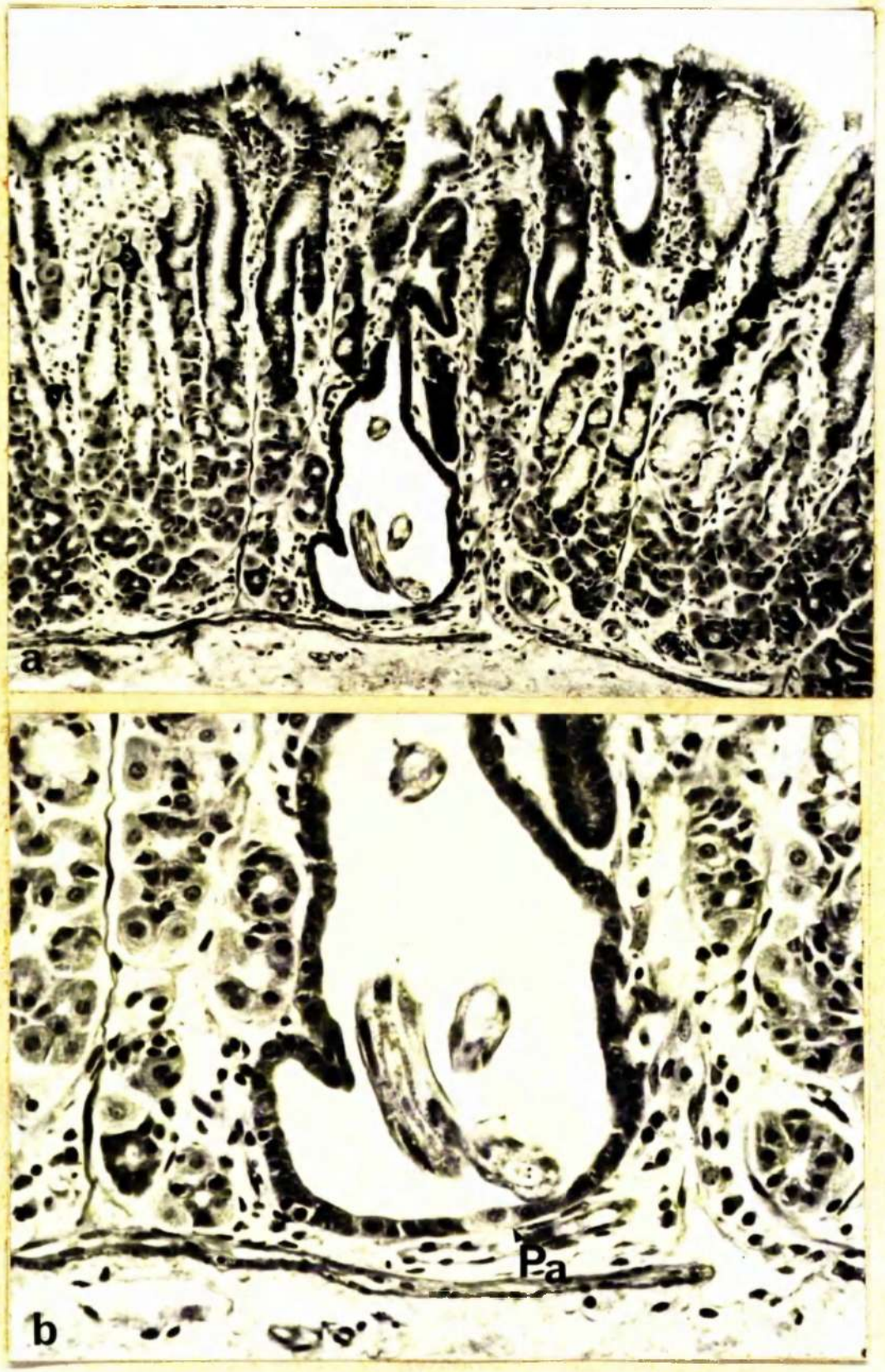

Figure 36. Day 4.

a) Slightly umbilicated nodule with a gland, moderately dilated by the presence of a larva, at the centre. Note that the surrounding glands appear normal. x 140.

b) Note the low cuboidal undifferentiated cells lining this gland and the presence of a single parietal cell (Pa) x 325.

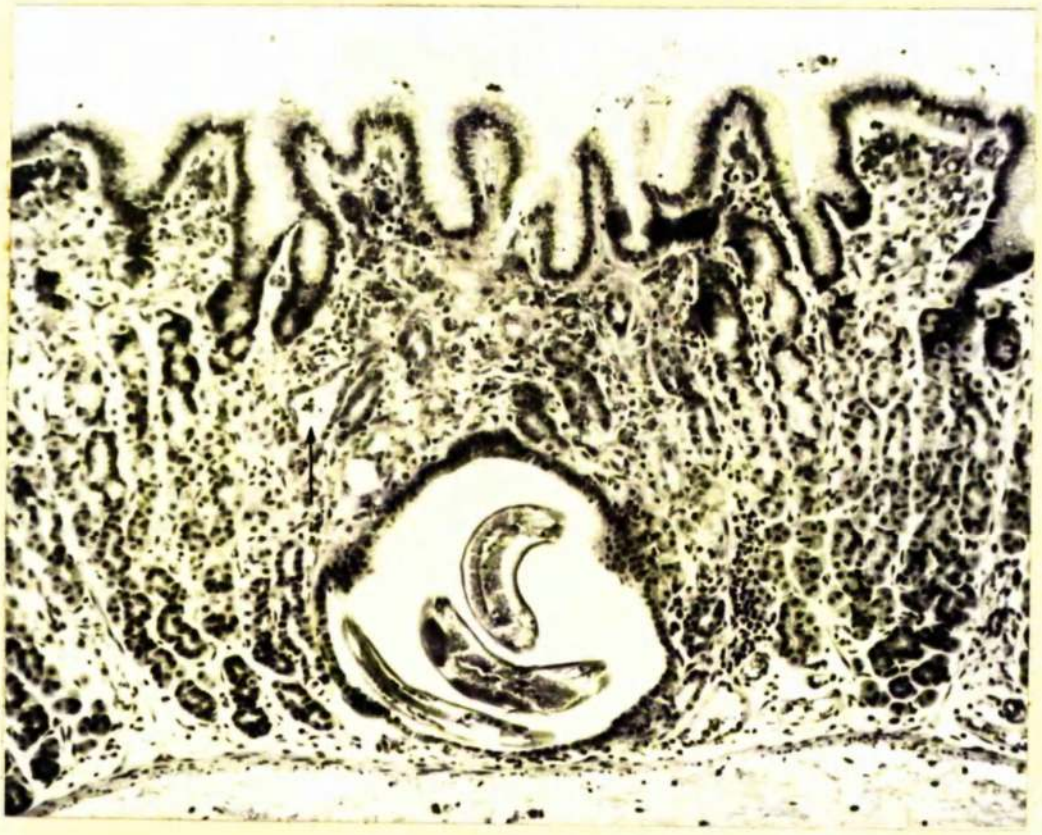

Figure 37. Day 10. The parasite is now larger and the gland more dilated. Note that the surrounding glands are normal although a few are slightly dilated and are lined by flattened epithelium (↑). x 140.

Figure 38. Day 17. The primary nodule. Raised umbilicated lesions in a fold and interfold area of the abomasum.

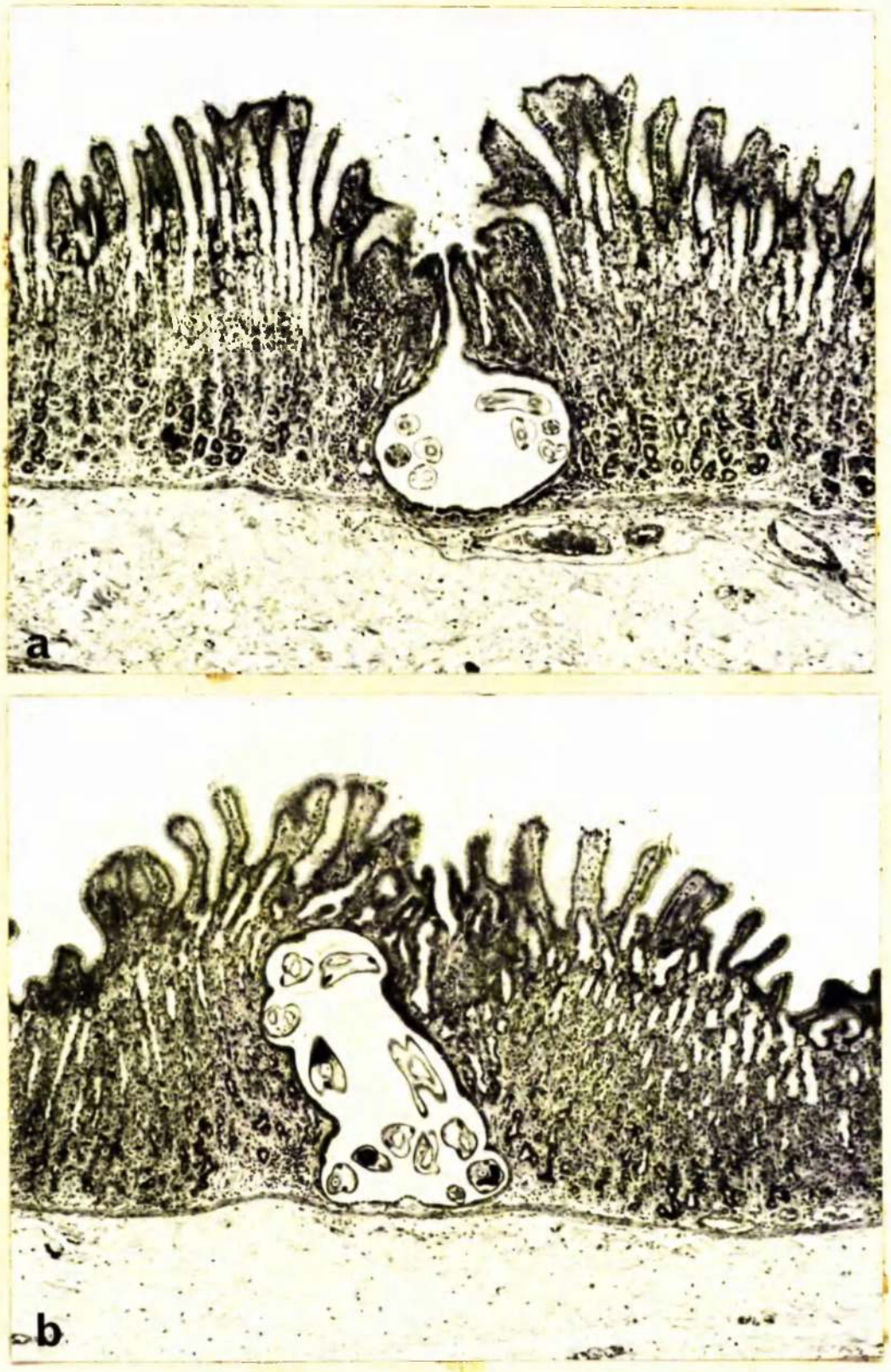

Figure 39. Day 17. a) Microscopic appearance of a primary nodule. x 45.

b) Microscopic appearance of a primary nodule. x 45.

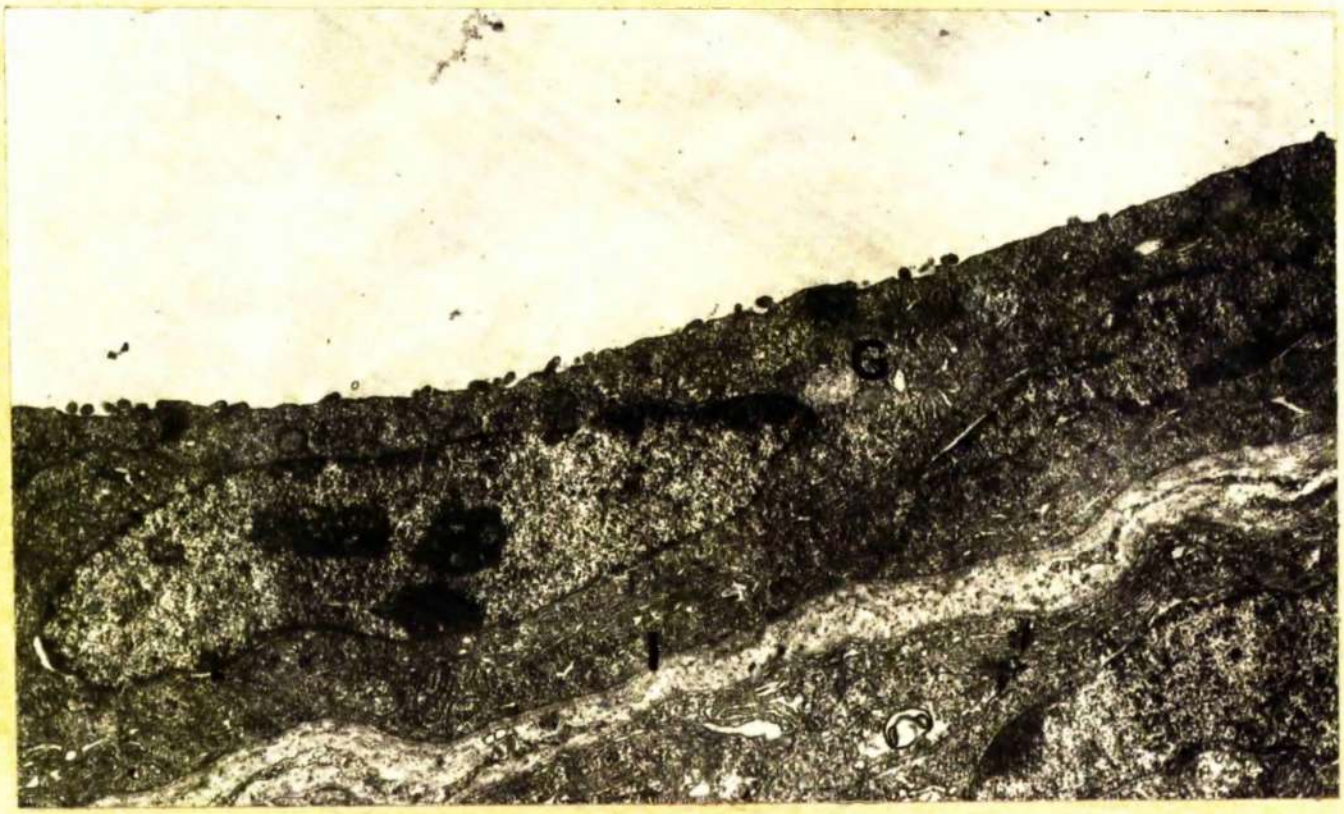

Figure 40. Day 4. Flattened undifferentiated cell lining parasitised gland. Note the oval granules (G) and the interdigitations of the lateral plasmalemmata (I). Fixation 4% glutaraldehyde. x 10,000.

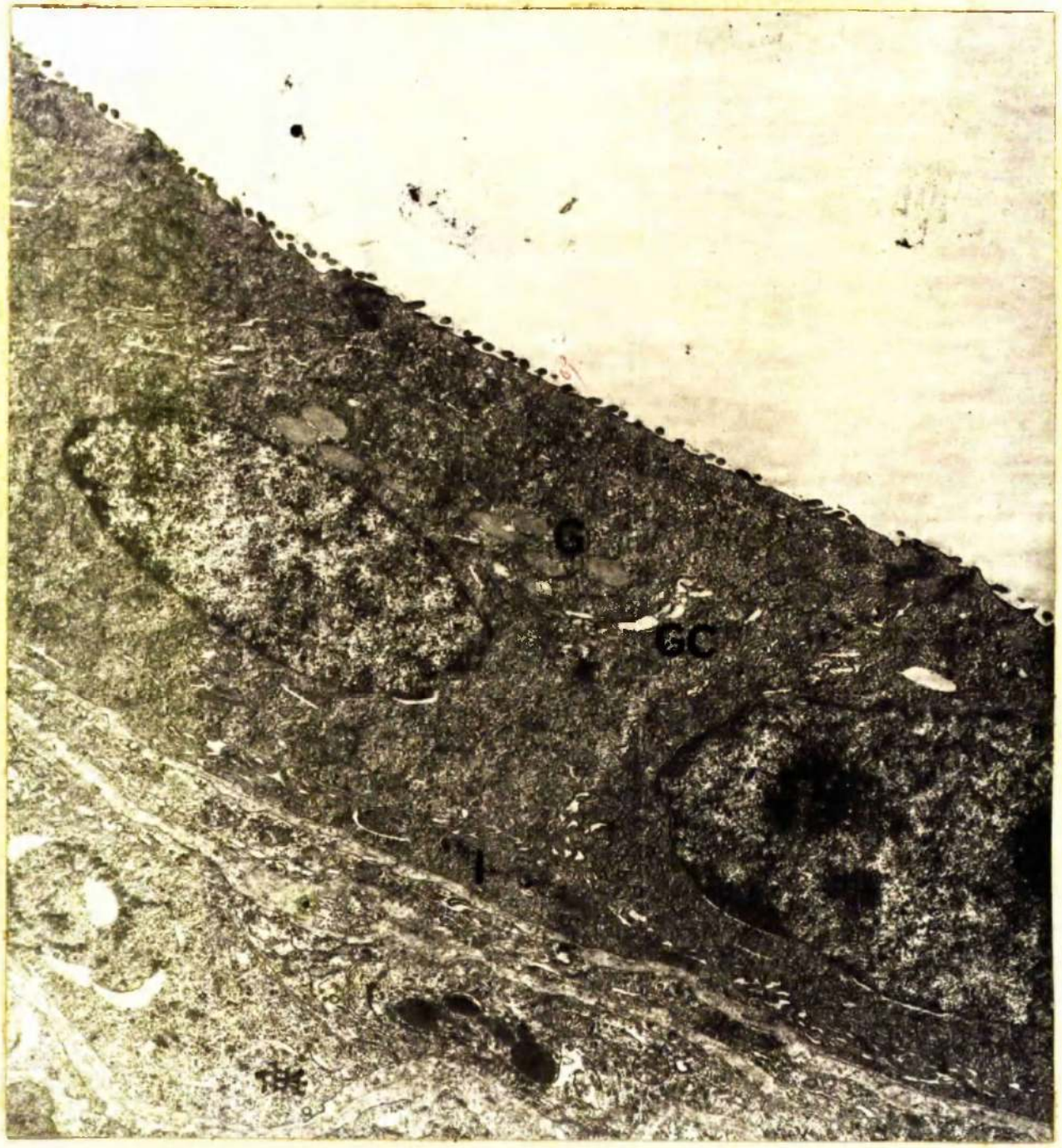

Figure 41. Day 10. Cuboidal cells lining parasitised gland. Note the oval and discoid granules (G), the apical golgi complex (GC) and the elaborate interdigitations of the lateral plasmalemmata (I). Fixation 4% glutaraldehyde. x 10,000.

Figure 42. Day 10. Cuboidal cells lining parasitised gland. Note the apical content of oval and discoid granules and the presence of a parasite in the lumen of the gland (P).
Fixation 4% glutaraldehyde. x 12,500.

Figure 43. Day 17. Columnar cell lining parasitised gland. Note the apically-situated oval granules (G), the supranuclear golgi complex (GC), and the interdigitations of the lateral plasmalemmata (I). Fixation 4% glutaraldehyde.

x 14,000.

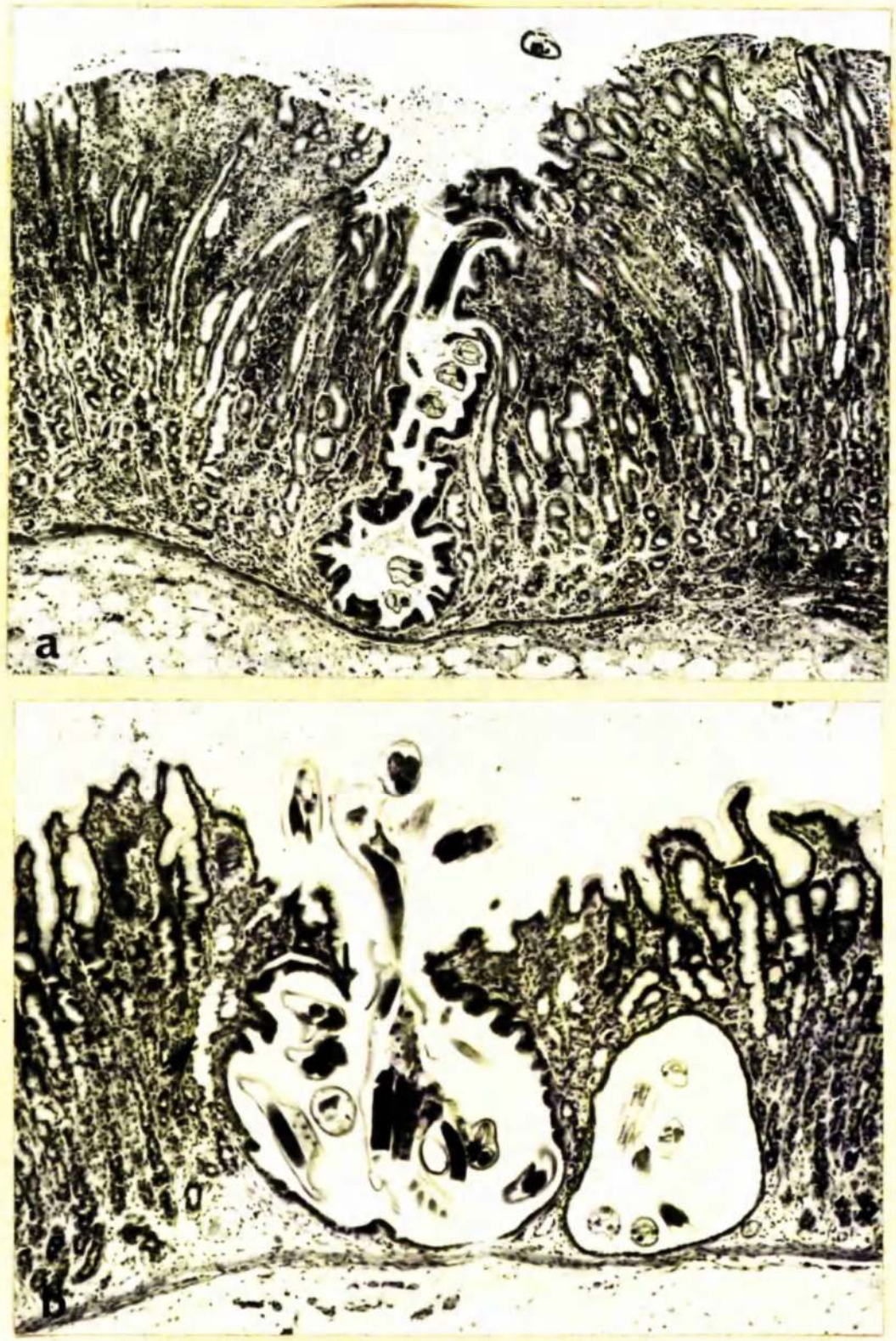

Figure 44. Day 18. a) Adult O. ostertagi emerging from a gastric gland. x 45.

b) Adult O. ostertagi emerging from a gastric gland. Note the stretching and dilatation of surrounding glands (↑). x 45.

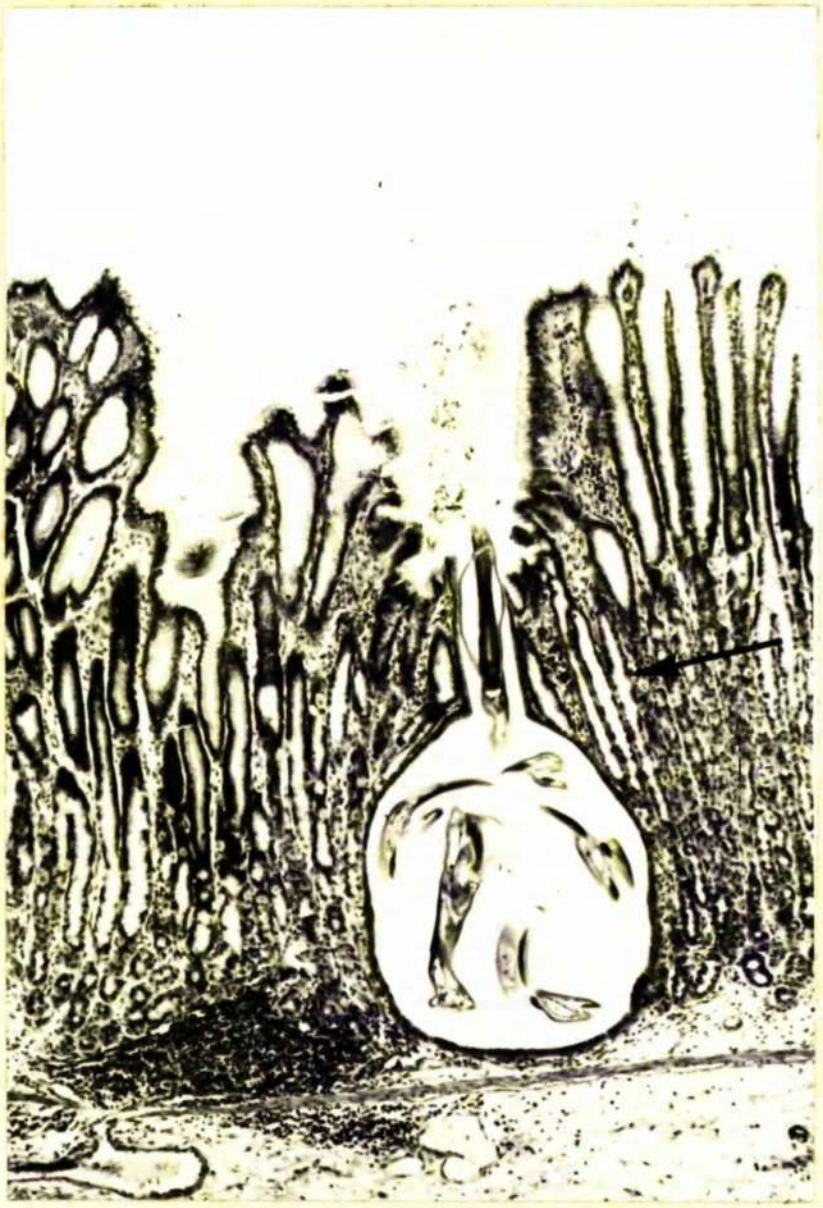

Figure 45. Day 20. Adult O. ostertagi emerging from a gastric gland. Note the stretching of the three immediate surrounding glands (↑). x 45.

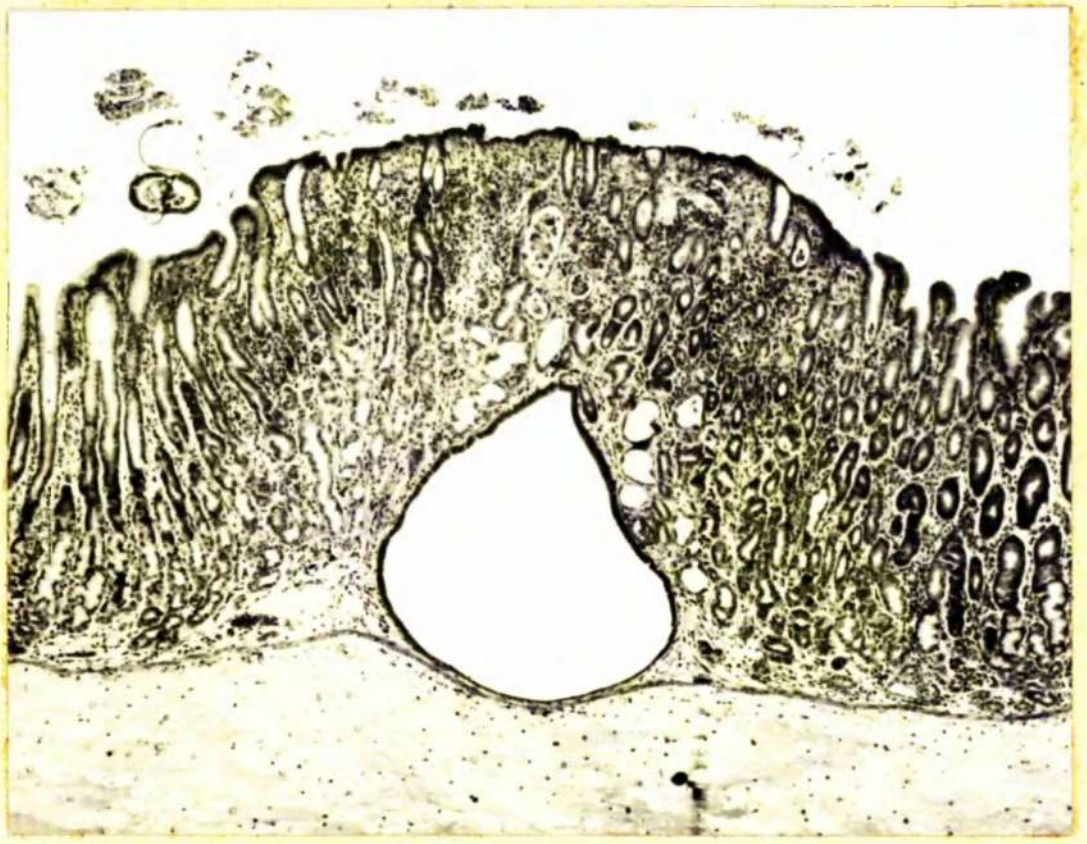

Figure 46. Day 20. Microscopic appearance of secondary nodule. The adult parasite has emerged leaving a distended gland surrounded by glands which are dilated and lined by flattened epithelial cells. x 50.

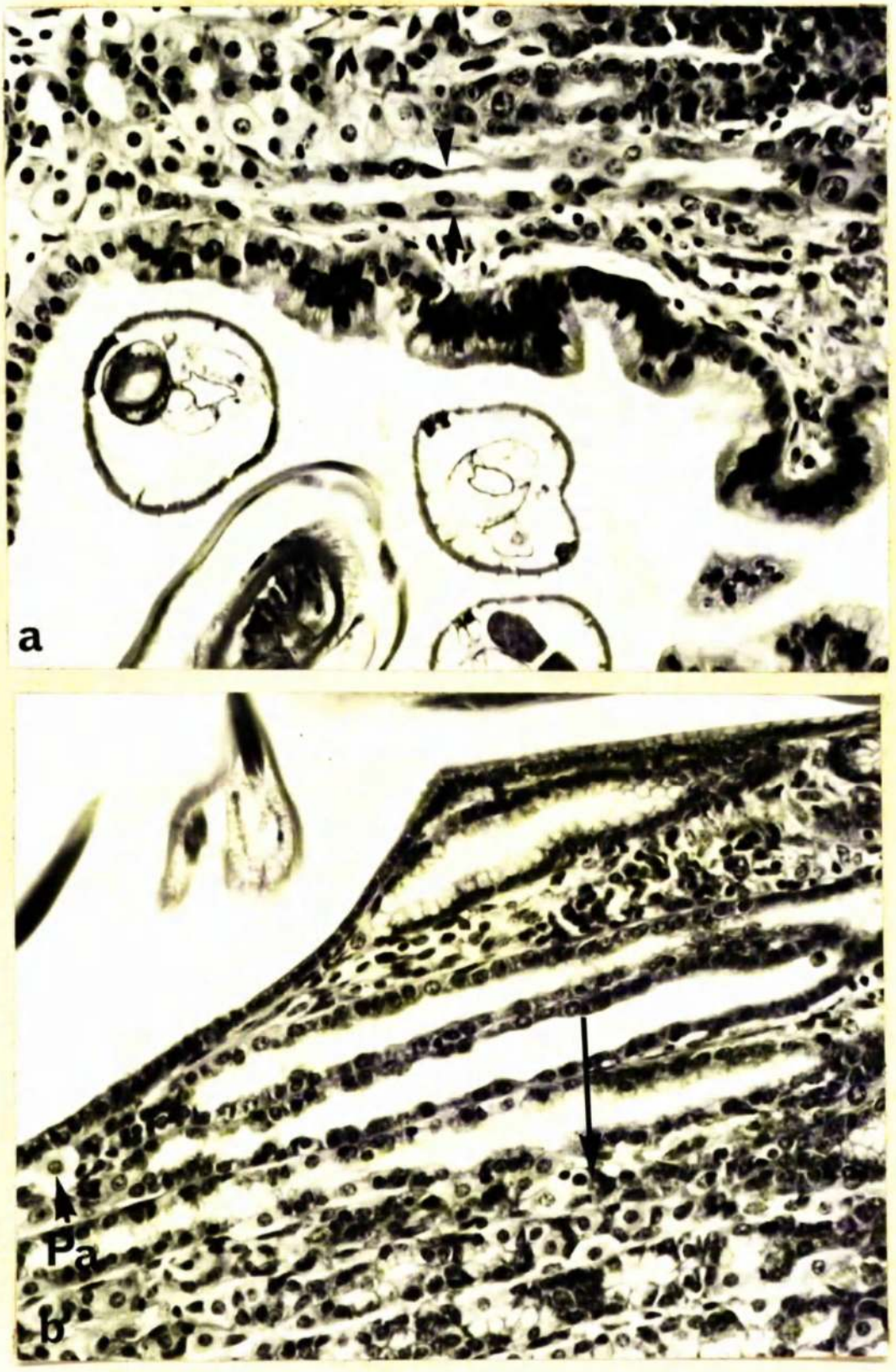

Figure 47. Day 18. a) Parasitised gland lined by tall mucus-secreting cells. The immediate surrounding gland is lined by flattened undifferentiated cuboidal cells (↑). The outer glands are still normal. x 520.

b) High power of Fig. 45. The three glands surrounding the parasitised gland are lined by cuboidal undifferentiated cells although parietal cells (Pa) are still present. The surrounding glands are normal (↑). x 260.

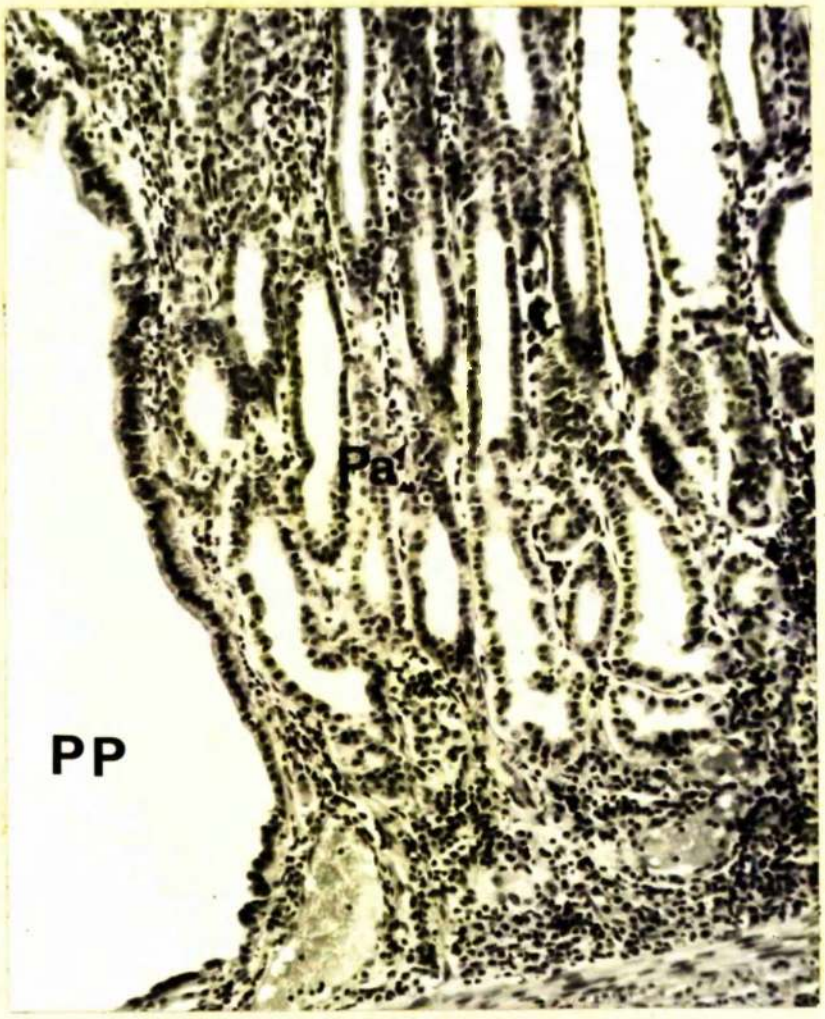

Figure 48. Day 25. Glands surrounding post-parasitised gland (PP). These glands are lined by low cuboidal cells which show no functional differentiation. Note single parietal cells (Pa) scattered throughout these undifferentiated cells. x 150.

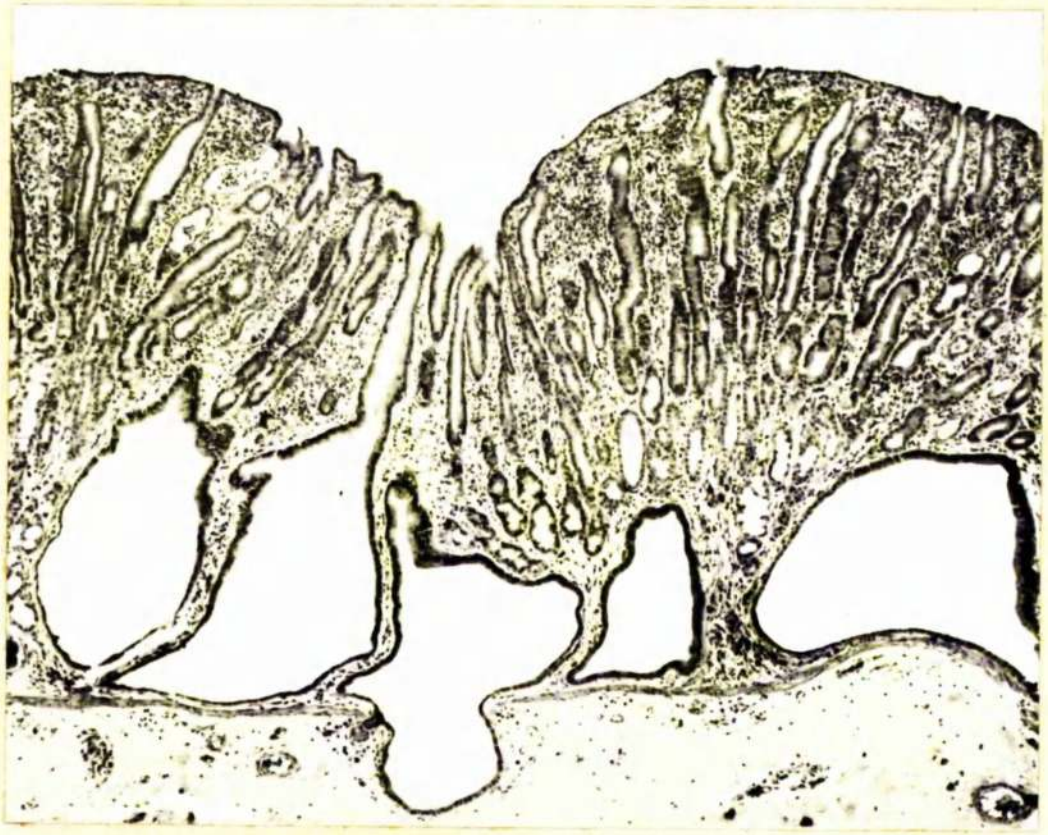

Figure 49. Day 25. Coalescence of secondary nodules with resultant loss of functional gastric mucosa over a considerable area. x 50.

Figure 50. Day 25. Area of overlap between two secondary nodules. The glands are lined by cuboidal rapidly-dividing (↑) undifferentiated cells. Parietal cells (Pa) can still be identified. x 150.

Figure 51. Day 25. Coalescence of secondary nodules.

Figure 52. Day 25. Individual nodules with a visible central orifice surrounded by an elevated area of hyperplastic cells.

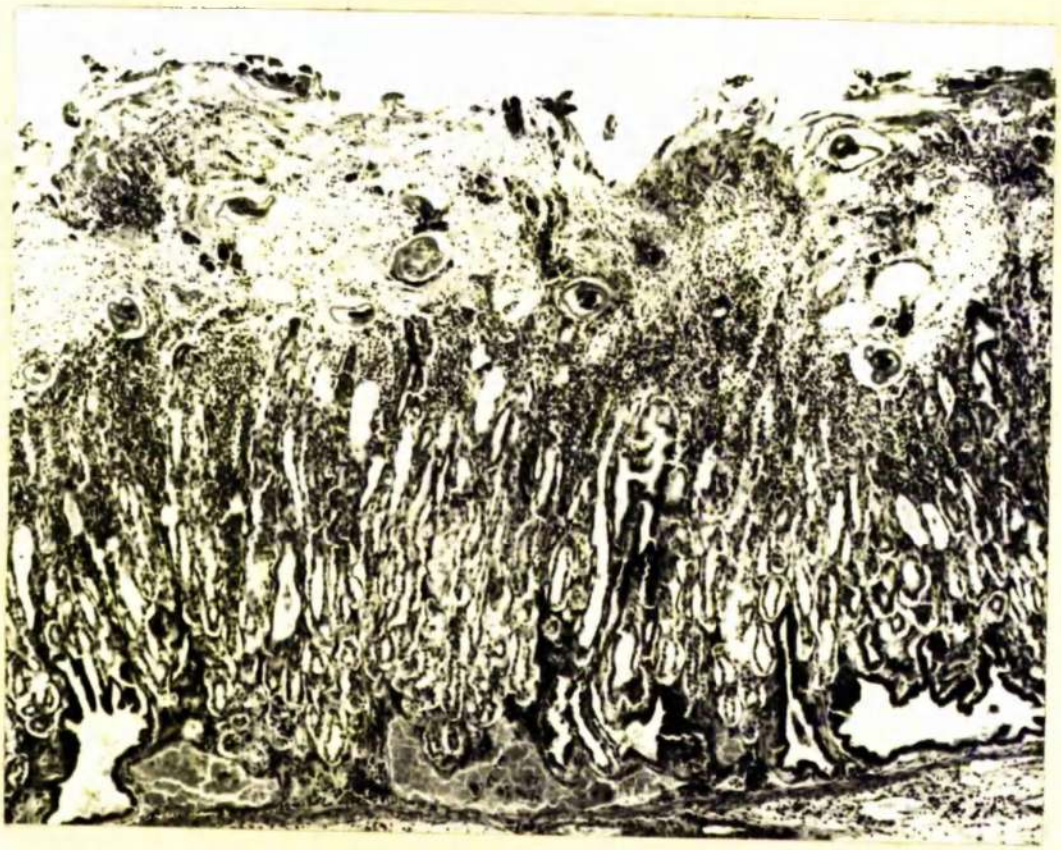

Figure 53. Day 24. Necrosis and sloughing of the surface mucous cells. Adult worms lie in an exudate of protein, polymorphs and clumps of bacteria. x 45.

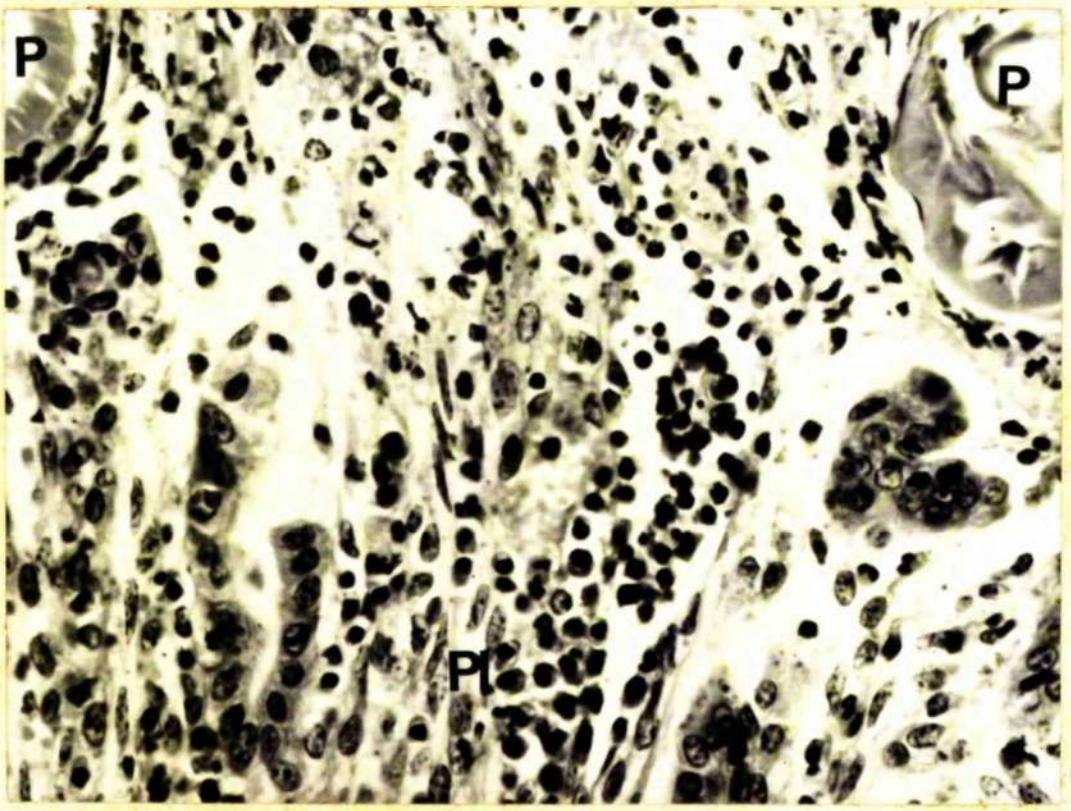

Figure 54. Day 24. Adult worm lying in a diphtheritic membrane. Note the large number of plasma cells in the adjacent lamina propria. x 325.

Figure 55. Day 24. Irregular plaques of diphtheritic membrane on the surface mucosa of the abomasum.

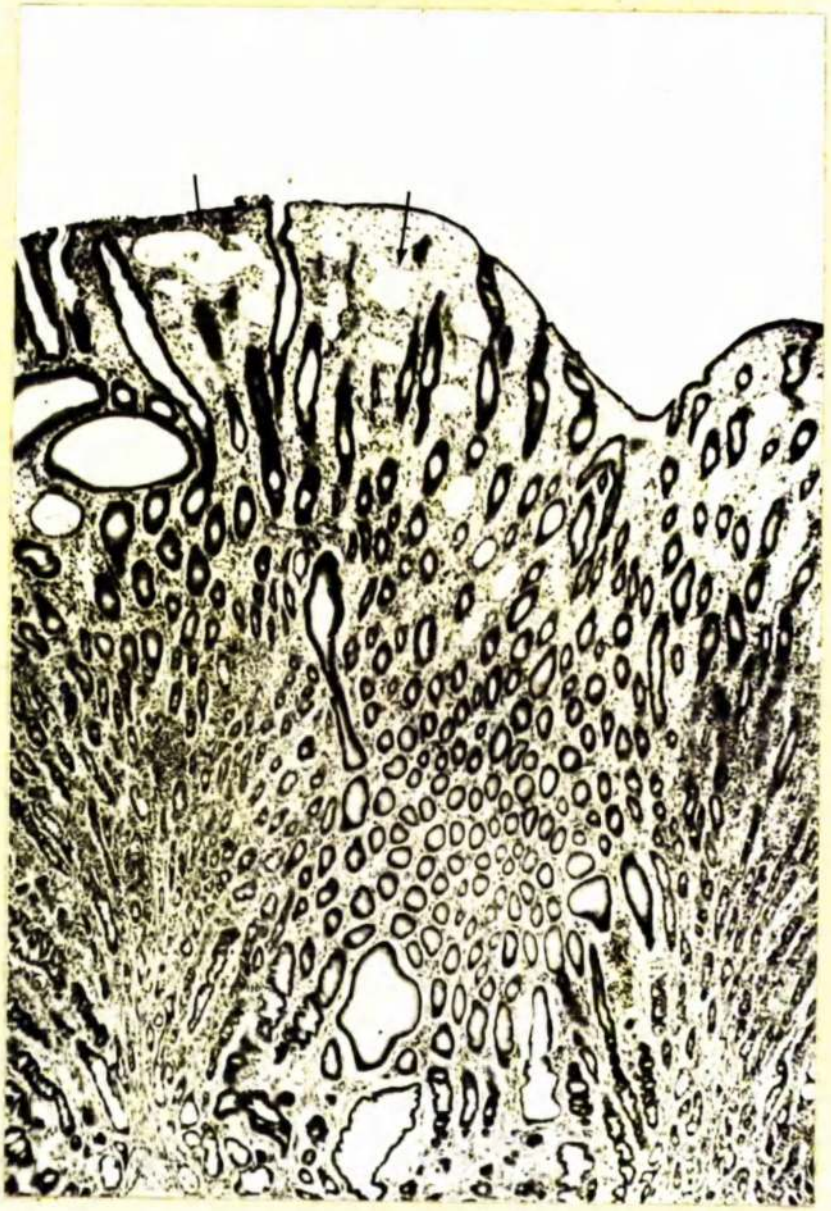

Figure 56. Day 27. Severe oedema of the hyperplastic gastric mucosa. Note the dilated lymphatics (↑) and the stretched surface mucous cells. x 52.

Figure 57. Day 21. Severe congestion and haemorrhage of the gastric mucosa. x 130.

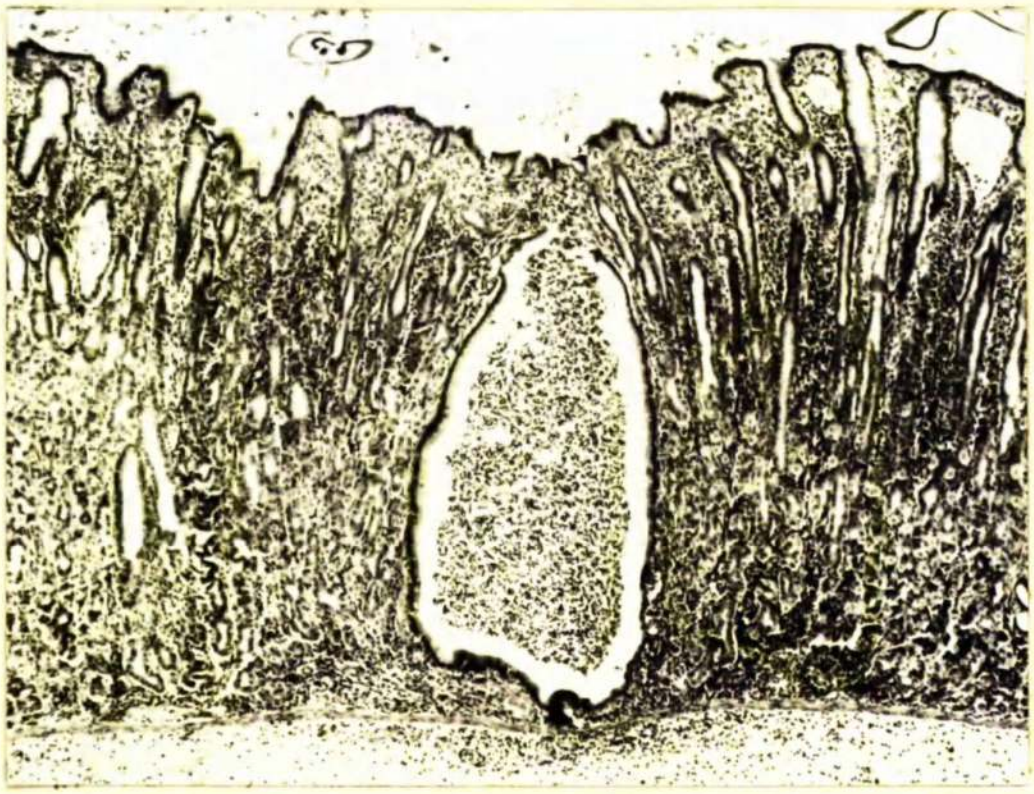

Figure 58. Day 26. Post-parasitised gland distended with purulent debri. x 45.

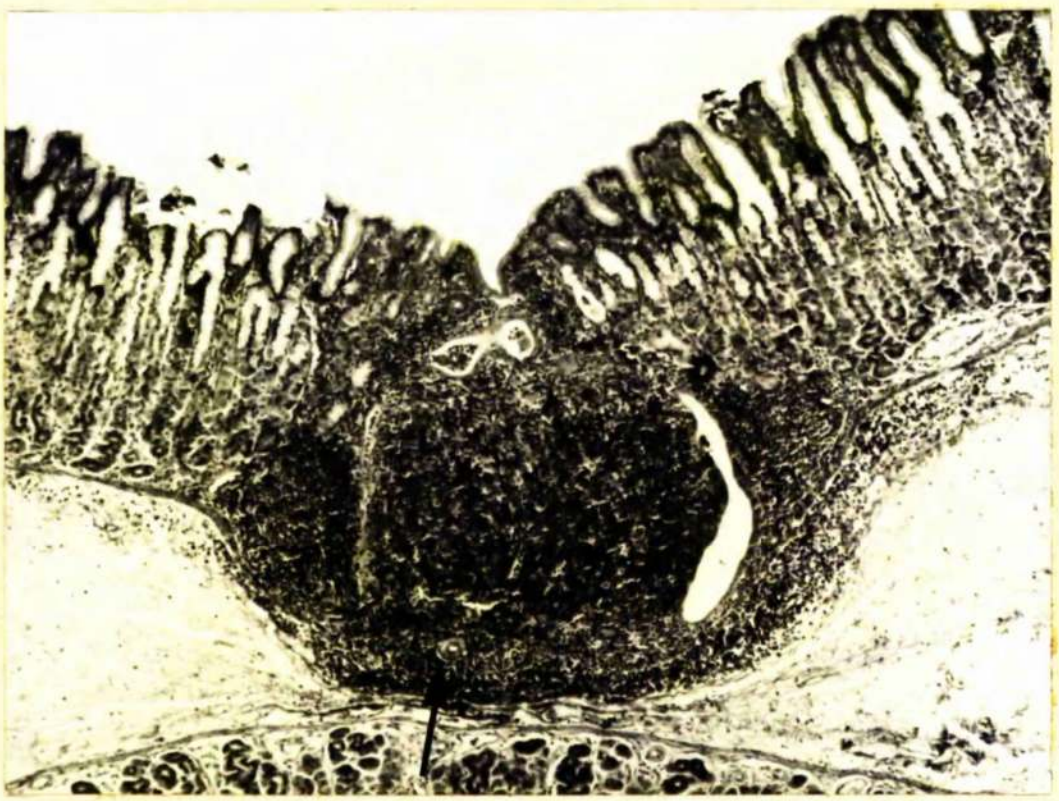

Figure 59. Day 29. Lymphoid nodule in the lower gastric gland area breaking through the muscularis mucosa to the submucosa. Note the presence of a small blood vessel (↑). x 50.

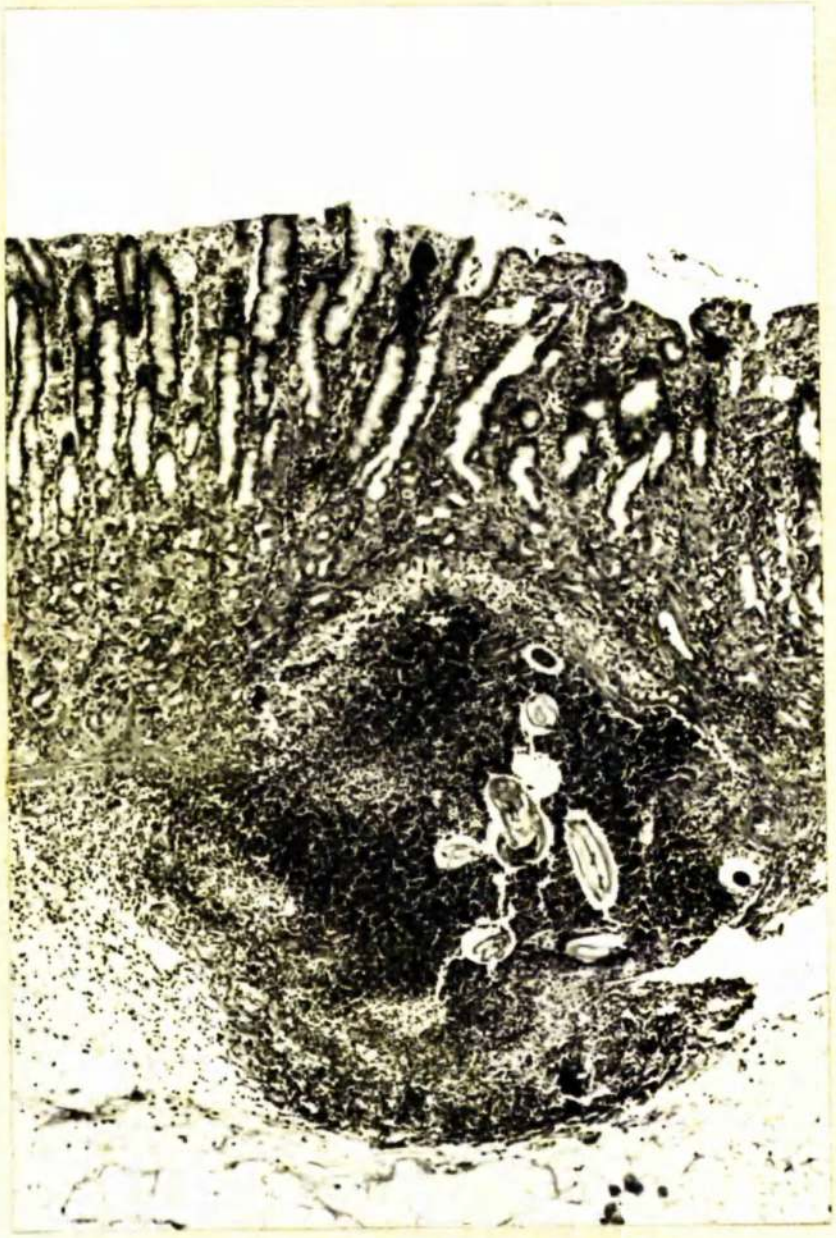

Figure 60. Day 27. Parasite breaking out of gastric gland into the submucosa. Note the intense associated eosinophil response. x 45.

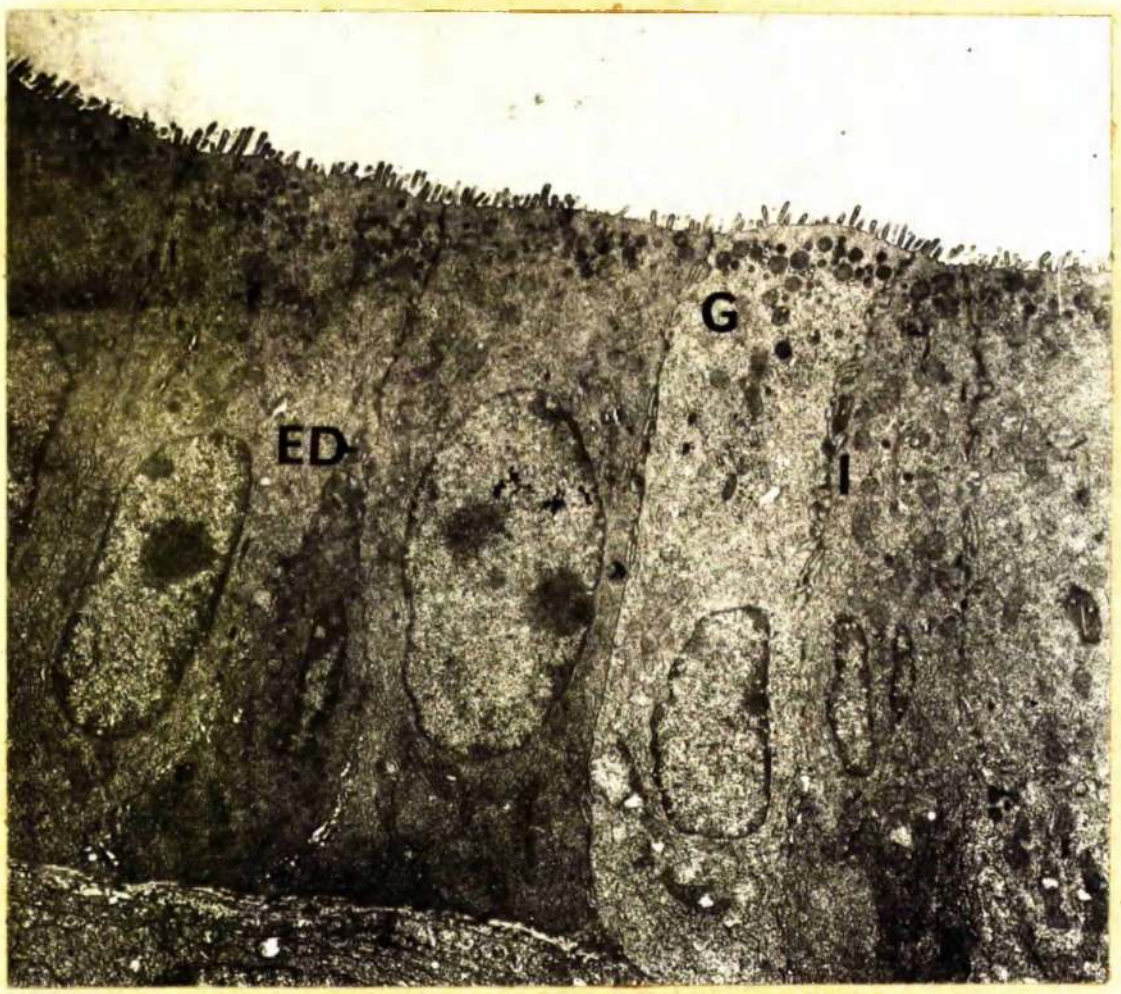

Figure 61. Day 22. Columnar cells lining gland which has formerly contained a parasite. Note the round and oval apical granules (G), the interdigitations of the lateral plasmalemmata (I) and the electron-dense material (ED) dilating the intercellular spaces. Fixation 1.5% glutaraldehyde. x 6,000.

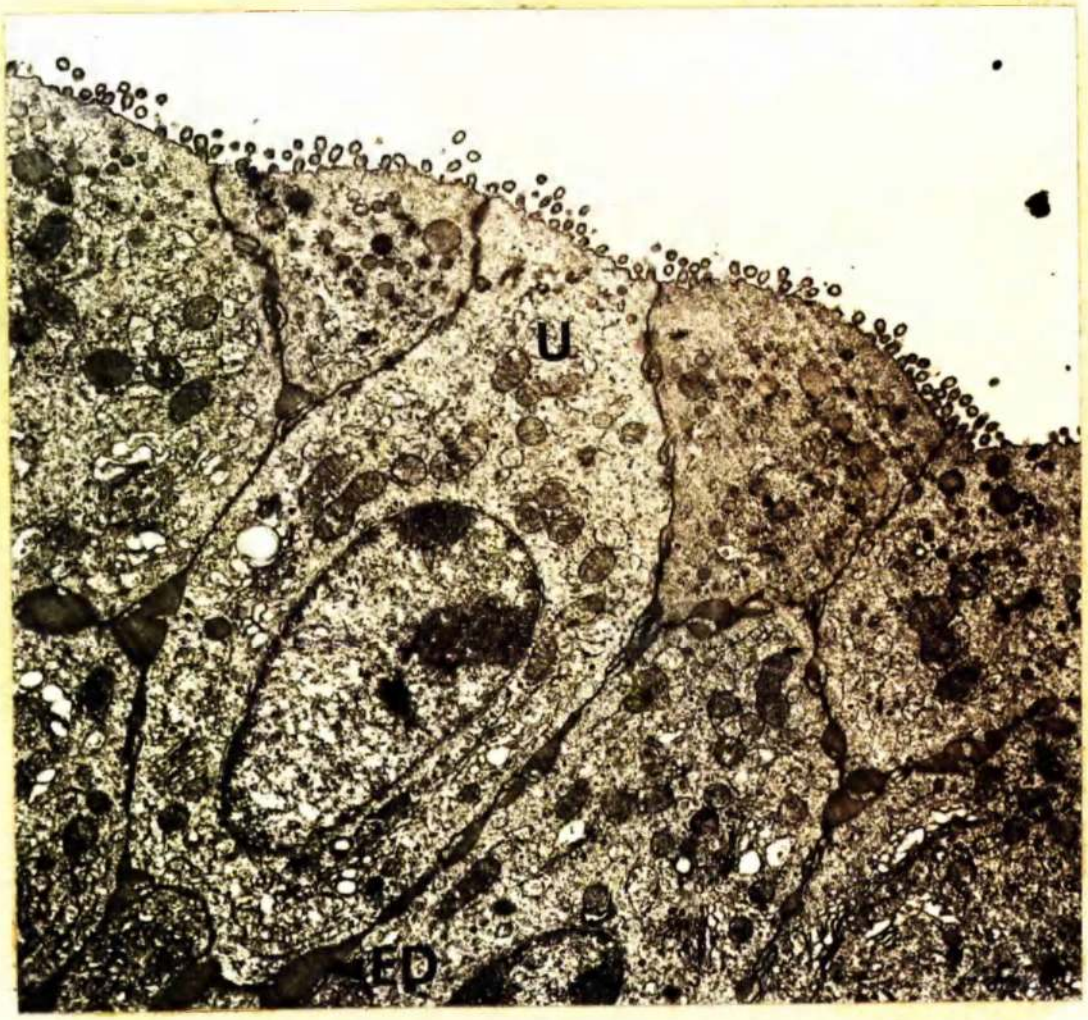

Figure 62. Day 25. Cells arranged in a pseudostratified fashion lining post-parasitised gland. Note the undifferentiated cell (U) and the electron-dense material (ED) lying between cells. Fixation 1·5% glutaraldehyde. x 10,000.

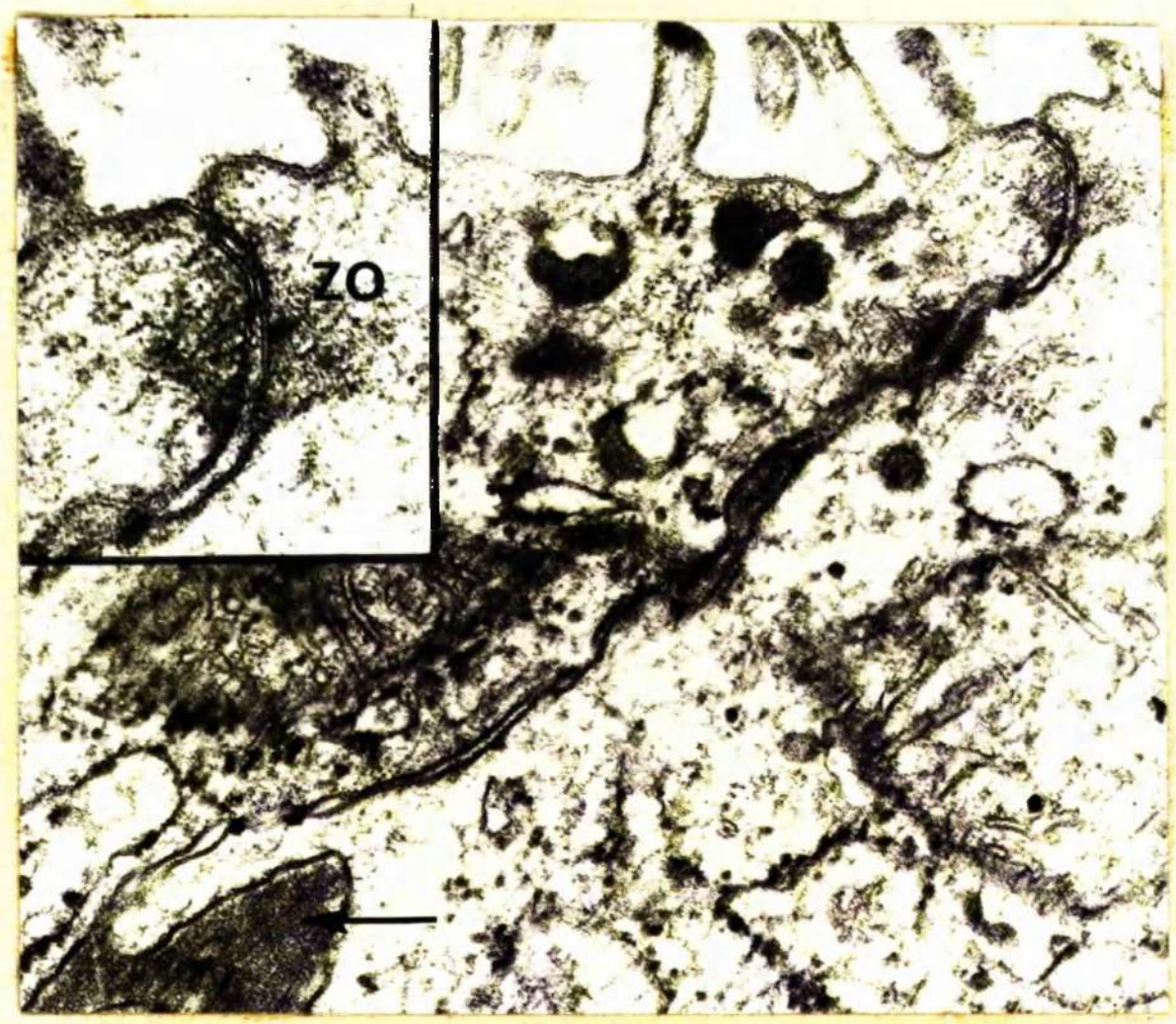

Figure 63. Day 25. Juxtaluminal segment of cells lining post-parasitised gland. Note the separation of the lateral plasmalemmata of the zonula occludens (ZO inset) and the electron-dense material (↑) lying in and dilating the intercellular space. Fixation 1% glutaraldehyde. x 75,000 (inset x 120,000).

Figure 64. Day 21. Stretched mucous neck cells lining dilated glands. Fixation 4% glutaraldehyde. x 12,500.

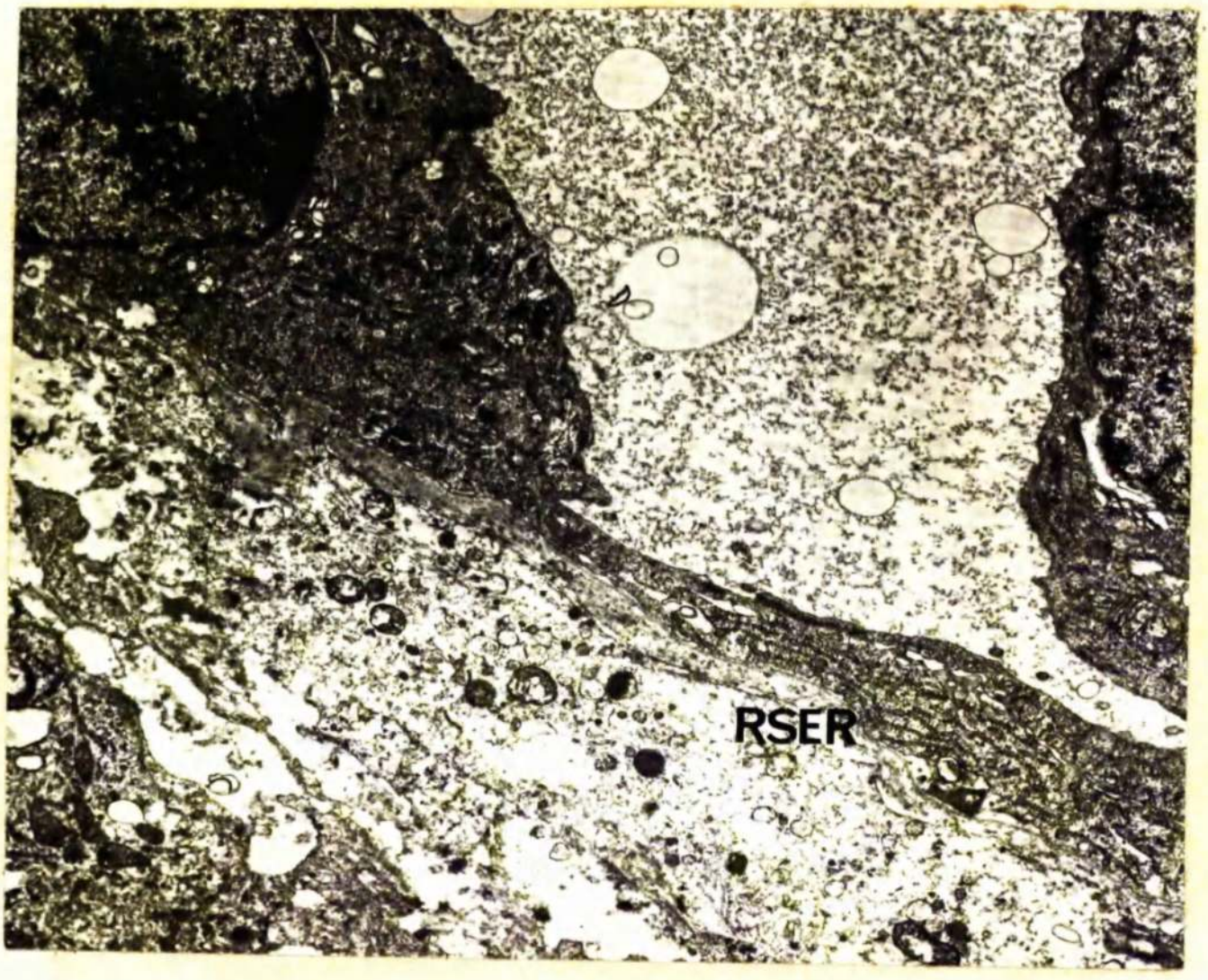

Figure 65. Day 21. Stretched zymogen cells, recognised by parallel stacks of RSER, lining dilated gland in the vicinity of a parasitised gland. Fixation 4% glutaraldehyde. x 10,000.

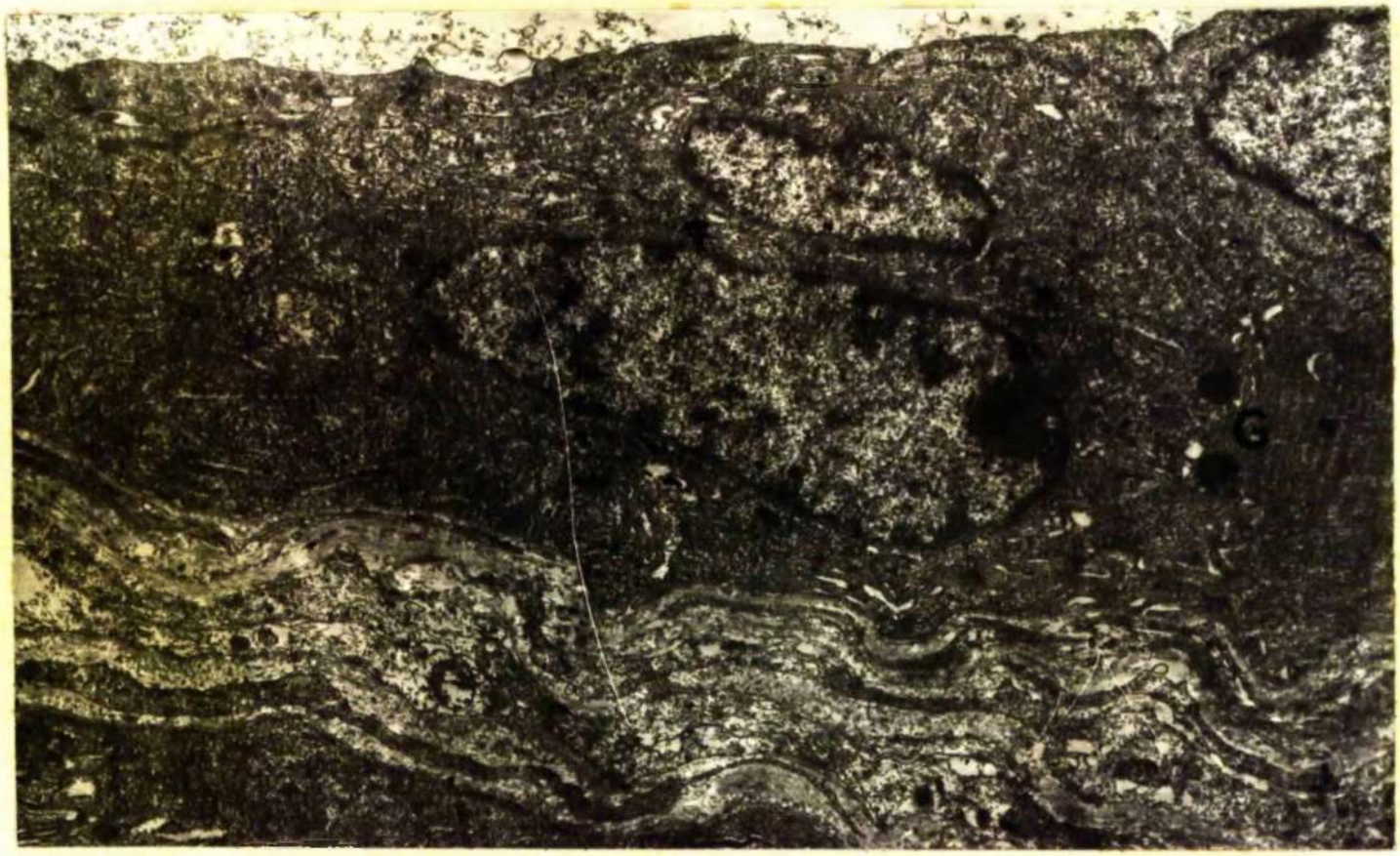

Figure 66. Day 23. Flattened zymogen cells lining dilated gland. Note the sparsity of pepsinogen granules. Fixation 4% glutaraldehyde. x 10,000.

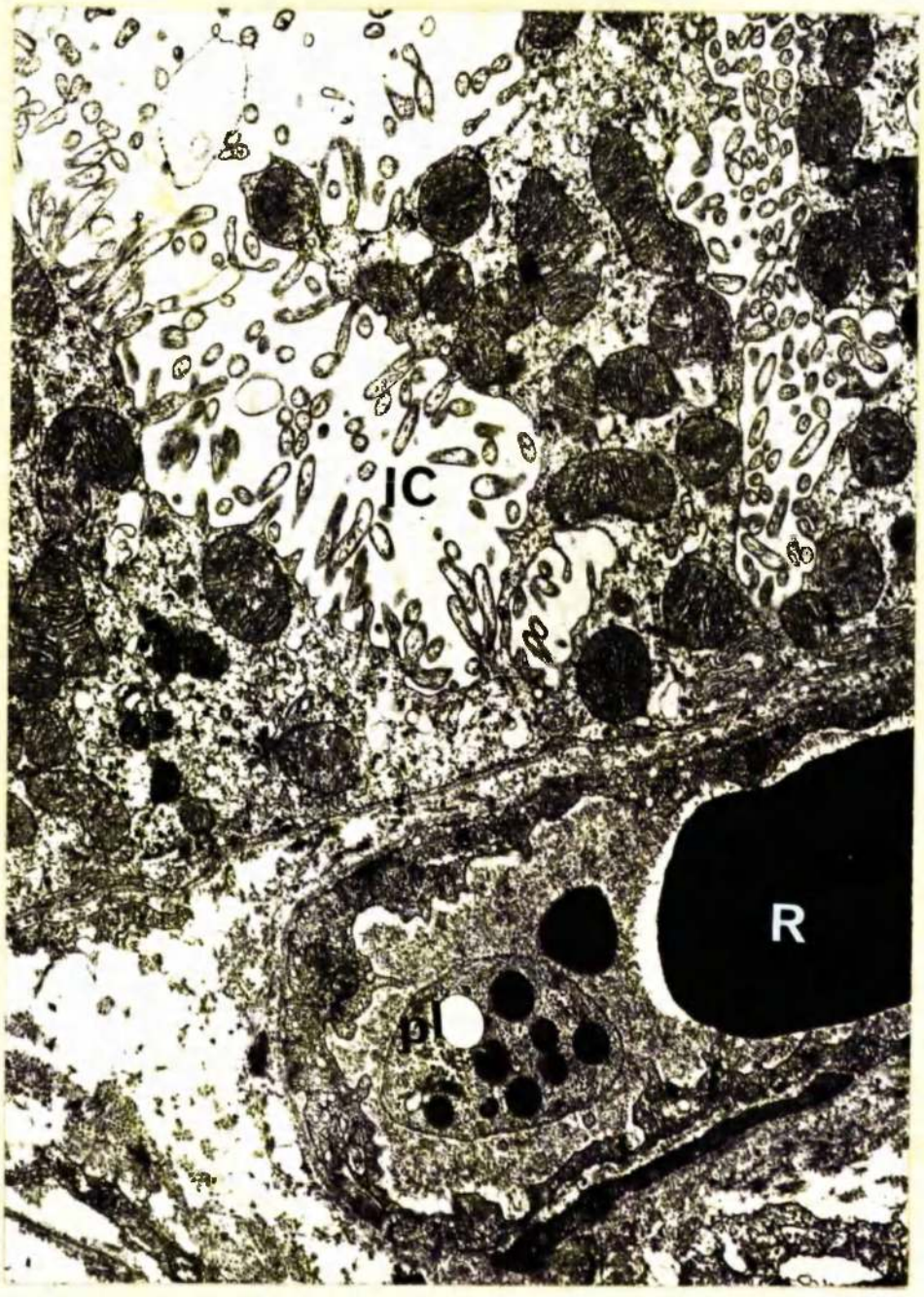

Figure 67. Day 23. Part of stretched parietal cell lining dilated gland. The intracellular canaliculi (IC) are markedly dilated and communicate directly with the lumen of the gland. Note the capillary in the lamina propria containing a red blood cell (R) and a platelet (pl).
Fixation 4% glutaraldehyde. x 12,500.

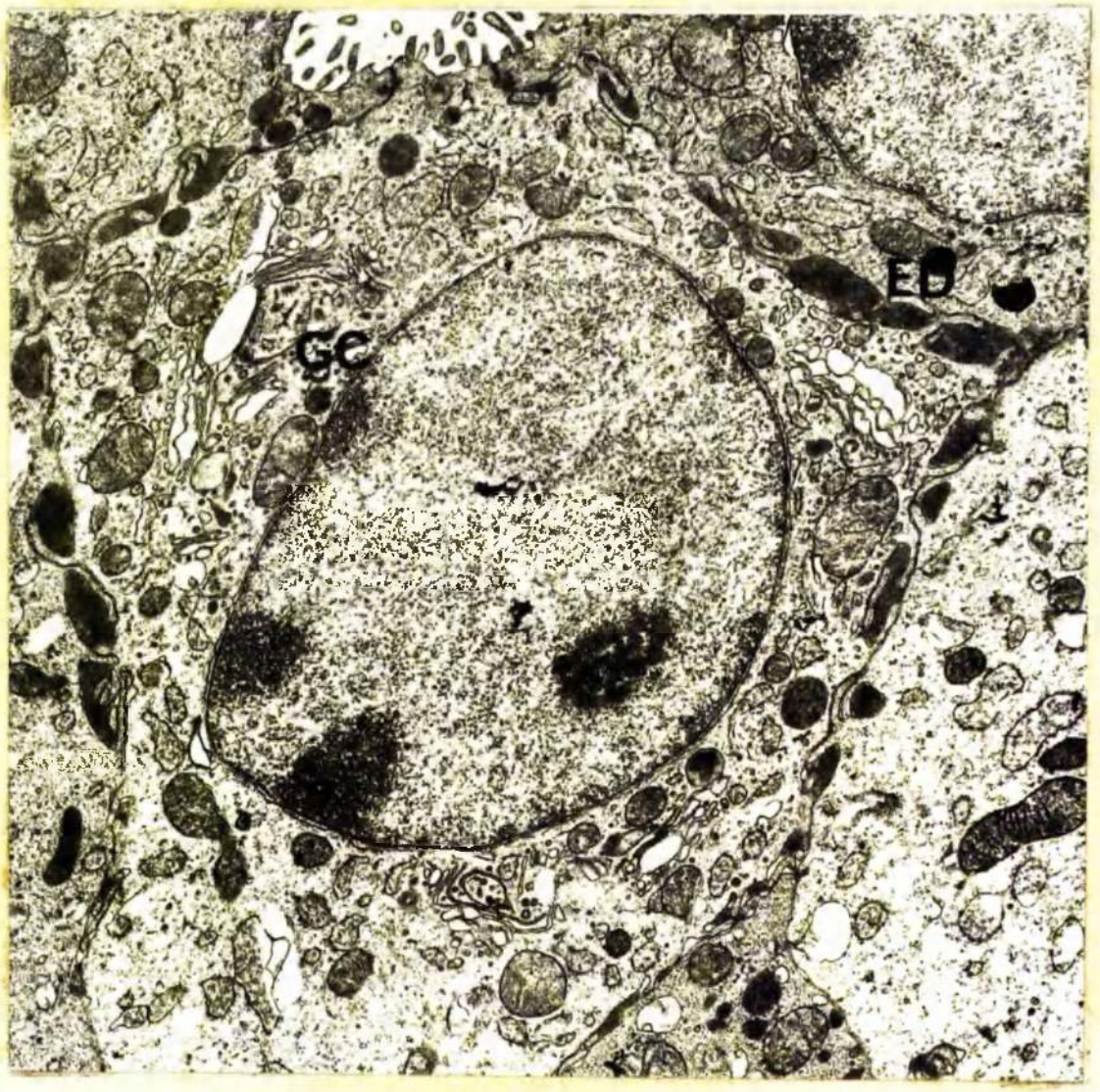

Figure 68. Day 27. Undifferentiated cell in hyperplastic non-functional mucosa. The nucleoplasm and the cytoplasm are of low electron density. Note the lack of structural features of any gastric epithelial cell. The golgi complex (GC) is extensive and the mitochondria are prominent. Electron-dense material (ED) dilates the intercellular spaces. Fixation 1% glutaraldehyde. x 12,500.

Figure 69. Day 30. Undifferentiated cell showing same structural features as Fig. 68. Fixation 1.5% glutaraldehyde. x 12,500.

Figure 70. Day 27. Juxtaluminal segment of undifferentiated cells showing electron-dense material (↑) lying in and dilating the intercellular space. Inset shows the material between the lateral plasmalemmata of the zonula occludens (ZO).
Fixation 1.5% glutaraldehyde. x 75,000 (Insert x 120,000).

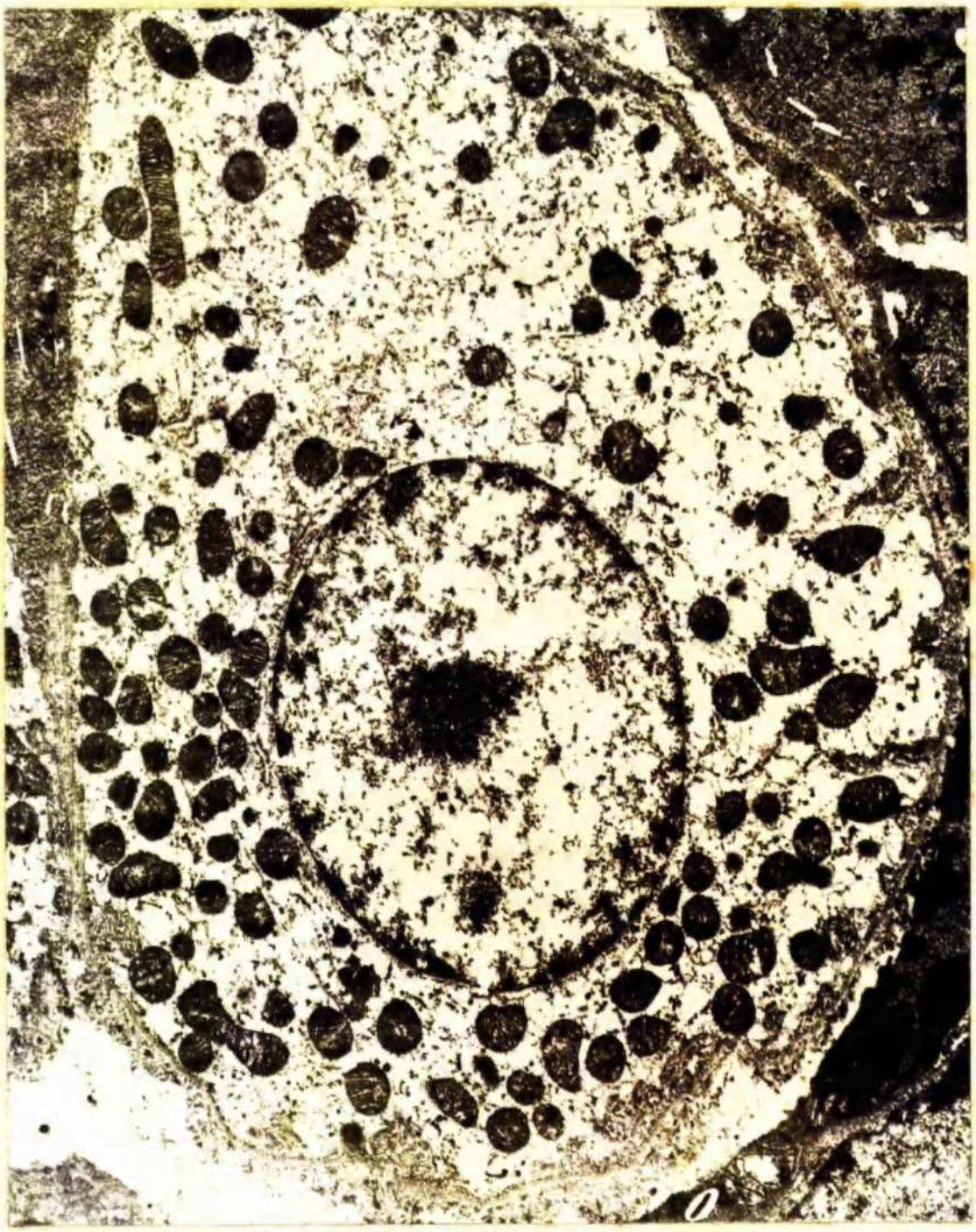

Figure 71. Day 22. Parietal cell with a degenerate pseudovacuolated cytoplasm and lacking intracellular canaliculi.

Fixation 4% glutaraldehyde. x 10,000.

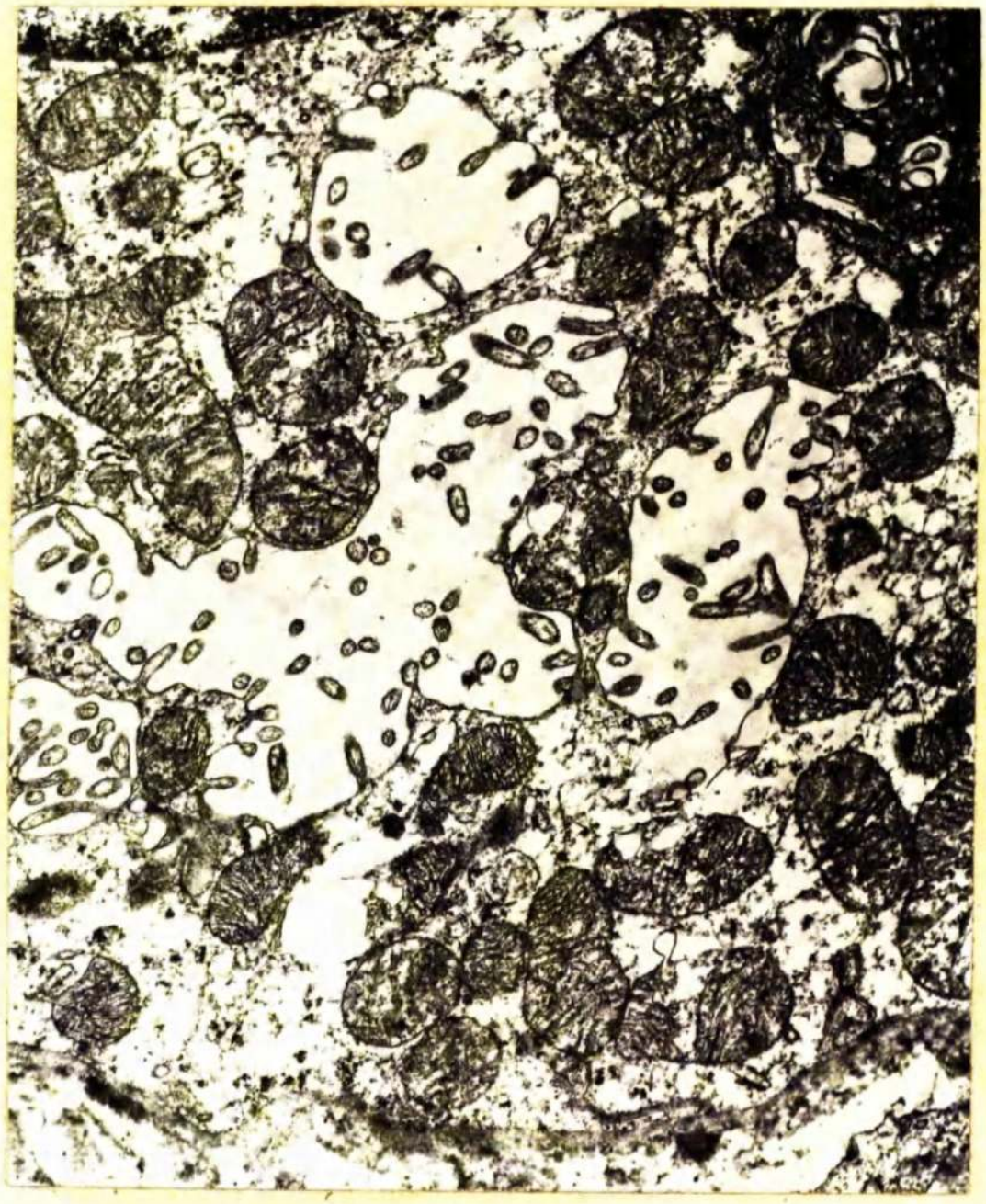

Figure 72. Day 25. Dilated intracellular canaliculi in a parietal cell. Note reduction in the number of microvilli. Fixation 4% glutaraldehyde. x 18,750.

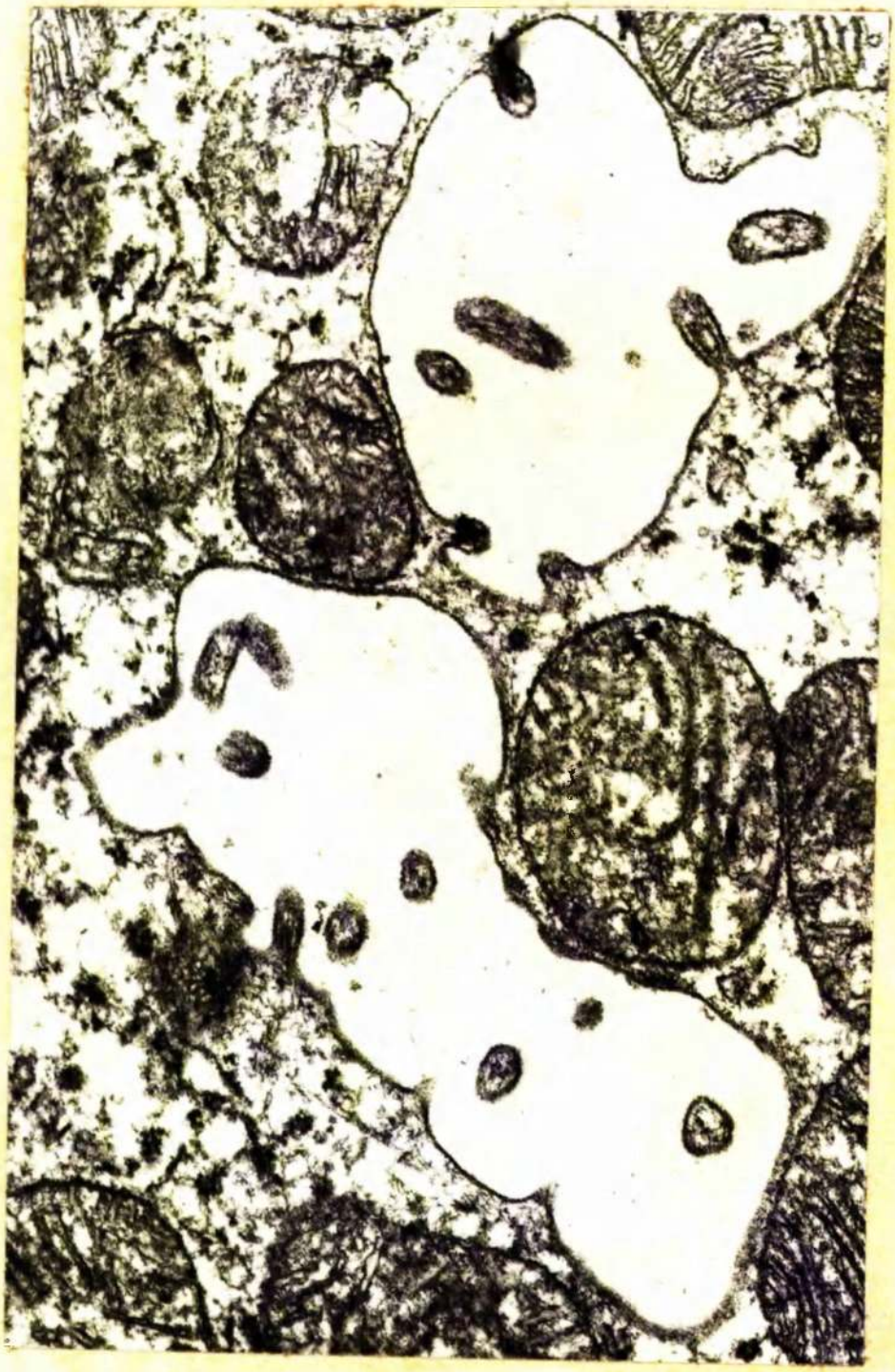

Figure 73. Day 27. Dilated intracellular canaliculi lined by a few microvilli. Fixation 4% glutaraldehyde. x 45,000.

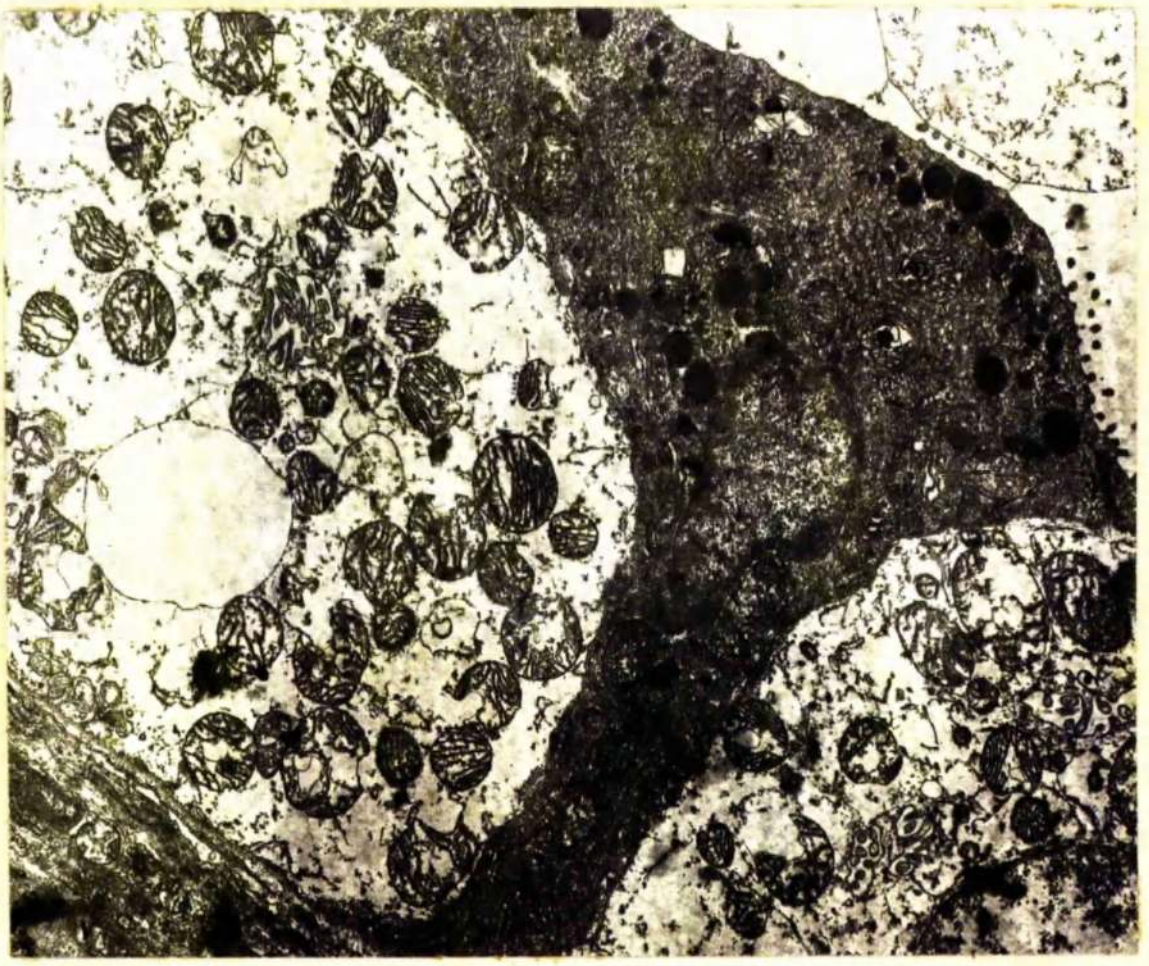

Figure 74. Day 25. Zymogen cell showing marked reduction in size and number of pepsinogen granules present. Note the degenerate pseudovacuolated cytoplasm in the associated parietal cells. Fixation 4% glutaraldehyde. x 8,000.

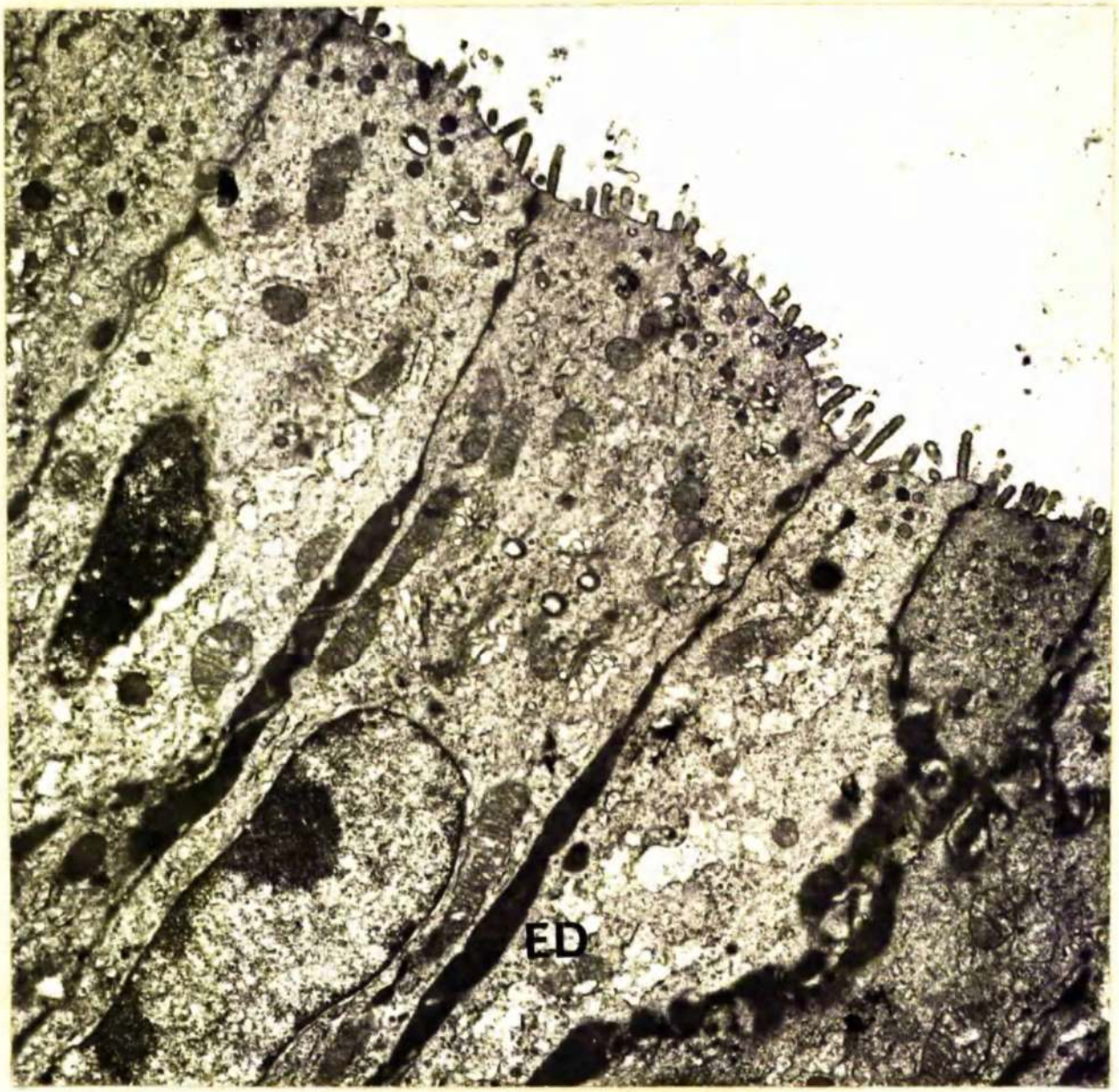

Figure 75. Day 29. Lateral boundaries of differentiating surface mucous cells are delineated by electron-dense material (ED). Fixation 1.5% glutaraldehyde. x 12,500.

Figure 76. Day 28. Surface mucous cells in area of submucosal oedema. The dilated intercellular spaces contain material of moderate electron density. Fixation 1.5% glutaraldehyde. x 9,000.

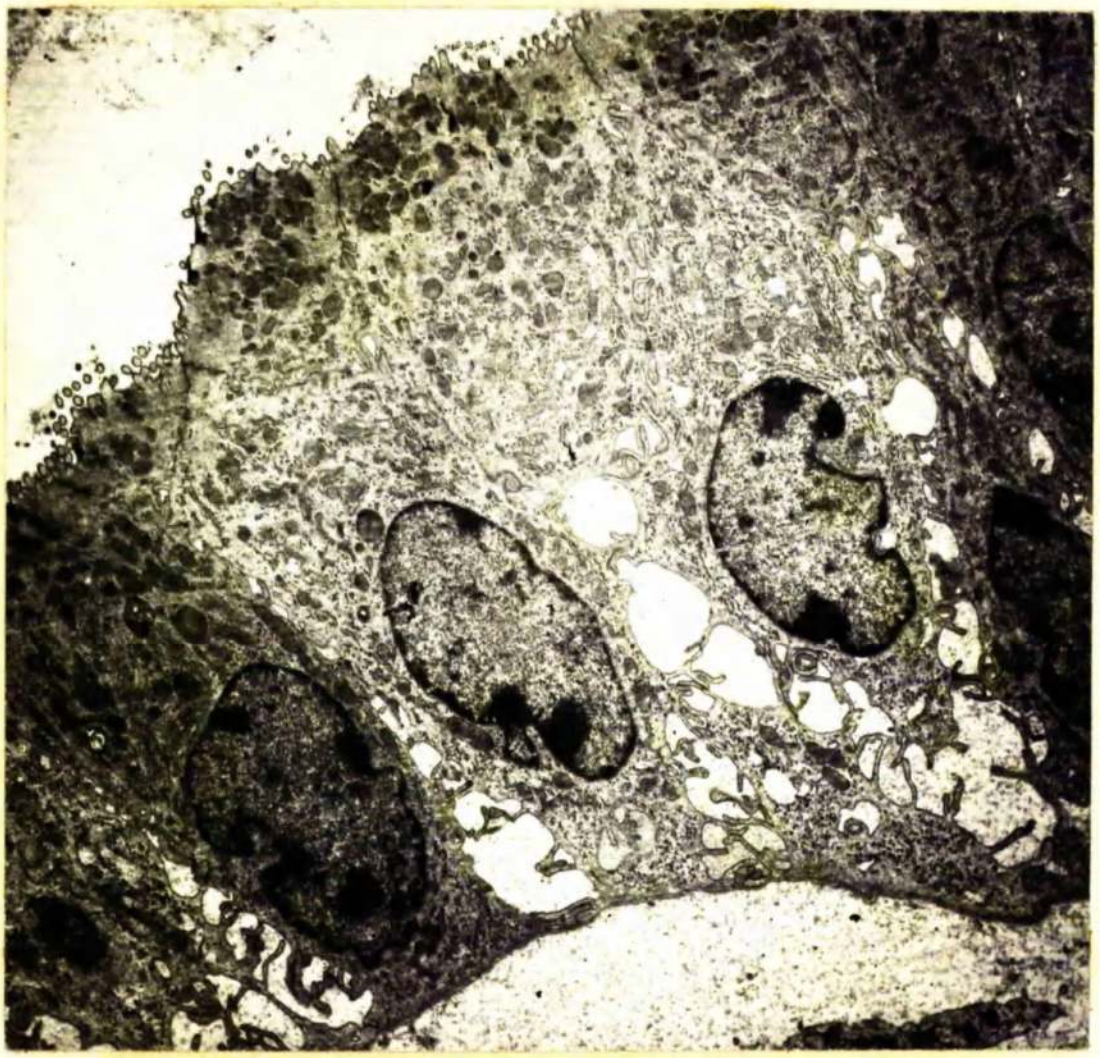

Figure 77. Day 28. Dilated intercellular spaces between surface mucous cells in area of submucosal oedema. Fixation 1% osmium tetroxide. x 6,000.

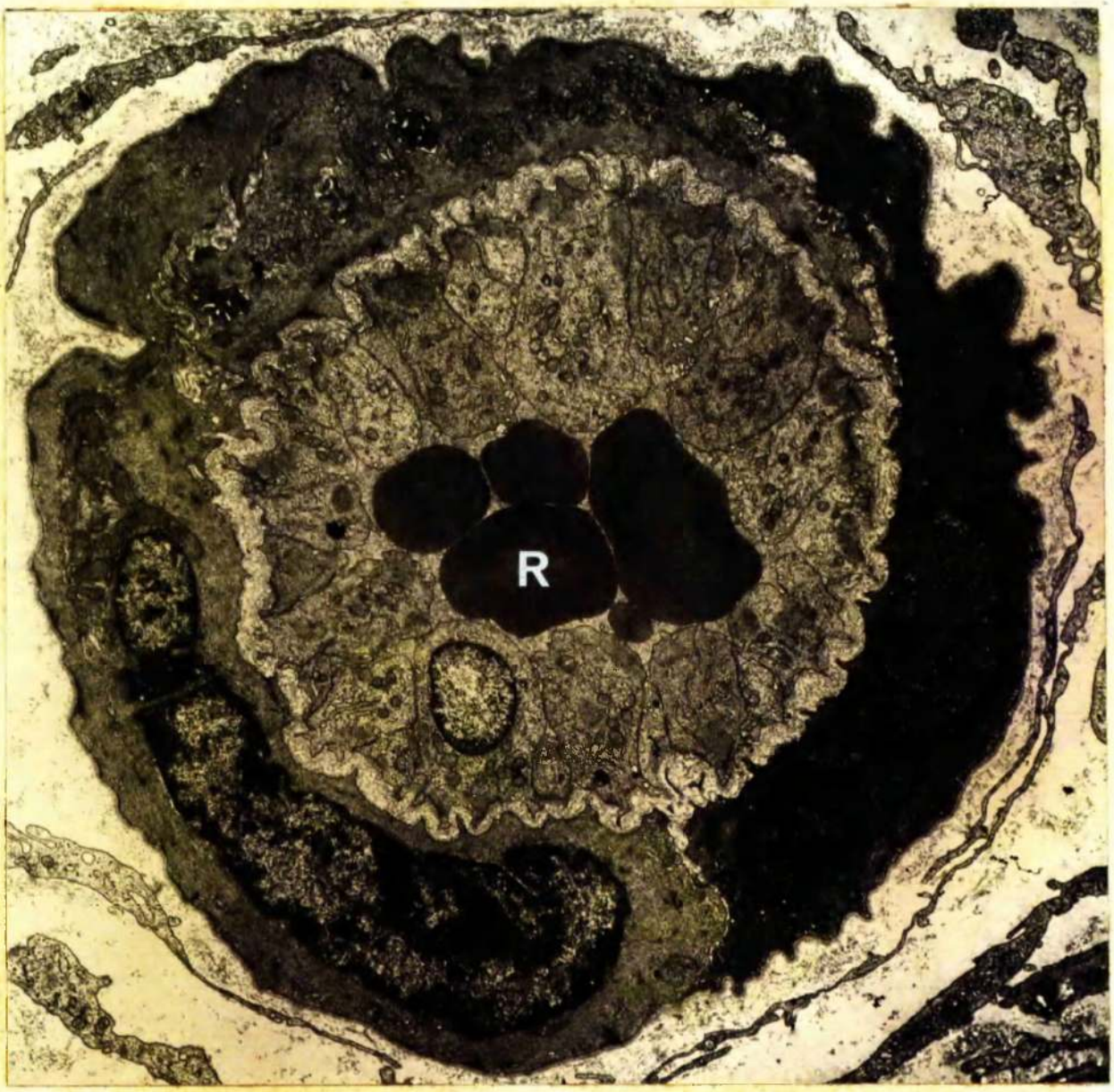

Figure 78. Day 25. Arteriole packed with red blood cells (R).
Fixation 1.5% glutaraldehyde. x 9,000.

Figure 79. Day 25. Capillary containing red blood cell (R) and a platelet (pl). Fixation 1.5% glutaraldehyde. x 12,500.

Figure 80. Day 27. Eosinophil leukocyte (Eo) and lymphocytes (L) in venule. Fixation 1% osmium tetroxide. x 10,000.

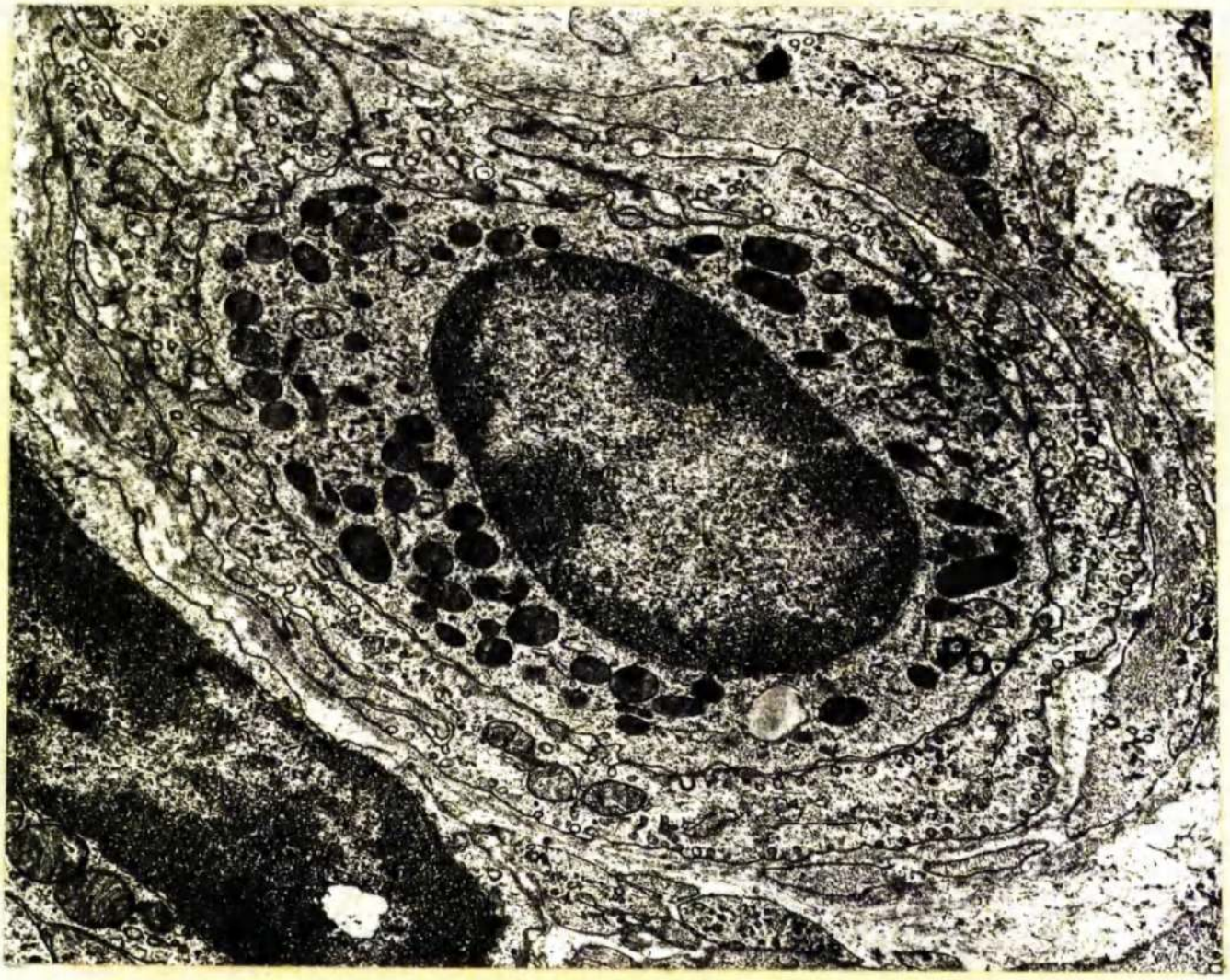

Figure 81. Day 26. Polymorphonuclear leukocyte (Po) in capillary. Fixation 1% osmium tetroxide. x 18,750.

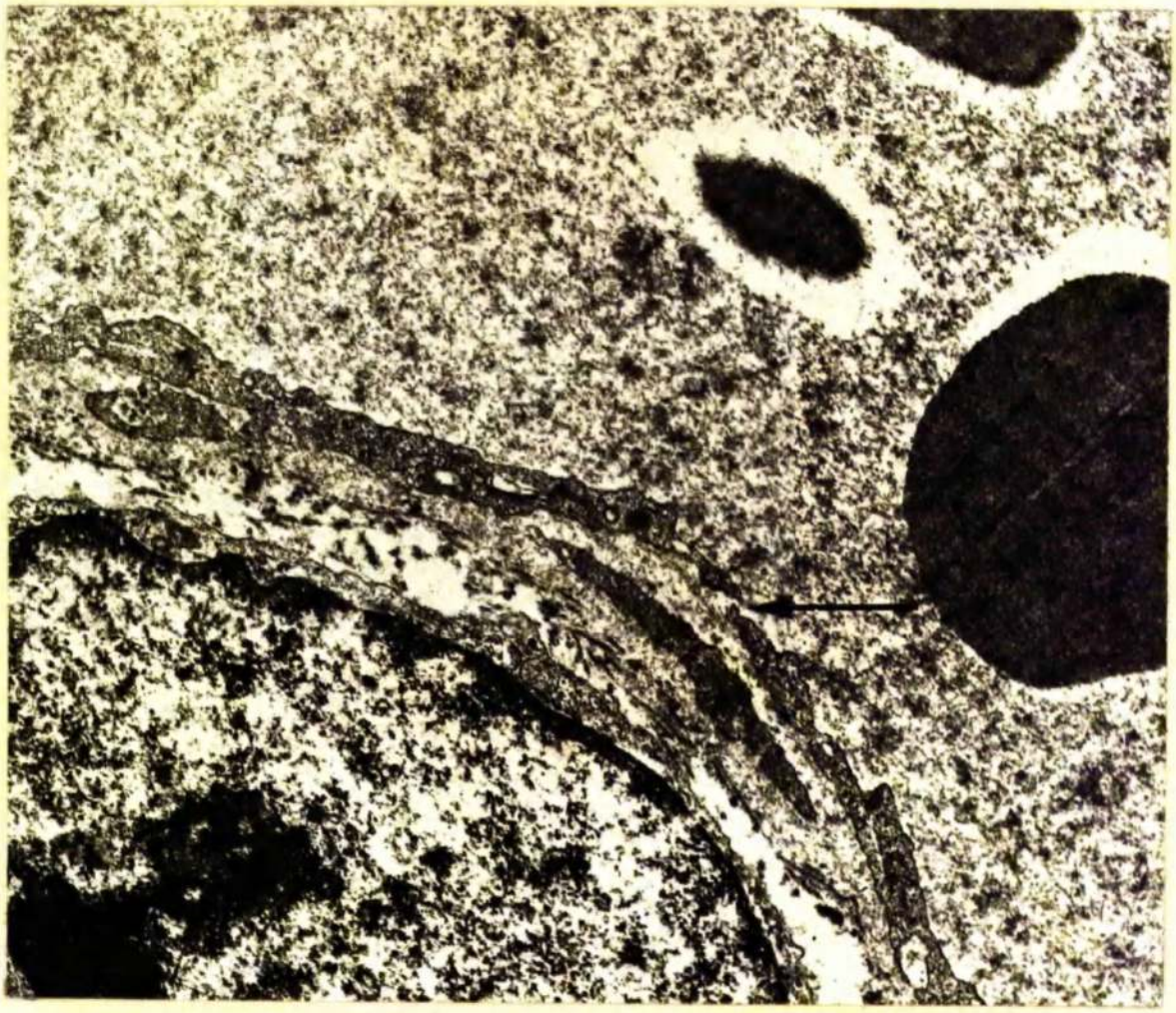

Figure 82. Day 28. Opening between two endothelial cells lining venule (↑). Fixation 4% glutaraldehyde. x 15,000.

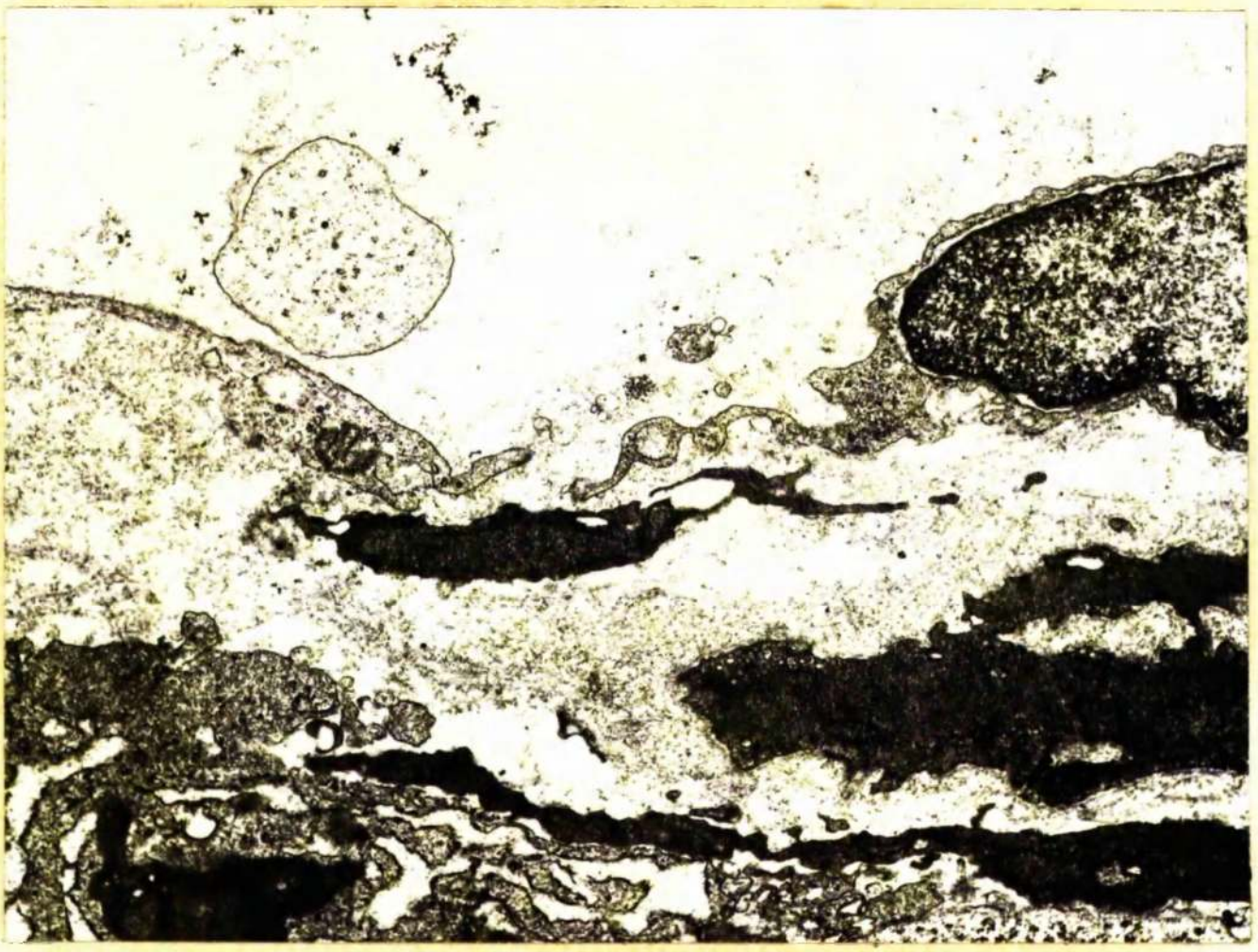

Figure 83. Day 27. Separation of lymphatic endothelial cells.

Fixation 1.5% glutaraldehyde. x 15,000.

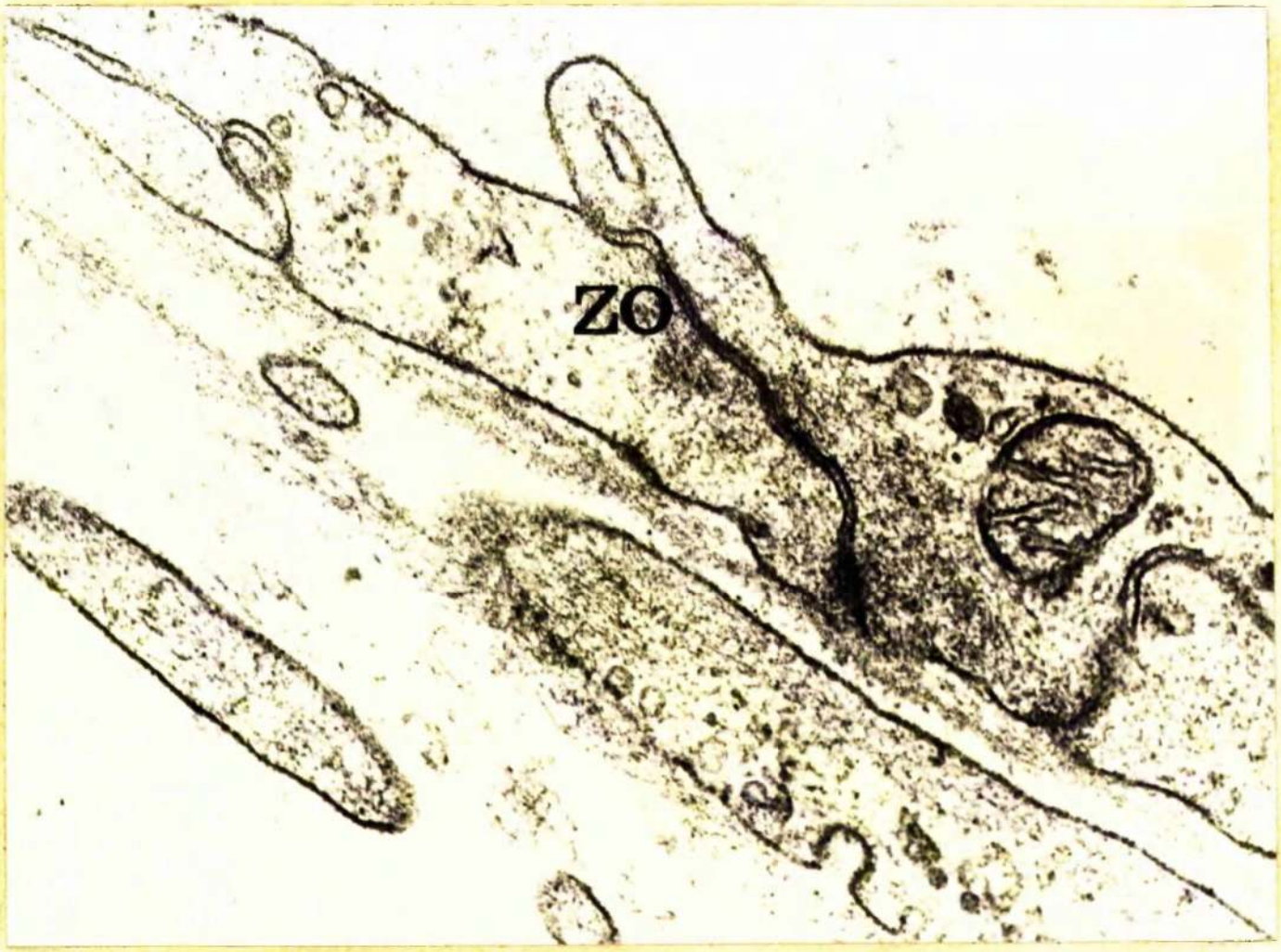

Figure 84. Day 27. Intact zonula occludens (ZO) between two endothelial cells in capillary. Fixation 1% osmium tetroxide. x 75,000.

Figure 85. Day 27. Macula occludens (MO) between two endothelial cells in capillary. Fixation 1% osmium tetroxide. x 75,000.

Figure 86. Day 63. Gastric mucosa has almost returned to normal. Note the distended gland which formerly housed a larva. The surrounding glands contain their full complement of mucous neck (MN), parietal (Pa) and zymogen cells (Z). x 140.

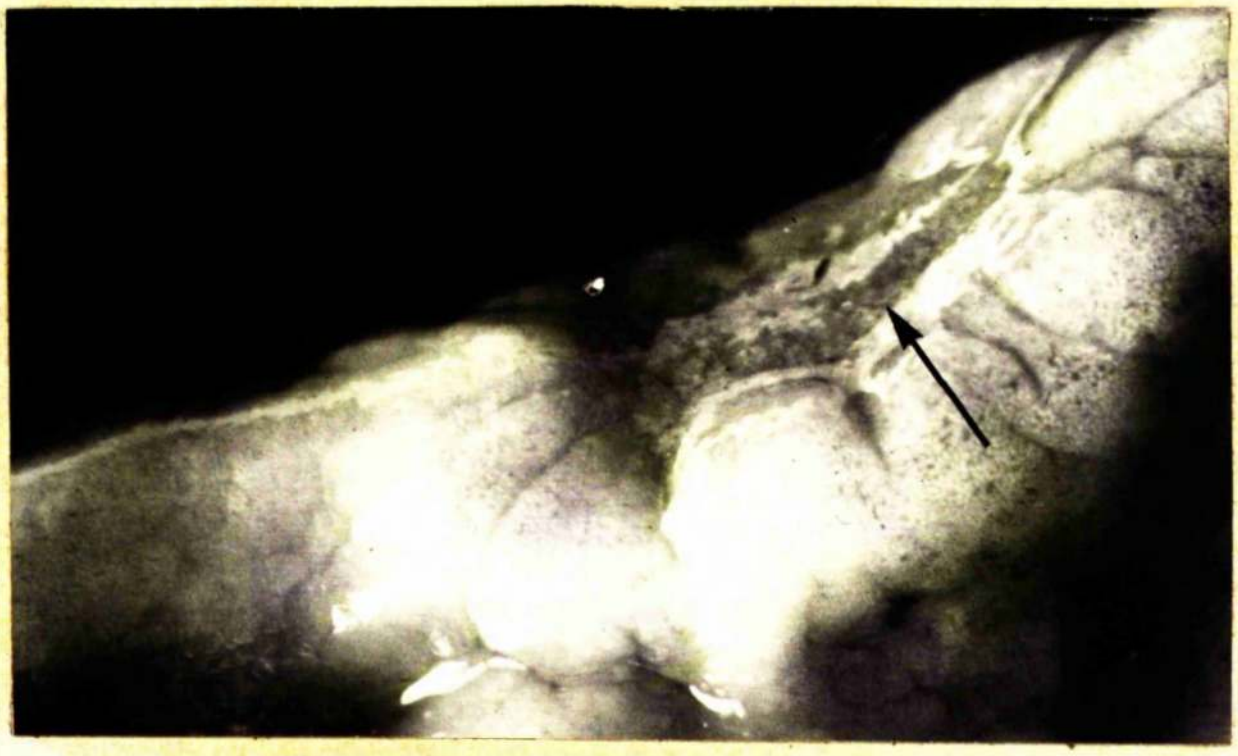

Figure 87. Day 42. "Thumb-print" lesion (↑).

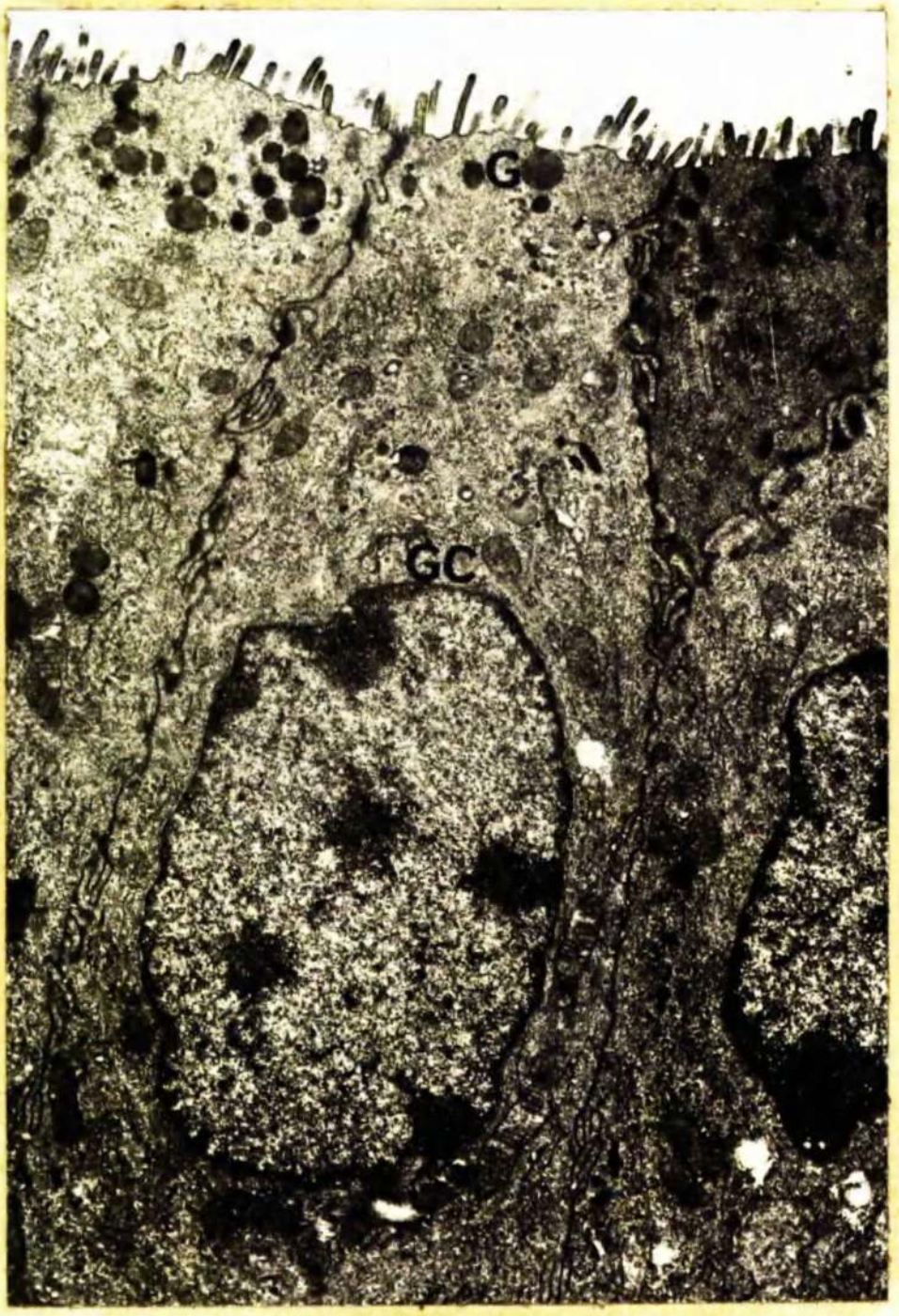

Figure 88. Day 35. Immature surface mucous cell. Note the round and oval granules (G) in apical cytoplasm, golgi complex (GC) capping the nucleus, localisation of mitochondria in basal cytoplasm and interdigitations (I) of the lateral plasmalemmata.

Fixation 1.5% glutaraldehyde. x 12,500.

Figure 89. Day 35. Developing mucous neck cell showing apical content of large round granules (G), extensive paranuclear golgi complex (GC) and fairly straight lateral plasmalemmata. Fixation 4% glutaraldehyde. x 15,000.

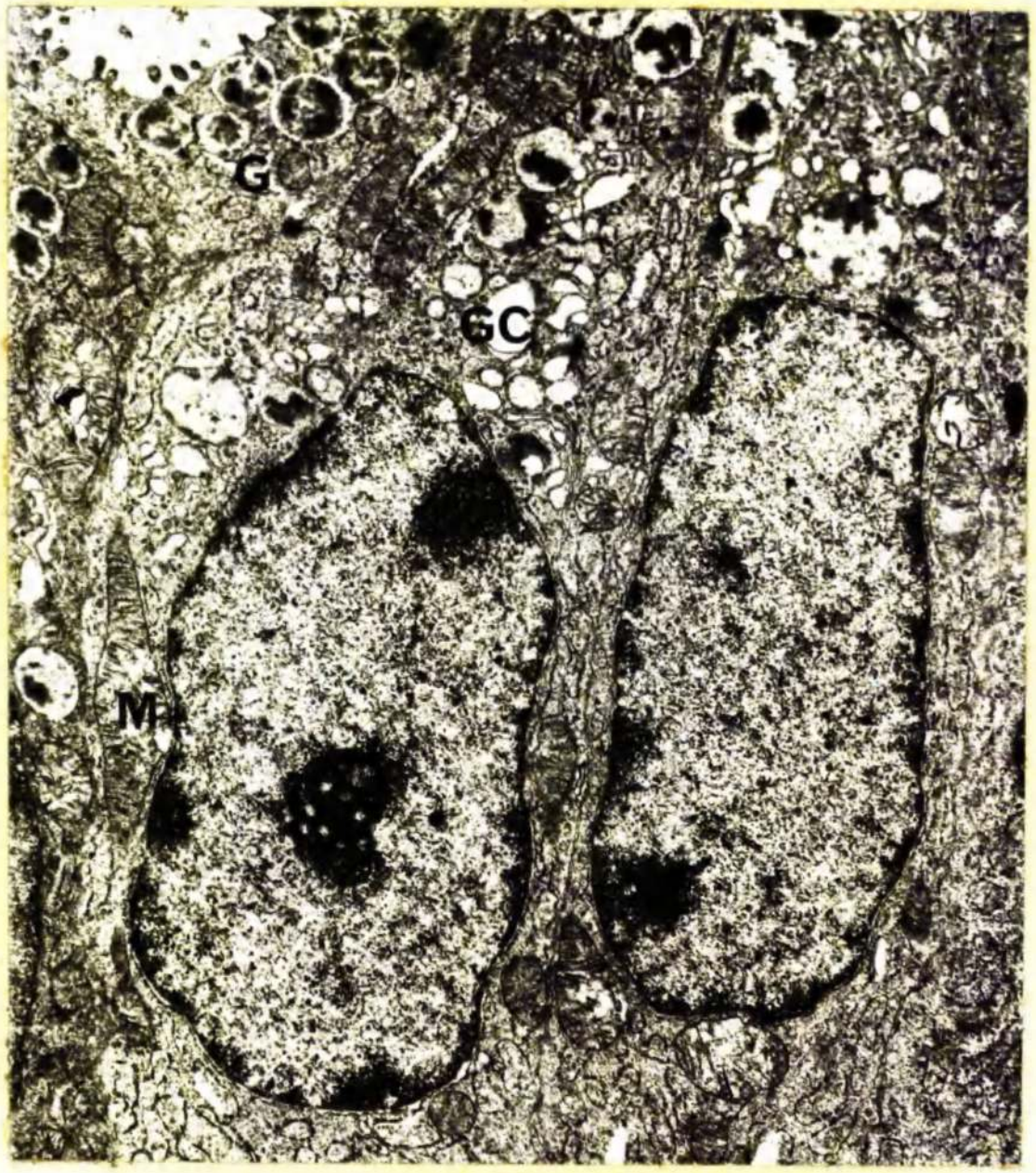

Figure 90. Day 42. Developing mucous neck cell showing elongated mitochondria (M), large round granules (G) in apical cytoplasm, extensive golgi complex (GC) and straight lateral plasmalemmata. Fixation 4% glutaraldehyde. x 12,500.

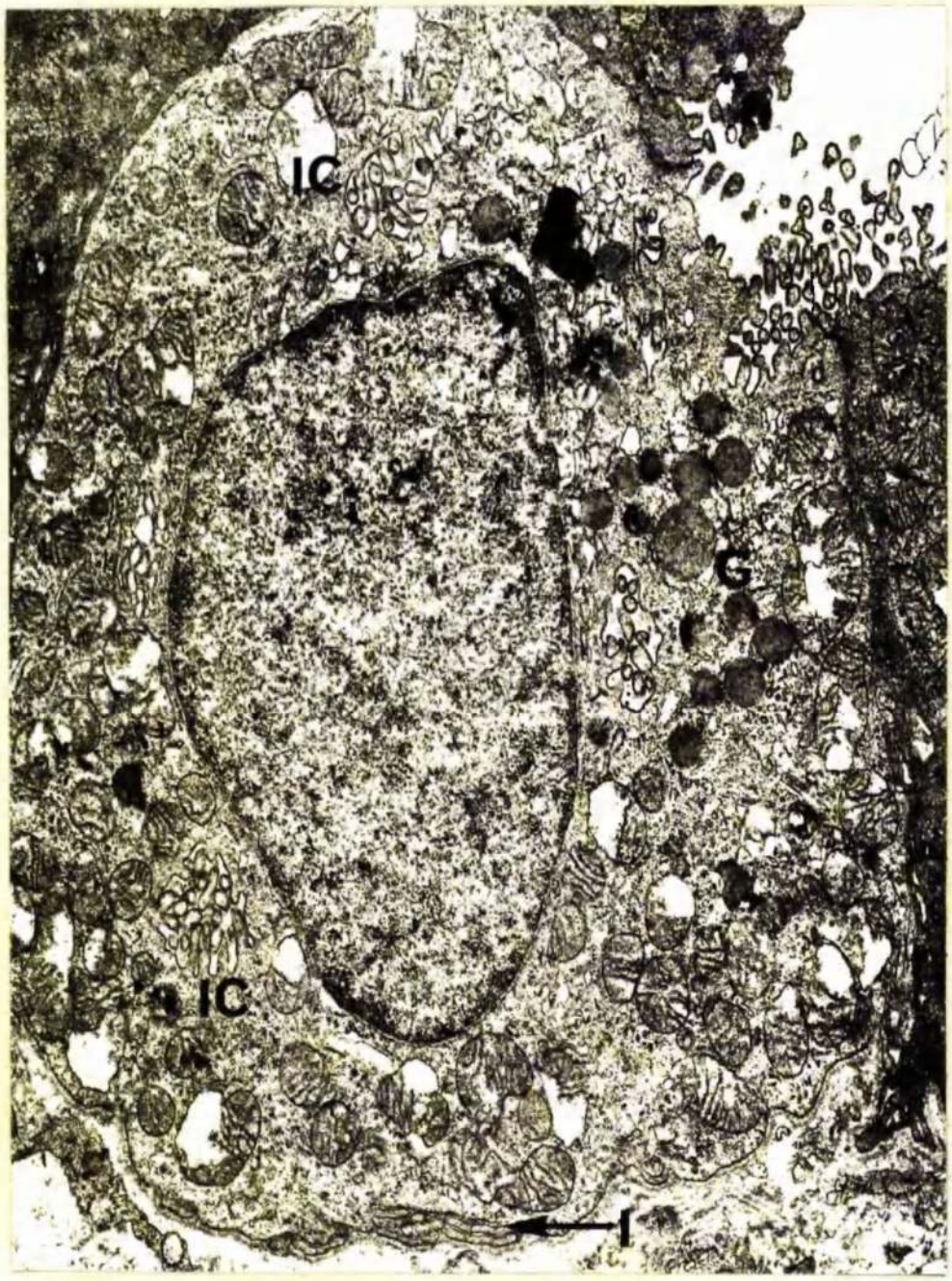

Figure 91. Day 29. Developing parietal cell showing poorly developed intracellular canaliculi (IC), granules (G) of moderate electron density and interdigitations of basal plasmalemmata (I). Fixation 1% glutaraldehyde. x 15,000.

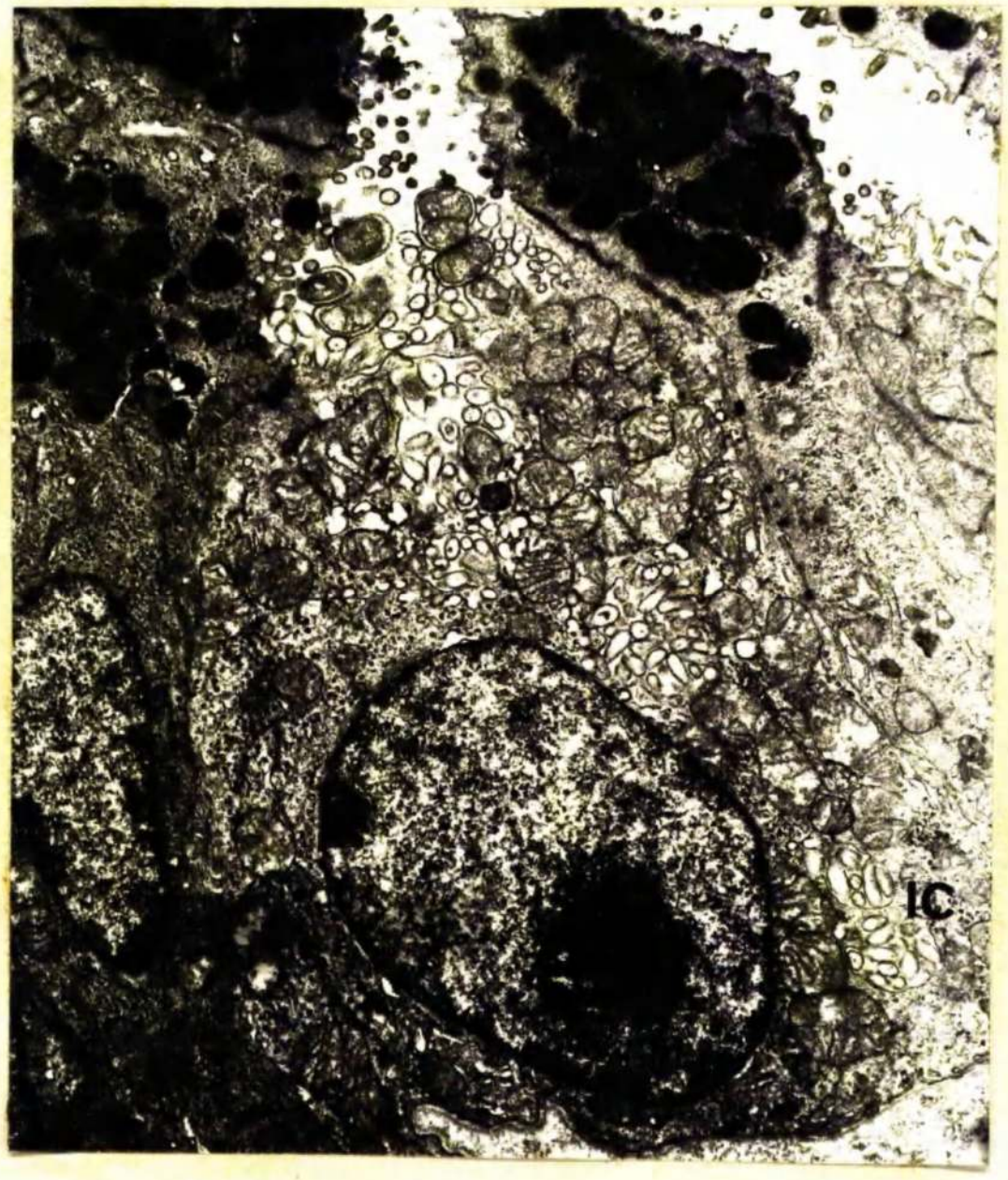

Figure 92. Day 30. Developing parietal cell showing poorly developed intracellular canaliculi (IC). Fixation 1.5% glutaraldehyde. x 10,000.

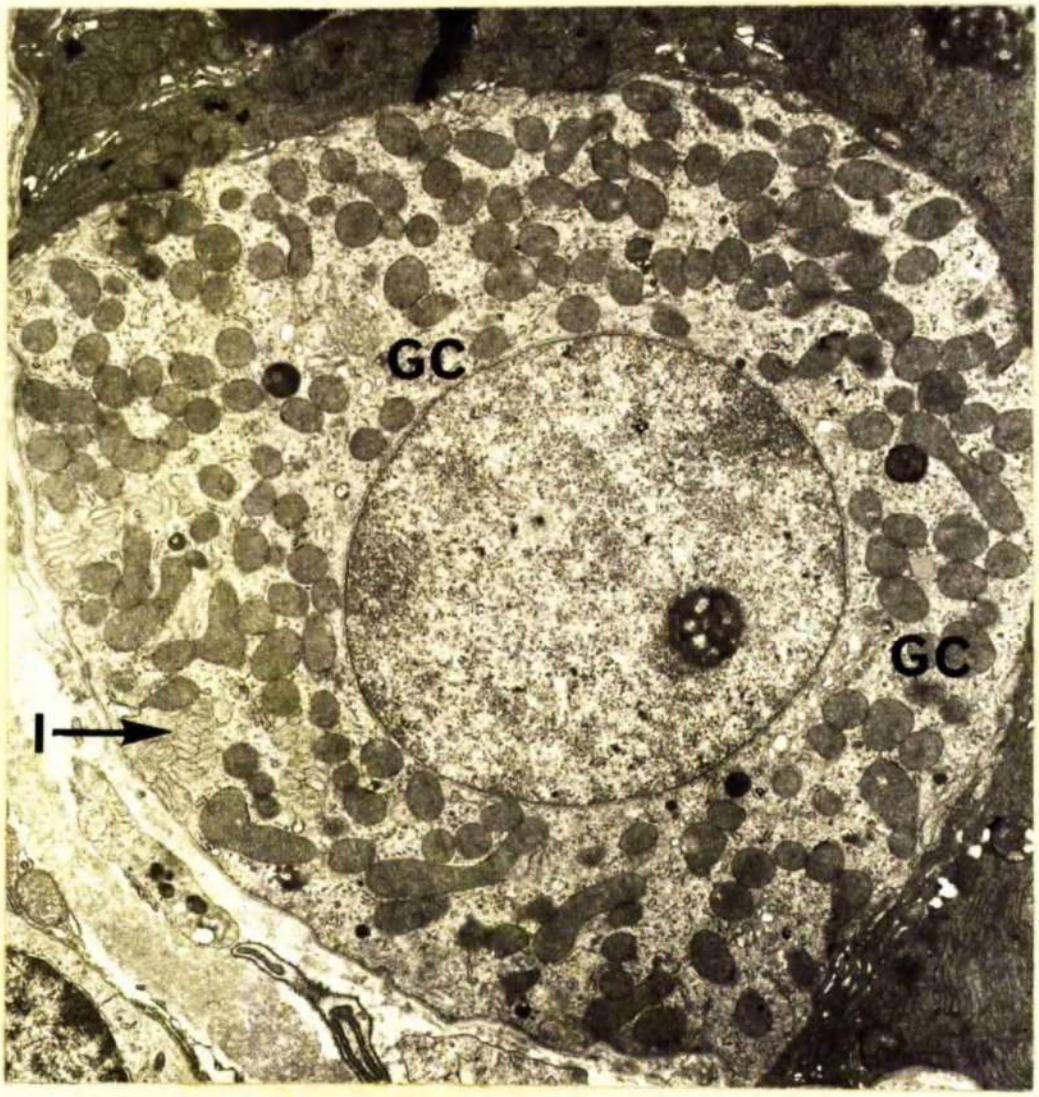

Figure 93. Day 35. Developing parietal cell showing lack of intracellular canaliculi, extensive paranuclear golgi complex (GC) numerous mitochondria lined by many transverse cristae mitochondriales and elaborate interdigitations (I) of basal plasmalemmata. Fixation 1.5% glutaraldehyde. x 10,000.

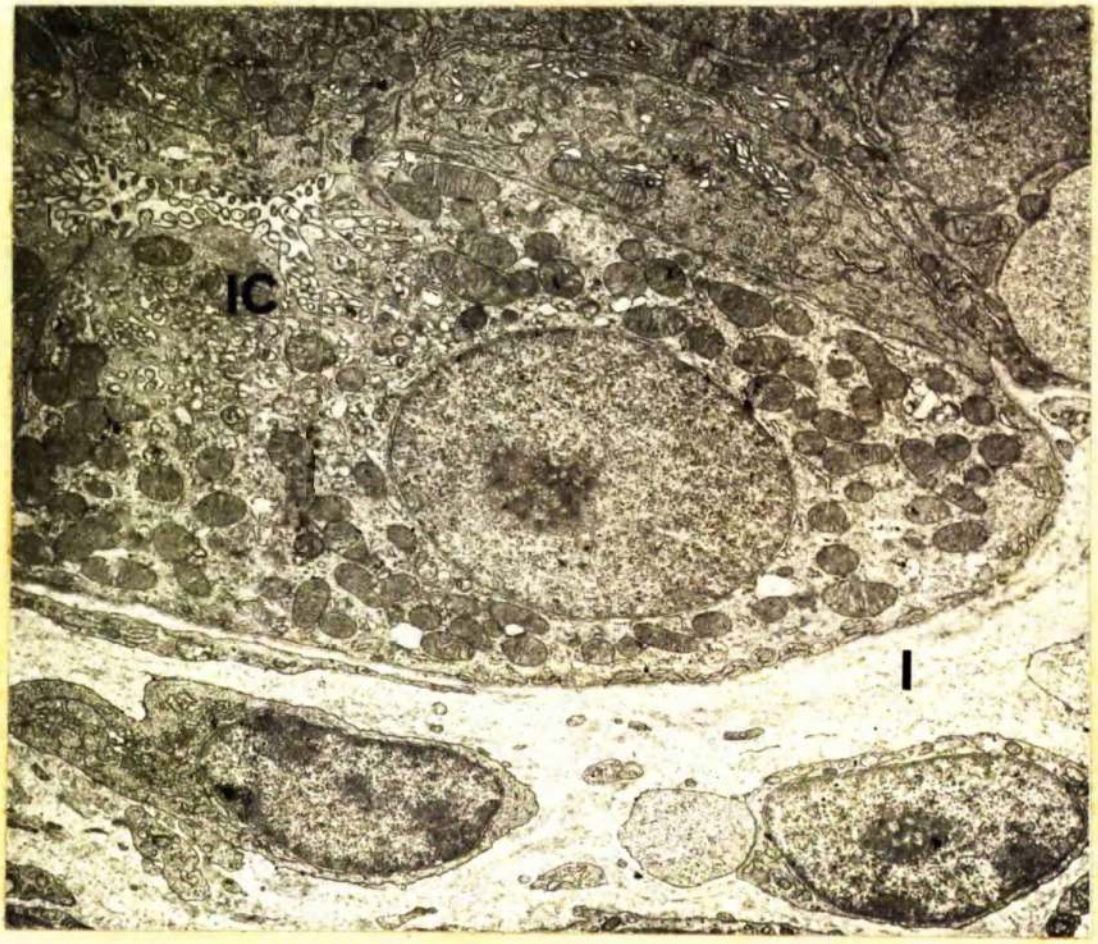

Figure 94. Day 35. Developing parietal cell showing limited development of intracellular canaliculi (IC) and interdigitations (I) of basal plasmalemmata. Fixation 1.5% glutaraldehyde. x 7,500.

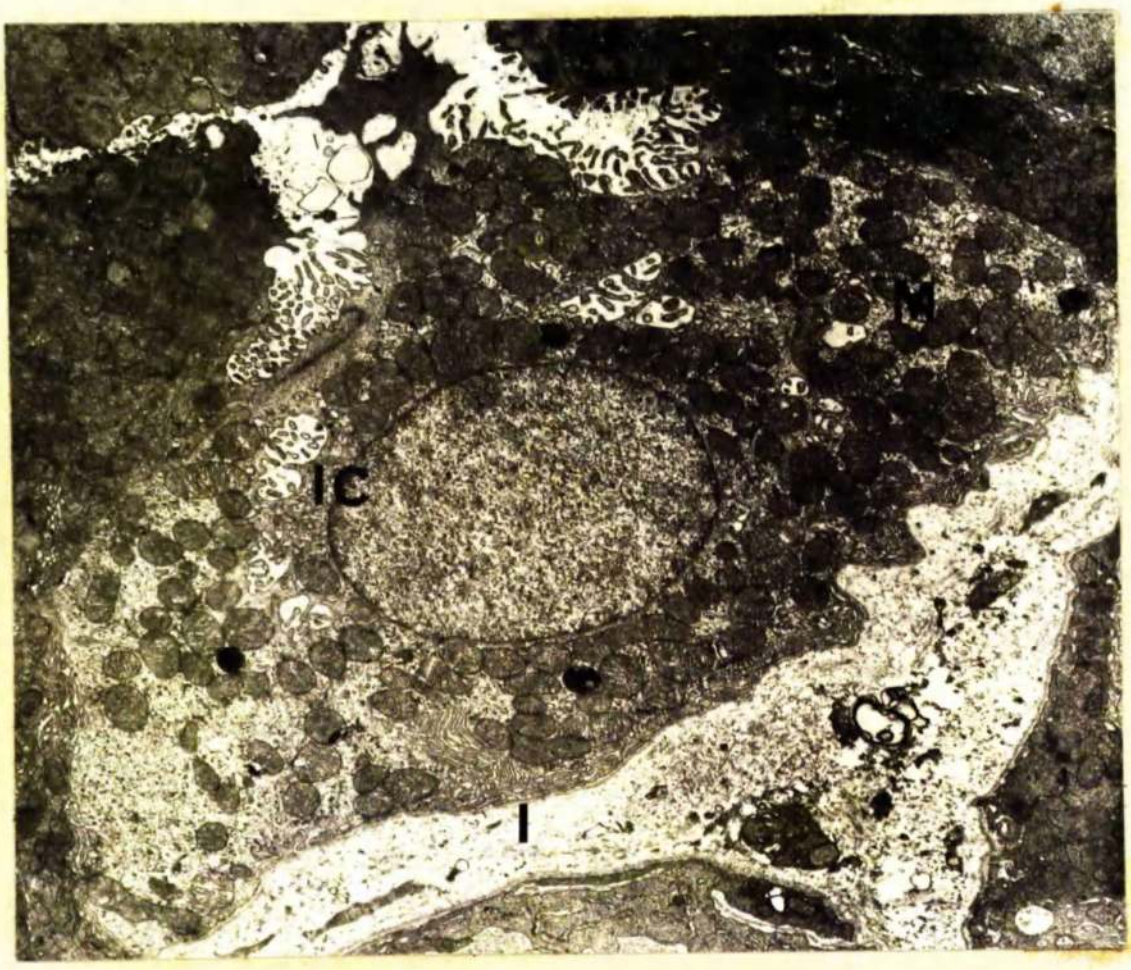

Figure 95. Day 42. Developing parietal cell showing limited development of intracellular canaliculi (IC), numerous mitochondria (M) with many transverse cristae mitochondriales, and elaborate interdigitations (I) of basal plasmalemmata. Fixation 1.5% glutaraldehyde. x 6,000.

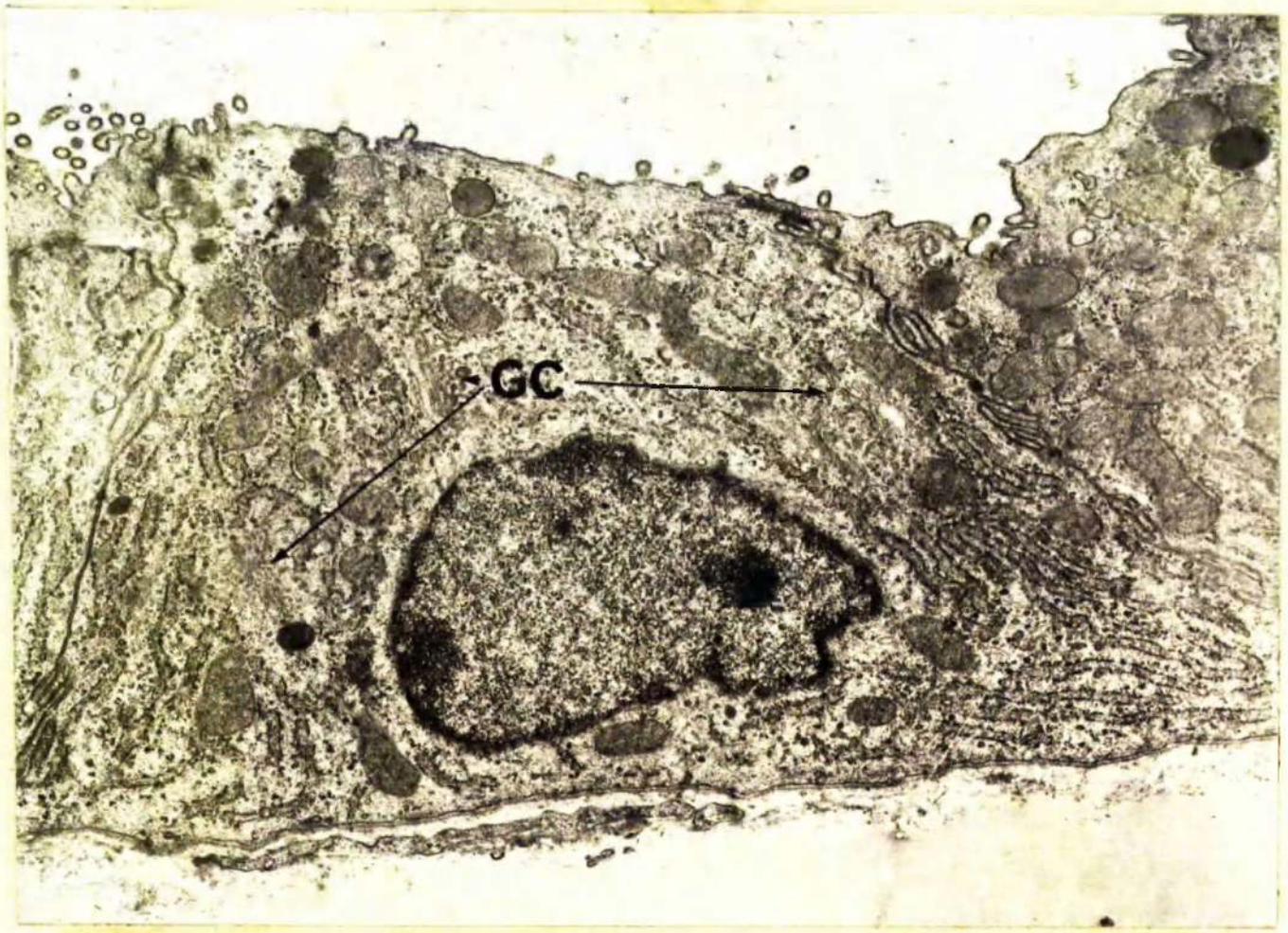

Figure 96. Day 35. Developing zymogen cells showing stacks of RSER parallel to the lateral and basal plasmalemmata and an extensive golgi complex (GC). Fixation 1.5% glutaraldehyde. x 12,500.

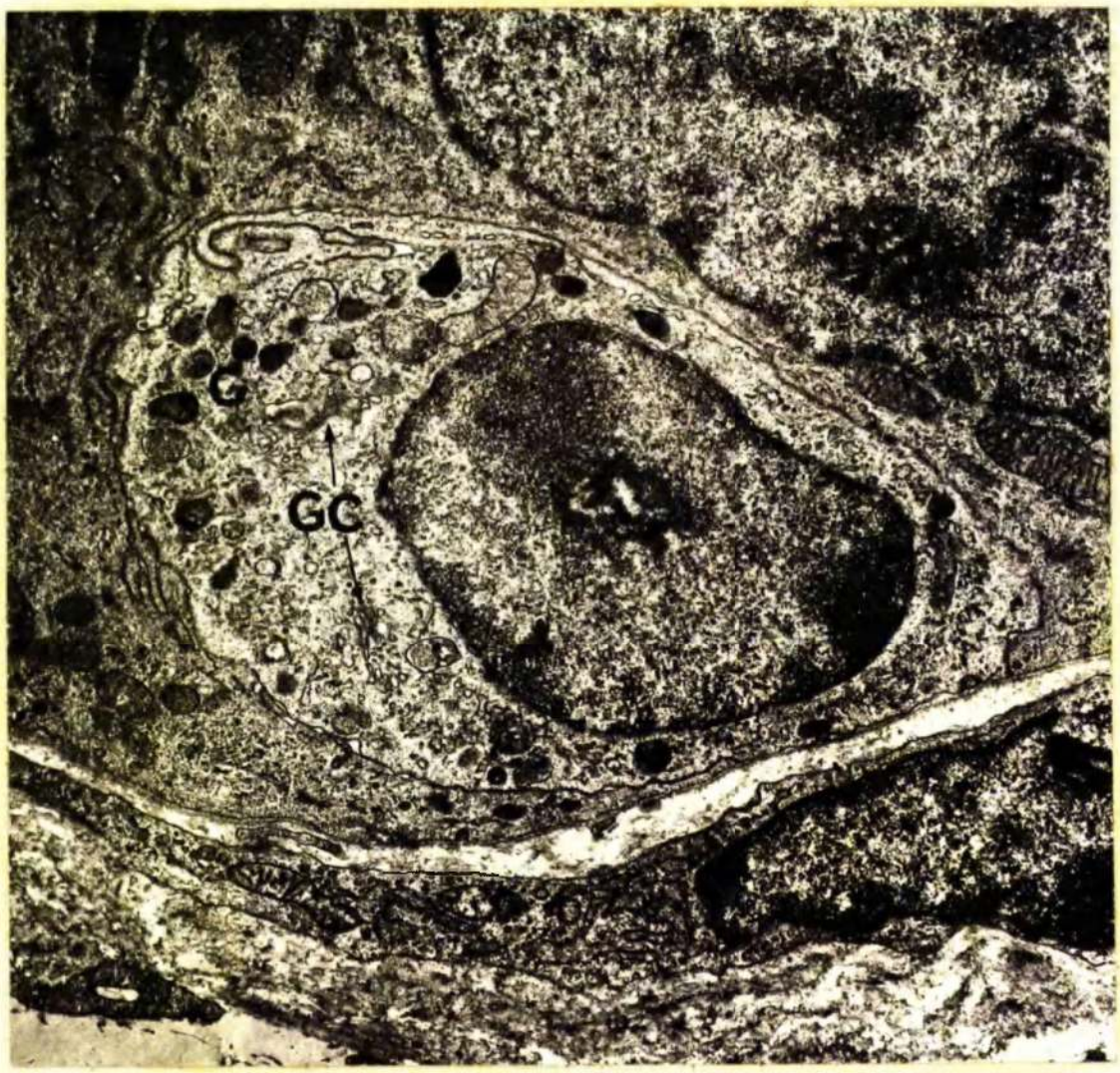

Figure 97. Day 35. Developing enterochromaffin cell containing a few electron-dense granules (G) and an extensive golgi complex (GC). Fixation 1.5% glutaraldehyde. x 12,500.

Figure 98. Day 25. Small lymphocyte containing centrioles (C) and mitochondria (M) with only a few cristae mitochondriales. Fixation 1% osmium tetroxide. x 25,000.

Figure 99. Day 25. Small lymphocyte containing Auer bodies (A). Fixation 1% osmium tetroxide. x 18,750.

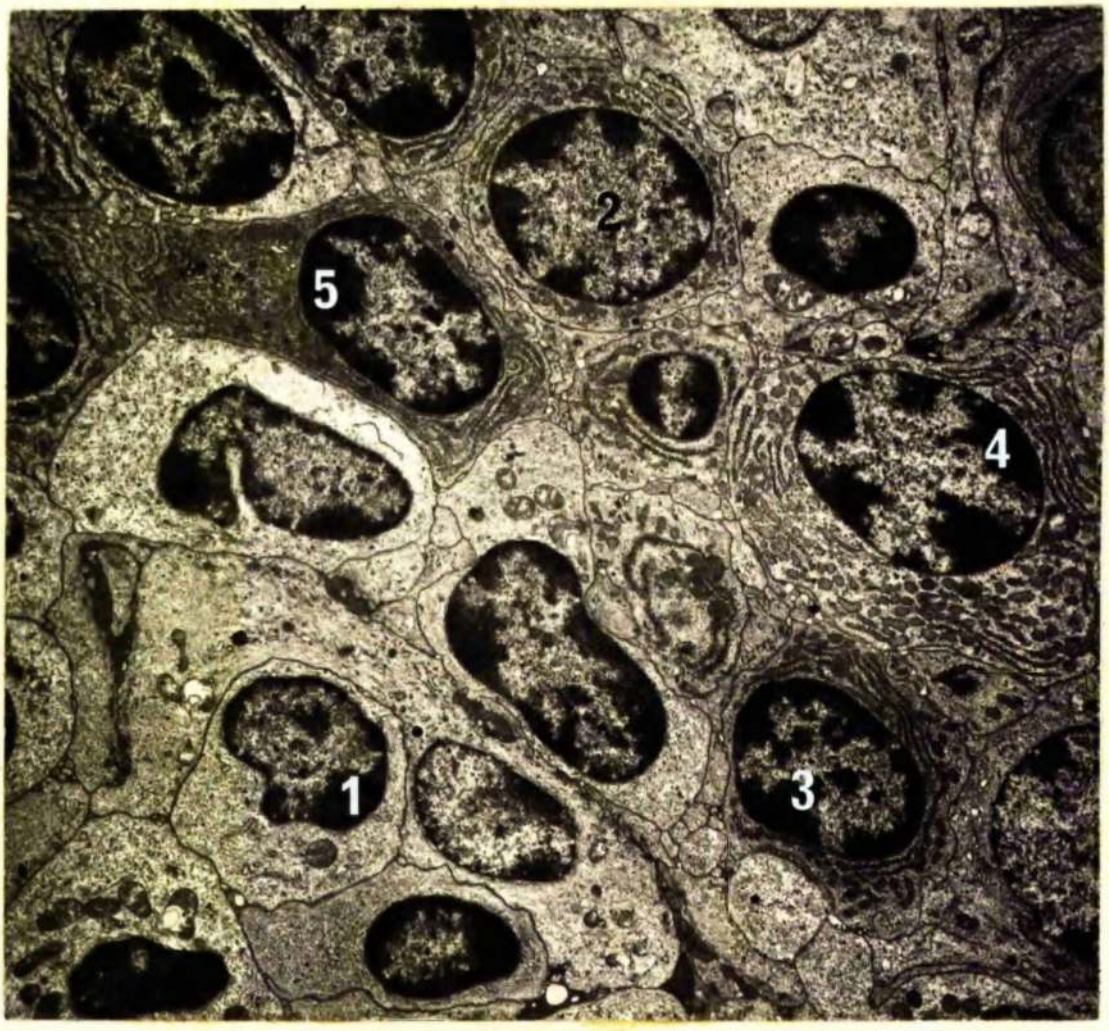

Figure 100 Day 25. A series of cells with increasing amounts of RSER appear to show a link between small lymphocytes and plasma cells (1→2→3→4→5)

Fixation 1.5% glutaraldehyde. x 6,000.

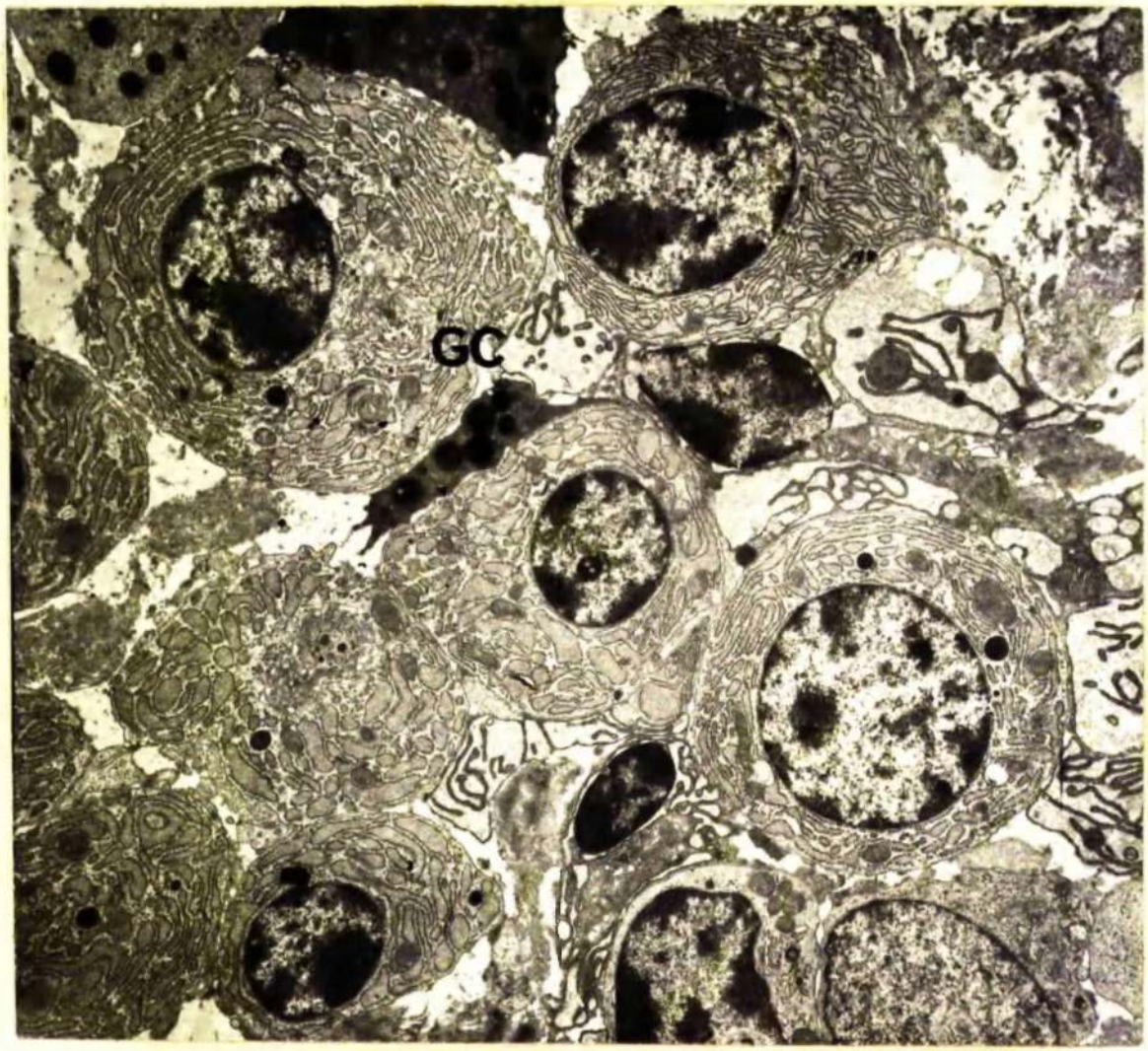

Figure 101. Day 23. Plasma cells in the surface mucosa. Note the extensive RSER and the large golgi complexes (GC). Fixation 1.5% glutaraldehyde. x 6,000.

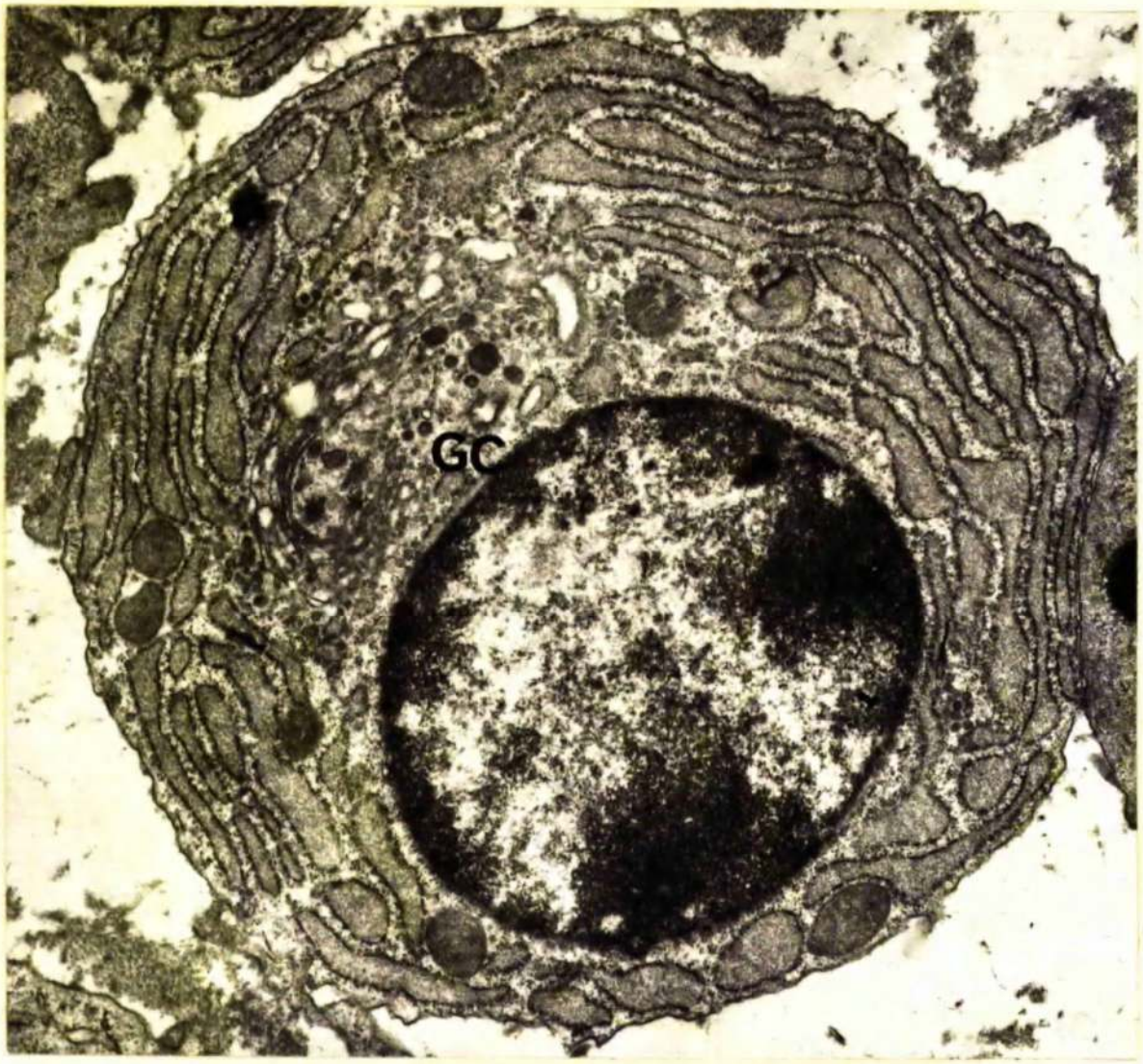

Figure 102. Day 25. Plasma cell showing numerous moderately dilated cisternae of RSER and a large paranuclear golgi complex (GC). Fixation 1.5% glutaraldehyde. x 18,750.

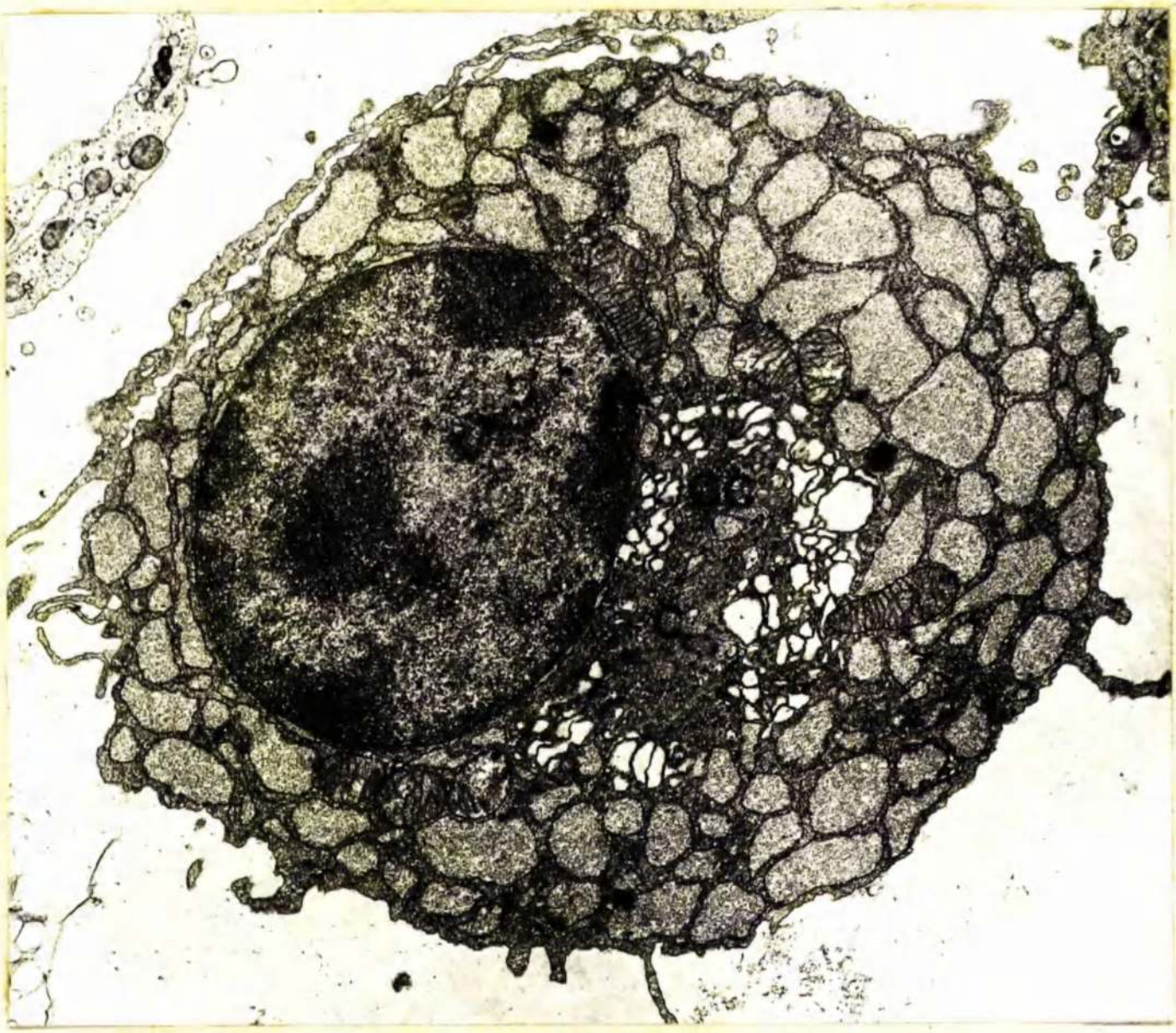

Figure 103. Plasma cell showing marked dilation of cisternae of RSER and extensive golgi complex (GC) with associated centrioles (C). Fixation 1.5% glutaraldehyde. x 12,500.

Figure 104. Plasma cell which appears to show uncoiling of RSER and an extensive golgi complex (GC).
Fixation 1% osmium tetroxide. x 10,000.

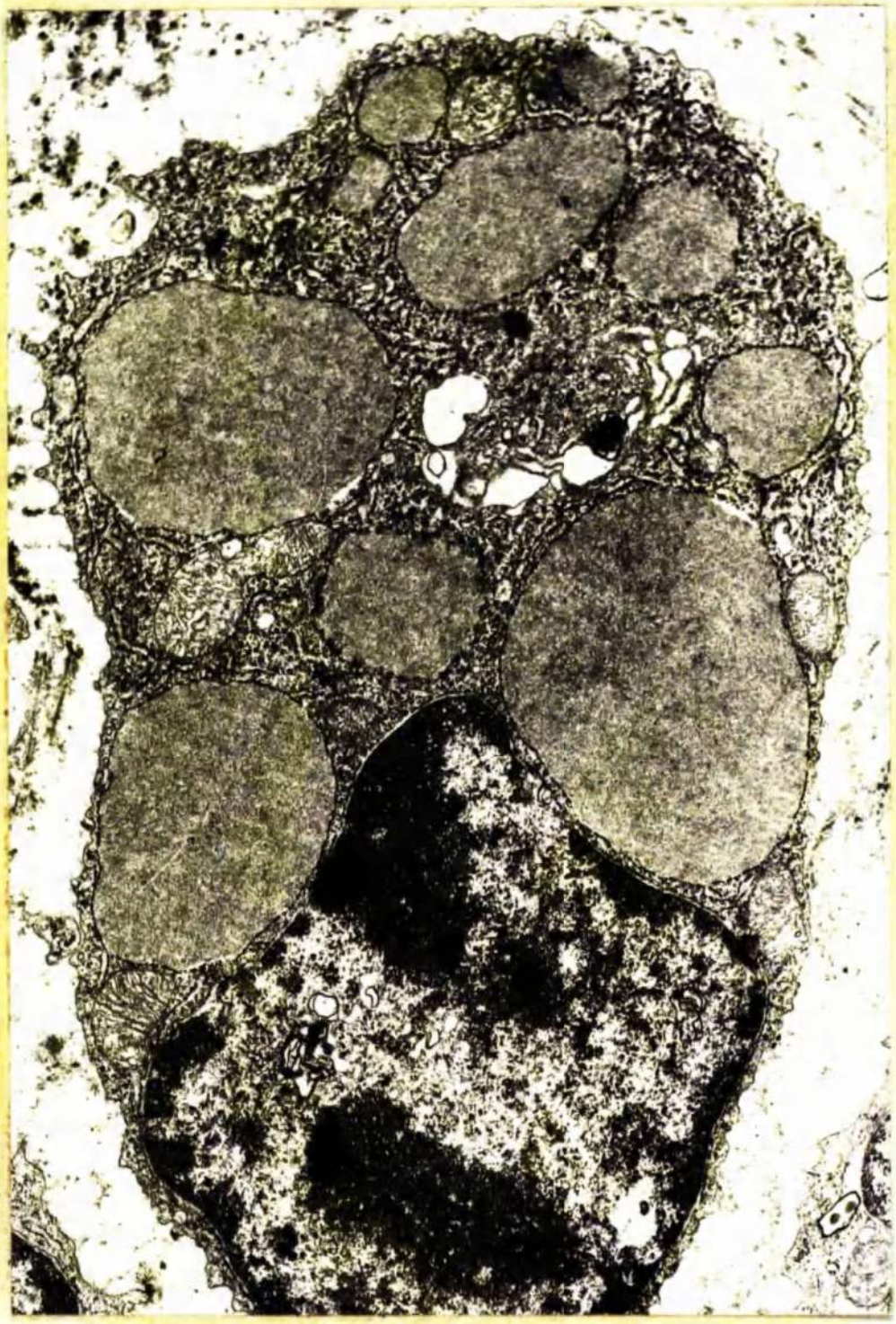

Figure 105. Plasma cell with cisternae of RSER greatly distended by electron-dense material to form Russell bodies. Fixation 4% glutaraldehyde. x 10,000.

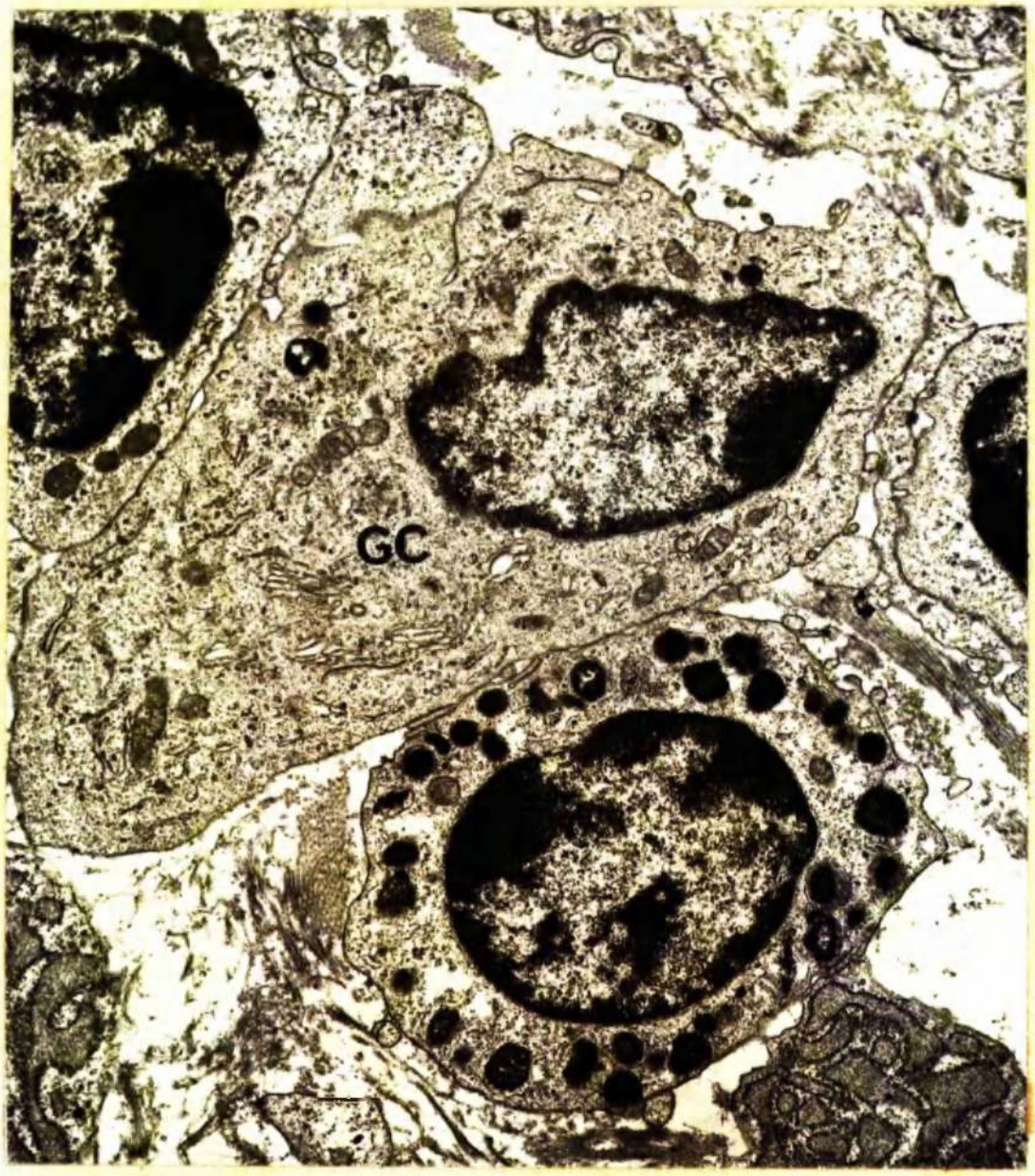

Figure 106. Macrophage lying in close proximity to mast cell. Note the abundant cytoplasm and the well-developed golgi complex (GC). Fixation 1.75% glutaraldehyde. x 12,500.

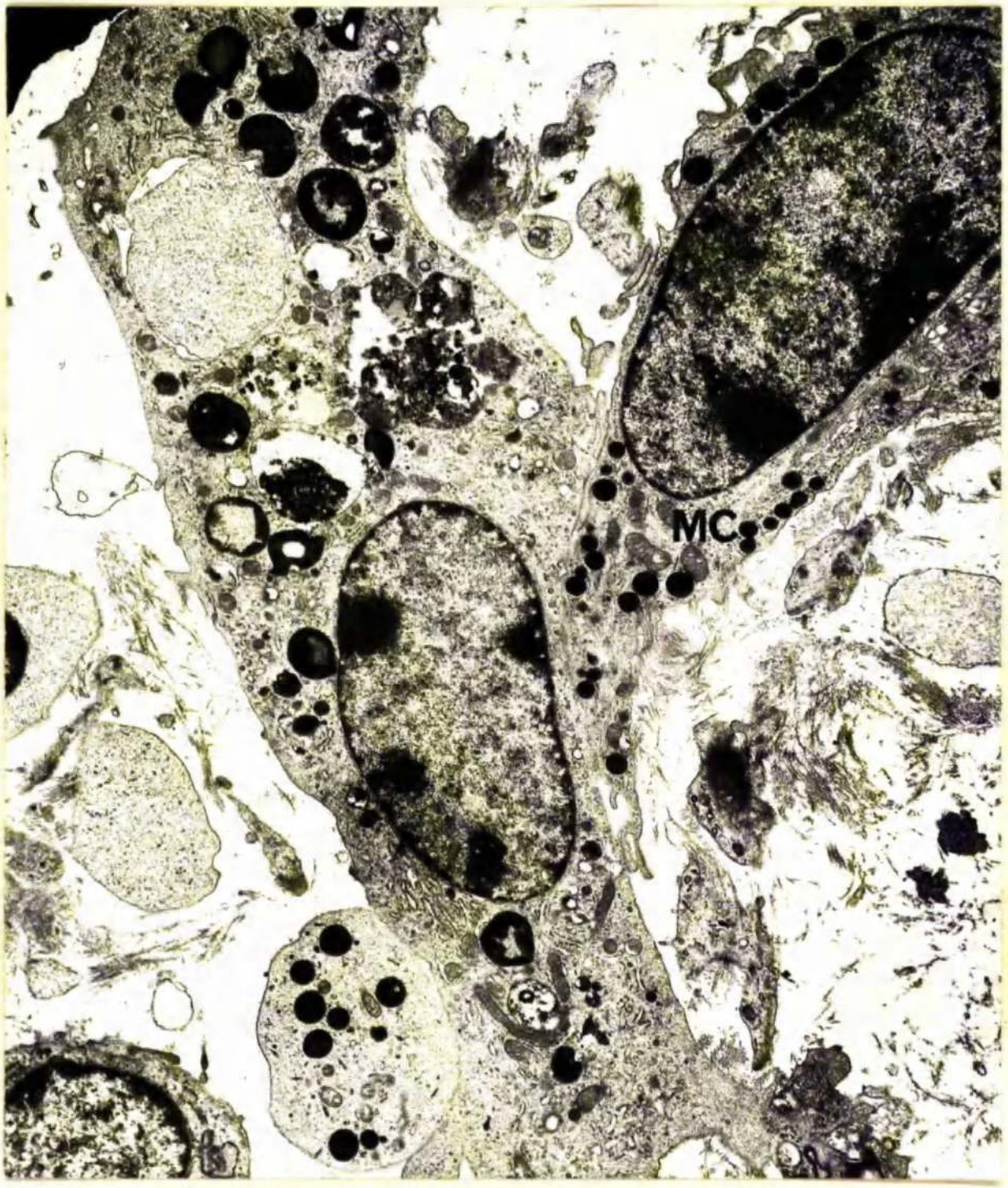

Figure 107. Macrophage with granules of varying size and morphology. Some of the granules may have been phagocytosed from the associated mast cell (MC). Fixation 1.75% glutaraldehyde. x 7,500.

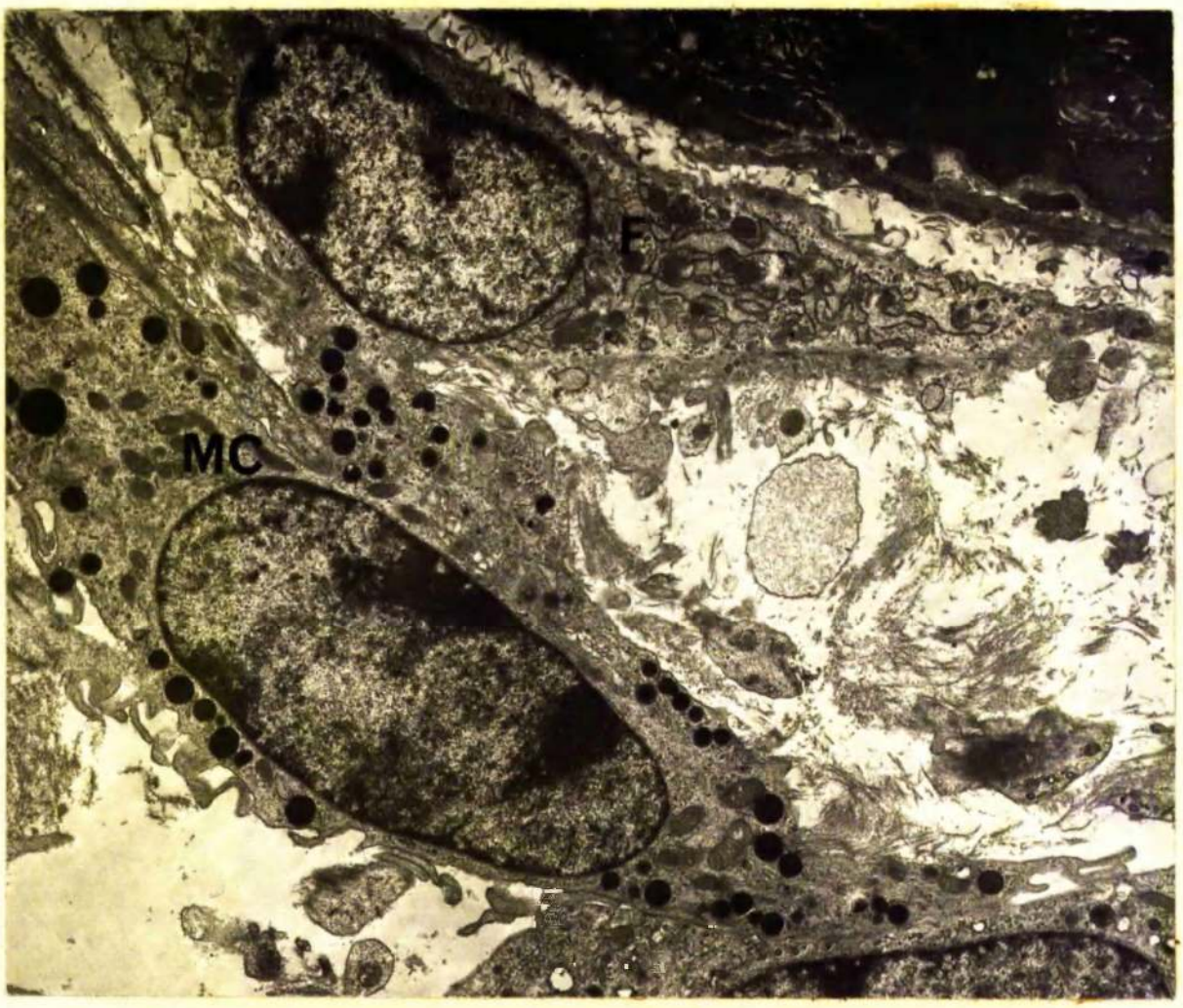

Figure 108. Fibroblast (F) apposed to epithelial basement membrane and mast cell (MC). Fixation 1.75% glutaraldehyde. x 6,000.

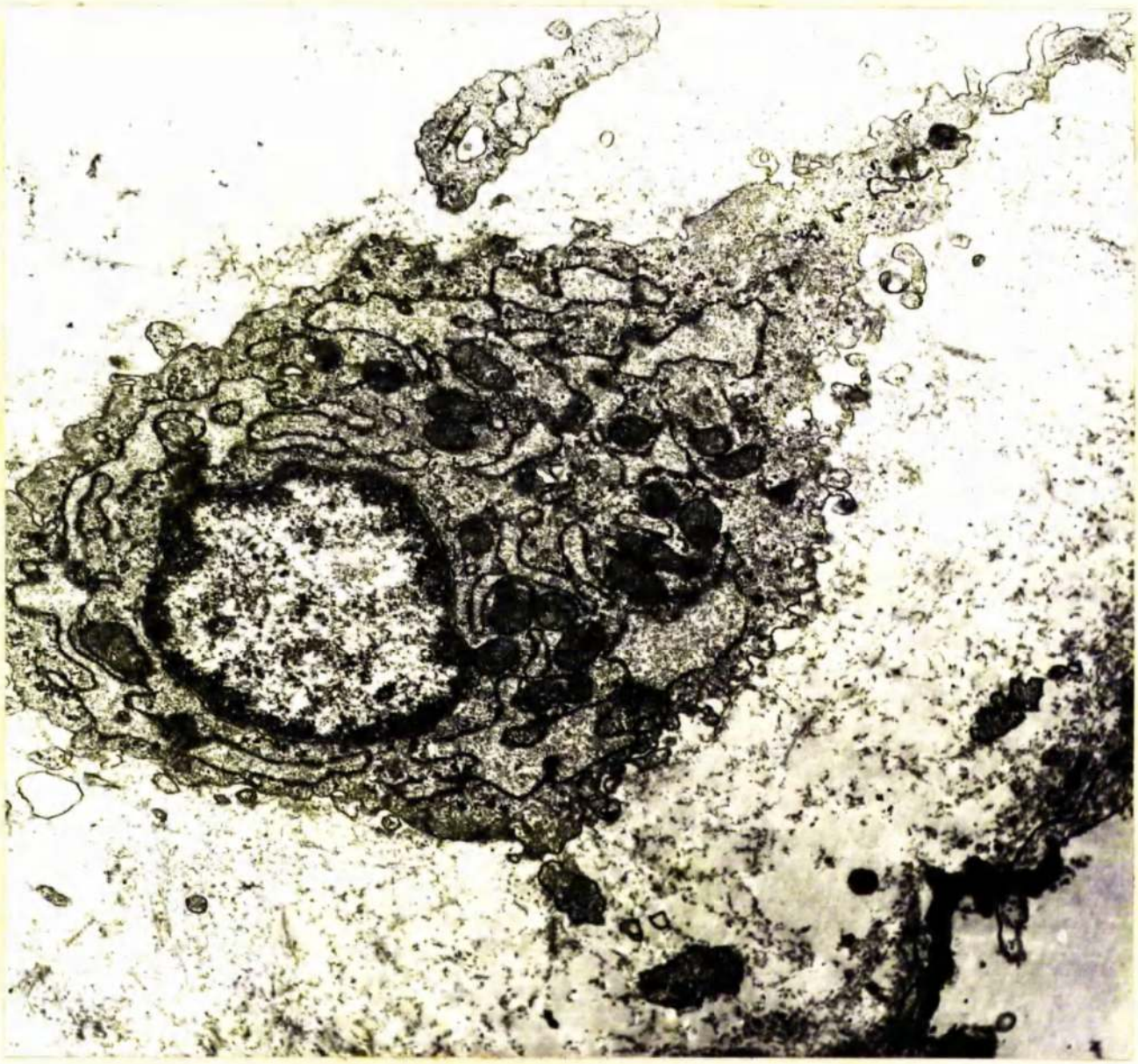

Figure 109. Fibroblast with abundant irregularly dilated and orientated cisternae of RSER with numerous interspersed oval mitochondria. Fixation 1.5% glutaraldehyde. x 18,000.

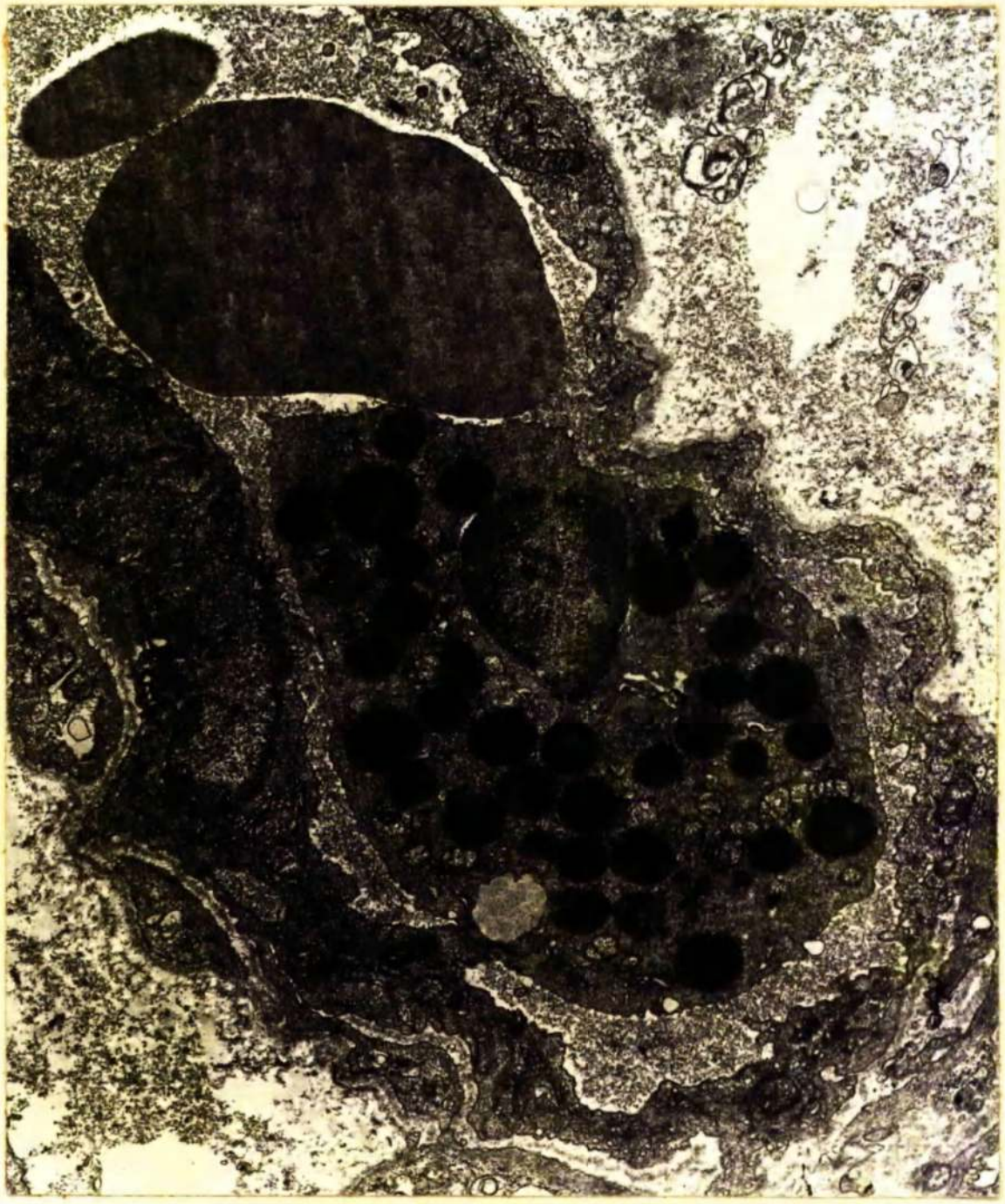

Figure 110. Eosinophil in venule. The cytoplasm is packed with round electron-dense amorphous granules. Fixation 1.5% glutaraldehyde. x 18,000.

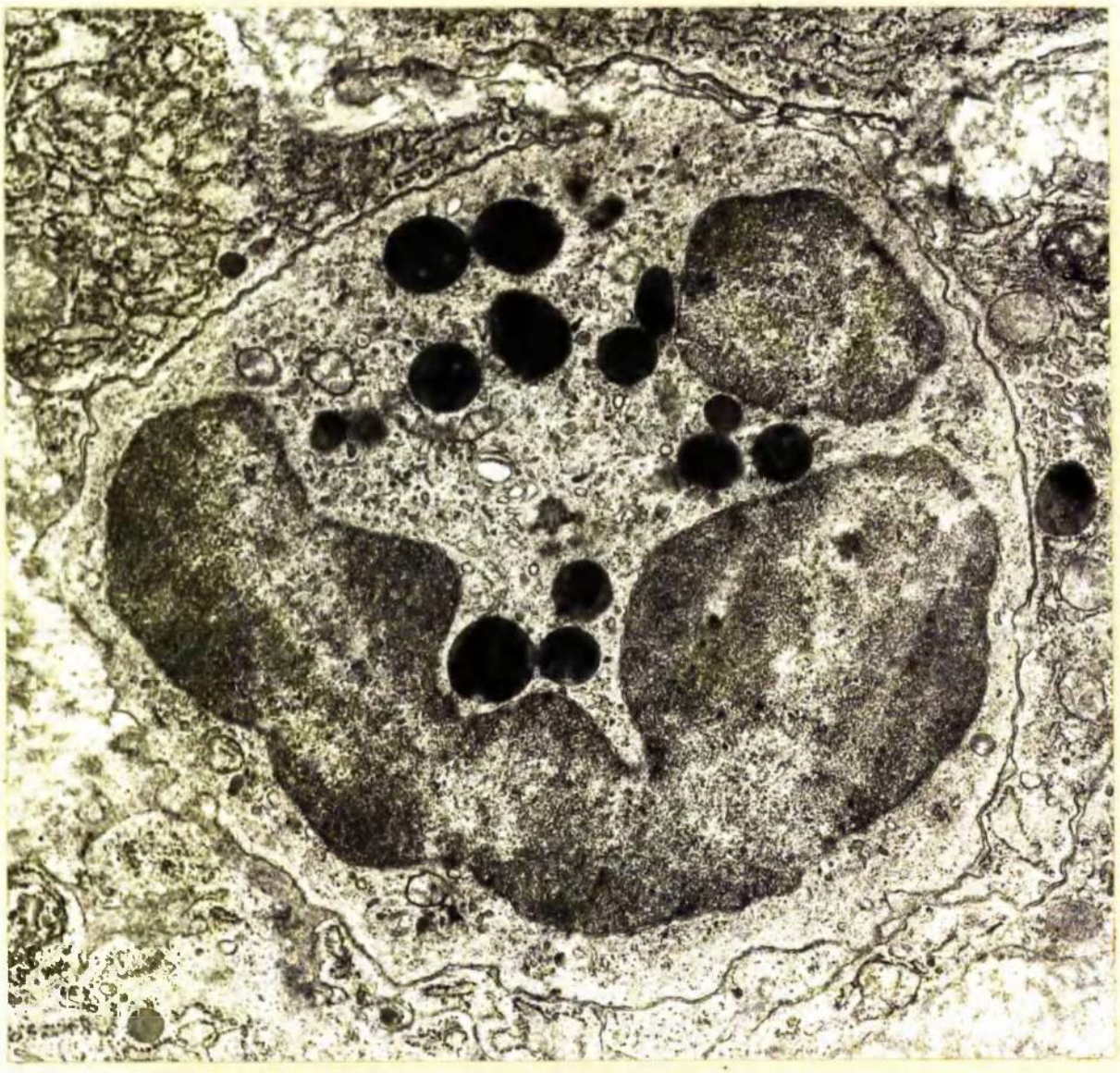

Figure 111. Eosinophil with reniform nucleus and numerous round and oval electron-dense amorphous granules.
Fixation 1.5% glutaraldehyde. x 18,750.

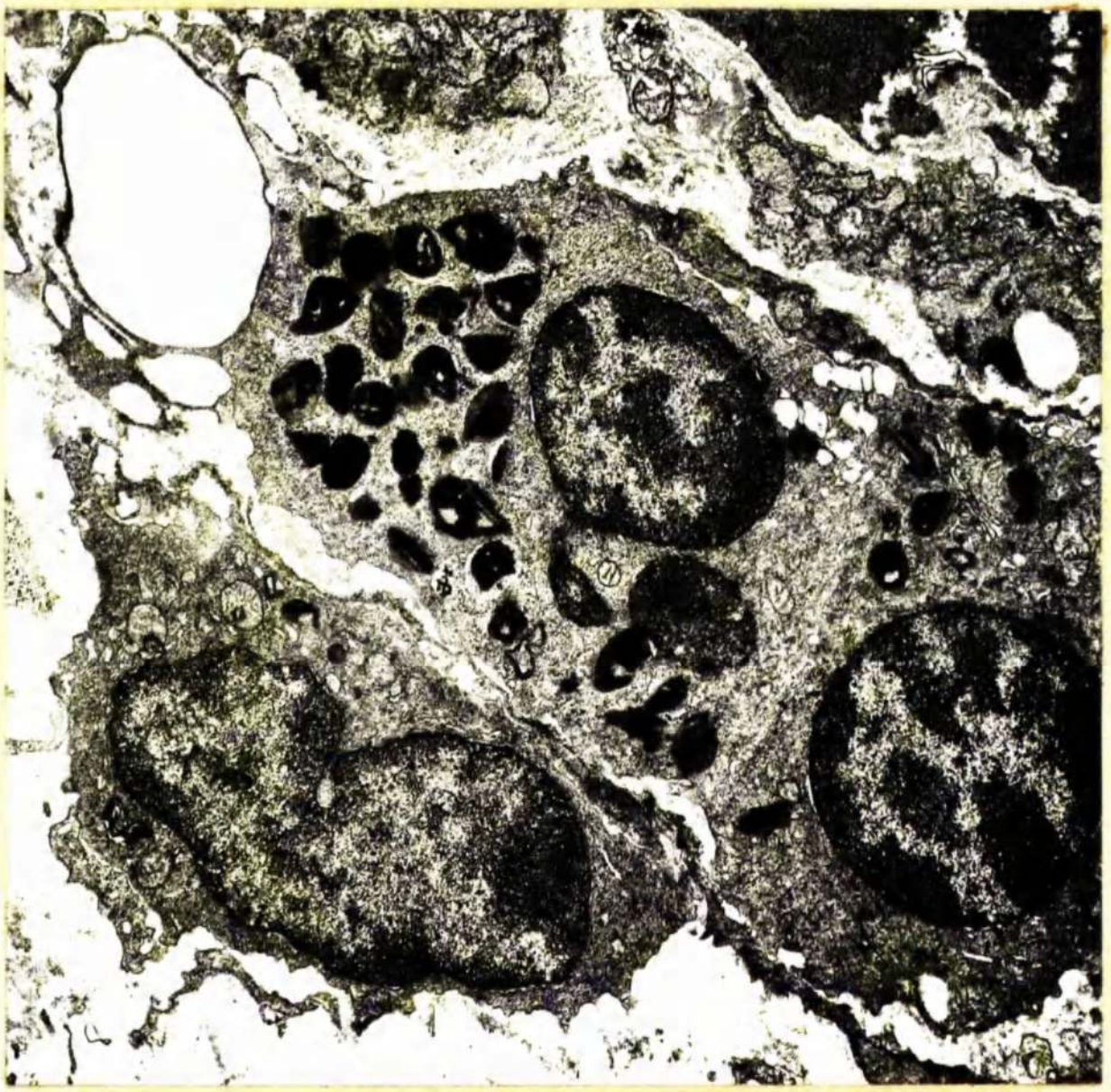

Figure 112. Eosinophil in lamina propria of gallbladder of parasitised sheep. Most granules are pear-shaped or cigar-shaped and have a patterned matrix usually with a central bar. Fixation 1.5% glutaraldehyde. x 12,500.

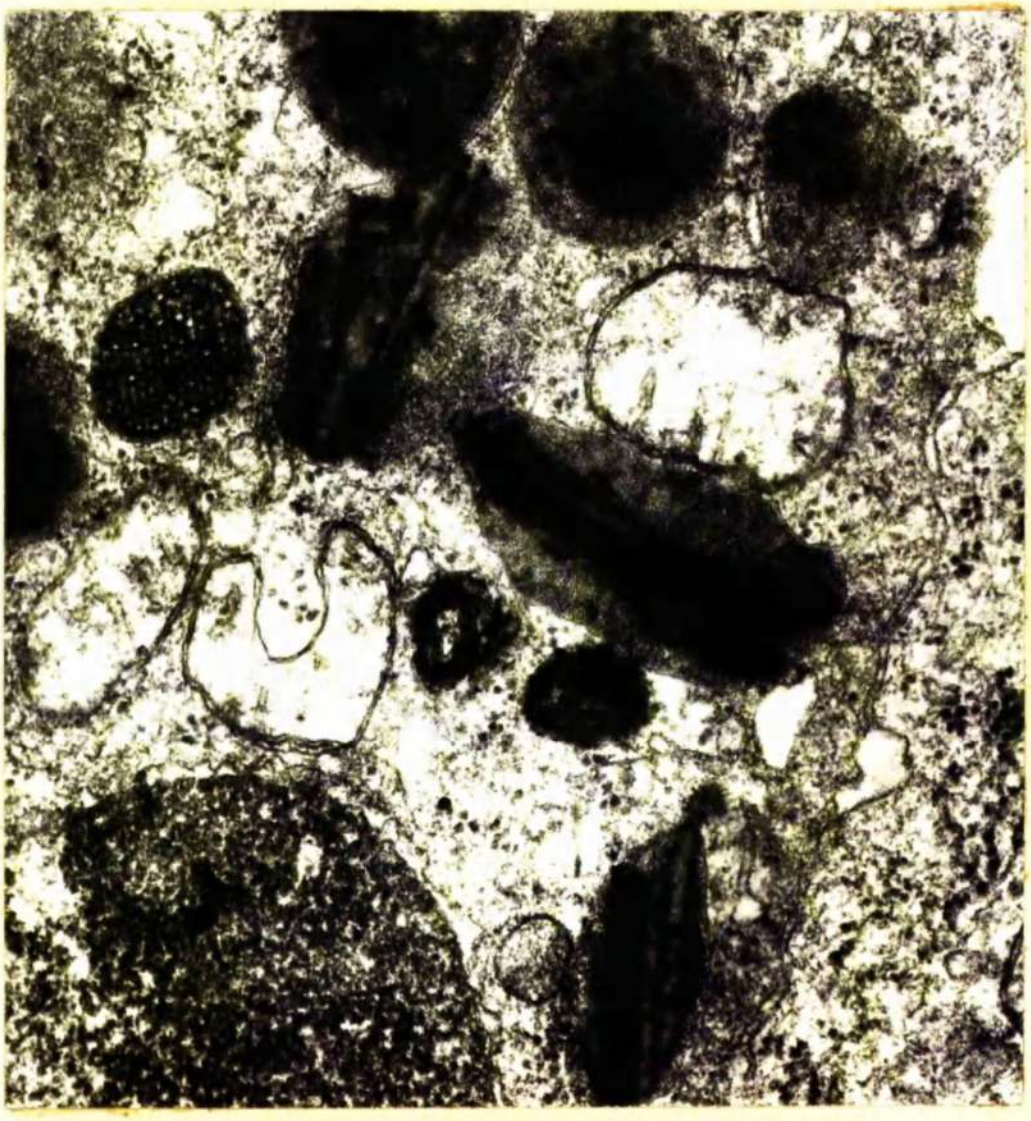

Figure 113. Granules in ovine eosinophil showing a variety of patterns. Fixation 1.5% glutaraldehyde. x 60,000.

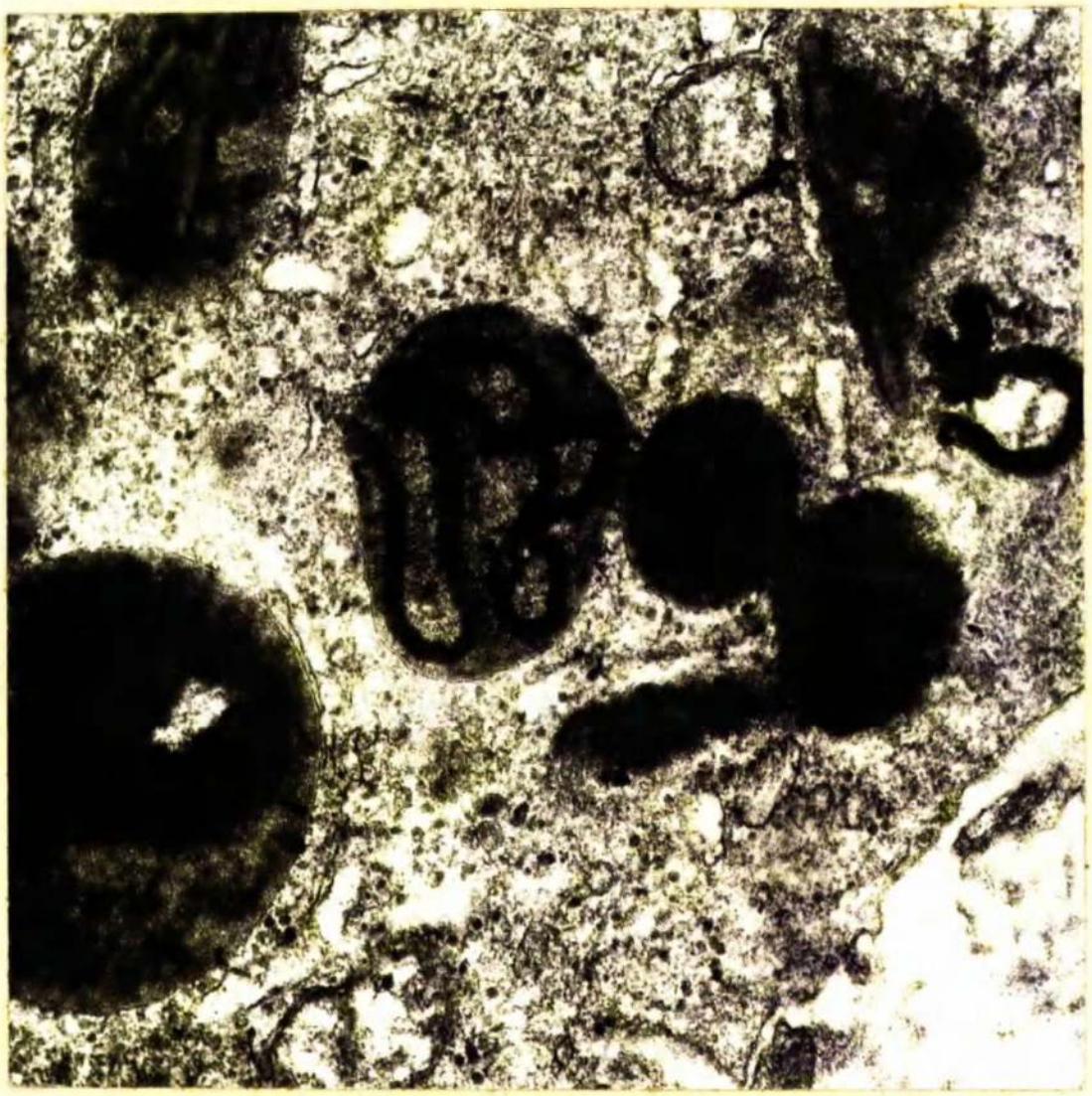

Figure 114. Granules in ovine eosinophil showing a variety of of patterns. Fixation 1.5% glutaraldehyde. x 60,000.

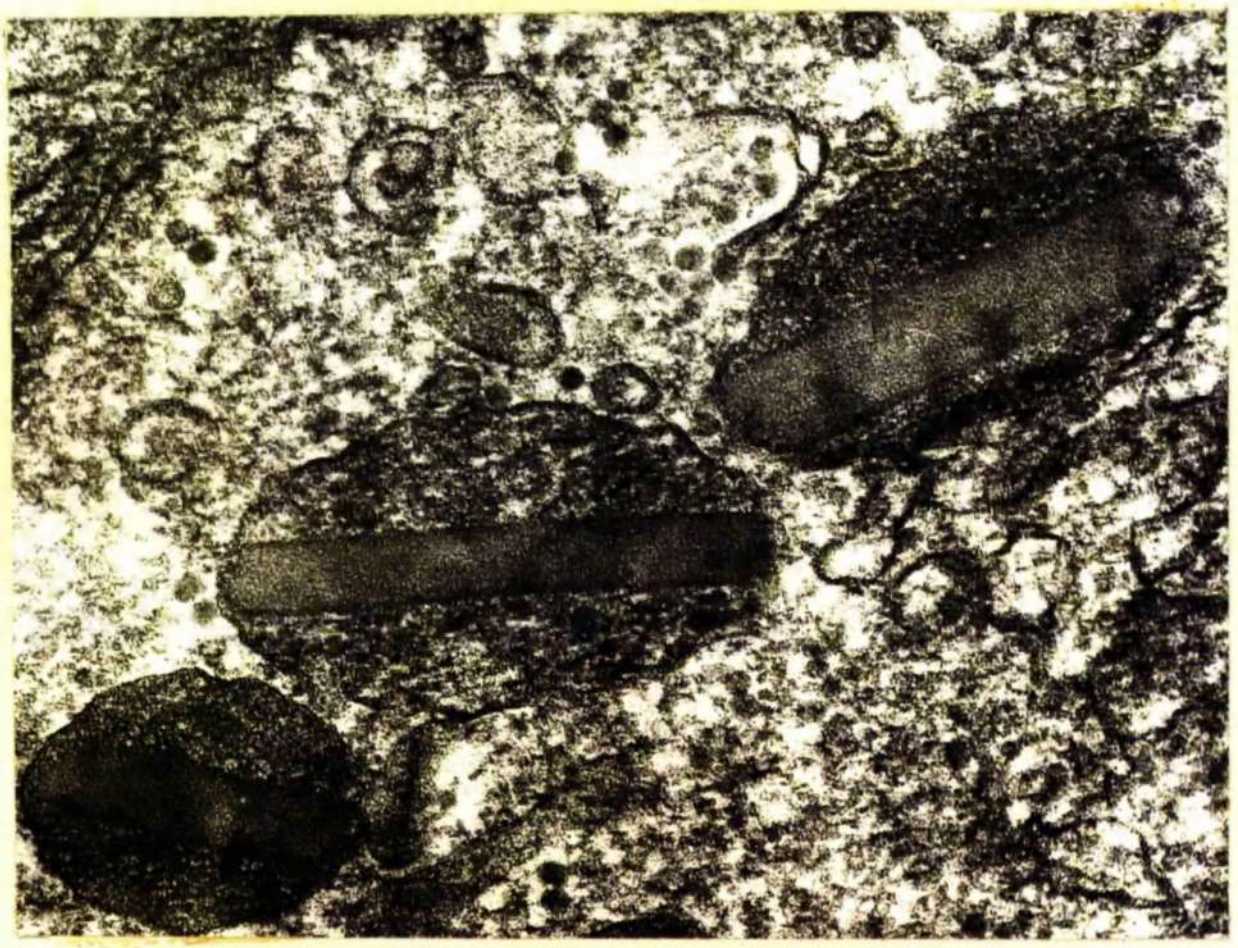

Figure 115. Cigar-shaped granules with a central rectangular bar in ovine eosinophil. Fixation 1.5% glutaraldehyde. x 120,000.

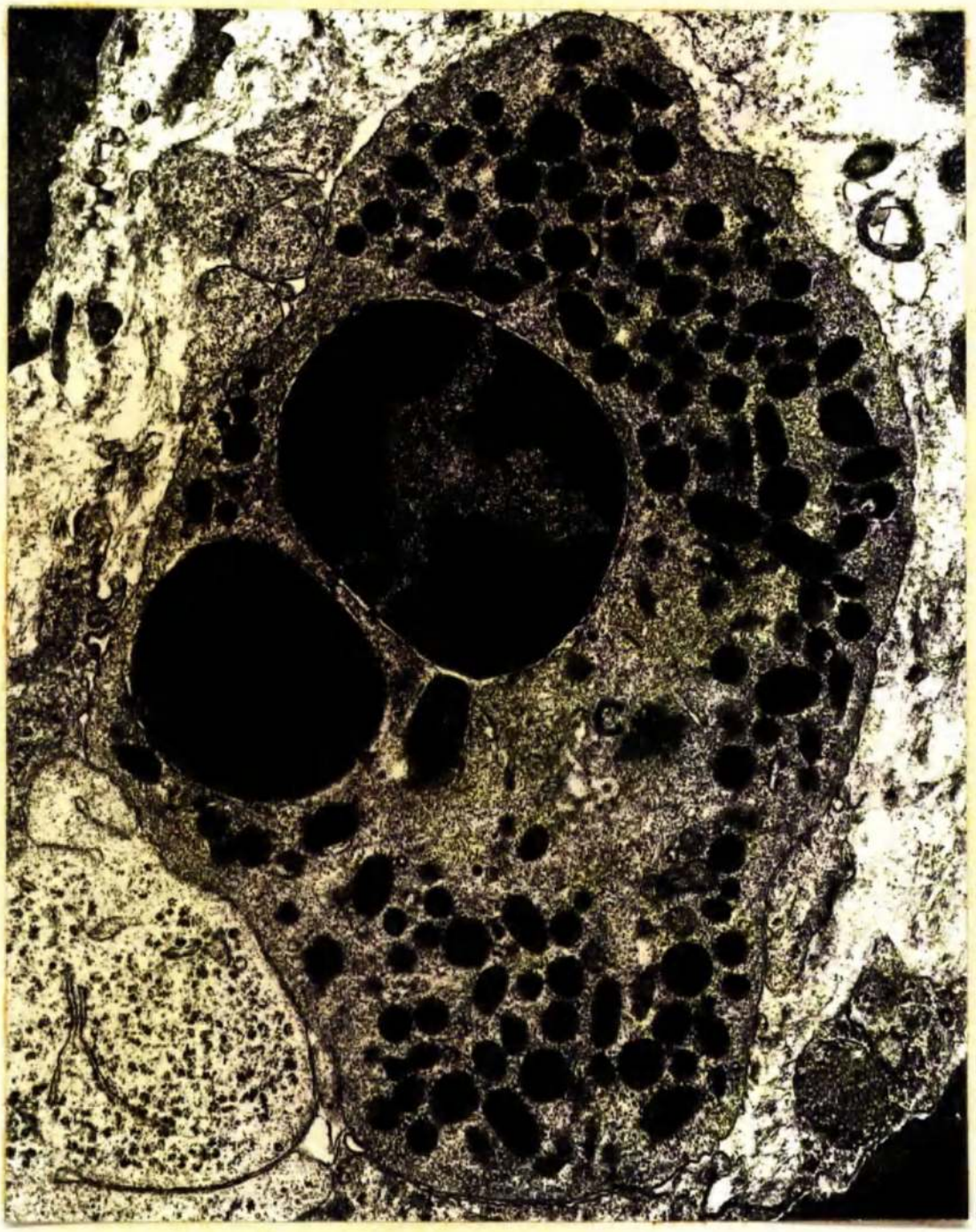

Figure 116. Polymorphonuclear leukocyte with a bilobed nucleus and numerous round, oval and elongated electron-dense granules. Note the centriole (C) in proximity to the nucleus. Fixation 1.5% glutaraldehyde. x 18,750.

Figure 117. Polymorphonuclear leukocyte apposed to capillary (Ca). Numerous round, oval and elongated granules and electron-dense particles of the nature of glycogen (*g*) are present in the cytoplasm. Fixation 1.5% glutaraldehyde. x 12,000.

SECTION IV

STRUCTURAL AND FUNCTIONAL CHANGES ASSOCIATED WITH THE USE OF THIABENDAZOLE IN BOVINE OSTERTAGIASIS

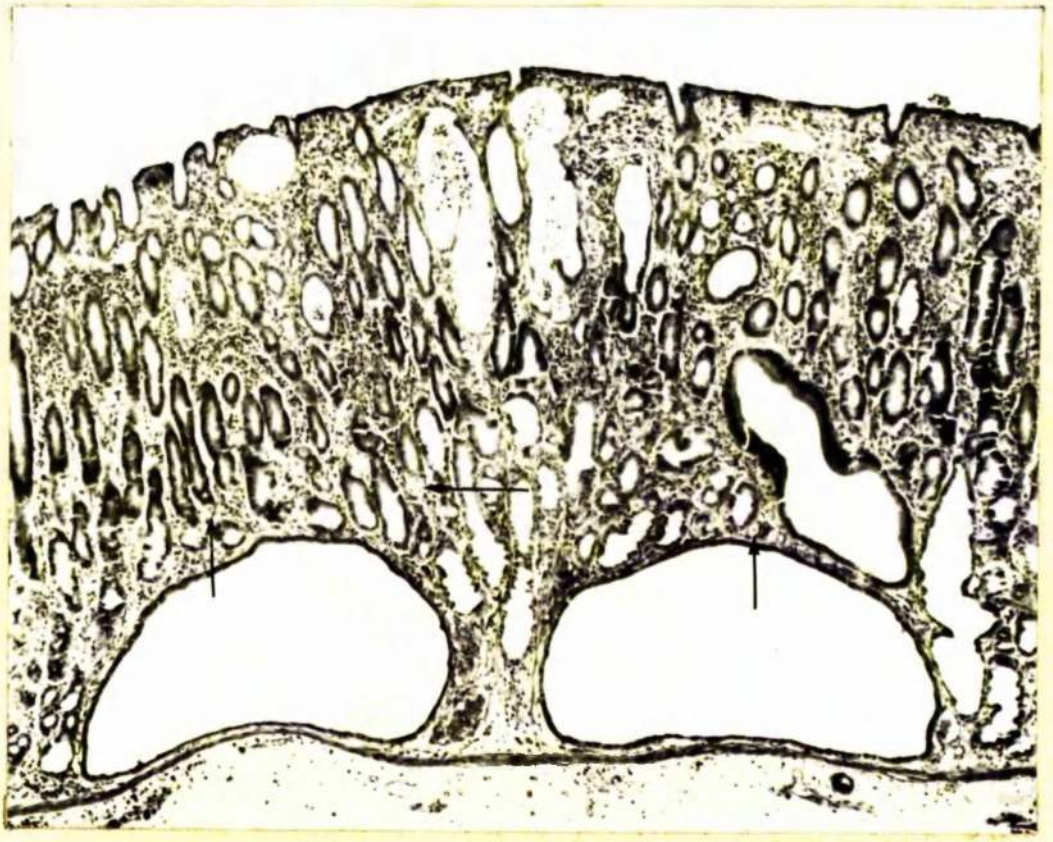

Figure 118. Day 28. Group 1. Coalescence of secondary nodules with resultant loss of functional gastric mucosa over a considerable area. Parietal cells (↑) can still be identified amongst the rapidly-dividing non-differentiated cells. x 50.

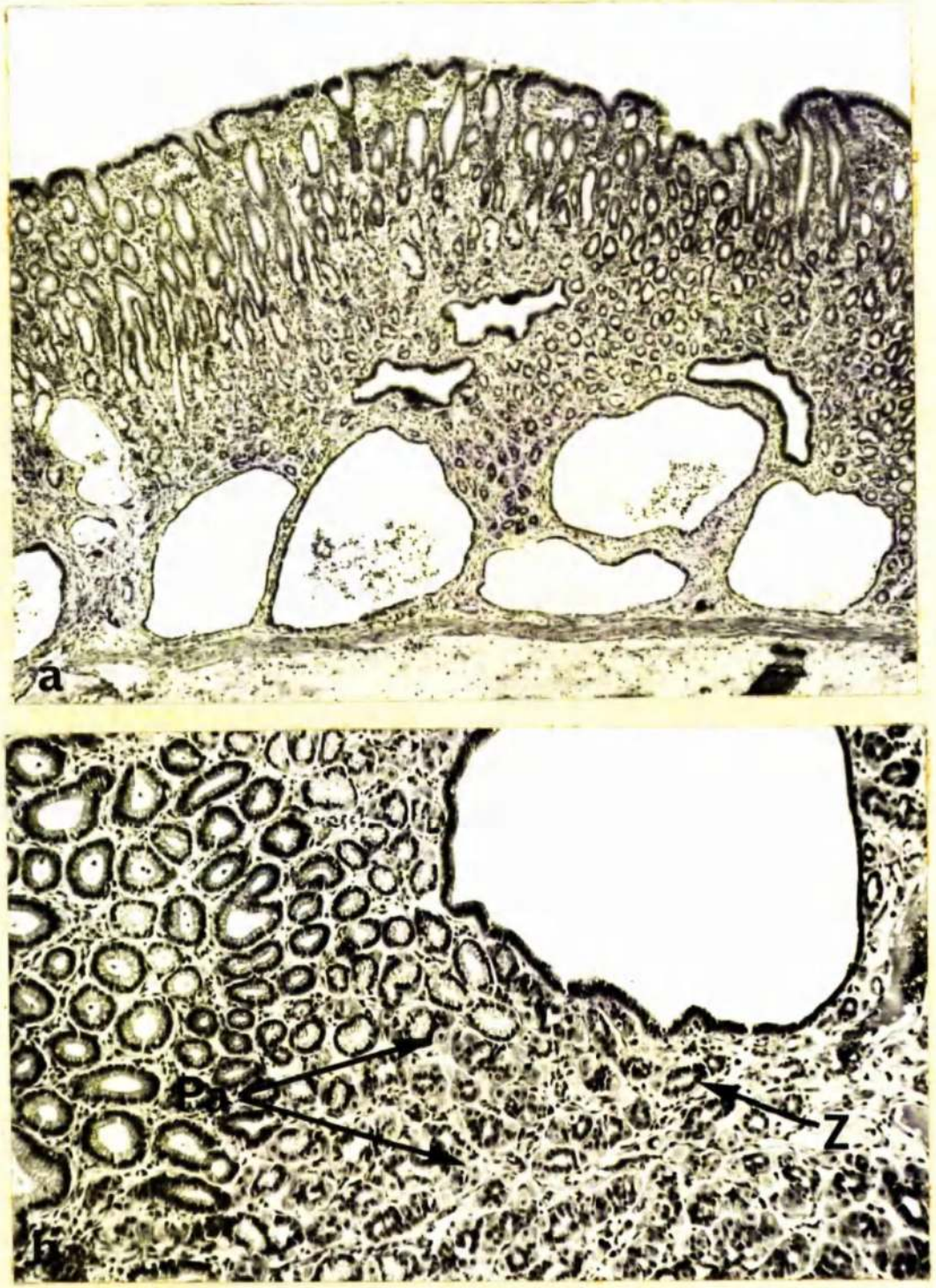

Figure 119 Day 28. Group 2.

a) Coalesced secondary nodules. Note the increase in the number of the parietal cells present in the hyperplastic mucosa. x 45.

b) High power of same area. Parietal cells (Pa) and zymogen cells (Z) are easily recognised. x 140.

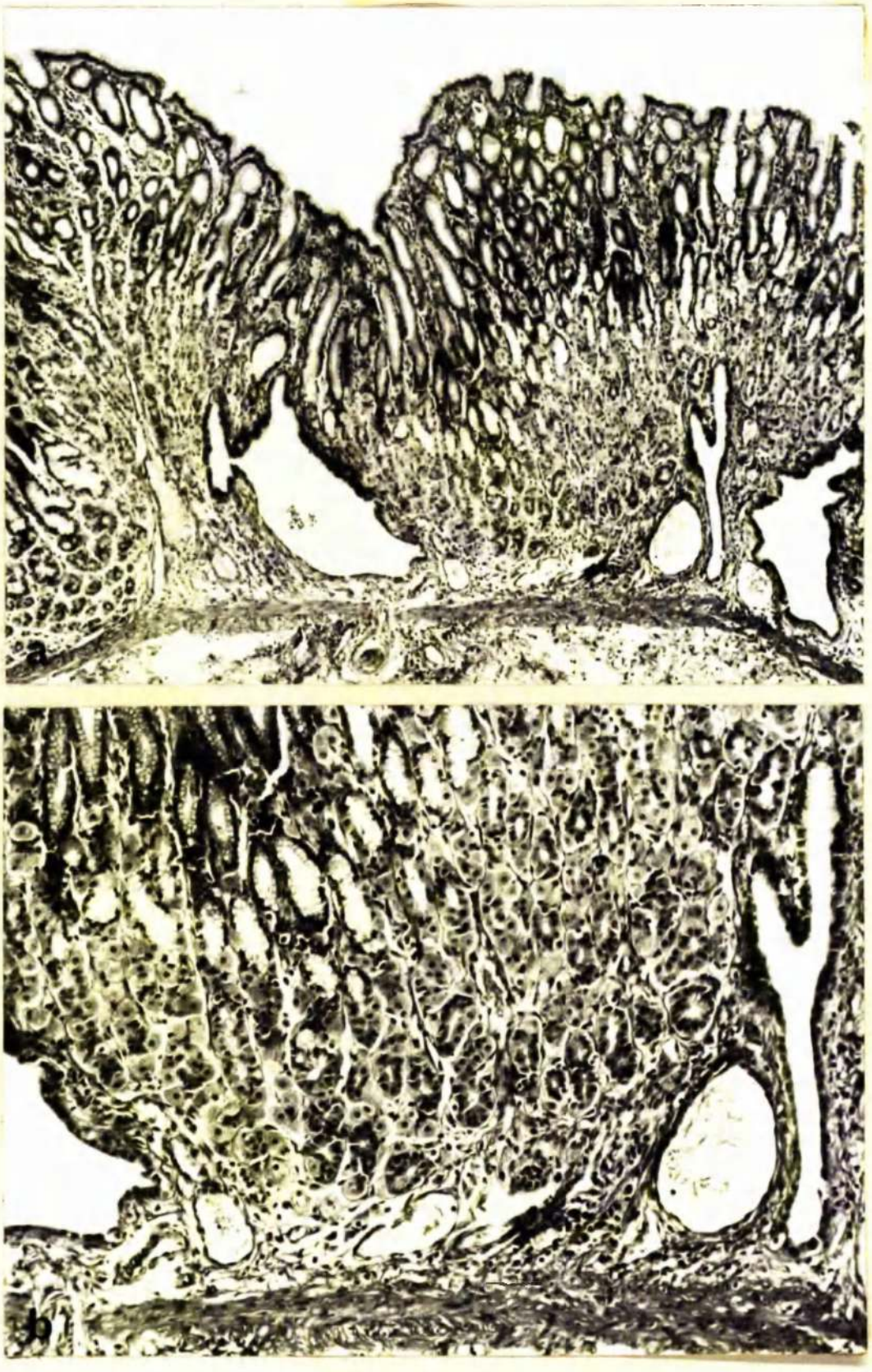

Figure 120. Day 28. Group 2.

a). Note the return of the parietal cell mass. x 45.

b) high power of same field. x 140.

Figure 121. Parietal cell in the gastric mucosa of an untreated calf (Group 1). The cytoplasm has a pseudovacuolated appearance and the intracellular canaliculi are markedly dilated and lined by only a few microvilli. Fixation 4% glutaraldehyde. x 12,500.

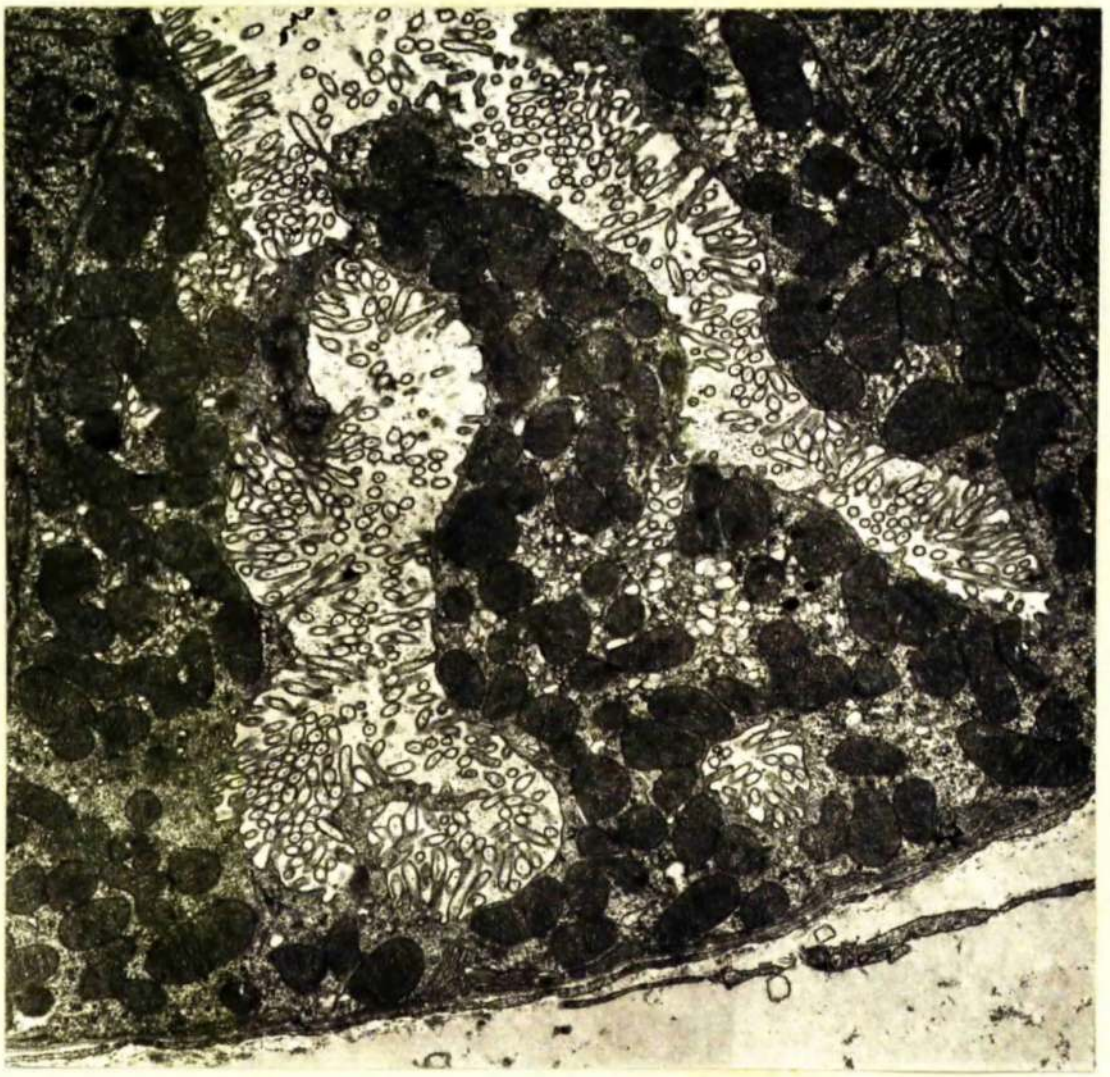

Figure 122. Parietal cell in the gastric mucosa of calf treated with Thiabendazole (Group 2). The intracellular canaliculi are extensive and are lined by numerous microvilli. Fixation 1.5% glutaraldehyde. x 10,000.

Figure 123. Parietal cell in gastric mucosa of calf treated with thiabendazole (Group 2). The intracellular canaliculi are extensive and lined by numerous microvilli. Note the dilated canaliculus (↑) lined by only a few microvilli. Fixation 1.5% glutaraldehyde. x 7,500.

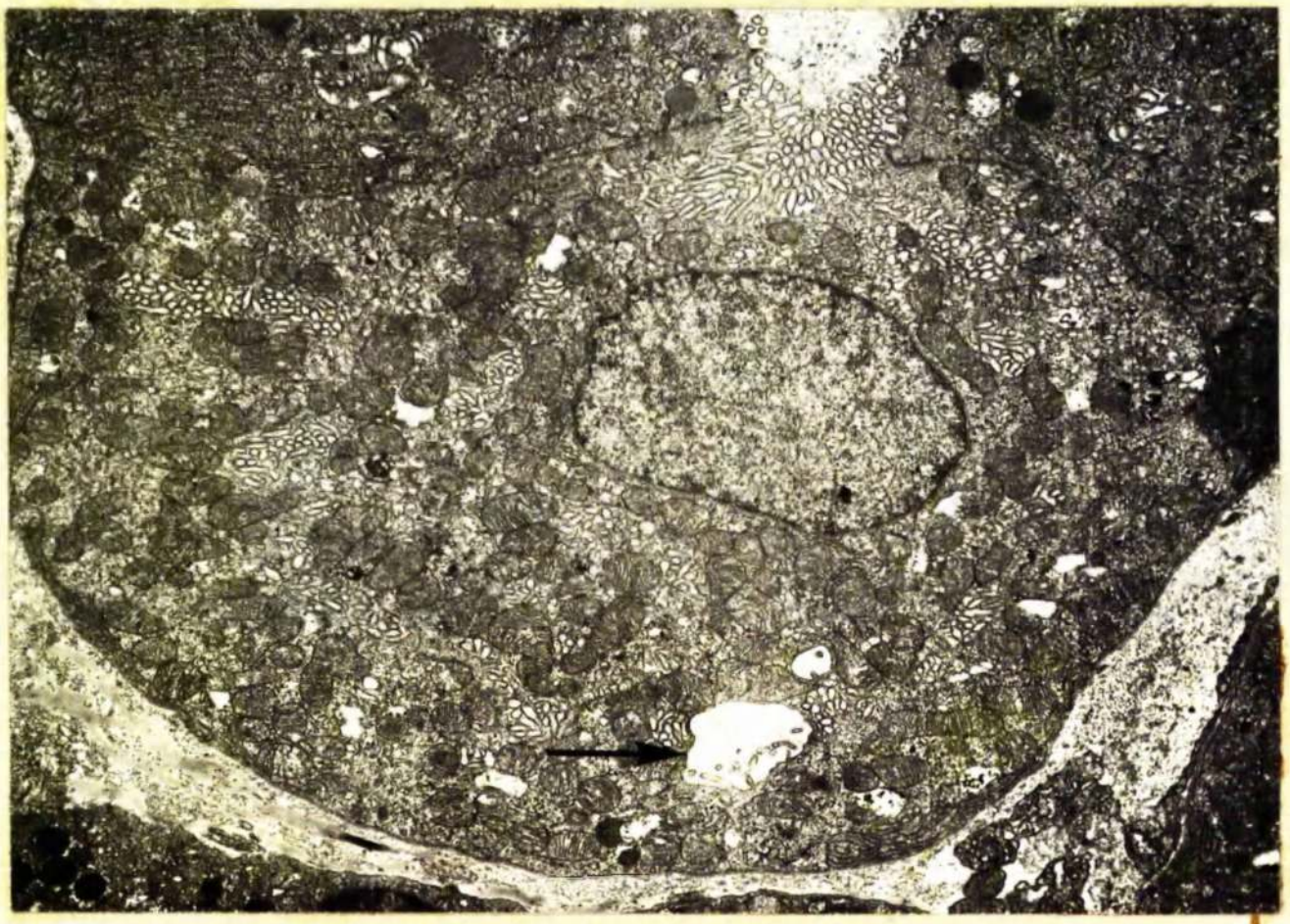

Figure 124. Parietal cell in gastric mucosa of calf treated with thiabendazole (Group 2). The intracellular canaliculi are extensive and lined by numerous microvilli. Note the dilated canaliculus (↑) lined by only a few microvilli. Fixation 1.5% glutaraldehyde. x 7,500.

SECTION V

THE GLOBULE LEUKOCYTE AND ITS DERIVATION FROM THE SUBEPITHELIAL MAST CELL

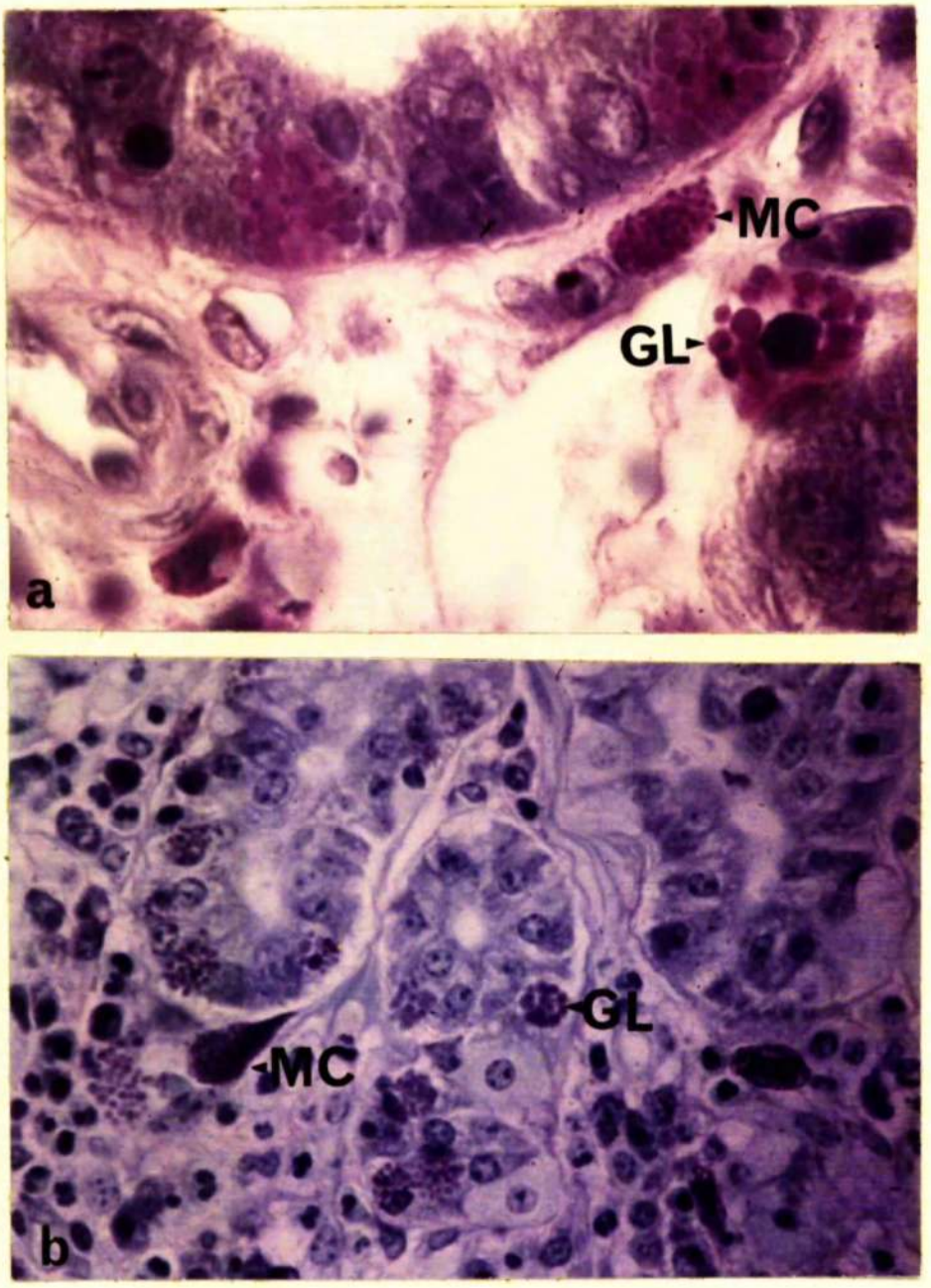

Figure 125. Toluidine blue (0.5% at pH 4.5)

a) Note the metachromasia of mast cell (MC) and GL granules. x 1050.

b) Note the metachromasia of mast cell (MC) and GL granules. x 420.

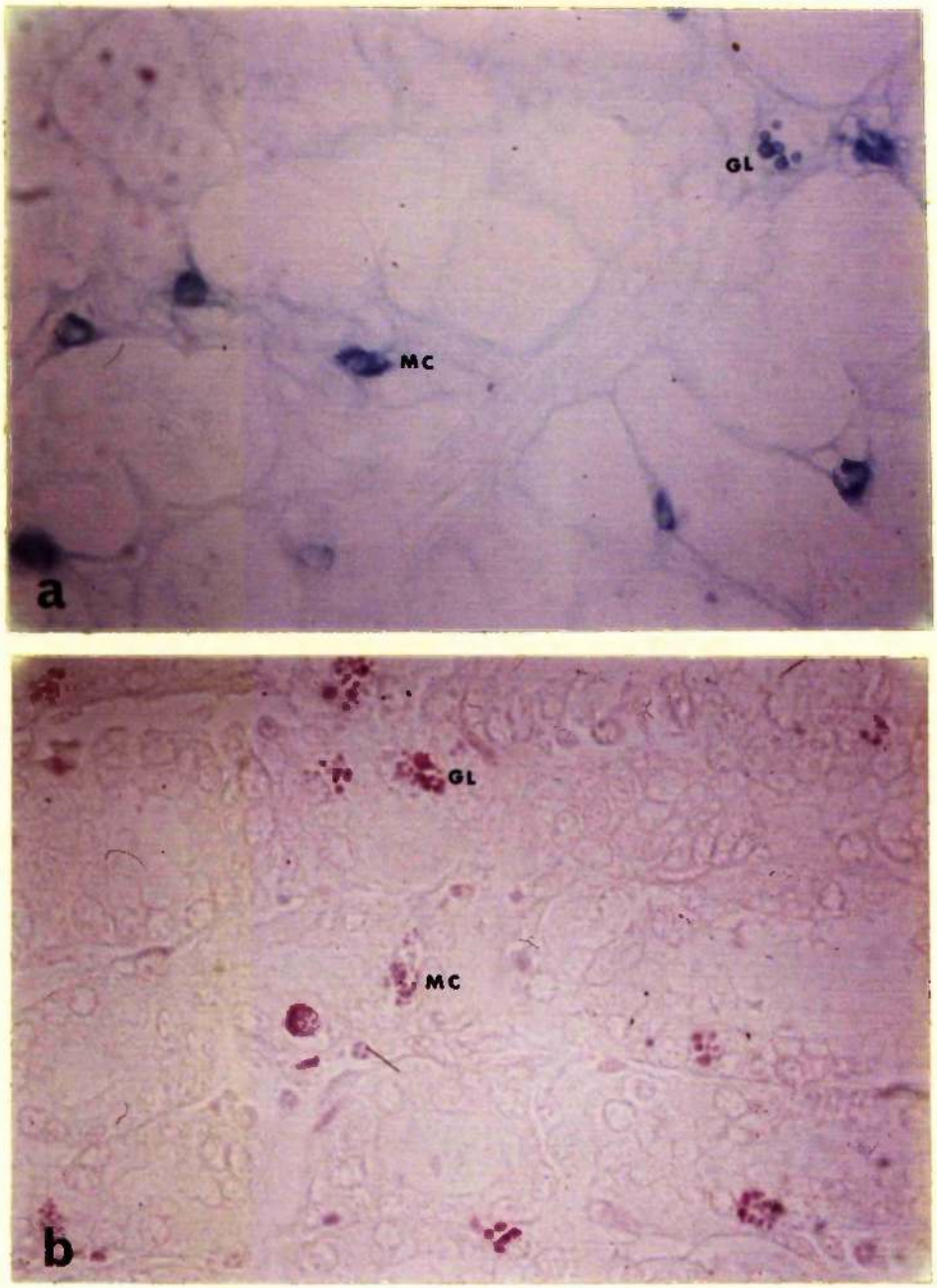

Figure 126. a) Astra blue (0.5% at pH 0.3). Mast cell granules (MC) stain bright blue. Note the rimming of GL granules with astra blue positive material. x 420.

b) Biebrich scarlet (0.04% at pH 10). Note the bright red staining of mast cell (MC) and GL granules. x 420.

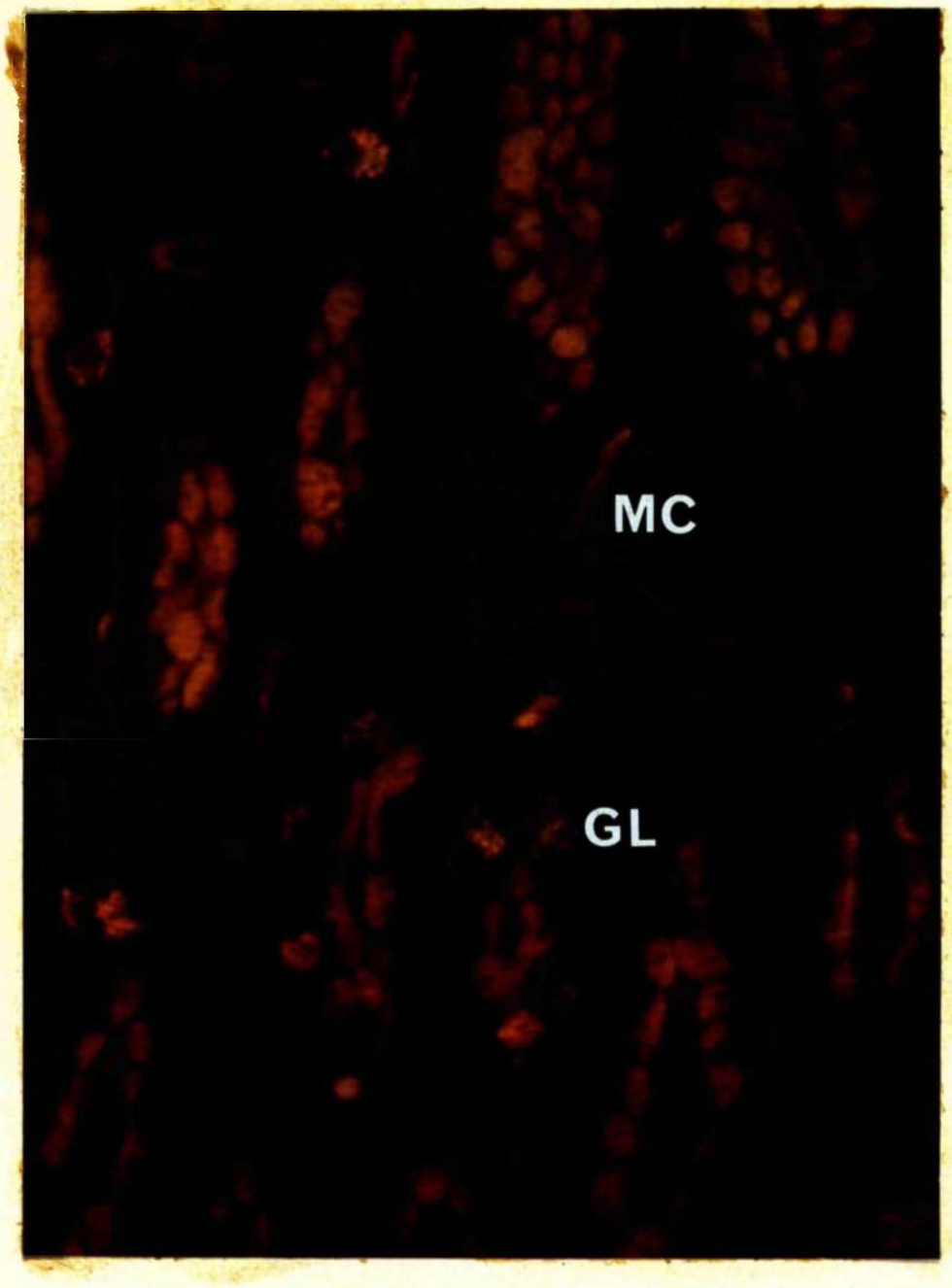

Figure 127. Acridine orange (0.001%). Mast cell granules (MC) fluoresce orange and GL granules fluoresce yellow to green. x 600.

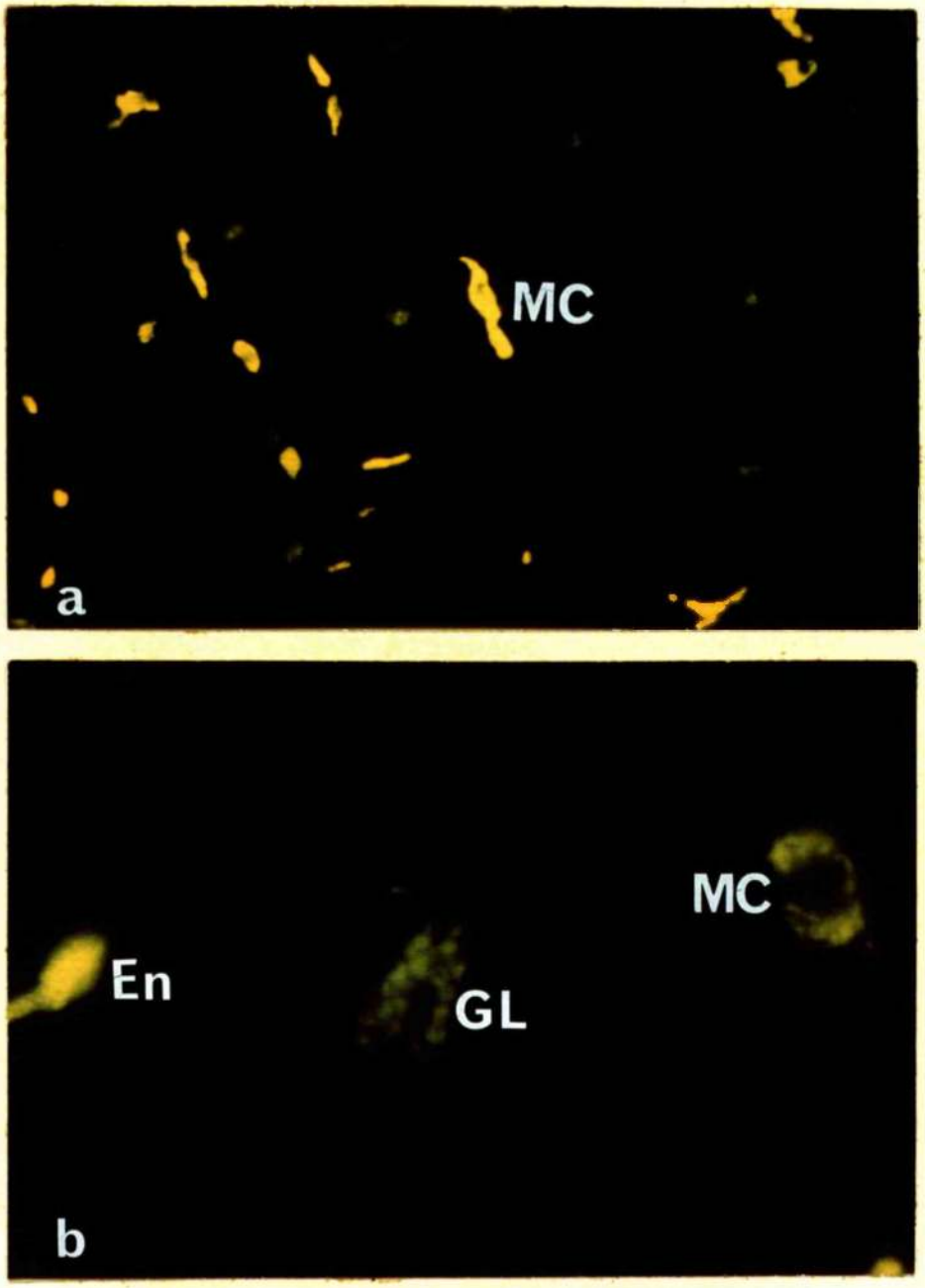

Figure 128. Falck technique for monoamines.

a) Note the bright yellow fluorescing granules in mast cells (MC). x 420.

b) GL granules show a patchy green fluorescence. Note the mast cell (MC) with green fluorescing granules and the enterochromaffin cell (En) with yellow fluorescing granules. x 1050

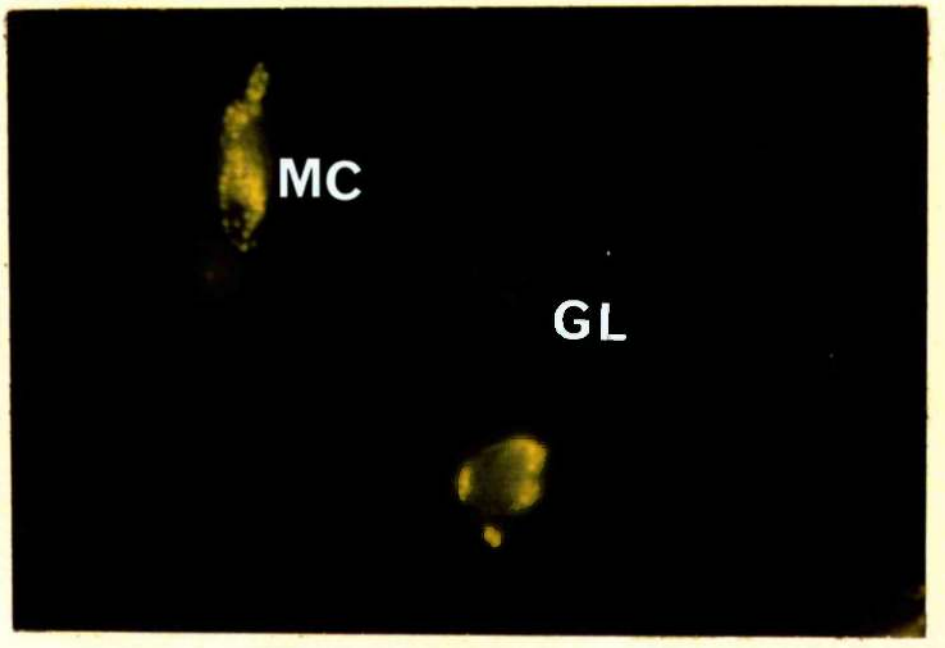

Figure 129. Falck technique for monoamines. Granules in mast cells (MC) show a yellow to green fluorescence. The intensity of fluorescence of GL granules is reduced. x 1050.

Figure 130. Acridine orange (0.001%). Transitional cells (TC) containing small granules which fluoresce orange and larger granules which fluoresce green or yellow. x 600.

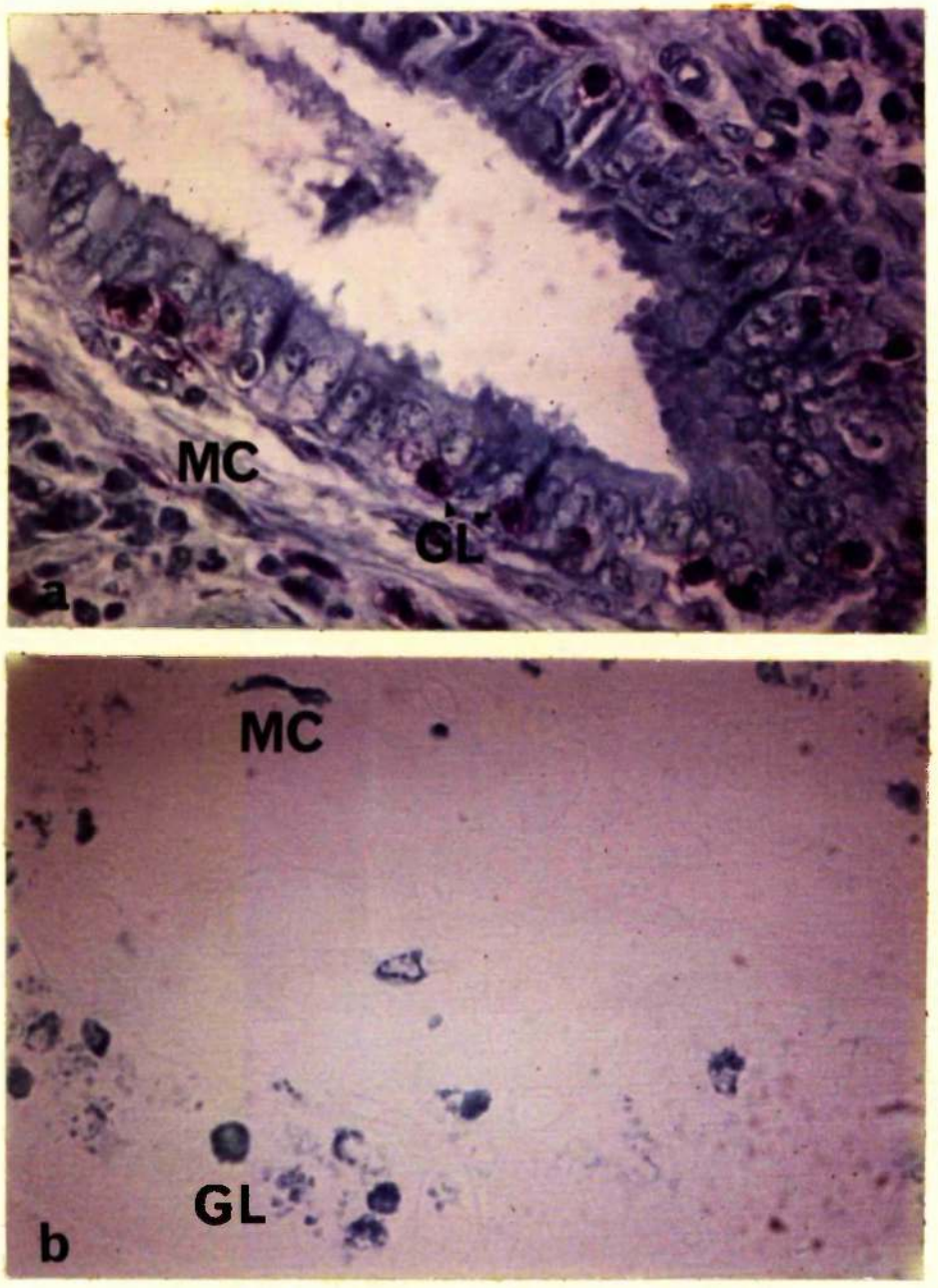

Figure 131. a) Toluidine blue (0.5% at pH 4.5). Bile duct in sheep infected with F. hepatica. Note the metachromasia of mast cell (MC) and GL granules. x 420.

b) Astra blue (0.5% at pH 0.3). Bile duct in sheep infected with F. hepatica. Mast cell granules (MC) stain bright blue. Note the range of blue staining of GL granules. x 420.

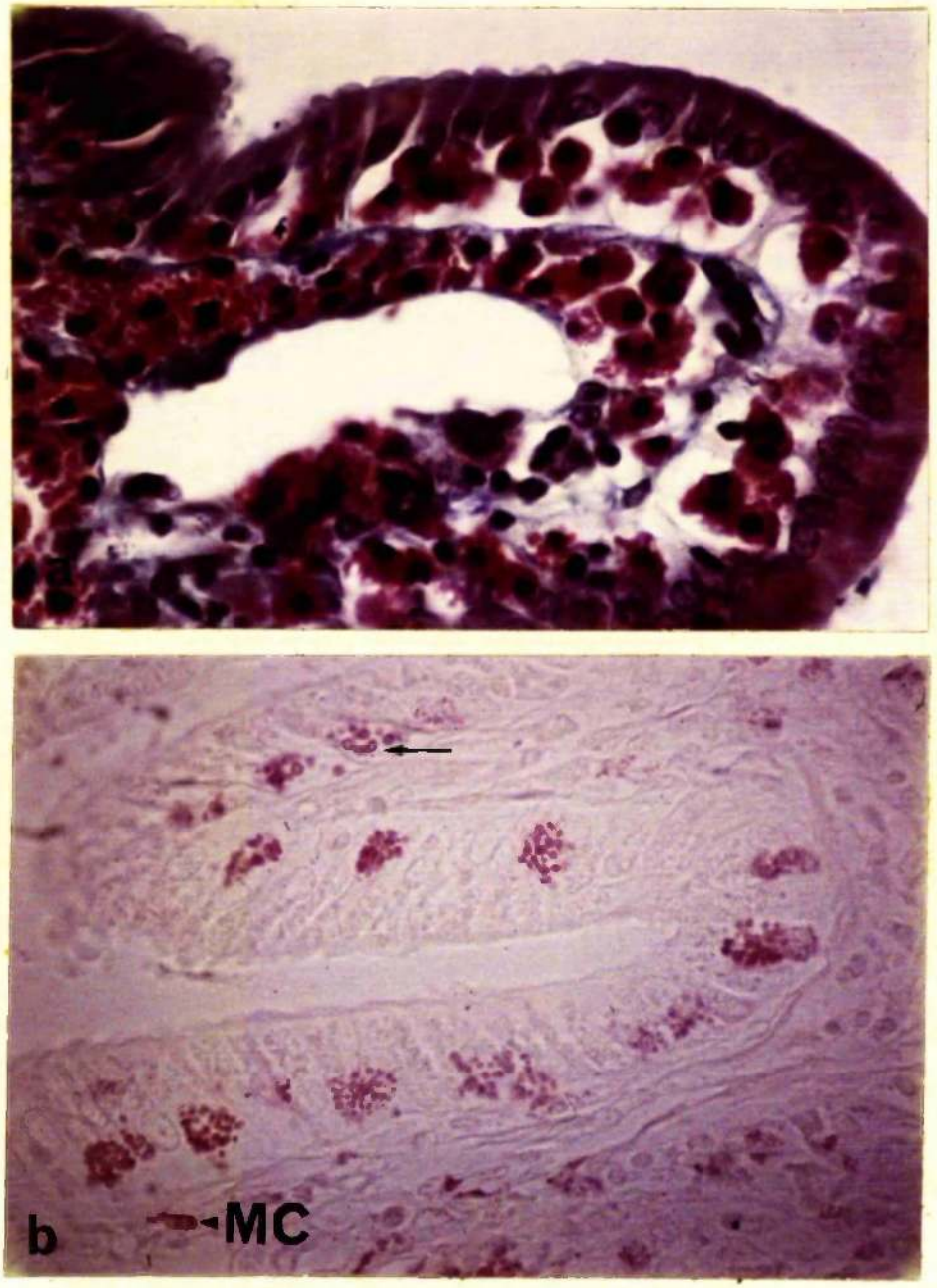

Figure 132. a) Picro-Mallory. Gallbladder in sheep infected with F. hepatica. Numerous GLs are present within the epithelium and in the lamina propria. x 420.

b) Biebrich scarlet (0.04% at pH 10). Gallbladder in sheep infected with F. hepatica. The mast cell (MC) and GL granules are bright red. Note the red halo around some granules (↑). x 420.

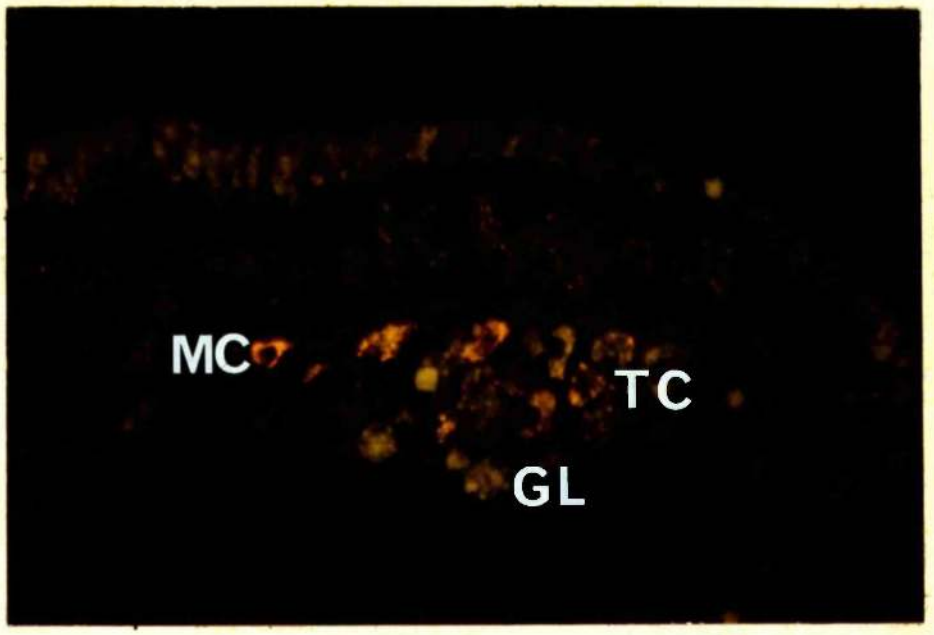

Figure 133. Acridine orange (0.001%). Bile duct in sheep infected with F. hepatica. Mast cell granules (MC) are orange, transitional cell granules (TC) are orange or green-yellow and those in GLs are green or yellow. x 420.

Figure 134. Subepithelial mast cell lying closely apposed to plasma cell (Pl) with markedly distended cisternae of RSER. Fixation 1.5% glutaraldehyde. x 18,000.

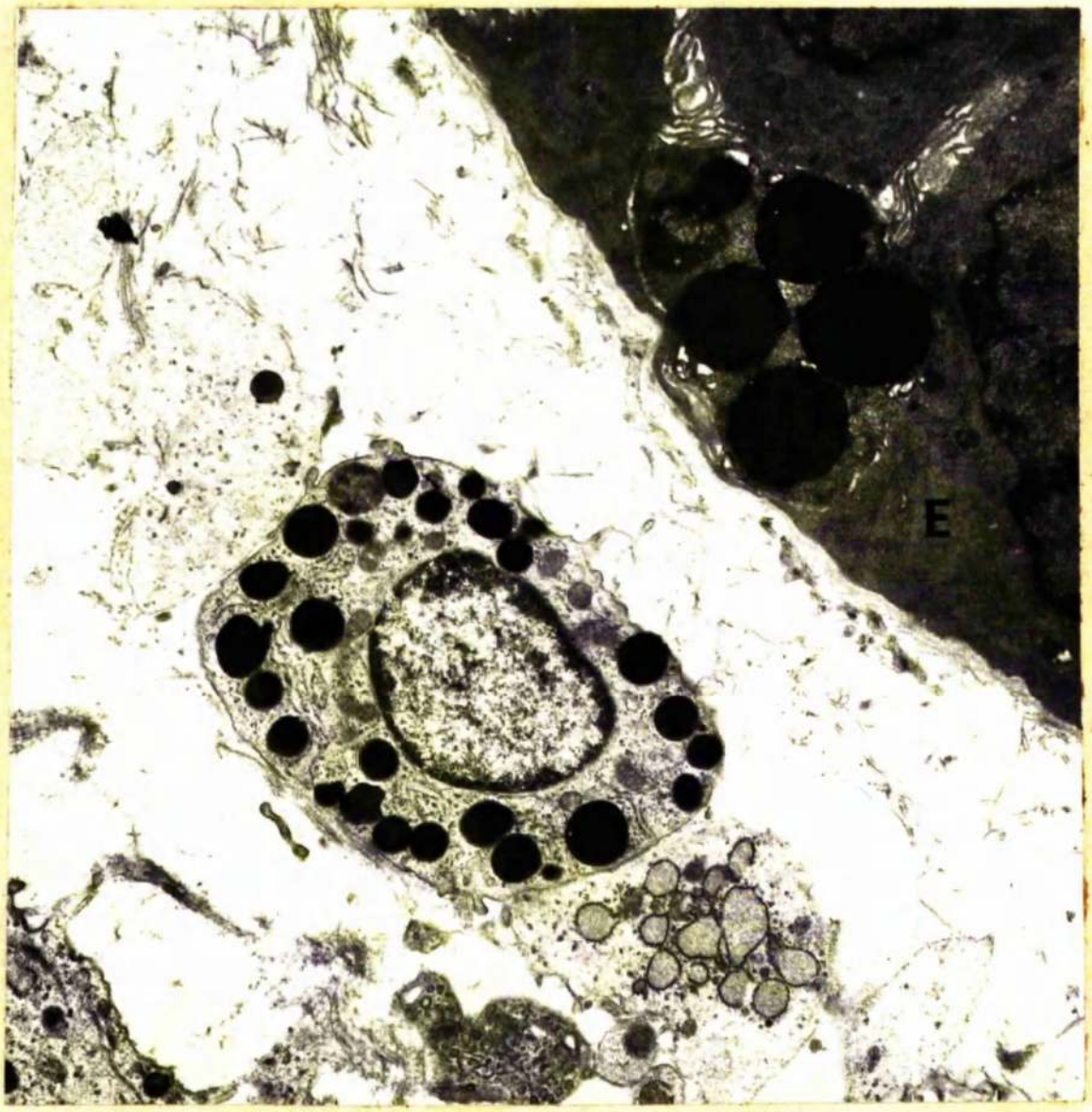

Figure 135. Mast cell bordering epithelial basement membrane. Part of GL can be seen within adjacent epithelium. Fixation 1.75% glutaraldehyde. x 10,000.

Figure 136. Mast cell showing range of changes in granules. Note the reticulated appearance of certain granules (↑). Fixation 1.5% glutaraldehyde. x 15,000.

Figure 137. Mast cell granules bounded by smooth-surfaced unit membranes. Note the rupture of the granule membrane (↑). Fixation 1.5% glutaraldehyde. x 75,000.

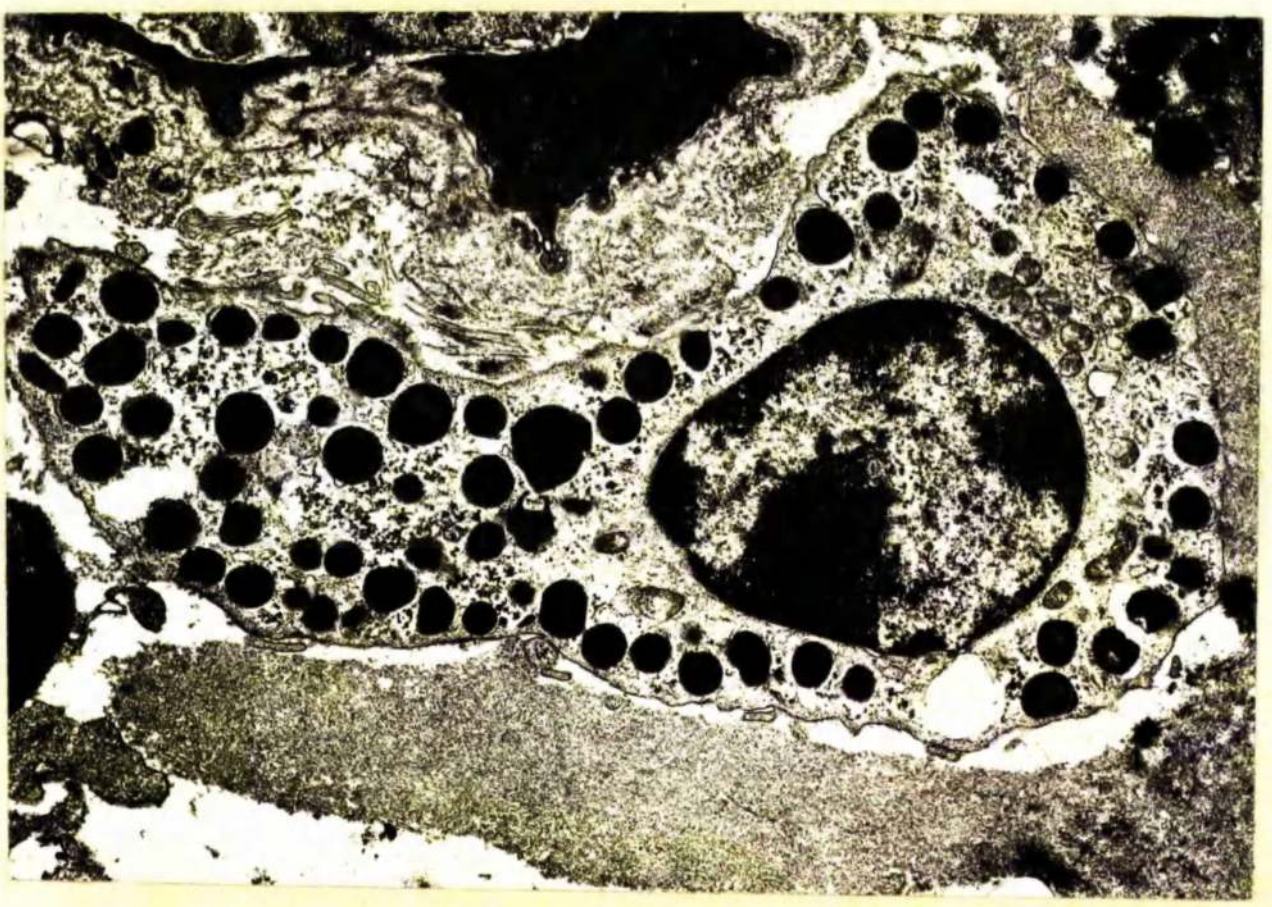

Figure 138. Mast cell containing complement of uniformly electron-dense amorphous granules. Fixation 1.75% glutaraldehyde. x 12,500.

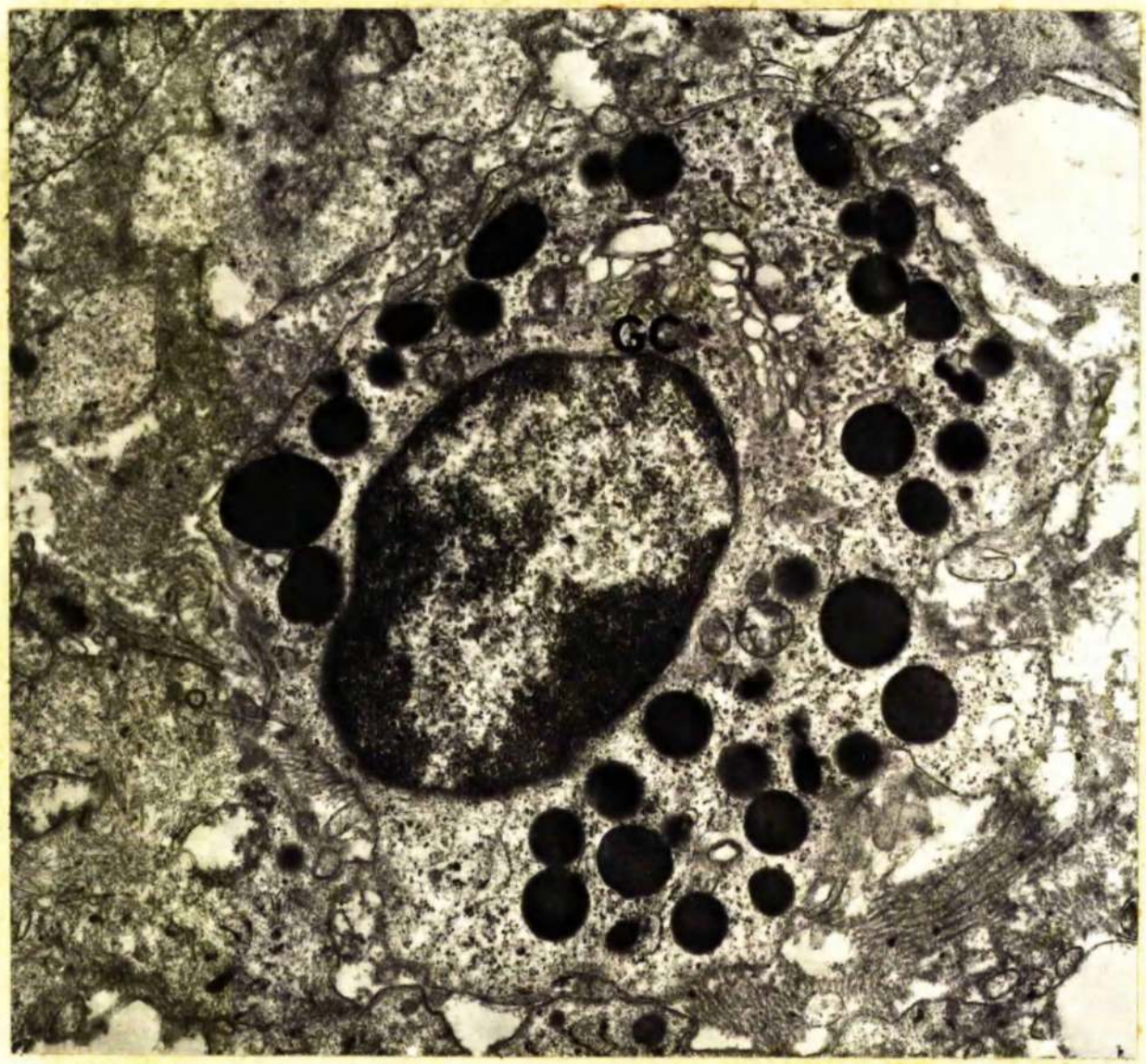

Figure 139. Mast cell with a well-developed golgi complex (GC). Fixation 1.75. glutaraldehyde. x 22,500.

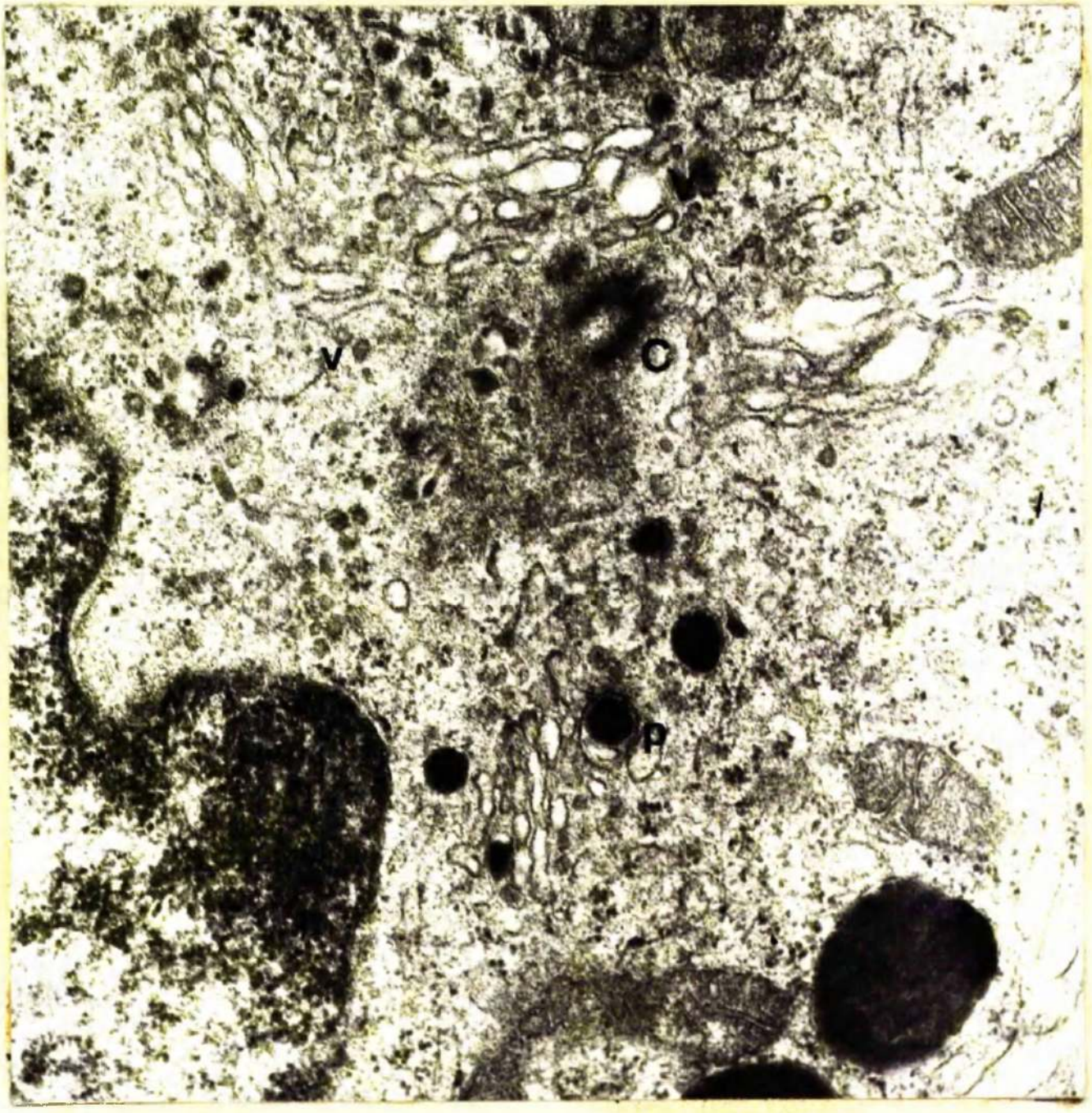

Figure 140. Golgi complex in mast cell. Many smooth-surfaced profiles are present; some are dilated to form vacuoles (V) and may contain electron-dense material, progranules (p). Note the associated vesicles (v) and centrioles (C). Fixation 1.5% glutaraldehyde. x 50,000.

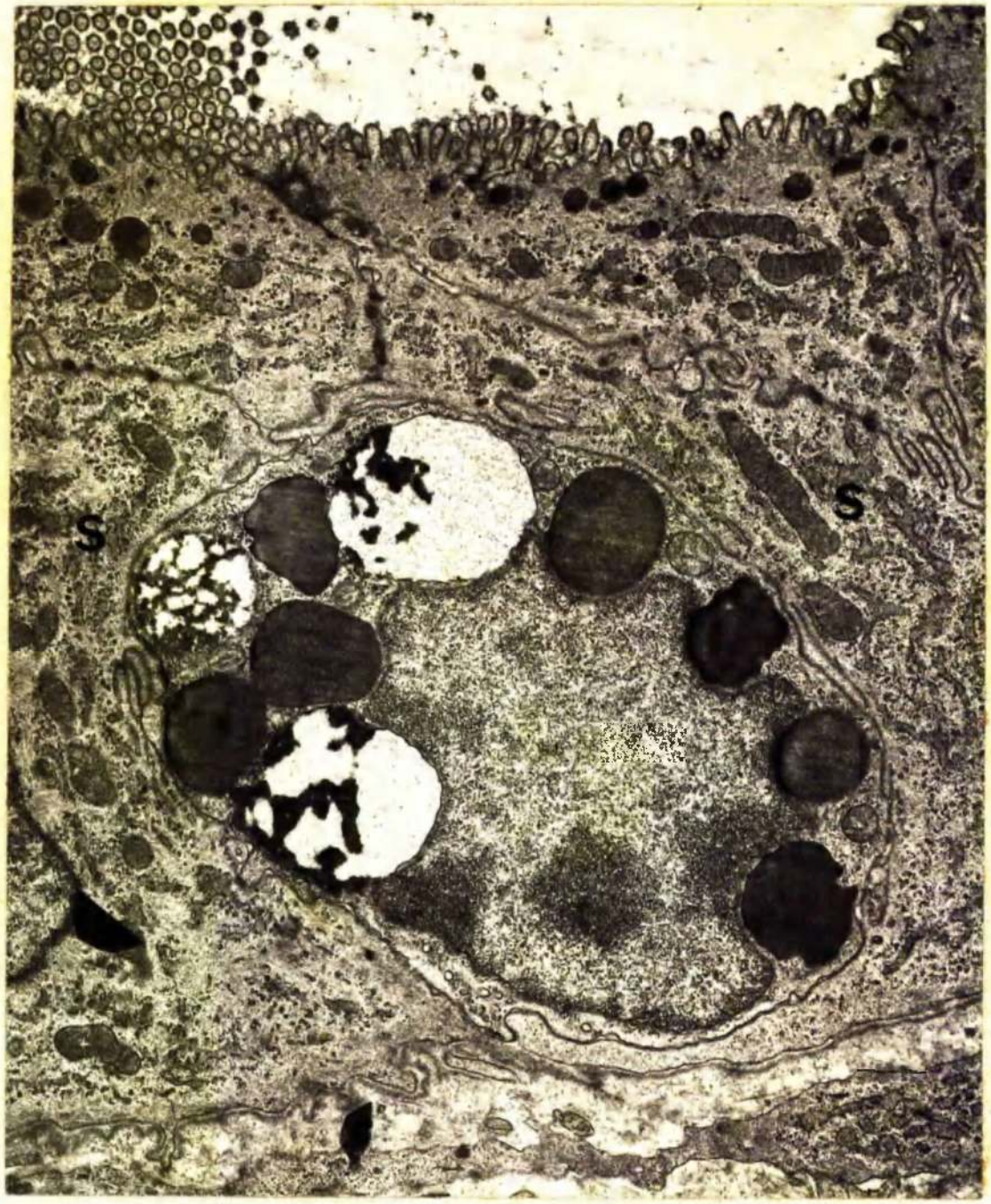

Figure 141. Globule leukocyte lying between surface mucous cells (S). Fixation 1% osmium tetroxide. x 12,500.

Figure 142. Smooth-surfaced membrane bounding GL granule. Fixation 1.5% glutaraldehyde. x 135,000.

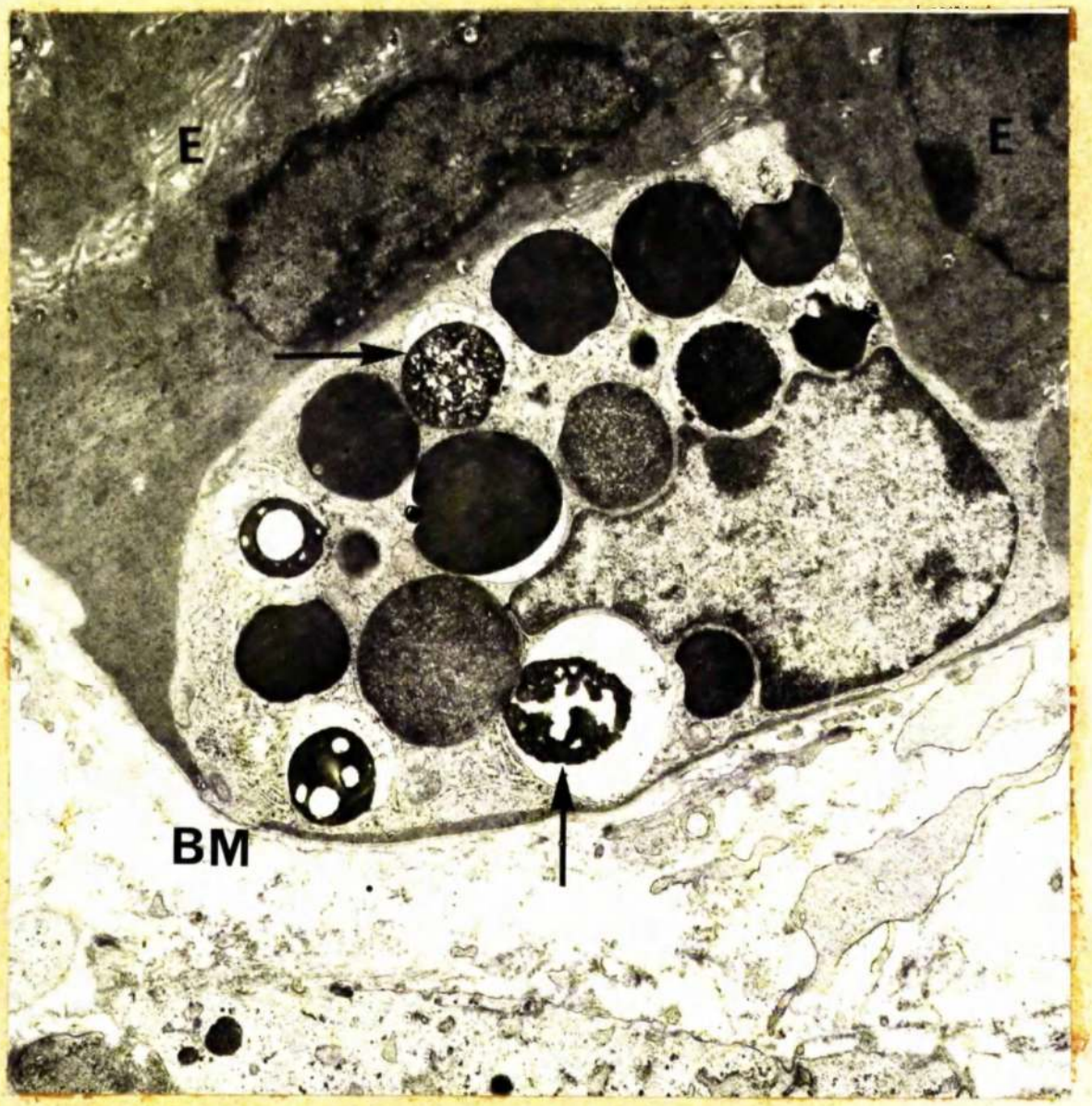

Figure 143. Globule leukocyte packed with granules some of which have a reticulated appearance (↑). A few cisternae of RSER and ribosomes are present. Fixation 1.75% glutaraldehyde. x 10,000.

Figure 144. Cell within the epithelium containing granules of varying size; some correspond to GL granules and others to mast cell granules. Fixation 1.5% glutaraldehyde. x 18,750.

Figure 145. Globule leukocyte lying between undifferentiated epithelial cells. It is packed with large granules some of which have a reticulated appearance (↑). Note the pseudo-vacuolated appearance of the cytoplasm. Fixation 1.5% glutaraldehyde. x 12,500.

Figure 146. Transitional cell in lamina propria. Note the range of granules present and the eosinophil (Eo). Fixation 1.5% glutaraldehyde. x 12,500.

Figure 147. Mast cell in lamina propria of gallbladder of parasitised sheep showing a range of granule changes. The cytoplasm contains many membrane-bound vacuoles (V). Fixation 1.5% glutaraldehyde. x 15,000.

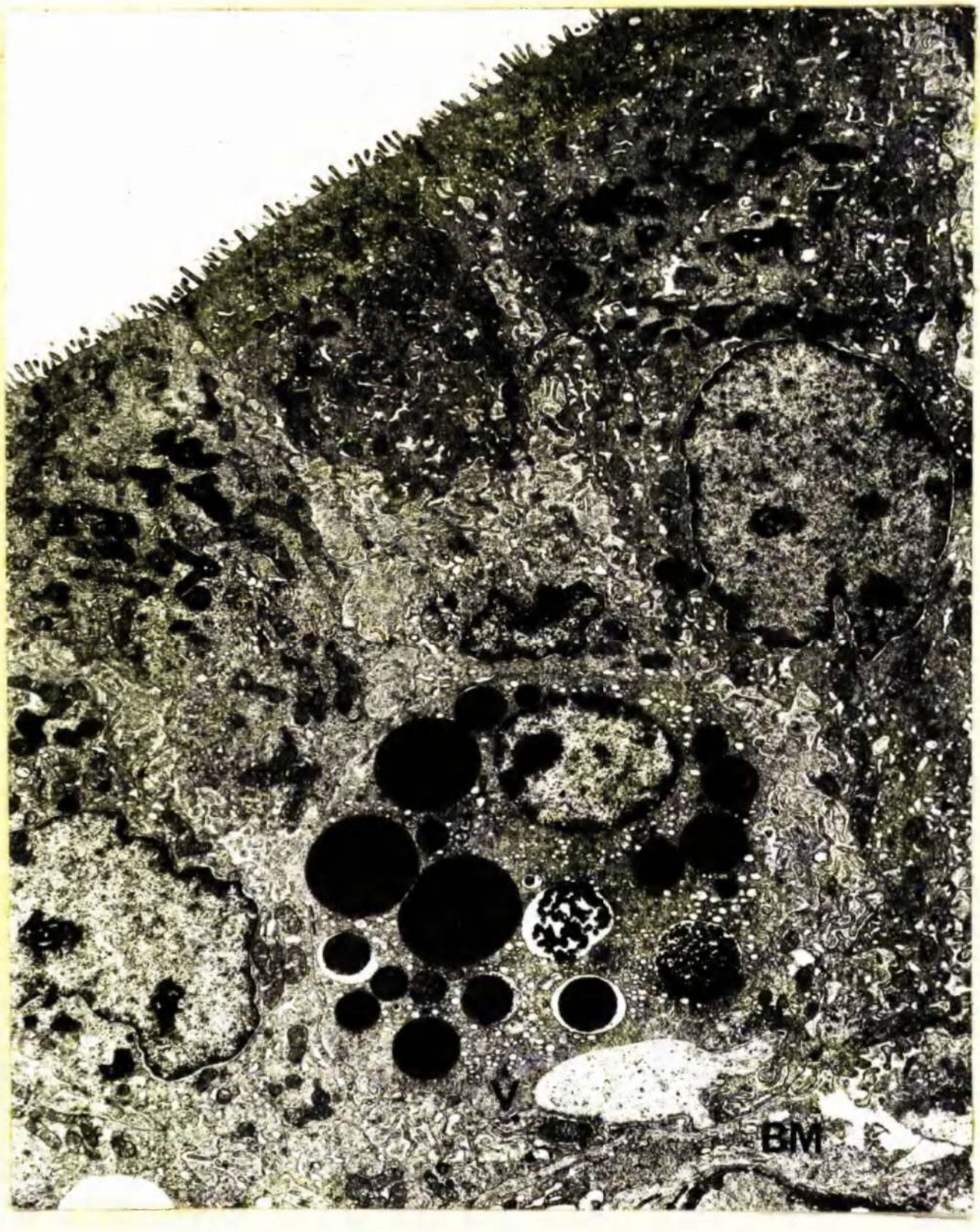

Figure 148. Globule leukocyte within the epithelium of gallbladder of parasitised sheep showing a range of granule size and structure. Note the presence of cytoplasmic vacuoles (V) as in mast cell of Fig. 147. Fixation 1.5% glutaraldehyde. x 6,000.

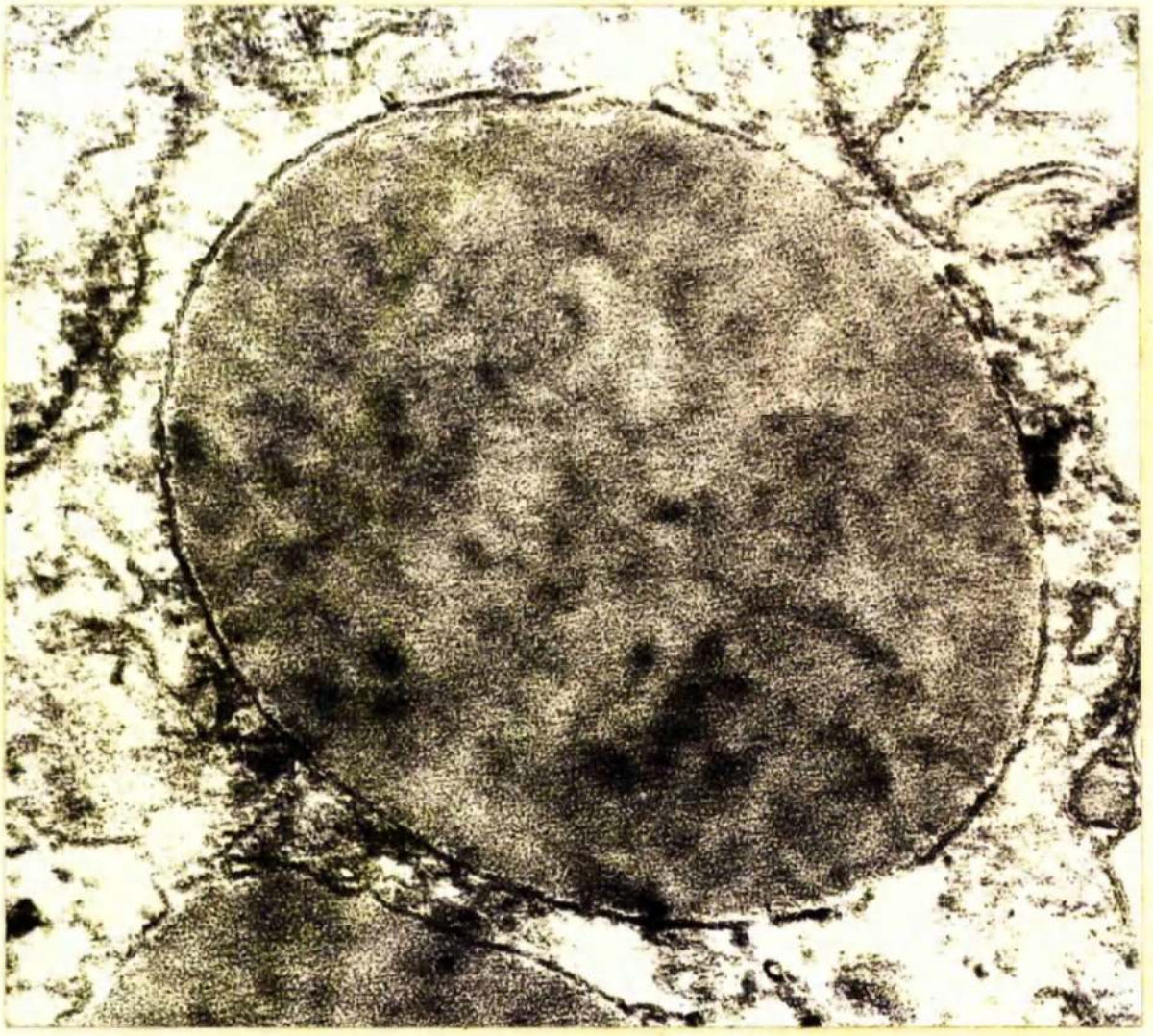

Figure 149. Granule in sheep GL bounded by a smooth-surfaced unit membrane. Fixation 1.5% glutaraldehyde. x 15,000.

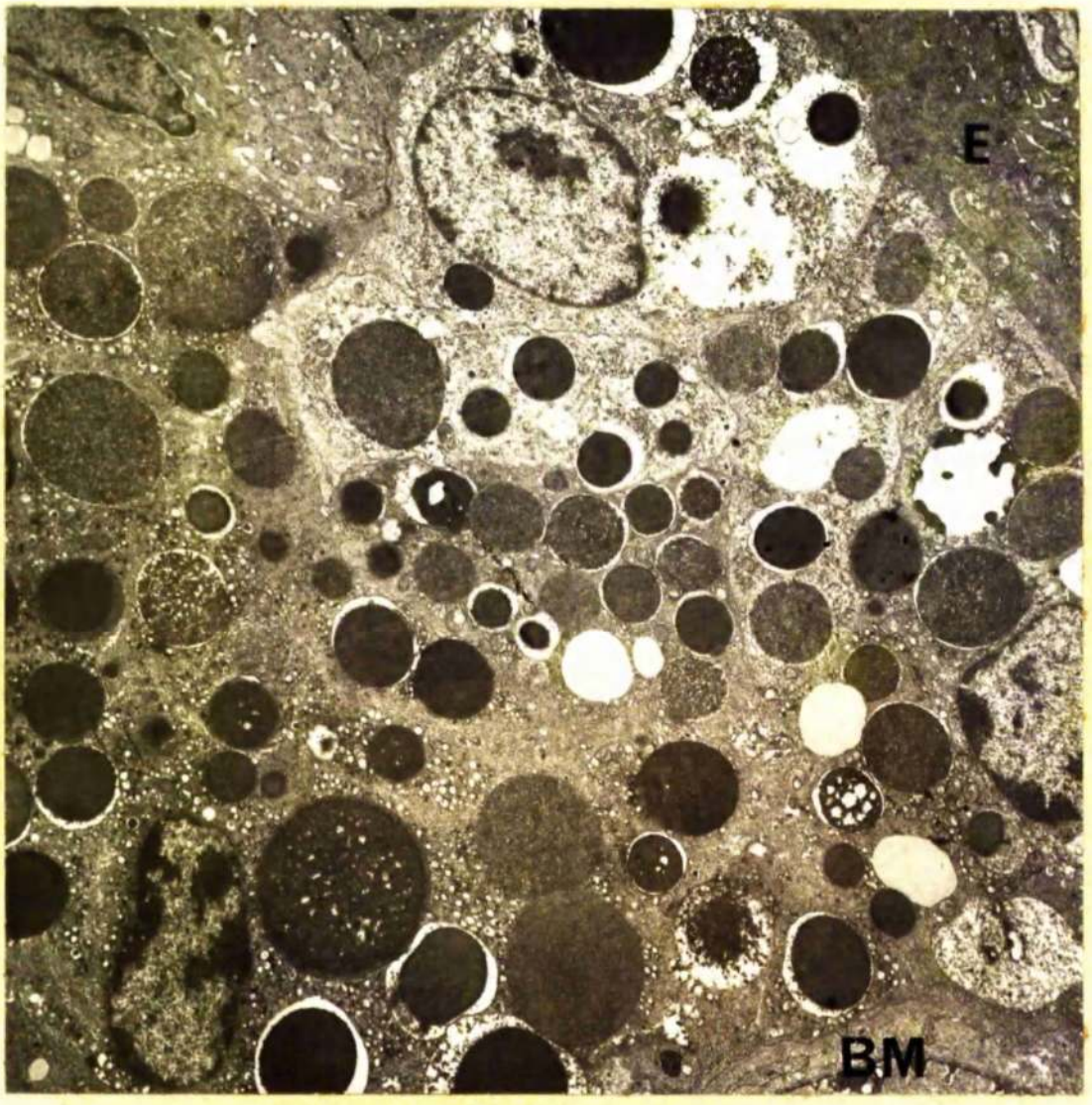

Figure 150. GLs with the epithelium of parasitised sheep showing a range of granule size and structure. Fixation 1.5% glutaraldehyde. x 6,000.

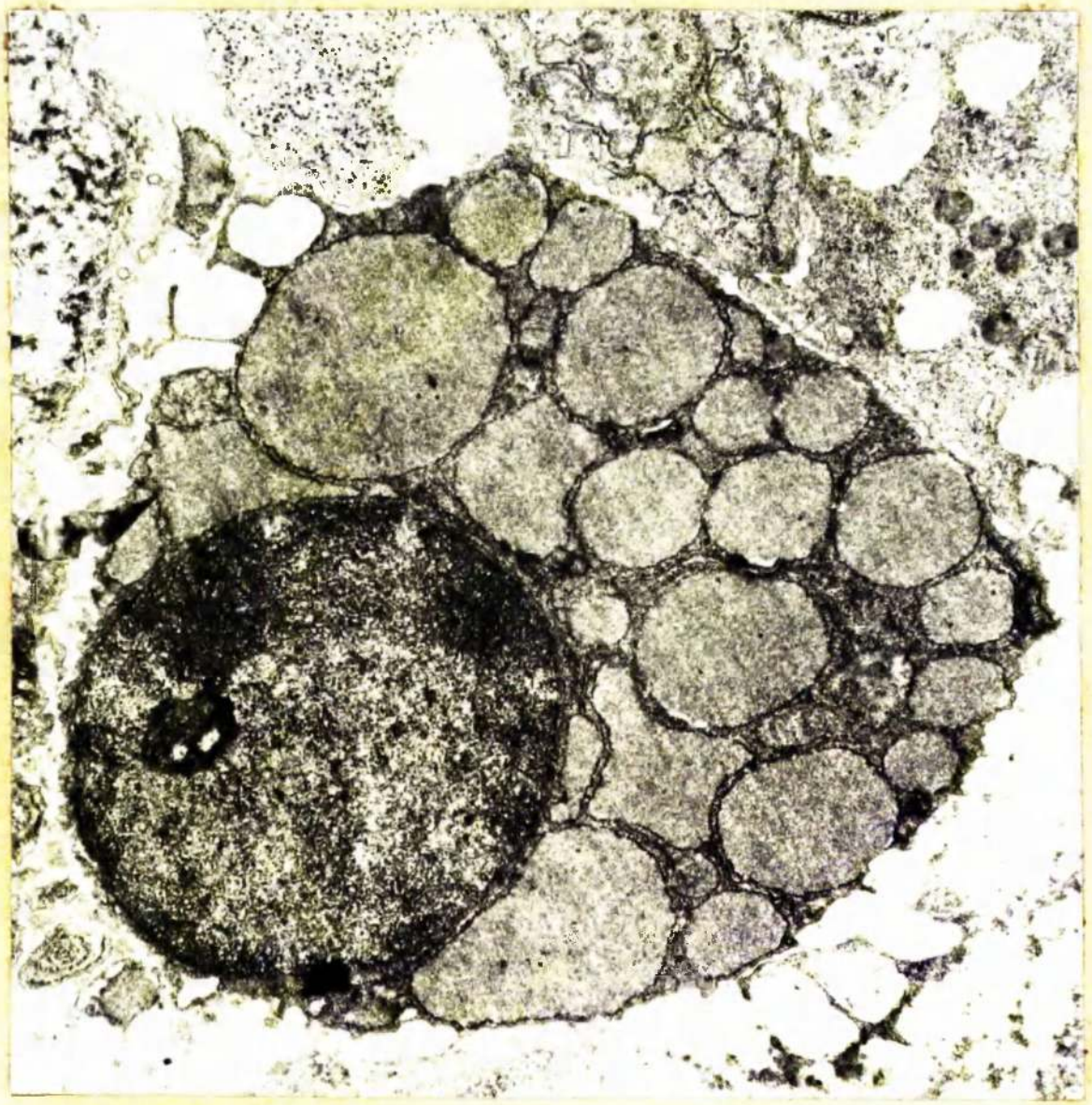

Figure 151. Russell body-containing cell in lamina propria of gallbladder of parasitised sheep showing distended cisternae surrounded by RSER. Fixation 1.5% glutaraldehyde. x 15,000.

SECTION VI

THE STRUCTURAL CHANGES IN THE BOWEL WALL ASSOCIATED WITH INCREASED PERMEABILITY TO MACROMOLECULES

Figure 152. Hyperplastic gastric mucosa produced by waves of development and emergence of inhibited larvae. Note the presence of an inhibited 4th stage larvae. x 50.

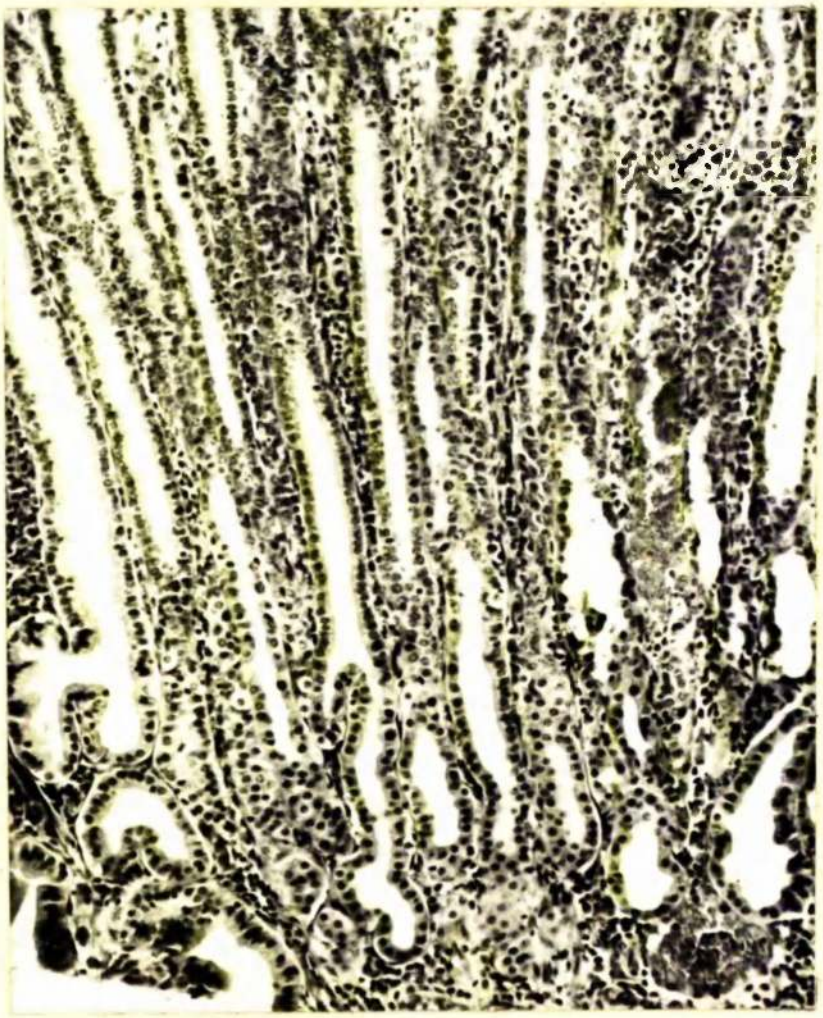

Figure 153. Rapidly-dividing undifferentiated cells in area joining two secondary nodules. x 140.

Figure 154. Coalescence of secondary nodules to form a markedly hyperplastic mucosa with a morocco-leather or crazy paving appearance.

Figure 155. Necrosis and sloughing of the surface mucous cells. Adult worms lie in an exudate of protein, polymorphs and clumps of bacteria. Note the hyperplastic gastric mucosa lined by rapidly-dividing undifferentiated cells. x 50.

Figure 156. Irregular plaques of diphtheritic membrane on the surface mucosa of the abomasum.

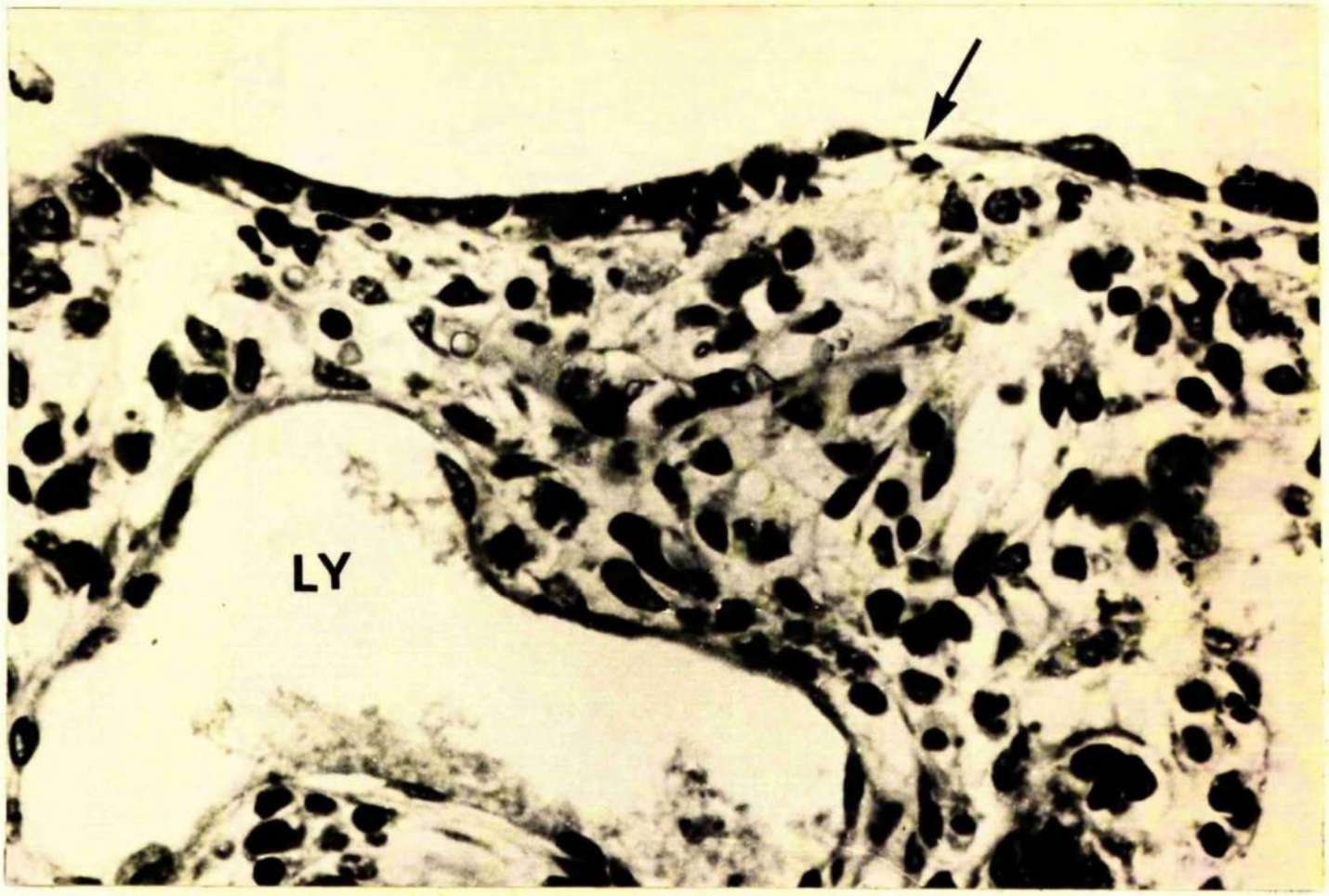

Figure 157. Stretched and flattened surface mucous cells (↑) in area of severe oedema. Note the dilated lymphatic (LY). x 410.

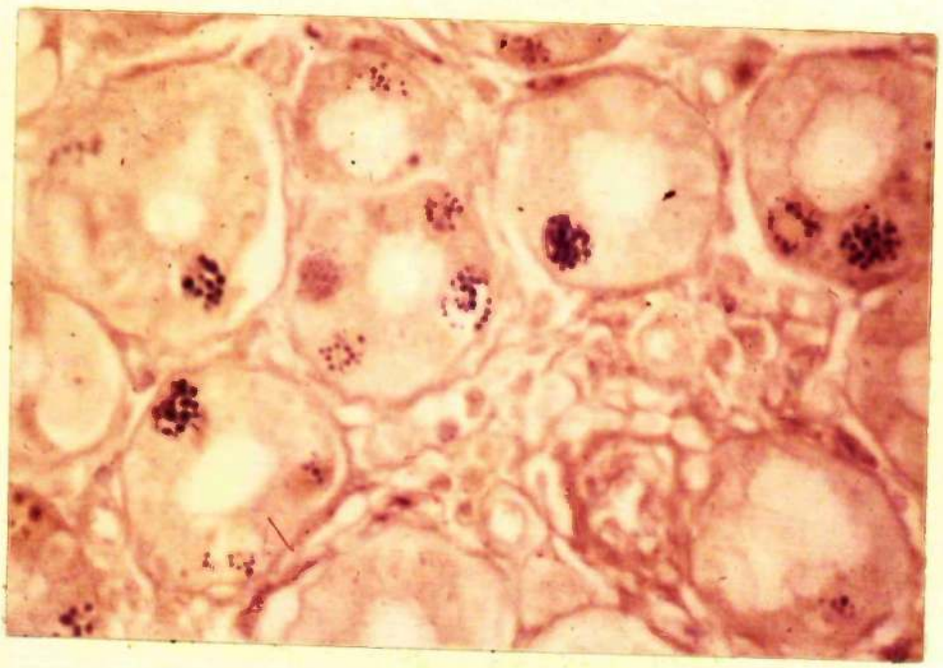

Figure 158. Globule leukocytes within gastric mucosa. Phosphotungstic acid-haematoxylin. x 420.

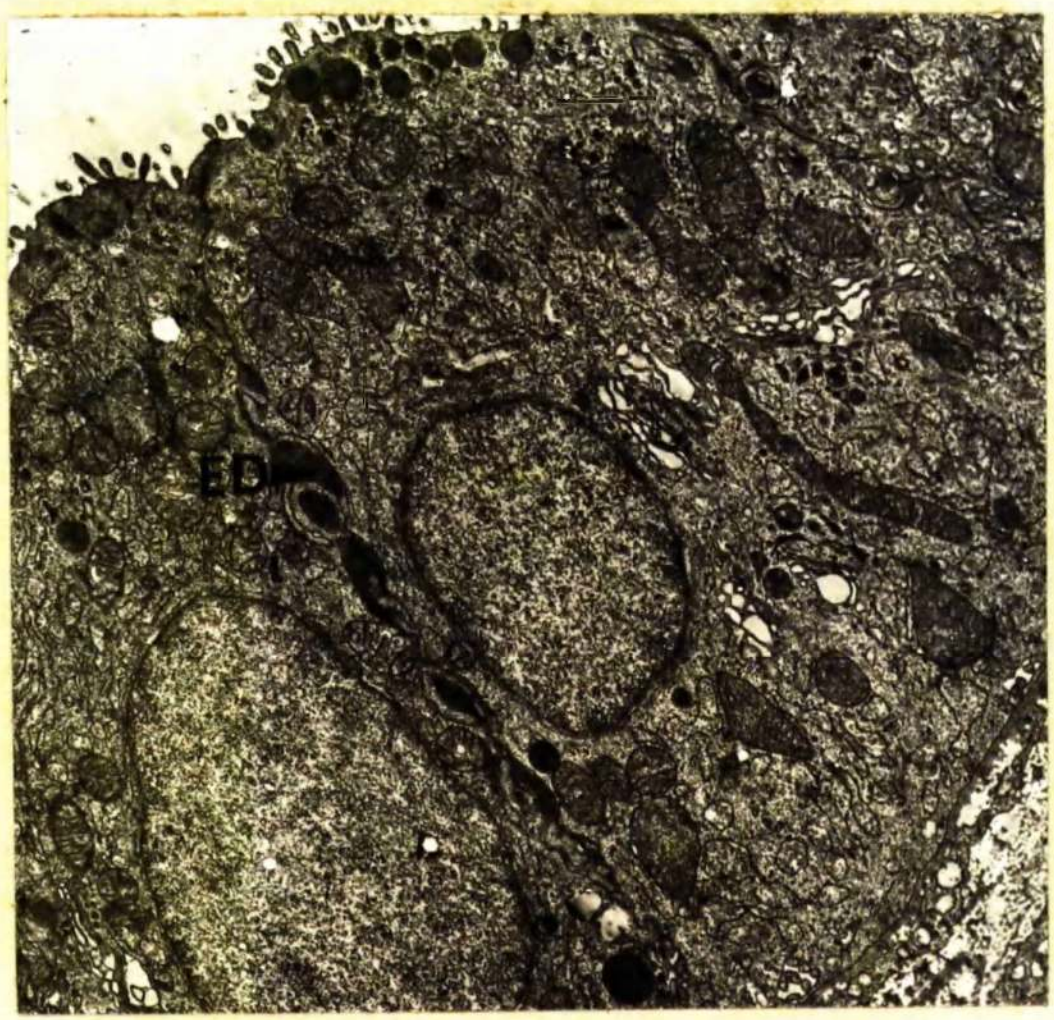

Figure 159. The cell boundaries of undifferentiated cells are delineated by electron-dense material (ED) lying between adjacent lateral cell membranes. Fixation 1.5% glutaraldehyde. x 15,000.

Figure 160. Electron-dense material (↑) lying between undifferentiated cells. Fixation 1.5% glutaraldehyde. x 15,000.

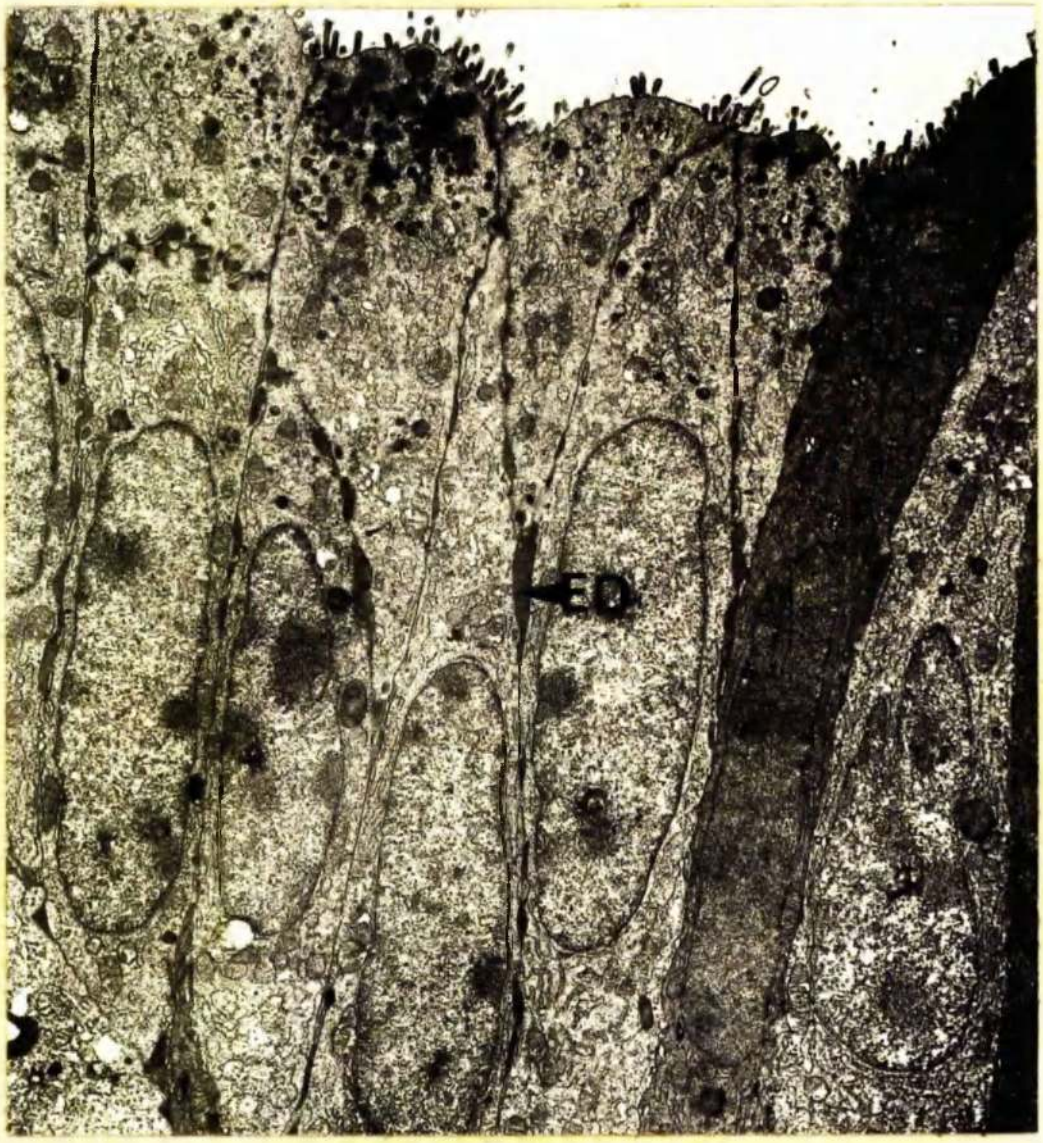

Figure 161. The borders of surface mucous cells are delineated by electron-dense material (ED) lying between adjacent lateral cell membranes. Fixation 1.5% glutaraldehyde. x 6,000.

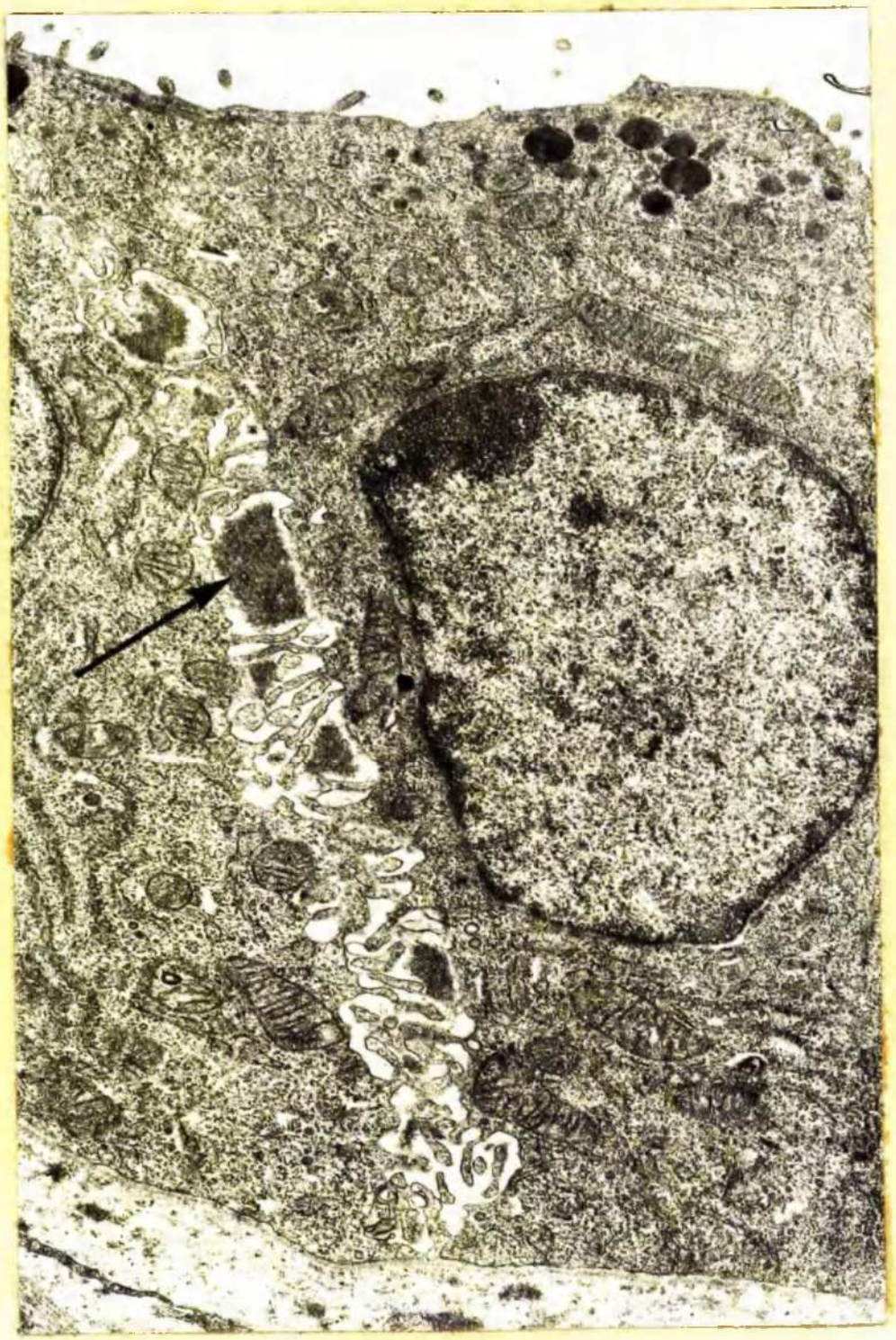

Figure 162. Patches of electron-dense material (↑) lying between relatively inactive zymogen cells. Fixation 4% glutaraldehyde. x 15,000.

Figure 163. Electron-dense material (↑) lying between undifferentiated cells. Note the membrane-bound vacuoles (V) filled with electron-dense material in the apical cytoplasm close to the lateral border of the cell. Fixation 1.5% glutaraldehyde. x 20,000.

Figure 164. Juxtaluminal segment of the lateral boundaries of undifferentiated cells. Note the separation of the lateral plasmalemmata forming the zonula occludens (ZO inset) and the electron-dense material (↑) lying between. Fixation 1.5% glutaraldehyde. x 75,000 (inset x 120,000).

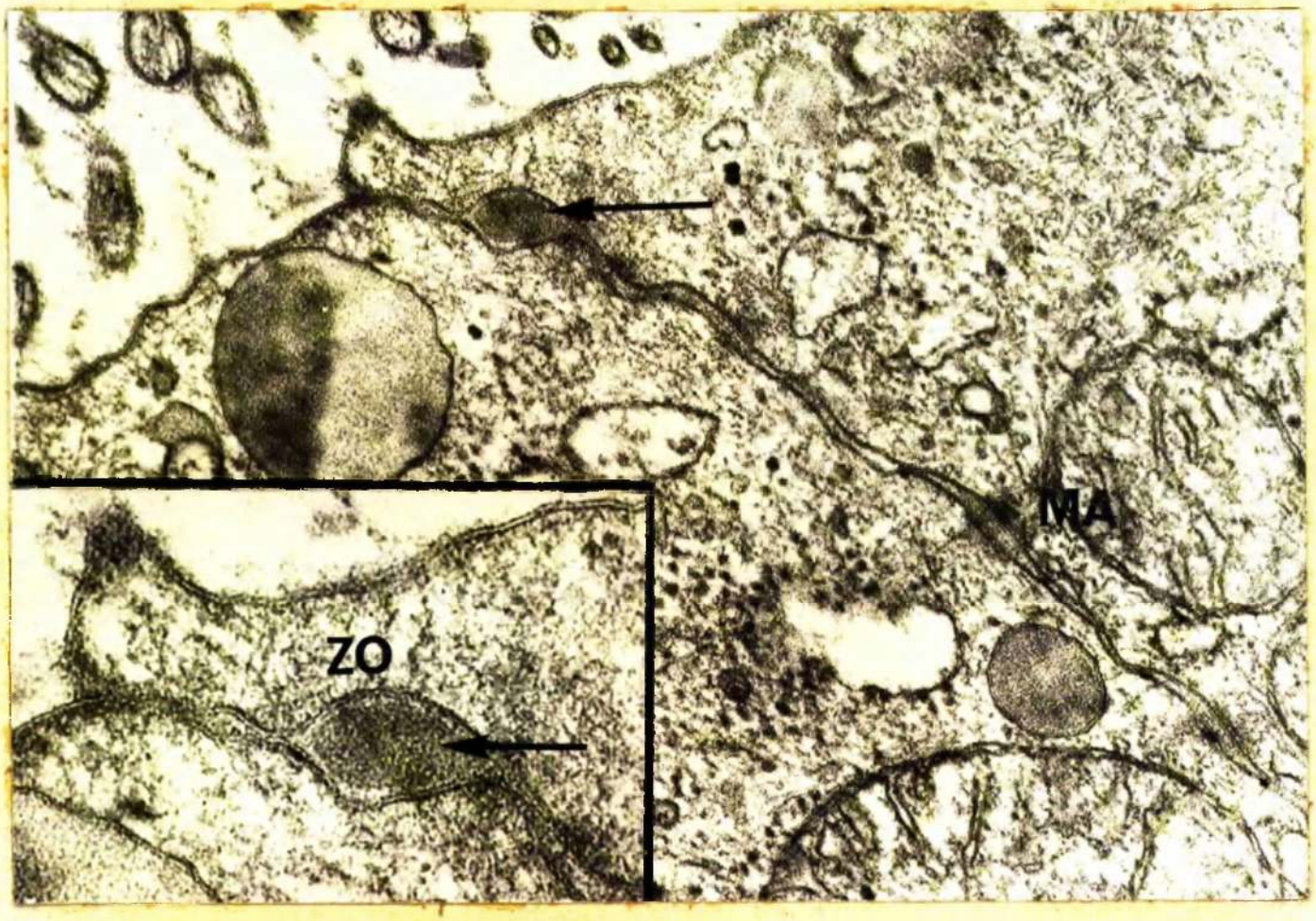

Figure 165. Juxtaluminal segment of the lateral boundaries of undifferentiated cells. Note the electron-dense material (↑) between the lateral plasmalemmata of the zonula occludens (ZO inset). The desmosomes (MA) show no structural changes. Fixation 1.5% glutaraldehyde. x 75,000. (inset x 120,000).

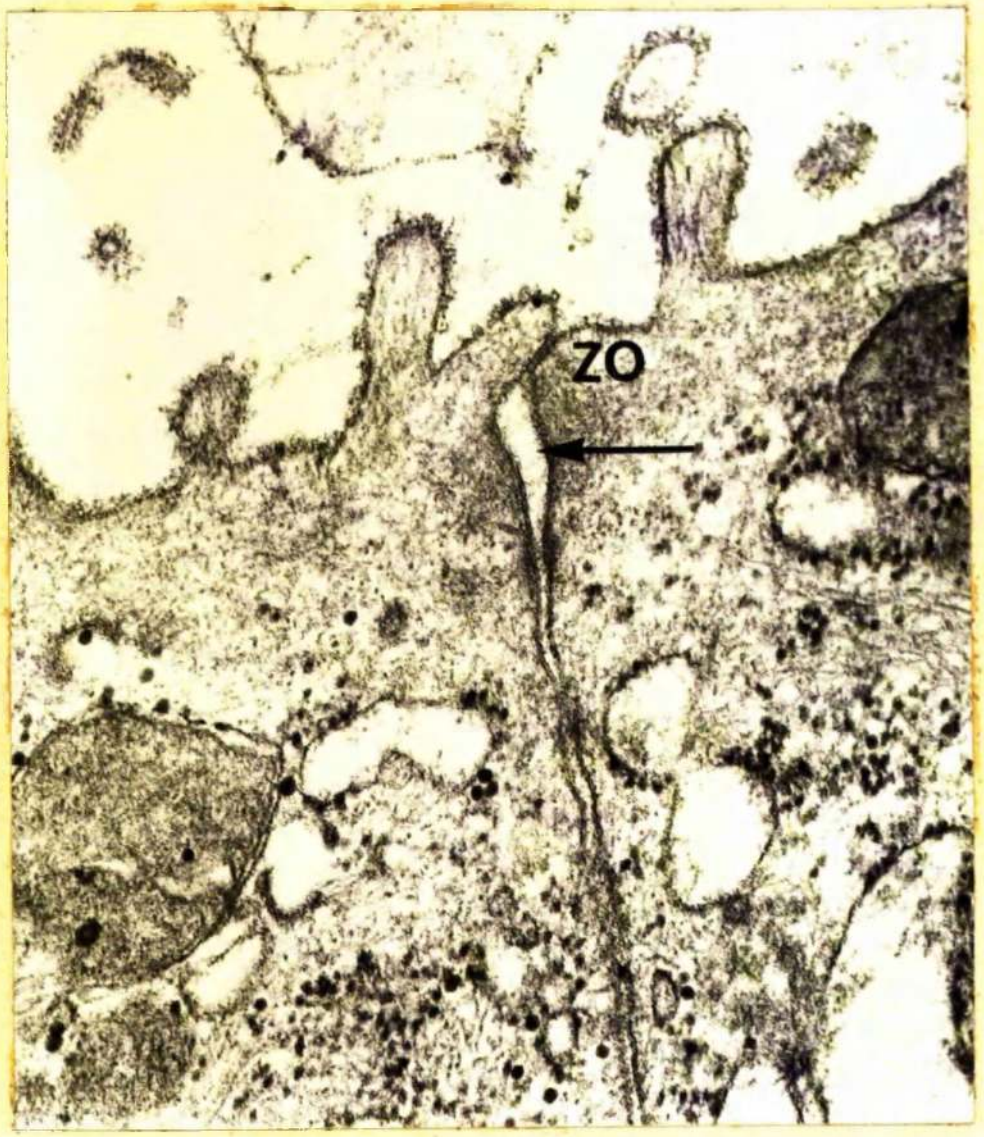

Figure 166. Juxtaluminal segment of undifferentiated cells. Note the shortened zonula occludens (ZO) and dilatation of the intercellular space (↑). Fixation 1.5% glutaraldehyde. x 75,000.

Figure 167. Complete separation of lateral plasmalemmata of the zonula occludens (ZO). Fixation 1.5% glutaraldehyde. x 112,000.

Figure 168. Partial separation of the lateral plasmalemmata of the zonula occludens (↑). Fixation 1.5% glutaraldehyde. x 75,000.

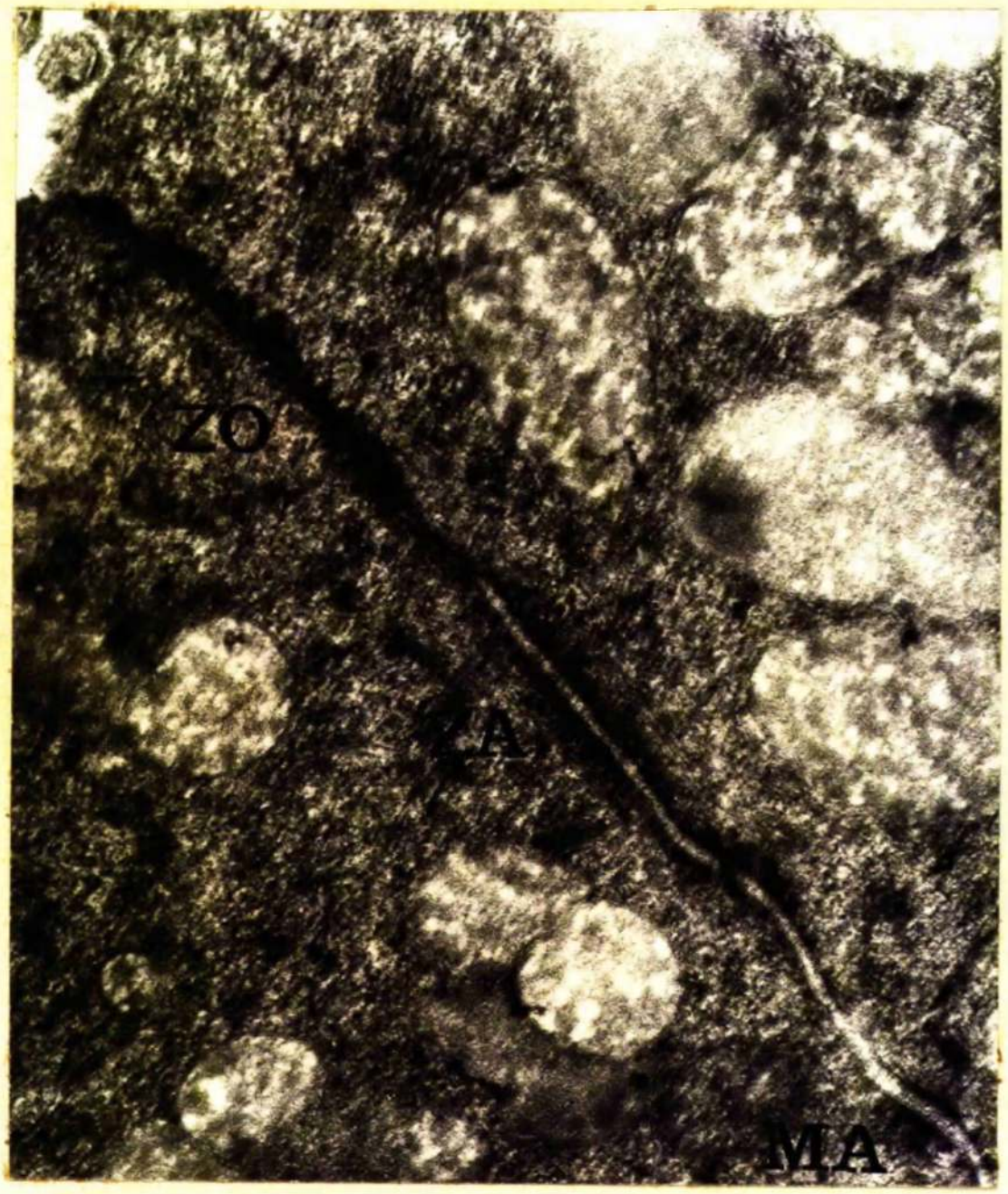

Figure 169. Tripartite junctional complex between surface mucous cells in the gastric mucosa of a parasite-free bovine. Note the long zonula occludens (ZO) and zonula adhaerens (ZA) and the desmosome (MA). Fixation 4% glutaraldehyde. x 75,000.

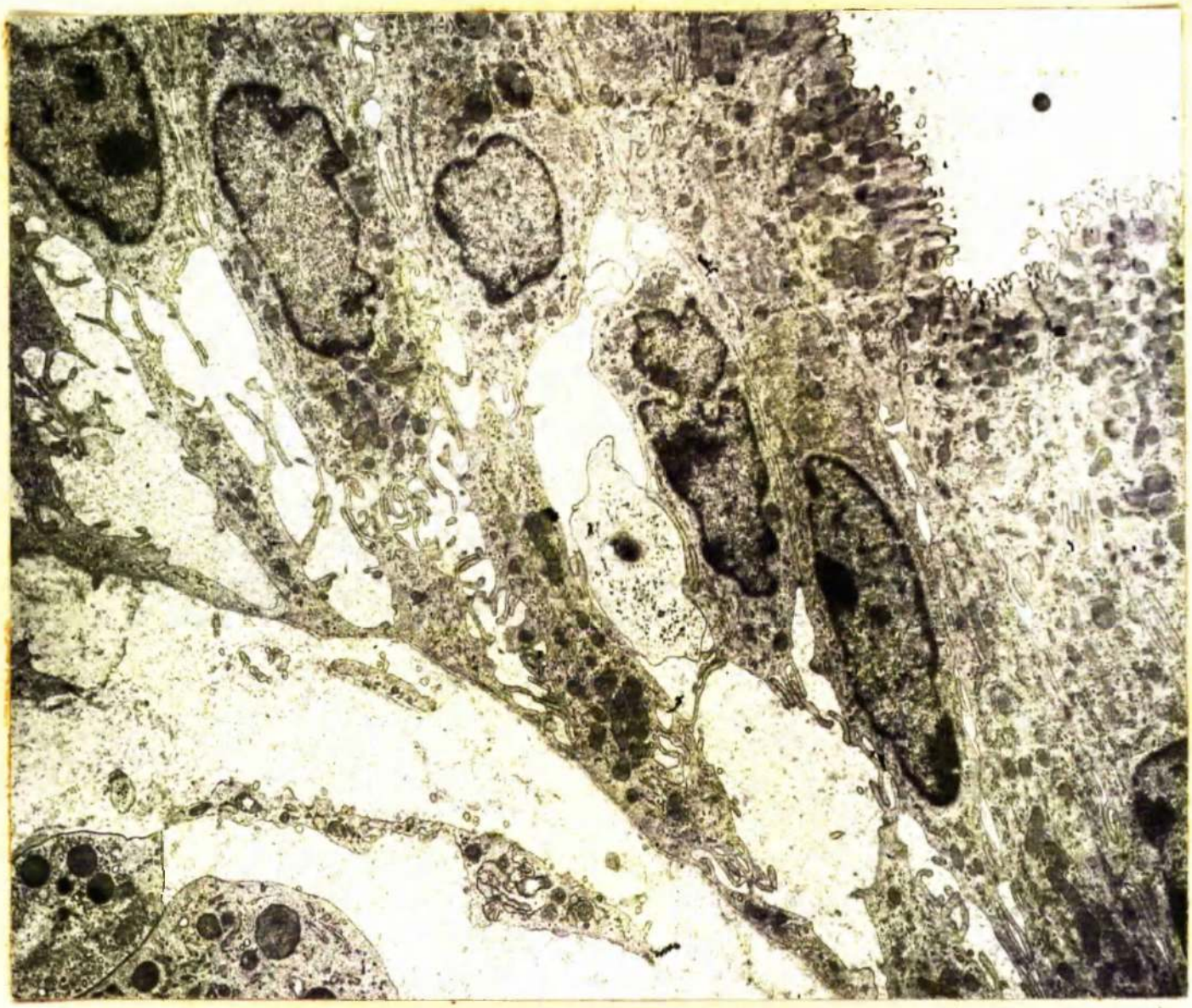

Figure 170. Surface mucous cells in an area of severe oedema. Note the marked dilatation of the intercellular spaces. Fixation 1% osmium tetroxide. x 9,000.

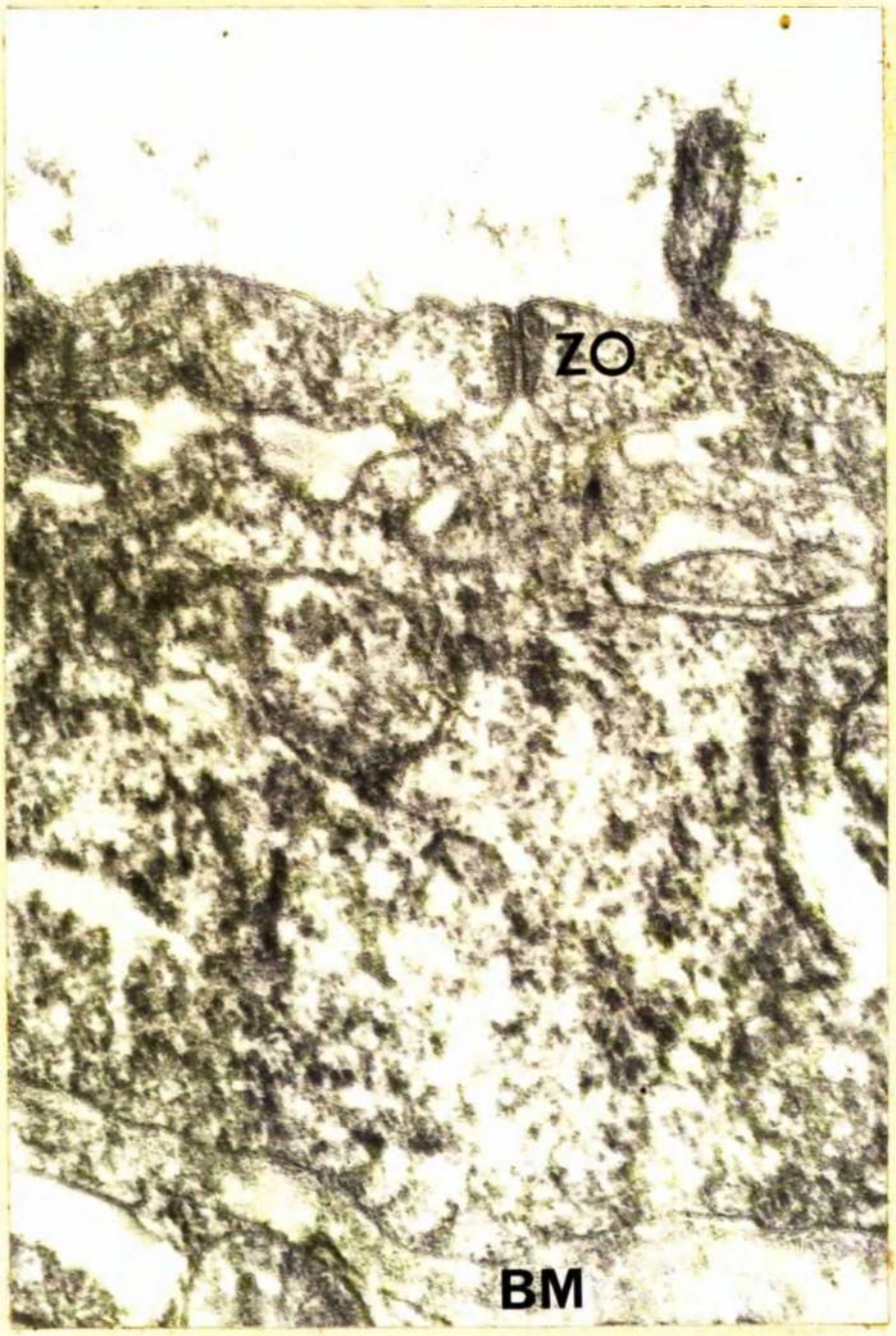

Figure 171. Shortened zonula occludens (ZO) joining flattened cells lining a dilated gland. Fixation 4% glutaraldehyde. x 75,000.

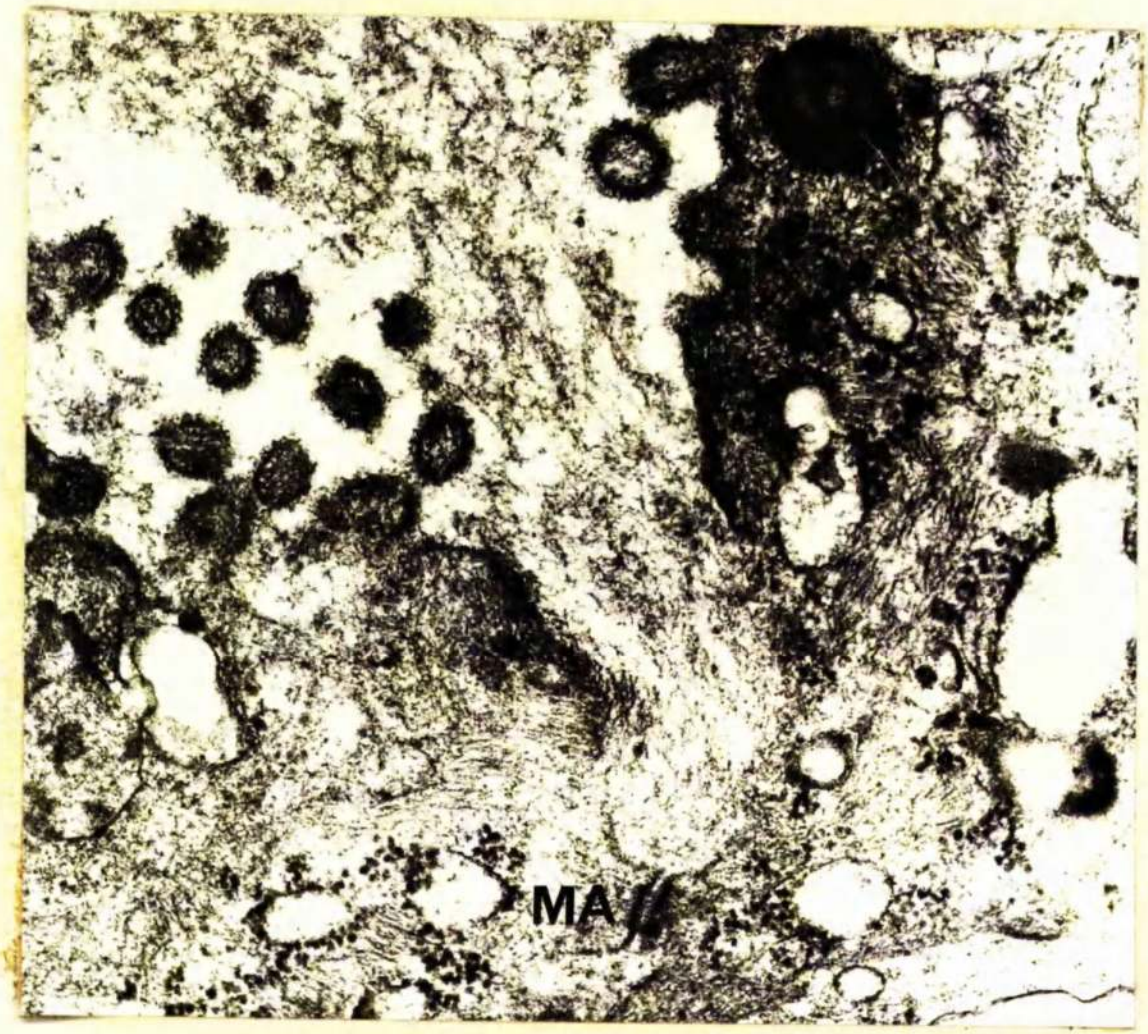

Figure 172. Flattened cells lining dilated gland are joined only by a desmosome (MA). Fixation 1.5% glutaraldehyde. x 56,000.

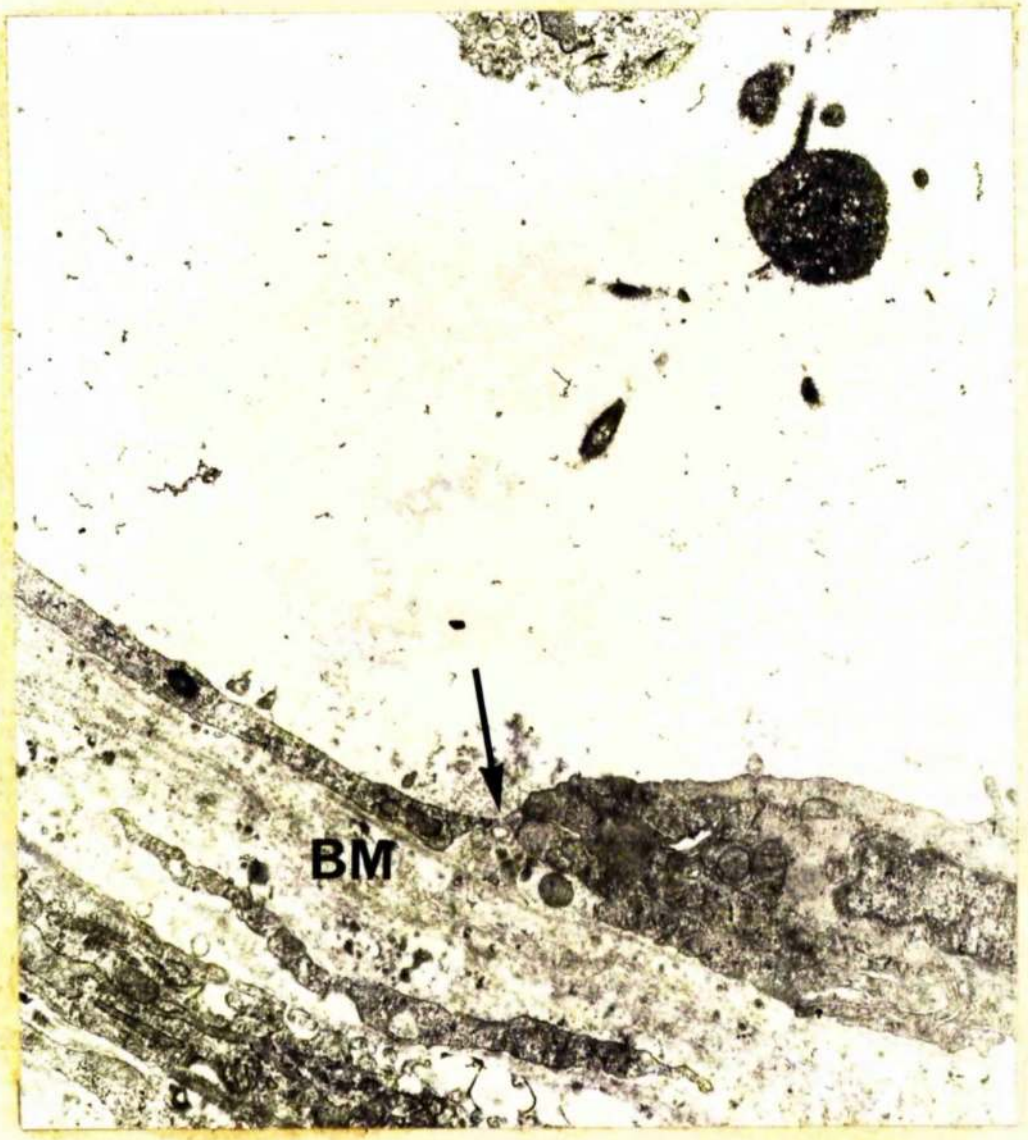

Figure 173. Flattened mucous cells in dilated glands. The cells are almost completely separated (↑). Fixation 4% glutaraldehyde. x 10,000.

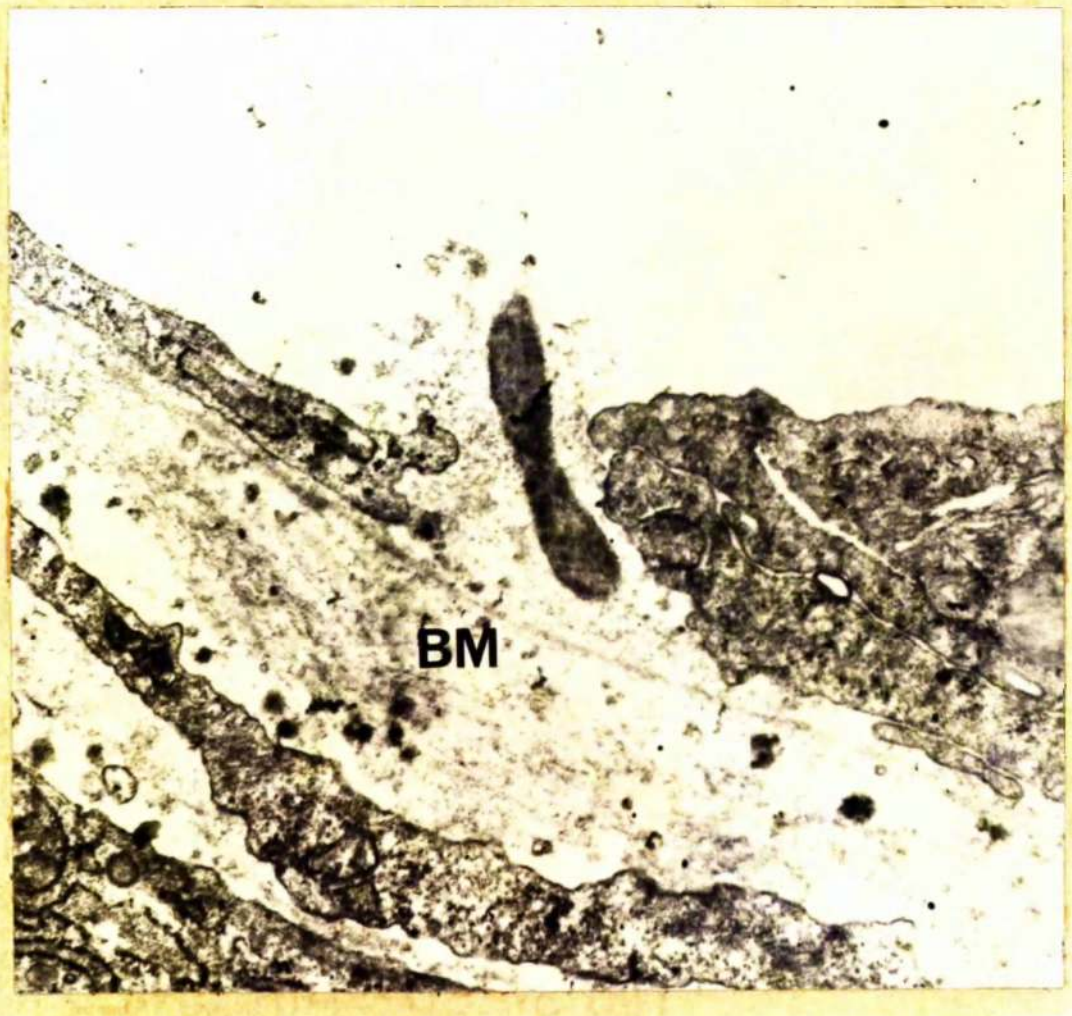

Figure 174. Complete separation of flattened mucous cells lining a dilated gland. Note the red blood cell between the separated cells. Fixation 4% glutaraldehyde. x 30,000.

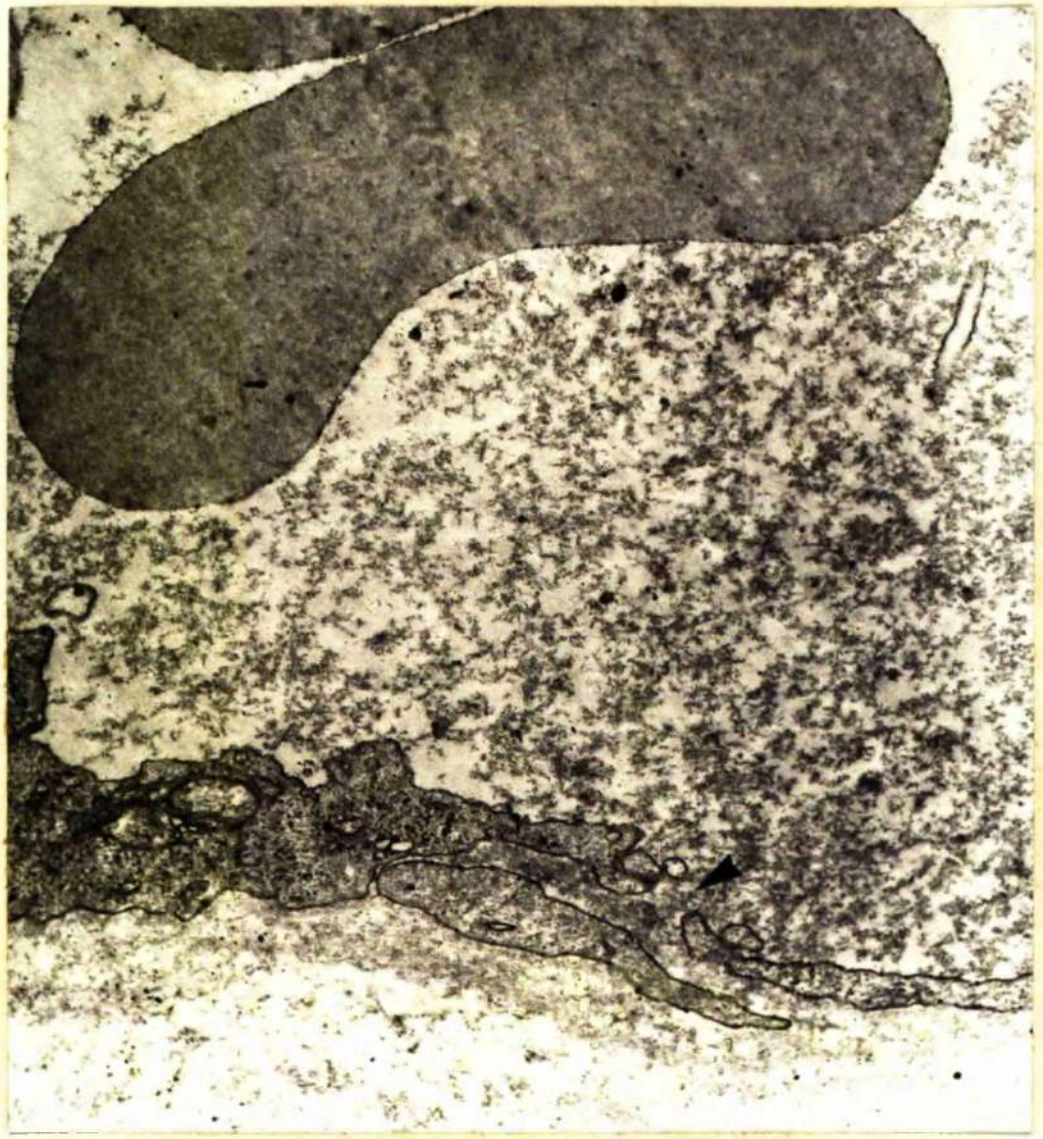

Figure 175. Separation of endothelial cells (↑) of venule. Fixation 4% glutaraldehyde. x 25,000.

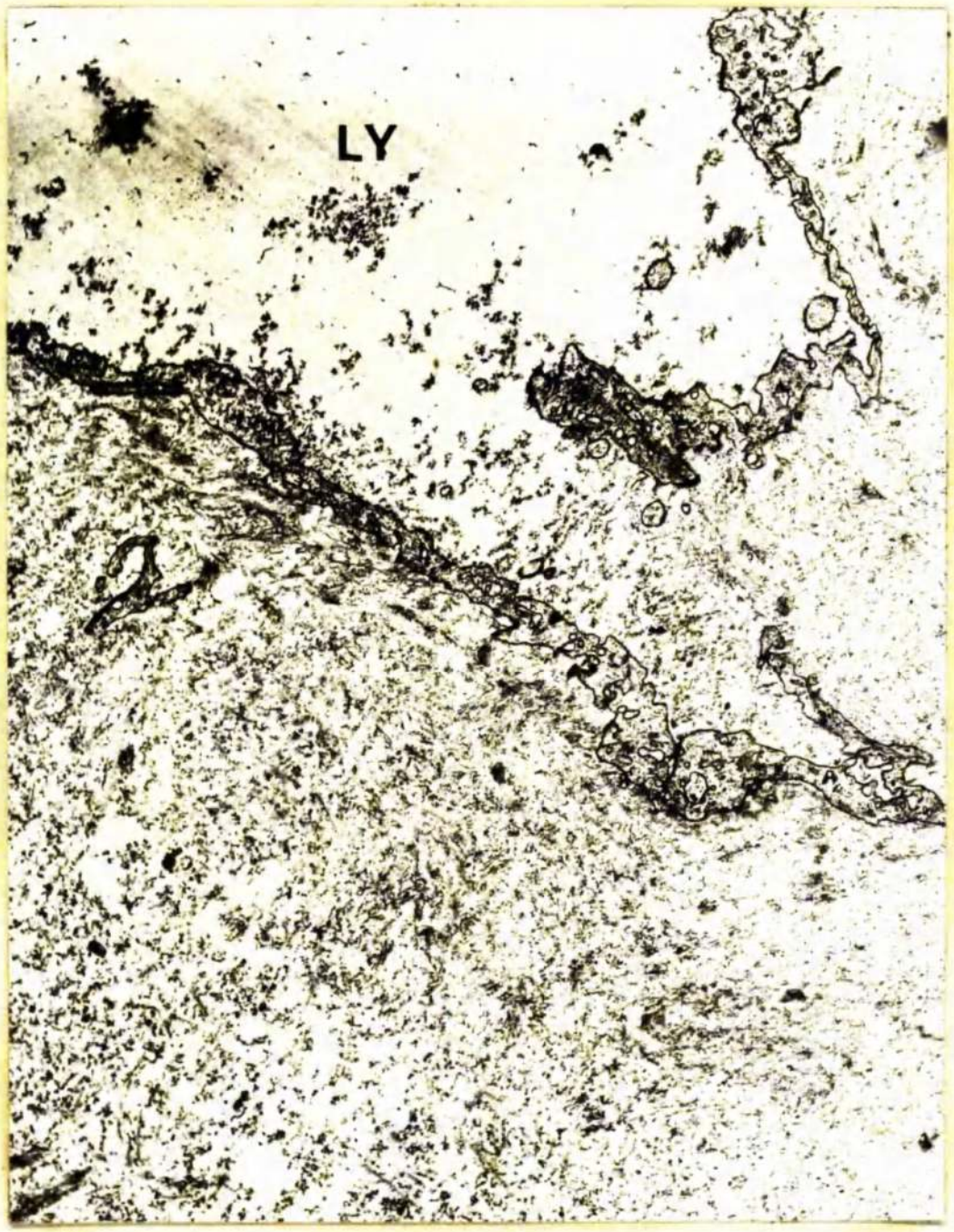

Figure 176. Dilatation of lymphatic and separation of endothelial cells. Fixation 1% osmium tetroxide. x 12,500.

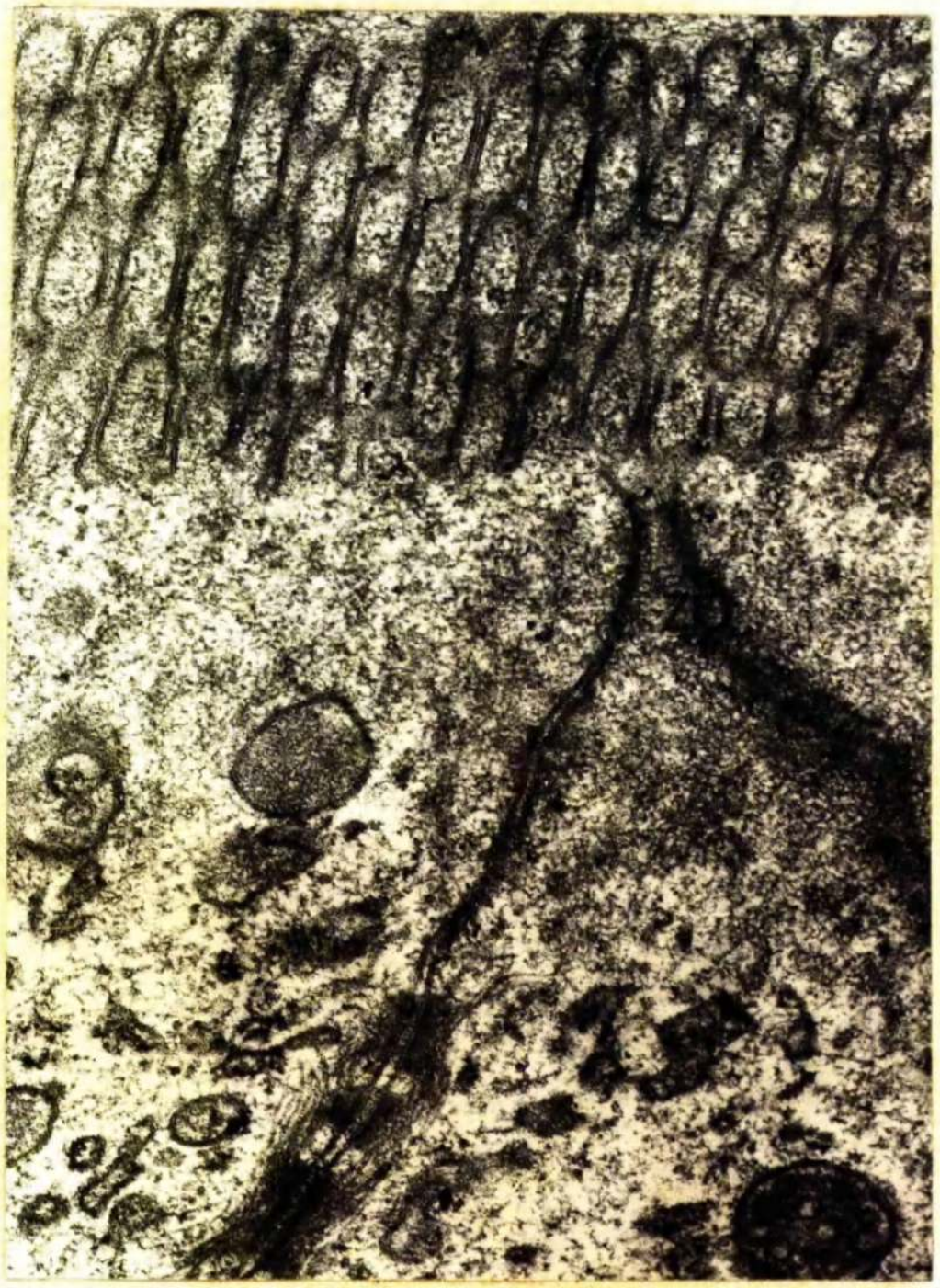

Figure 177. Tripartite junctional complex between surface cells in small intestine. The zonula occludens (ZO) forms a complete seal. Fixation 1% osmium tetroxide. x 75,000.